CRYSTAL ENGINEERING OF SOME 2-PYRIMIDINONES AND UNSYMMETRICAL UREAS

A Thesis
Submitted for the Degree of
Doctor of Philosophy

By
SUMOD GEORGE

School of Chemistry
University of Hyderabad
Hyderabad 500 046
India

April 2004

CRYSTAL ENGINEERING OF SOME 2-PYRIMIDINONES AND UNSYMMETRICAL UREAS

A Thesis
Submitted for the Degree of
Doctor of Philosophy

By
SUMOD GEORGE

School of Chemistry
University of Hyderabad
Hyderabad 500 046
India

April 2004

To
My Parents

STATEMENT

I hereby declare that the matter embodied in this thesis entitled "**Crystal Engineering of Some 2-Pyrimidinones and Unsymmetrical Ureas**" is the result of investigations carried out by me in the School of Chemistry, University of Hyderabad under the supervision of **Prof. Ashwini Nangia**.

In keeping with the general practice of reporting scientific observations due acknowledgements have been made wherever the work described is based on the findings of other investigators.

Sumod George

Hyderabad
April 2004

CERTIFICATE

Certified that the work "**Crystal Engineering of Some 2-Pyrimidinones and Unsymmetrical Ureas**" has been carried out by **Sumod George** under my supervision and that the same has not been submitted elsewhere for a degree.

Dean

School of Chemistry

Dean
School of Chemistry
University of Hyderabad
Hyderabad-500 046, India

Prof. Ashwini Nangia

Thesis Supervisor

ACKNOWLEDGEMENT

I wish to express my deep and profound thanks to my supervisor, **Prof. Ashwini Nangia** for his constant encouragement, guidance and thought provoking discussions throughout my Ph.D programme. I have been able to learn a great deal from him and consider my stay with him as a rewarding experience in my life.

It is a pleasure for me to thank Prof. Gautam R. Desiraju for useful discussions, encouragements and inspiring lectures. I feel very fortunate to be associated with him.

I thank Prof. E.D. Jemmis, Dean, School of Chemistry and former Deans and faculty members of the School for their co-operation on different occasions.

I would like to thank Dr. René Masse, Laboratoire de Crystallographie, Grenoble, France, Prof. Jean-François Nicoud, Université Louis Pasteur, Strasbourg, France, Dr. Vincent M. Lynch, University of Texas, Austin, USA, Prof. Thomas C. W. Mak, The Chinese University, Hong Kong for helpful discussion, their assistance with X-ray data on compounds studied and analyzed in this thesis. Thanks are also to Drs. Muriel Bagieu-Beucher, Yvette Le Fur, M. Muthuraman and C.K. Lam for helpful discussions and X-ray data collections.

I wish to thank my labmates Drs. V.R. Thalladi, A. Anthony, N.N.L. Madhavi, K.S. Srinivasan, R. Thaimattam, Ram K.R. Jetti, Ashok Varma, Sanjay Sarkhel, T. Praveen Kumar, V.S. Senthil Kumar and P. Vishweshwar, Messrs Venu R. Vangala, K.V.V.M. Sairam, B. Balakrishna Reddy, A. Srinivasulu, B. Srinivas, L. Srinivas Reddy, C. Malla Reddy, Rahul Banerjee, Binoy K. Saha, Dinabandhu Das, Sunil K. Panigrahi, Aparna Vema, Saikat Roy, Archan Dey, J. Jeevan Kumar, M. Ravi kumar, Prashant V. Bhat, Tejender Singh Thakur, K.C. Srikanth and N. Jagadeesh Babu. Their constant support and friendly nature has made my stay in the campus joyful and wonderful.

There are lot of people who have helped me and it is difficult to mention all their names here but I thank all of them equally and profoundly. To name a few are M.K. Uttaman, Satyen Saha, Anil Kumar, Romesh Singh, Suvvada Srinivas, B.K. Srinivas, B. Kishore Babu, V. Chandrashekar, S. Perumal, P.P. Muhamad Ali, Maju Joe, T.K. Prasad, A.R. Biju, Tamal Ghosh, S. Philip Anthony, N. Jayaprakash and M. Mariappan.

I thank all the non-teaching and technical staff of the School of Chemistry for their kind help on various occasions. I would like to thank P. Raghaviah, S. Satyanarayana, Bhaskar Rao and Hemanth Kumar who are associated with X-ray diffractometer, NMR, IR and powder XRD machines.

I thank the DST for a fellowship for carrying out my research.

Blessings, affection, vision and support from my parents has made me what I am today. Support and care from my brothers, sisters and my wife Jincy during my research has generated a great feeling and I am very proud of them. I oblige all my achievements to them. Lastly and most importantly I thank almighty God for blessings and giving me strength throughout my life for all my endeavours.

Sumod George

PREFACE

The design of molecular solids and materials with desirable structure and property is a very important, though difficult, goal in current scientific research. Crystal engineering is a rapidly developing interdisciplinary field that can be used for designing solids with a synthetic plan for controlling the structure and properties of molecules in the condensed phase. *Crystal Engineering*, *CrystEngComm* and *Crystal Growth & Design* are three specialized journals devoted to this area of research which indicates the relevance of this particular area in current chemical research. This thesis mainly deals with an attempt towards developing molecules with polar layers and 3D arrangements for materials with useful properties.

Crystal engineering deals with the synthesis and rationalization of crystal structures. The design strategy is facilitated by the identification of recurring or robust structural units, namely supramolecular synthons. Some recent crystal design examples are illustrated in Chapter 1.

Chapter 2 explains synthesis and crystal structure of the initial set of three neutral pyrimidin-2-ones. Their hydrogen bonding interactions are explained in terms of C–H···O and C–H···N interactions leading to layered structures. The aromatic chromophore is aligned with respect to the polar axis in the crystal at an angle close to the optically ideal value 54.74°. The isostructurality in these crystal structures is explained.

Crystal engineering uses various strategies for controlling the packing in the solid state. The salt methodology is to crystallize organic molecules as their ionic salts. Chapter 3 deals with the characterization of chloride and nitrate salt adducts of pyrimidinones by X-ray diffraction and analysis of their crystal packing. Structural features and 2D polar layers are explained in terms of the robustness of C–H···O

synthons. The frequent recurrence of mirror plane symmetry in these structure is explained through *ab initio* calculations.

Chapter 4 discusses the studies carried on a series of *meta*-substituted phenyl pyrimidinones. The preference for 2D polar layer arrangement observed in this series is explained through the shape of the aryl pyrimidinone molecule and the geometry of interactions between hydrogen bonding functional groups. A model is proposed to account for the recurrence of the 2D polar layer assembly in these crystal structures.

The crystal structure of three miscellaneous pyrimidinone derivatives, one neutral and two salts, are explained in Chapter 5. Their packing is explained in terms of weak C–H···O, C–H···N hydrogen bonds as well as ionic interactions.

Chapter 6 describes the design, analysis and properties of some unsymmetrical urea crystal structures. Self complementary functional groups in crystal engineering such as halo···nitro, ethynyl···nitro and *N,N*-dimethylamino···nitro that form one-dimensional hydrogen bonded structures are incorporated into the urea scaffold. The main idea that the strong hydrogen bonded urea α-network and the weak X···NO_2 interactions would orient in orthogonal directions is demonstrated successfully. Crystal structures directed by the NO_2···I and NO_2···H–C≡C– interactions are isostructural and contain the structure directing urea tapes while the less polarisable bromo, chloro and flouro derivatives form the urea···nitro hydrogen bond synthon. The $N(Me)_2$ derivative crystallizes in a centrosymmetric space group with a hydrogen bond network that is nearly identical with non-centrosymmetric iodo and ethynyl derivatives.

Salient crystallographic details of the crystal structures discussed in this thesis have been given in Chapter 7. A full list of atomic coordinates is available upon request from Prof. Ashwini Nangia, University of Hyderabad (ansc@uohyd.ernet.in).

Hyderabad
April 2004

Sumod George

CONTENTS

CHAPTER FIVE

C–H···O AND C–H···N HYDROGEN BONDING IN SOME DIVERSE *N*-ARYLPYRIMIDINONE DERIVATIVES

CHAPTER SIX

CRYSTAL ENGINEERING OF SOME UNSYMMETRICAL UREAS

CHAPTER ONE

CRYSTAL ENGINEERING AND SUPRAMOLECULAR CHEMISTRY

1.1 Introduction

One of the goals of modern day chemistry is the construction of larger and larger molecular assemblies. In the area of covalent chemistry these large structures are the numerous synthetic targets being followed in laboratories around the world.[1] Many of these molecules are complex natural products with vital biological activity. To quote from the book Classics in Total Synthesis by K.C. Nicolaou[2] "*Construction of Nature's molecules in the laboratory from atoms and/or simple molecules, a process known as total synthesis, is one of the most demanding human practices*". From the synthesis of strychinine[3] in 1950's, modern organic synthesis has flourished in the last fifty years. The successful total synthesis of complex natural products like palytoxin,[4] taxol[5] and brevetoxin B,[6] to name a few, illustrates the mastery of chemists in the construction of covalent bonds. However these triumphs have come at a great price. Even when total synthesis is performed in a convergent manner, the multistep routes are not only time consuming but also expensive in terms of materials required and persons employed. As the need for larger and larger structures for mesoscale assembly and materials science grows, the feasibility of utilizing the covalent bond to act as the glue that holds the molecular pieces together becomes very difficult. This realization has prompted chemists to seek other strategies for the construction of extended structures and this leads to the chemistry of noncovalent synthesis, namely supramolecular chemistry. Supramolecular chemistry is defined as "*chemistry beyond the molecule*" by Lehn.[7] In the same manner that molecular chemistry deals with atomic assemblies, held together by covalent bonds, supramolecular organic chemistry is about the chemistry of molecular assemblies that are held together by noncovalent intermolecular bonds.[8] A through knowledge of the

molecular recognition process[9] permits the design of small, relatively simple building blocks which have the information inbuilt to self assemble into a larger structure (Figure 1). This idea is illustrated from the elegant work of Fraser Stoddart.[10] The dicarboxylic acid **1,** which possesses a π-excessive hydroquinone ring, can thread through the macrocyclic cavity of the π-deficient tetra cationic cyclophane **2** stabilized by aryl-aryl interaction to form a psuedorotaxane molecule $[\mathbf{1.2}]^{4+}$. The psuedorotaxane $[\mathbf{1.2}]^{4+}$ thus formed further self assemble to supramolecular arrays through carboxylic acid dimer O–H···O hydrogen bonds and then into macroscopic conglomerate through van der Waals and extended π-π stacking interaction. Figure 1 shows all aspects of supramolecular hierarchy in action.

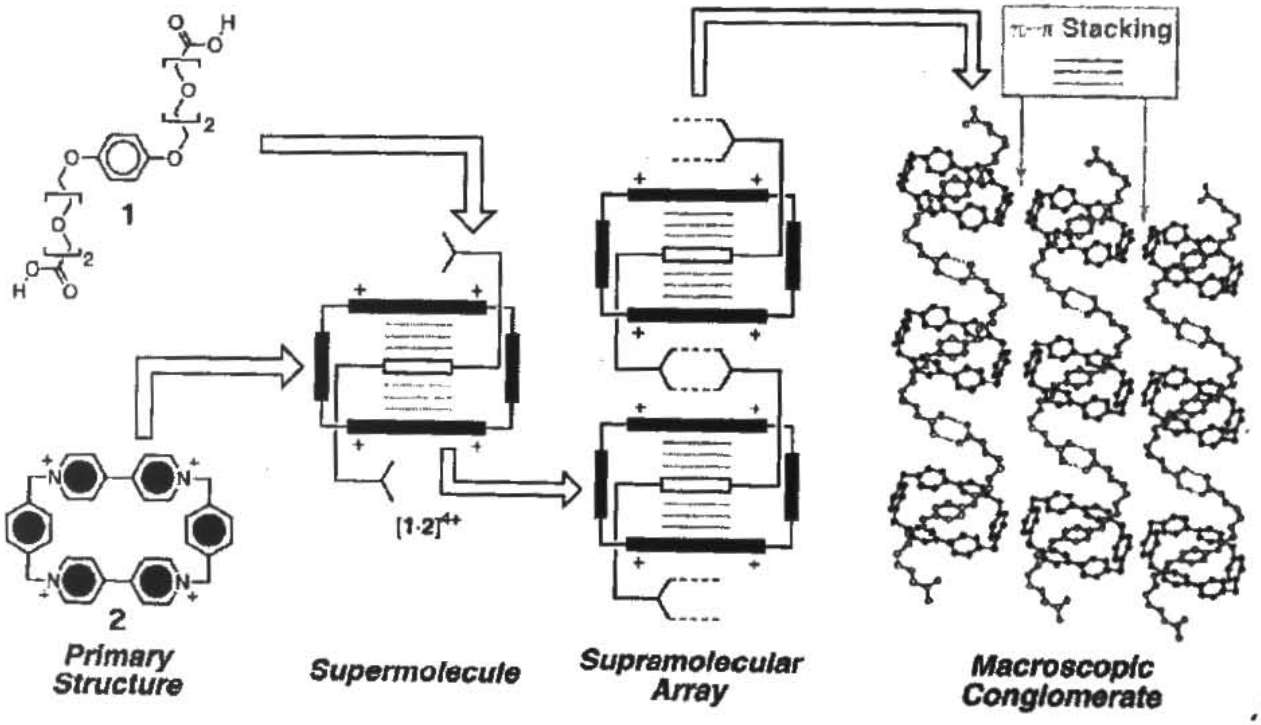

Figure 1. Supramolecular hierarchy illustrated using the $[\mathbf{1.2}]^{4+}$complex. Simple building blocks have information inbuilt to self assemble into a large structure.

The emergence of supramolecular chemistry has done much to initiate a paradigm shift over the past two decades where concepts like molecular recognition and self assembly[11] are transferred from biological processes into chemical

nanosystems through the medium of synthesis. Non covalent interactions have been used by materials scientists to make (synthesize) artificial cells and supramolecular chemists have assembled catenanes and rotaxanes.[11,12] Perhaps the highest levels of supramolecular sophistication is found in living systems, consisting of elegant supramolecular assemblies of organic biomolecules.[13] There are three main branches of supramolecular chemistry: one in which hydrogen bonding plays a key role,[14] another in which weaker noncovalent interactions, such as stacking of aromatic rings,[15] are the main forces, and a third in which coordination of ligands to metal ions is the central idea.[16]

1.2 Crystal Engineering

Today "Crystal Engineering"[17] is viewed as supramolecular chemistry in the solid state *i.e.* the construction of crystalline materials from molecules or ions using non-covalent interactions. The word "Crystal Engineering" was first introduced by a physicist named Pepinsky[18] at the meeting of American Physical Society held in Mexico City in August 1955 in an abstract entitled "*Crystal Engineering: a new concept in crystallography*". This idea was elaborated by Schmidt during the period 1950 to 1970 to address the issue of crystal packing in the context of organic solid state photochemical reactions of cinnamic acids and amides.[19] A more general definition of crystal engineering was given by Desiraju[20] in 1989 as *"the understanding of intermolecular interactions in the context of crystal packing and in the utilization of such understanding in the design of new solids with desired physical and chemical properties"*. An important goal in this area is to synthesize solids with specific and tunable properties. One can design materials that have nonlinear optical,[21] magnetic[22] or catalytic properties.[23] In order to obtain nonlinear optical materials molecules or ions must be organized in a non-centrosymmetric arrangement, for magnetic materials they must be positioned so that communication

between spins is facilitated, and for chemical separations the materials must be able to house trapped molecules or ions. In other words, to build useful materials, we must be able to control how the building block molecules or ions can be assembled into architecture with desirable structures. The development of organic solid state chemistry required a proper theory of crystal packing.[19] With the discovery of the remarkable electromagnetic rays called X-rays by William Conrad Röntgen in 1895 and later Max Theoder von Laue's discovery that X-rays are diffracted from crystals, solid state chemists have taken the advantage of this accurate structure determination technique. Crystal structures are mediated by intermolecular interactions and the most reliable method of obtaining reliable information on these interactions is through crystallography. With the increasing number of accurate X-ray crystal structures that are being reported because of CCD (charged coupled device) 2D area detector technology, structural chemists started looking for organic crystals that can act as catalysts, microporous materials, frequency doublers and also applications in areas such as molecular modelling and drug design.[24] The realization that a crystal is *supermolecule par excellence*, with atoms and covalent bonds being replaced by molecules and intermolecular interactions further added recognition to crystal engineering as the supramolecular equivalent of organic synthesis and brought it to the main stream of chemical sciences.[25]

1.3 Intermolecular Interactions and Supramolecular Synthons

Intermolecular interactions are primarily responsible for the formation and crystallization of supermolecules in the solid state. They are present between atoms that are not directly bonded or linked by a conjugated framework.[26] The development of crystal engineering relies on advancing understanding of the factors that control the packing of molecules in the solid state. Fundamental to such an approach is the rationalization of intermolecular interactions by elucidating the criteria, which control

the dominance of one type of interaction over another. It is well known that almost all the intermolecular forces, except van der Waals interactions, are of electrostatic origin. From a crystal engineering view point they are classified according to the their distance dependence and directionality. Intermolecular interactions are divided into two classes: isotropic, medium-range forces and anisotropic long-range forces. Isotropic forces define the shape of the individual molecules, size and close packing. These forces include C···C, C···H and H···H interactions. Isotropic forces include van der Waals forces, which act between all atoms and molecules. These can be repulsive or attractive depending on the distance between the interacting non-bonded atoms and are responsible for the gross packing arrangements. Although these forces are individually weak they become quite significant when considered together. Anisotropic interactions on the other hand include interactions among N, O, S, Cl, Br, I or between any of these elements and carbon or hydrogen. Ionic forces are extremely long range in nature. Such interactions are found between metal ions and oxygen or nitrogen or halogen atoms and are quite specific.

It was Corey[27] (1967) who introduced the term synthon to simplify the synthesis of complex natural products and other molecules. Recognizing that crystal engineering is the solid state equivalent of supramolecular synthesis, Desiraju[28] defined supramolecular synthons as *structural units within supermolecules which can be formed and/or assembled by known or conceivable synthetic operations involving intermolecular interactions*. Supramolecular synthons play the same focusing role in supramolecular synthesis that conventional synthons do in molecular synthesis. Supramolecular synthons are the smallest structural unit that contain crystallization information. Therefore the goal of crystal engineering is to identify synthons that are robust enough to be exchanged from one crystal structure to another, which ensures generality and predictability. The advantage of using the synthon approach is that it

offers a simplification in the understanding of crystal structures. Some common synthons as well as those that will appear in this thesis are shown in scheme 1.

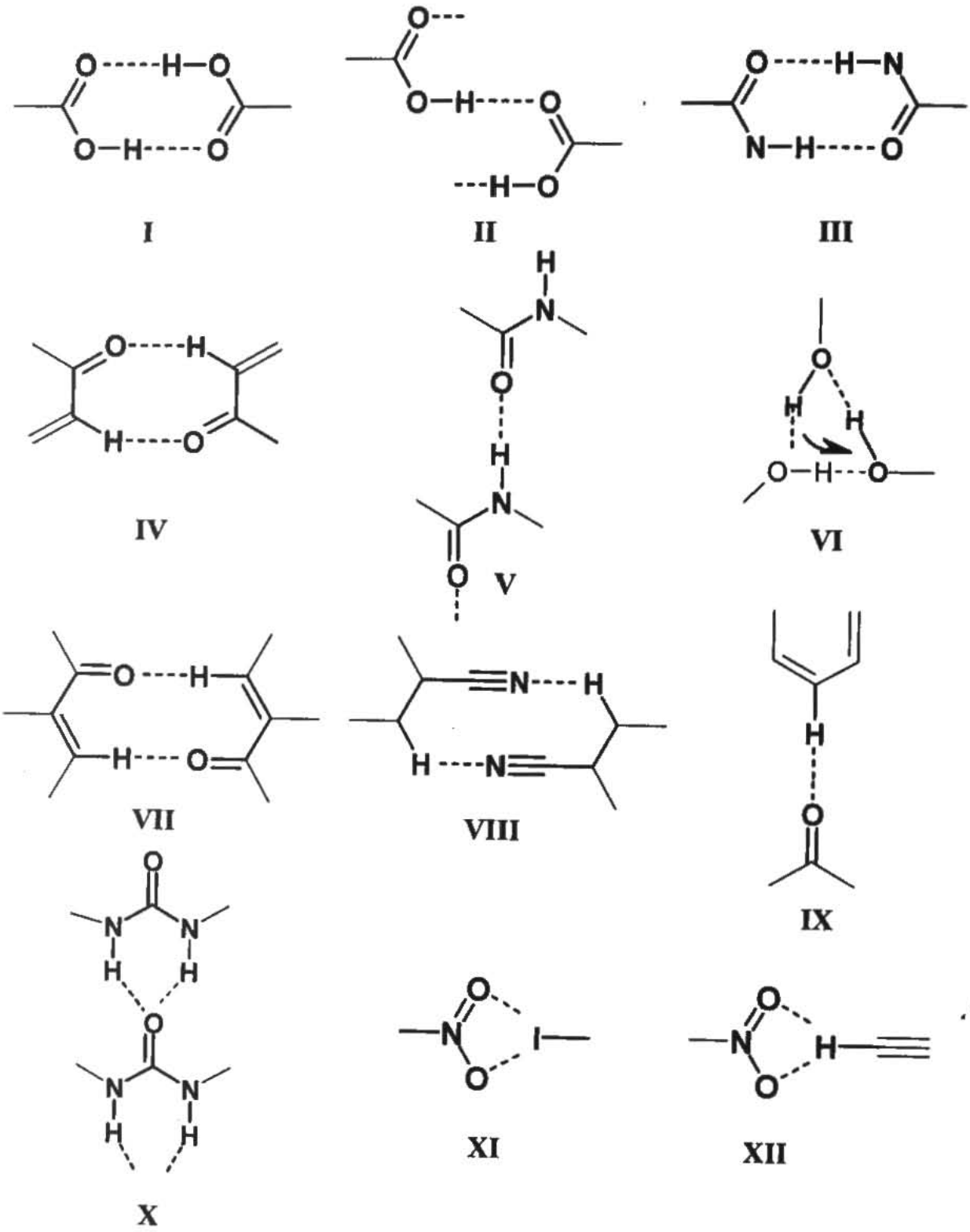

Scheme 1. Examples of some common supramolecular synthons (**I-VIII**). Synthons **IX-XII** will appear in this thesis.

1.4 Constructing Structures using Hydrogen Bonds

Hydrogen bond is the most recognized and well studied noncovalent interaction due to its frequent occurence in organic solids and biological molecules. Hydrogen bonding combines strength (a prerequisite for stability) with directionality (a prerequisite for reproducibility). Etter,[29] Leiserowitz and Schimdt,[30] Jeffrey and Saenger,[31] Desiraju[32] and Taylor and Kennard[33] have carried out extensive studies of solid-state structures of organic compounds in the last two decades. Hydrogen bonds are formed when a donor with an available acidic hydrogen atom is bought into contact with an acceptor carrying available non-bonding lone pairs of electrons. The hydrogen bond, primarily electrostatic in nature, has possibly been quoted most often as the architect in design strategies in crystal engineering. The directional and selective behaviour of hydrogen bonding makes it ideal for the construction and stabilization of large noncovalently linked molecular architectures. Many theoretical[34] approaches to understanding the nature of hydrogen bond have been advanced but none are completely satisfactory in explaining all of the properties of the hydrogen bond. A hydrogen bond is a summation of several contributions, where the importance of each contribution depends on the precise nature of the systems involved. The prediction of hydrogen bonding patterns has traditionally been based on conventional strong intermolecular interactions such as O–H···O and N–H···O. However for a complete understanding of the criteria, which determine the molecular packing, subtle effects such as size, shape and the role of weak intermolecular interactions should be taken into account.

Hydrogen bond networks control molecular architectures in the solid state. Hydrogen bonds were used as design element in solid-state organic chemistry.[29b] Hydrogen bonds direct the co-crystallization of diarylureas[35] and acyclic imides.[36] Whitesides and coworkers[37] have exploited the strong multiply hydrogen bonded lattice formed between cyanuric acid and melamine to construct large nanometer

scale structures. Hexagonal network structures of cyanuric acid · melamine (**CA · M**), thiocyanuric acid · melamine (**TCA · M**) are shown in figure 2.[38] Crystal structure determination showed that both these structures have similar features except that N–H···O hydrogen bonds in (a) are replaced by N–H···S hydrogen bonds in (b). Stoddart and Philp[11,39] explain how self-assembly idea in natural systems can be used in unnatural systems.

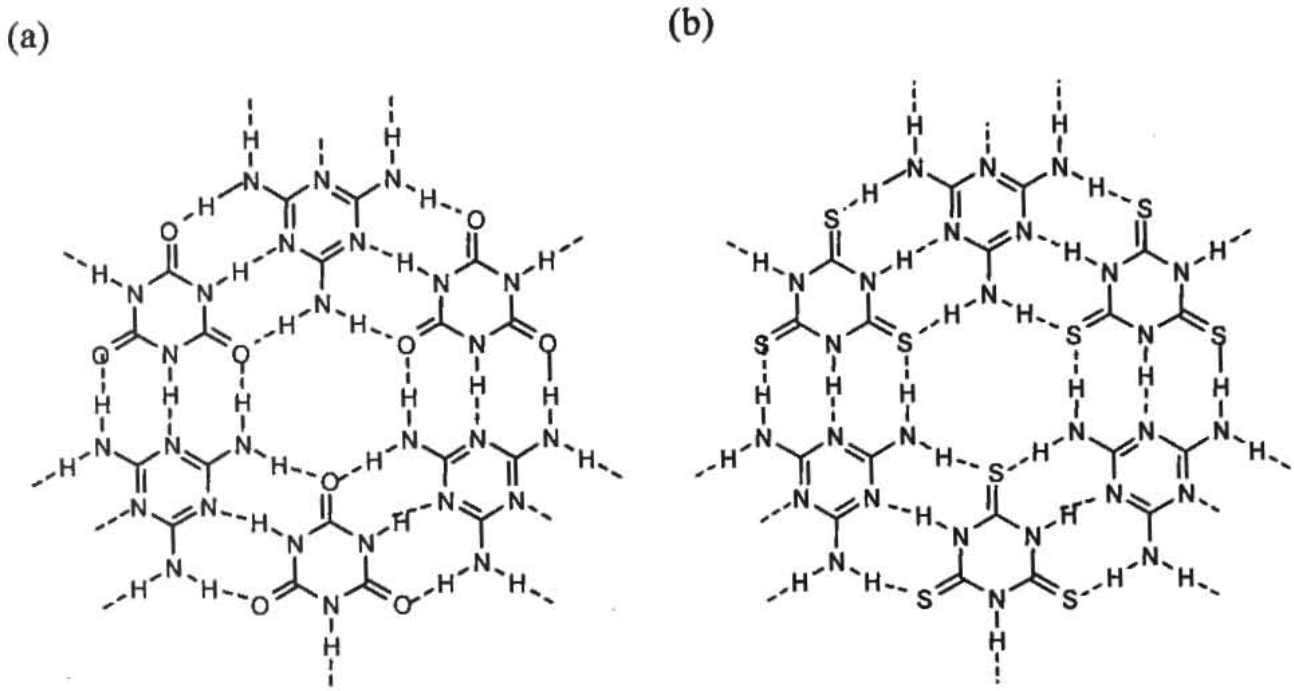

Figure 2. The stable hexagonal lattice formed between (a) cyanuric acid and melamine (**CA · M**) (b) thiocyanuric acid and melamine (**TCA · M**). Structures dominated by strong and weak hydrogen bonds.

Forces that can be categorized as weakly directional interactions include C–H···O and C–H···N hydrogen bonds,[40] C–H···π,[41] Hal···Hal interactions.[42] C–H···O and C–H···N hydrogen bonds are important in a wide variety of chemical and biological systems.[43] Many of their characteristics are like that of the strong O–H···O and N–H···O hydrogen bonds.[44] They are electrostatic in nature and have long-range distance character (Table 1). The effects of weaker hydrogen bonds on the crystal

structure are very subtle and therefore rationalization of their importance is a challenge. Analysis and comparison of crystal structures is possible using supramolecular synthons,[28] graph sets[45] and networks.[46] Recently Ohkita and coworkers[47] have synthesized the elusive graphyne network using weak C–H···N hydrogen bonding interaction shown in figure 3. Here the weak C–H···N hydrogen bond plays a directing role in determining the crystal structure. Molecular assemblies stabilized by C–H···O and C–H···N hydrogen bonds are illustrated in Chapter 2, 3 and 4.

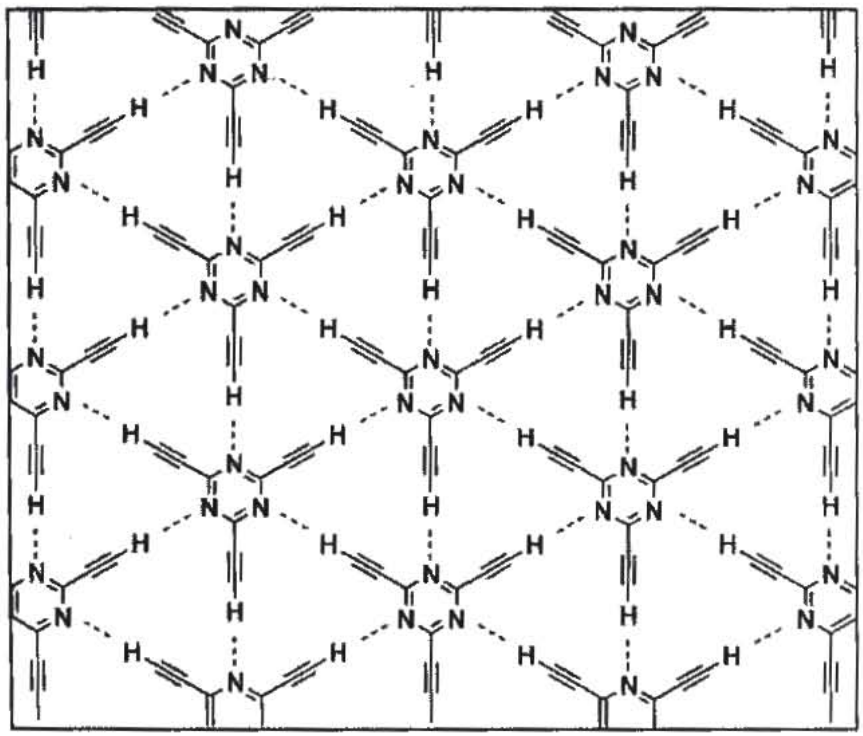

Figure 3. The two-dimensional hexagonal network structure formed by 2,4,6-triethynyl-1,3,5-triazine,[47] a structure dominated by weak hydrogen bonds. Note the similarity with the structure in figure 2 which is an indication that weak hydrogen bonds are also capable of forming robust and symmetric patterns.

Table 1. Some properties of strong and weak hydrogen bonds.

	Very Strong	Strong	Weak
Bond energy (–kcal/mol)	15-40	4–15	<4
Examples	$[F–H\cdots F]^-$ $[N–H\cdots N]^+$ [P–OH···O=P	O–H···O=C N–H···O=C O–H···O–H	C–H···O C–H···N O–H···π
IR ν_s relative shift	>25%	5–25%	< 5%
Lengthening of X–H (Å)	0.05–0.2	0.01–0.05	≤ 0.01
D(X···A) range (Å)	2.2–2.5	2.5–3.2	3.0–4.0
d(H···A) range (Å)	1.2–1.5	1.5–2.2	2.0–3.0
θ(X–H···A) range (°)	175-180	130–180	90–180
Effect on crystal packing	Strong	Distinctive	Variable
Utility in Crystal Engineering	Unknown	Useful	Partly useful
Electrostatics	Significant	Dominant	Moderate

1.5 Crystal Engineering of Organic Salts

Organic salts have been studied in crystal engineering for understanding their hydrogen bonding patterns and designing structural patterns.[48] Due to their high thermal and mechanical stability, crystallinity and less volatility organic salts are preferred compared to their neutral counterparts. Generally, various intermolecular forces, weak and strong, such as van der Waals interactions, dipole-dipole interactions and hydrogen bonding, stabilize organic crystals. In general, a molecule with large hyperpolarisability (β) has a larger dipole moment (μ), which leads to stronger dipole-dipole interactions between the molecules. However the large μ results in anti-parallel centrosymmetric packing. Developing solids with noncentrosymmetric structures is important because they are associated with useful physical properties. In salts, columbic interactions could override the dipolar

interactions that provide a strong driving force for centrosymmetric crystallization in neutral compounds. The use of ionic compounds further improves the chance of achieving a noncentrosymmetric crystal structure because, in addition to the rationale described above, the counter ions separate and screen the dipolar chromophores from one another, thus reducing the undesirable dipole-dipole interactions (Figure 4). It is of note that one of the strategies in crystal engineering is to dissect and insulate different types of intermolecular interactions from one another. Due to the above reasons and ease of synthesis many groups have shown the potential of organic salts in fields such as non linear optics.[49]

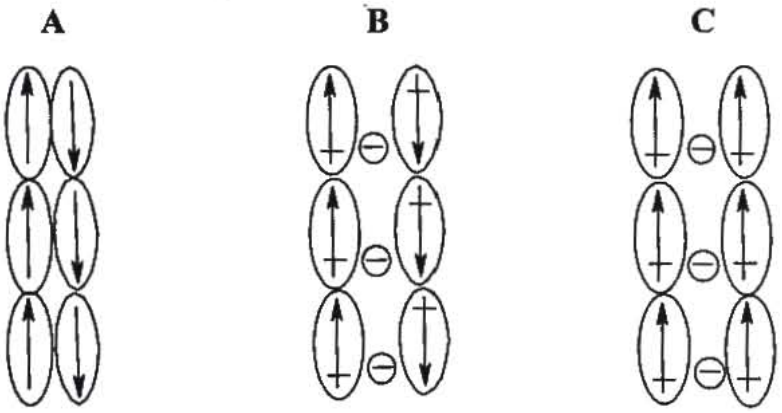

Figure 4. Anti parallel arrangement of molecular dipoles typical for a covalent compound (A), antiparallel arrangement of molecular dipoles for a salt (B), and parallel arrangement of molecular dipoles for a salt (C).

One advantage of using salts is that the counter ions can be varied easily and this makes this approach a highly successful one to engineer a variety of crystalline materials. Salts can give rise to good efficient physical properties when combined with the correct counter ion. Nakanishi's group[50] has used 4-amino-1-methylpyridinium benzene sulfonate salts with different substituents of hydroxy, methoxy, methyl, chloro or bromo group at *para* position and obtained colourless crystals. These salts were found to crystallize in noncentrosymmetric structures and

many of them were found to have useful physical properties like second harmonic generation (SHG). Uosaki *et. al.*[51] have studied a series of noncentrosymmetric cocrystals prepared from 2-amino-5-nitropyridine and achiral benzenesulfonic acids. These were found to be colourless with high melting point and hyperpolarisability. In general, the large β values of ionic species are due to strong electron acceptor and electron donor characteristics of the cation and anion parts respectively. Therefore many ionic π-conjugated compounds are highly polarized when a proper substituent is introduced at the opposite end of π-conjugated system to the ion part. This polarity can be used as a design element in crystal engineering.

Masse *et. al.* have reported tetra(4-methoxyphenyl)phosphonium iodide salt $C_{28}H_{28}O_4PI$ (MOPPI), a crystal built with quasi octupolar tetrahedral chromophores having quadratic nonlinear optical properties which shows that organic salts are as flexible as many other building blocks in crystal engineering.[52]

Recently Klinowski and coworkers[53] have reported the structural characterisation of a novel salt formed by the hydrothermal reaction between trimesic acid and 1,2-bis(4-pyridyl)ethane in the presence of cadmium(II) ions. It was found that trimesic acid anion forms sheets with the bipyridinium cations and solvent molecules occupy the interlayer spaces (Figure 5). The layers are stabilized by weak and strong hydrogen bonds.

Ward *et. al.*[54] have exploited properties of the unique two-dimensional hydrogen bonded sheets directed by hydrogen bonds between six guanidinium protons and the six lone pairs of the organosulfonate oxygen. The two dimensional layers when connected with aromatic pillars form a brick-like molecular architecture or a discrete double layer which can accommodate various guests. These observations demonstrate that crystal engineering can be simplified by selecting robust 2D-networks. Crystal engineering of some robust 2-pyrimidinone salt layers will be explained in Chapter 3.

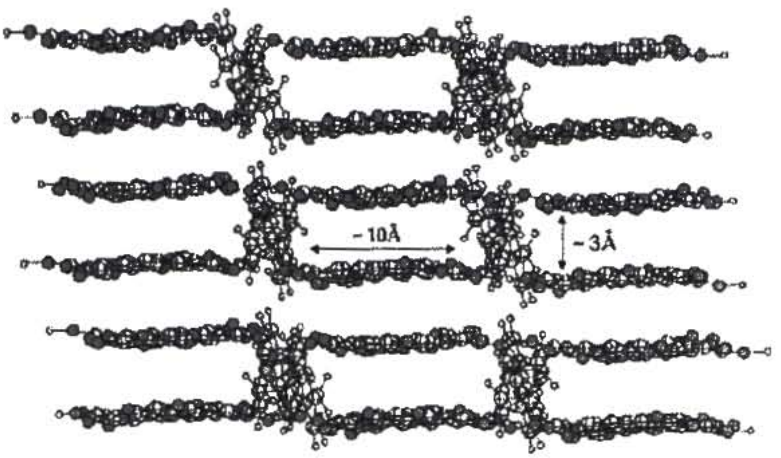

Figure 5. The layered structure formed by trimesic acid anion. The bipyridinium cations and solvent molecules occupy the interlayer spaces.

Figure 6 shows an example from Nangia's[55] group where even weak interactions, like C–H···O, when placed appropriately can lead to a target layered structure. The molecule 4,4-bis(4'-biphenylyl)cyclohexa-2,5 dienone **3** (Figure 6a) was designed with hydrogen bonding donor-acceptor groups in the quinone ring and the biphenyl groups oriented in the third dimension. The molecule assembled in a layer motif *via* C–H···O hydrogen bonded tape and the phenyl rings formed pillars in the open frame work which includes solvent guest molecules, as shown in figure 6c.

(a)

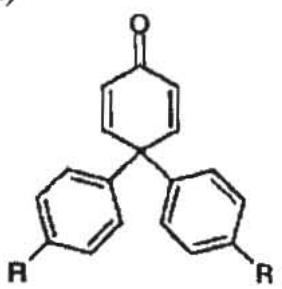

R = Ph

3

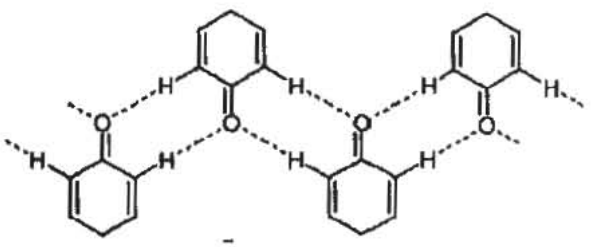

benzoquinone tape synthon

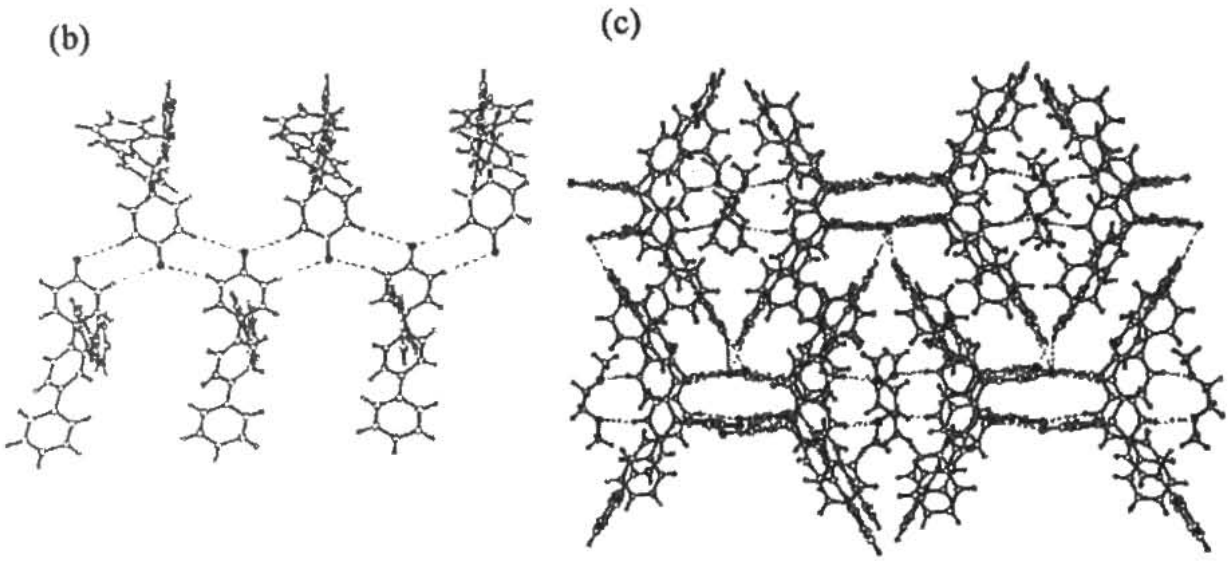

Figure 6. (a) 4,4-bis(4'-biphenylyl)cyclohexa-2,5-dienone **3** and the expected benzoquinone C–H···O tape. (b) C–H···O hydrogen bonded tape seen in the crystal structure viewed in the *bc*-plane. (c) The crystal structure viewed down the *c*-axis and the inclusion of 1,2-dimethoxyethane guest in the hydrophobic cavity. A network of C–H···O hydrogen bonds between the host-guest and host-host stabilize the structure.

1.6 Nonlinear Optics

The formation of crystal possessing a polar axis, a property shown by many organic and inorganic materials is one of the remarkable aspects of solid-state chemistry. Properties like nonlinear optics (NLO),[21,56] which are associated with polar materials are current targets in nanomaterials science. Materials with nonlinear optical property can be used in devices which process and store information efficiently. An important nonlinear effect is second harmonic generation (SHG), which is used for frequency doubling of infrared and other electromagnetic radiation. Early nonlinear optical materials were inorganic compounds such as lithium niobate ($LiNbO_3$) and potassium dihydrogen phospate (KDP). But slowly it was realized that organic materials have SHG efficiency that is greater by several orders in magnitudes, quick response time and structurally flexible due to variety of synthetic methods.

Several efficient quadratic NLO materials are based on one-dimensional charge transfer molecules, *e.g. p*-nitroaniline.

Design of NLO active materials is a challenge in crystal engineering. Absence of an inversion centre is the primary requirement for second order NLO effects. But due to high ground state dipole moment and the more efficient packing of molecules across the inversion centre most of the molecules tend to pack in centrosymmetric space groups. According to Kitaigorodskii,[57] molecules tend to undergo shape simplification, which results in dimers and then higher order aggregates to adopt close packing in solids. The most frequently occurring space group in crystallography $P2_1/c$ (36 %) has the inversion centre as a symmetry element. About 75 % of all organic compounds crystallize in centrosymmetric space group.[58] There are several methods adopted by various research group to over come this problem. Paul and Curtin[59] showed that certain crystal symmetries tend to be favoured by certain types of molecular structure, *e.g* by putting a substituent at the *ortho* or *meta* position of the aryl ring the tendency towards noncentrosymmetry can be increased. Scheme 2 shows some molecules which crystallize in noncentrosymmetric space group with nonlinear optical properties because an asymmetry was introduced in them. Several research groups have introduced hydrogen bonding groups to direct molecular alignment in the solid ensuring physical properties.[60] Hollingsworth[61] and Hulliger[62] have shown that channel-type inclusion compounds hold considerable promise in the design of solids that possess tunable bulk properties. Lin and coworkers[63] has illustrated that diamondoid networks have the potential to produce SHG activity along with high thermal stability. Another approach is to use octupolar[64] systems, which overcome many of the disadvantages with dipolar molecules, because they do not have a permanent dipole moment. Other strategies are incorporating molecular chirality[65] and use of coulombic interactions.[49]

Some strategies towards polar solid layers and some SHG active compounds obtained are described in Chapter 3, 4 and 6.

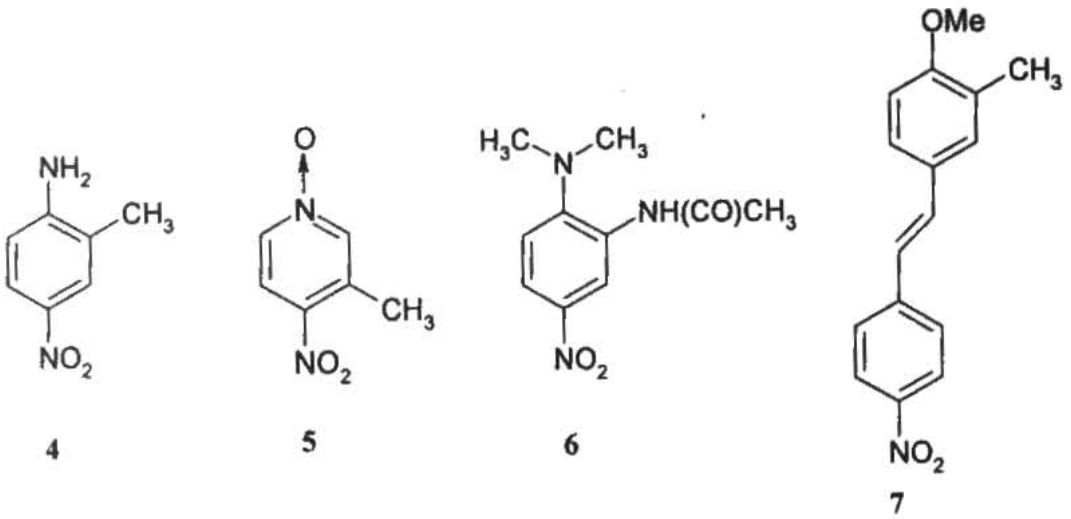

Scheme 2. Molecules **4-7** crystallizes in noncentrosymmetric space groups due to asymmetry in the molecule.

1.7 Isostructurality

The phenomenon of isomorphism is known for more than two centuries with the growth of potassium alum crystals from a saturated solution of ammonium alum. Kitaigorodskii was the first to review isostructurality behaviour in organic compounds.[57] Kàlmàn and coworkers[66] have reported pairs of isostructural cardenolides and bufadienolides. The C–H···O interaction in the crystal structure of 2-oxa-4-androstene-3,17-dione **8** was replaced by a C–O–H···O hydrogen bond in its isostructural 6α-hydroxy analogue **9**, is an example of isostructurality from our group (Figure 7).[67]

(a)

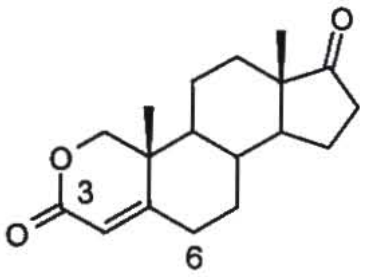
O
O
3
6

8

(b)

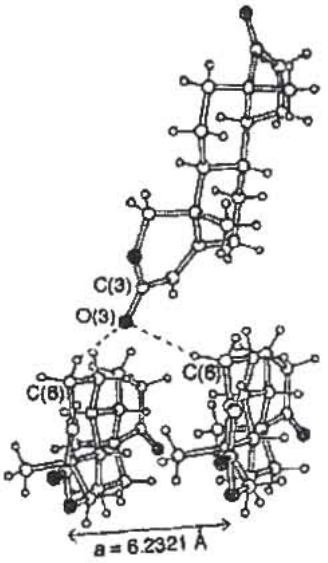
C(3)
O(3)
C(6)
C(8)
a = 6.2321 Å

(c)

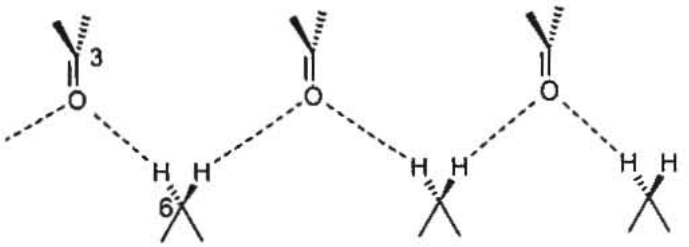
3
O
H
H
6
O
H
H
O
H
H

(a')

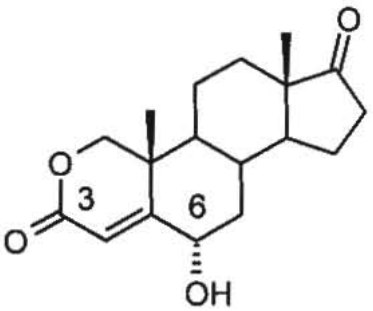
O
O
3
6
O
OH

9

(b')

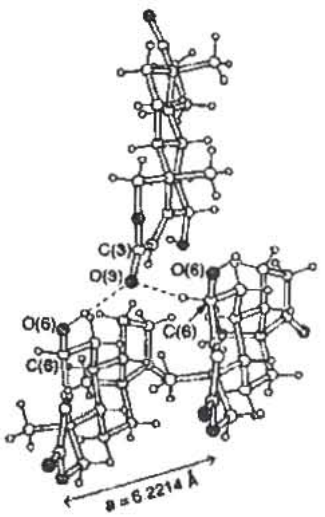
C(3)
O(3)
O(6)
O(6)
C(6)
C(6)
a = 6.2214 Å

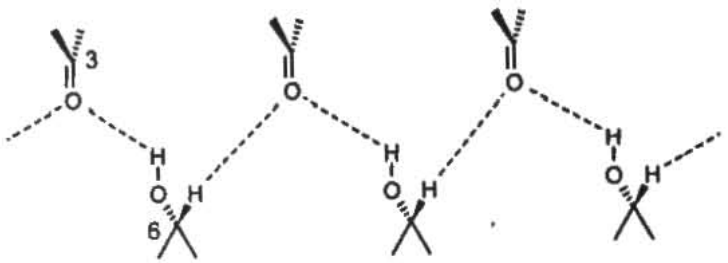

(c')

Figure 7 (a) 2-Oxa-4-androstene-3-17-dione **8** (b) its crystal structure and (c) the C–H···O synthon. (a') 6α-Hydroxy-2-oxa-4-androstene-3,17-dione **9**, (b') its crystal structure and (c') C–O–H···O synthon. Note the identity of *a*-axis and the similarity in hydrogen bonding and arrangement of molecule in both these structures. The C–O–H···O in (a') is replaced by C–H···O hydrogen bond in (a).

Kàlmàn[68] has suggested two parameters, which quantify the extent of isostructurality between two crystal structures. They are the unit cell similarity index (Π) and isostructurality index ($I_i(n)$).

$$\Pi = \left| \frac{a+b+c}{a'+b'+c'} \right| - 1 \cong 0$$

where a, b, c and a', b', c' are orthogonalized lattice parameters of the related structures. For a pair of completely isostructural crystals Π should be close to zero.

$$I_i(n) = \left[1 - \left(\frac{\sum_i \Delta R_i^2}{n} \right)^{1/2} \right] \times 100$$

The isostructurality index, ($I_i(n)$) is a measure of the degree of internal isostructurality where n is the number of distance differences (ΔR_i) between the absolute coordinates of identical non-hydrogen atoms within the same section of asymmetric units of related structures. $I_i(n)$ should be close to 100% for isostructural crystals. The concept of isostructurality is used in comparing crystal structures in Chapter 2, 3 and 6.

Controlling molecular assembly in one dimension is the first step in designing molecular solids.[69] Many of the strategies employed to control molecular aggregates in one dimension can be extended towards the design of two-dimensional aggregates. Urea functionality is found to be sufficiently reliable and persistent units that will self assemble into one dimensional α-network held together *via* two anti N–H protons of one molecule donating to the carbonyl oxygen atom of a neighbouring molecule to form bifurcated N–H···O hydrogen bonds.[70] Fowler and coworkers[71] have shown that two-dimensional networks can be designed by choosing molecules such as urylenedicarboxylic acids (Figure 8a) that will form two independent sets of one-dimensional self complementary hydrogen-bonded infinite chains oriented in orthogonal arrays. The urea portion of these molecule forms the α-network that is cross-linked by a second chain pattern formed between the carboxylic acid substituents. This approach has the advantage that the networks self-assemble to give predictable patterns. Urea scaffold was also used to control molecular aggregation even in the third dimension. Hollingsworth *et. al.*[72] have shown that the cocrystal formed between urea and α,ω-dinitrile molecules contain the same α-network formed by the two urea *anti* N–H protons. On the other hand, hydrogen bonds between the terminal cyano groups and the *syn*-N–H proton donors of urea molecules form a heteromeric chain as shown in the figure 8b. These $CN(CH_2)_nCN$/urea cocrystals offer the flexibility that orientation of adjacent urea chains can be controlled to give an antiparallel arrangement when n = 4 or a parallel arrangement when n = 3 or 5. When n exceeds 5 urea self assemble to form channel inclusion complexes.

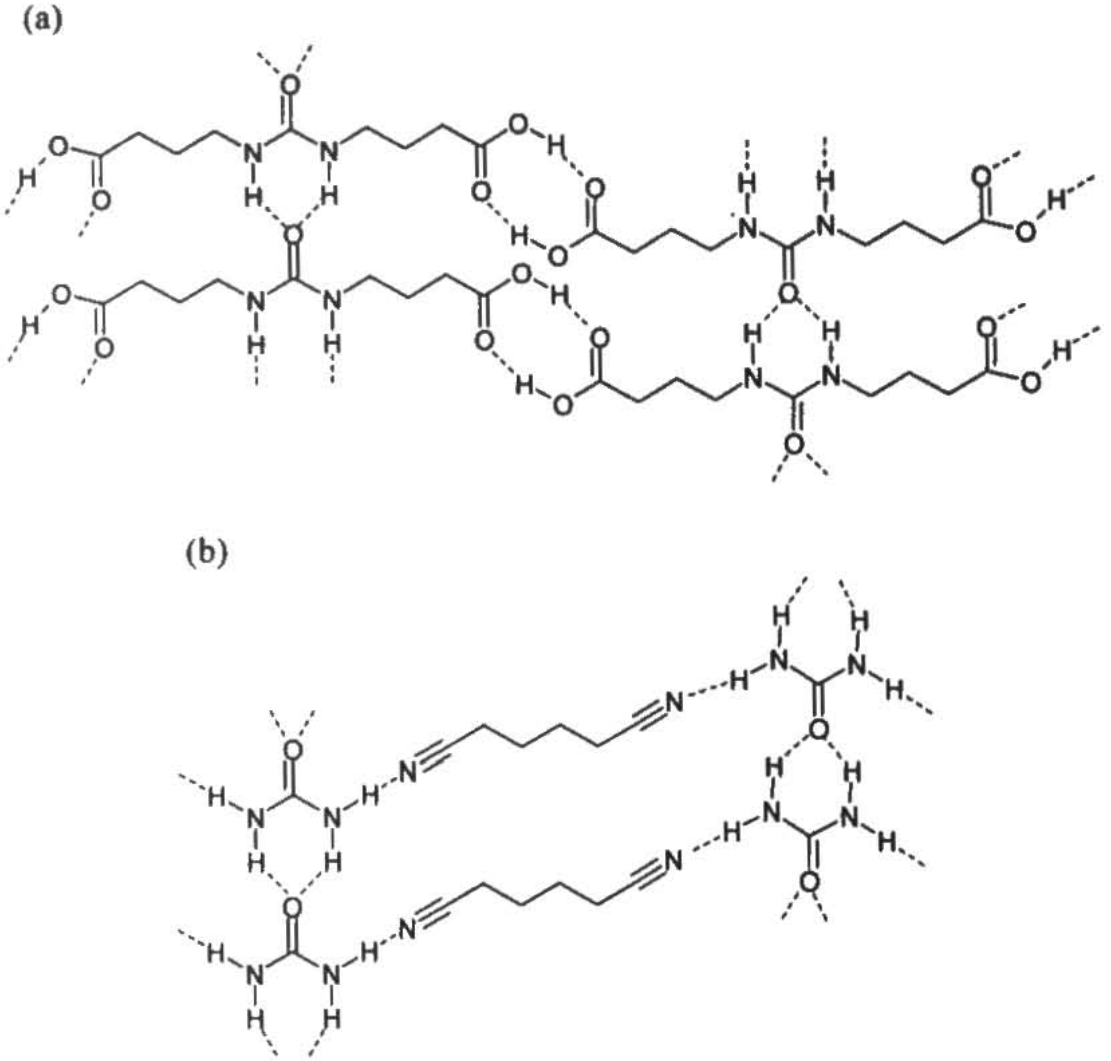

Figure 8. (a) Layered structure formed in urylenedicarboxylic acid formed by the two self-complementary functional groups. (b) Two dimensional layer in which urea forms a complex with the α,ω-dinitrile groups.

The topology of urea assembly has not only been used in small molecule self–assembly process but also in macrocyclic rigid systems. Urea scaffold was incorporated into the macrocyclic molecules, which further self-assembled into capsules[73] and nanotubes,[74] which can trap guest molecules of suitable size. Design of solid structures using urea and some common self-complementary functional group in crystal engineering will be shown in Chapter 6.

1.9 Crystal Engineering of Some 2-Pyrimidinones

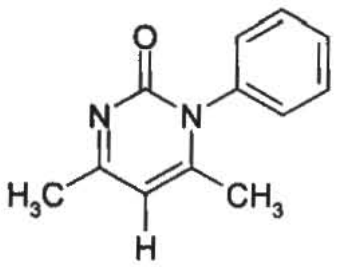

10

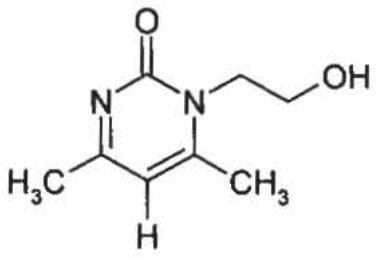

11

In the above background, the present thesis is presented. Pyrimidinone molecule **10** was used earlier in our lab as a precursor for making non-natural β-lactam analogues.[75] Pyrimidinones are synthesized by condensing acetyl acetone with urea molecule in a single step. This simplicity in making the molecule makes it flexible and valuable for structural studies. Molecules with different substituents can be synthesized and their packing modes in the crystal structures can be studied. We noted that a closely related molecule 1,2-dihydro-*N*-(2-hydroxyethyl)-4,6-dimethylpyrimidin-2-one **11** crystallizes in the chiral space group $P2_1$. Pyrimidinone derivatives are rich in C–H donors and have acceptors like oxygen, nitrogen, phenyl and crystallizes easily from common solvents like chloroform, methanol, ethyl acetate and their mixture with hexane. Since this molecule is having only C–H donors they can form weak C–H···O hydrogen bonds. Based on hydrogen bonding pattern and close packing arguments we expected that structures of pyrimidinone would self assemble similar to the α-network found in the crystal structures of urea molecule (Figure 9). The N–H···O hydrogen bond in urea would be replaced by C–H···O interactions in pyrimidinones. Such studies will highlight and reinforce the hydrogen bond mimicry idea observed in the steroid project in our group (Figure 7).

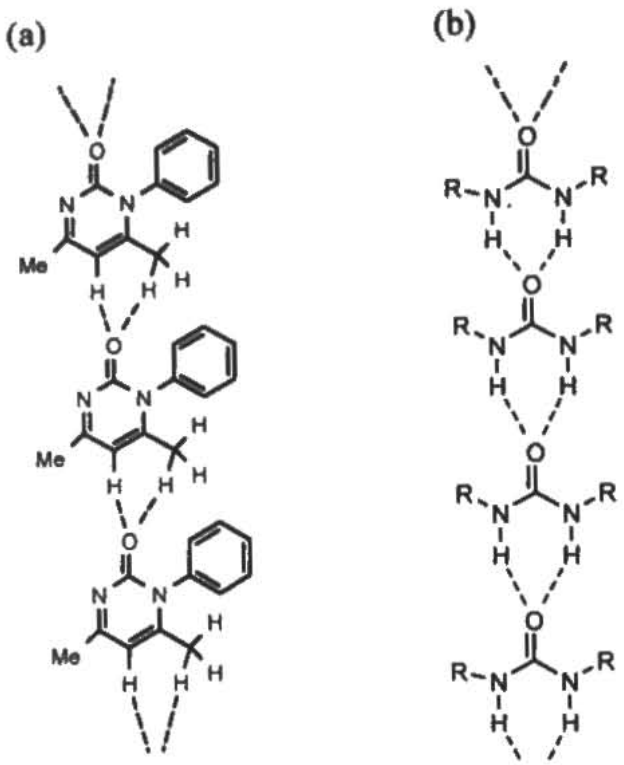

Figure 9. (a) The C–H···O hydrogen bonding pattern expected in pyrimidinone **10** molecule. (b) The α-network formed by N–H···O hydrogen bond seen in the crystal structure of urea. Comparison of both the structures show that pyrimidinones are masked ureas which would self assemble in the same manner using the weak hydrogen bonds.

During the course of this project Schmuck and Lex[76] have shown that the N–H···O hydrogen bond found in the discrete dimers of chloride salt of 5-amidopyridinium-pyrrole-2-carboxylate (Figure 10a) is isofunctionally replaced by the C–H···O bond in the chloride salt of 5-(guanidinocarbonyl)pyrrole-2-carboxylic acid (Figure 10b). The binding geometries were found to be very similar as shown in the Figure 10. The recurrence and consistent packing can be attained due to the limited number of donors and acceptors.

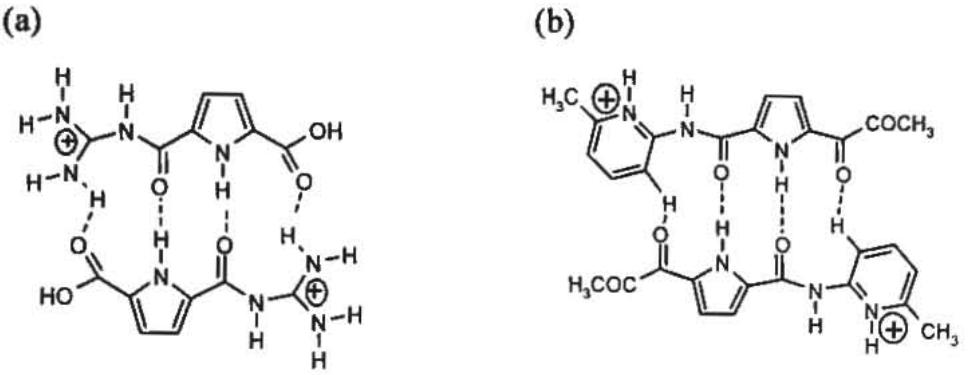

Figure 10. (a) Schematic representation of the dimer formed by the chloride salt of 5-(guanidinocarbonyl)pyrrole-2-carboxylic acid (b) chloride salt of 5-amidopyridinium-pyrrole-2-carboxylate. The chloride ion is not shown in the figure.

1.10 References

1. K.C. Nicolaou, D. Vourloumis, N. Wissinger and P.S. Baran, *Angew. Chem. Int. Ed.*, **2000**, *39*, 44.
2. K.C. Nicolaou and E.J. Sorenson, *Classics in Total Synthesis*, Wiley-VCH, Weinheim, **1996**.
3. R.B. Woodward, M.P. Cara, W.D. Ollis, A. Hunger, H.V. Daeniker and K. Schenker, *J. Am. Chem. Soc.*, **1954**, *76*, 4749.
4. E.M. Suh and Y. Kishi, *J. Am. Chem. Soc.*, **1994**, *116*, 11205.
5. K.C. Nicolaou, Z. Yang, J.J. Liu, H. Ueno, P.G. Nantermet, R.K. Guy, C.F. Claiborne, J. Renaud, E.A. Couladouros, K. Paulvannan and E.J. Sorenson, *Nature (London)*, **1994**, *367*, 630.
6. K.C. Nicolaou, E.A. Theodorakis, F.P.T.J. Rutjes, J. Tiebes, M. Sato, E. Unterseller and X.–Y. Xiao, *J. Am. Chem. Soc.*, **1995**, *117*, 1173.
7. J.-M. Lehn, *Supramolecular Chemistry*, VCH, Weinheim, **1995**.
8. J.-M. Lehn, *Angew. Chem., Int. Ed. Engl.*, **1990**, *27*, 89.

9. S.H. Gellman, (ed.) Special issue on molecular recognition, *Chem. Rev.*, **1997**, *97*, 1231-1713.
10. M. Asakawa, P.R. Ashton, G.R. Brown, W. Hayes, S. Menzer, J.F. Stoddart, A.J.P. White and D.J. Williams, *Adv. Mater.*, **1996**, *8*, 37.
11. D. Philp and J.F. Stoddart, *Angew. Chem., Int. Ed. Engl.*, **1996**, *35*, 1154.
12. A.R. Pease, J.O. Jeppesen, J.F. Stoddart, Y. Luo, C.P. Collier and J.R. Heath, *Acc. Chem. Res.*, **2001**, *34*, 433.
13. (a) R.E. Hubbard, *Encyclopedia of Life Science*, **2002**, Macmillian Publishers Ltd, p342. (b) L.M. Greig and D. Philp, *Chem. Soc. Rev.*, **2001**, *30*, 287. (b) J.S. Lindsey, *New J. Chem.*, **1991**, *15*, 153.
14. (a) J.C. MacDonald and G.M. Whitesides, *Chem. Rev.*, **1994**, *94*, 2383. (b) L.J. Prins, D.N. Reinhoudt and P. Timmerman, *Angew. Chem., Int. Ed.*, **2001**, *40*, 2382. (c) A. Casnati, F. Sansone and R. Ungaro, *Acc. Chem. Res.*, **2003**, *36*, 246.
15. (a) E.A. Meyers, R.K. Castellano, and F. Diedrich, *Angew. Chem., Int. Ed.*, **2003**, *42*, 1210. (b) W.B. Jennings, B.M. Farrell and J.F. Malone, *Acc. Chem. Res.*, **2001**, *34*, 885. (c) C.A. Hunter, K.R. Lauson, J. Perkins and C.J. Urch, *J. Chem. Soc., Perkin Trans 2.*, **2001**, *5*, 651.
16. (a) J.P. Sauvage, *Acc.Chem. Res.*, **1998**, *31*, 611. (b) M. Fujita, *Acc. Chem. Res.*, **1999**, *32*, 53. (c) D.L. Caulder and K.N. Raymond, *Acc. Chem. Res.*, **1999**, *32*, 975. (d) P.J. Stang, *Chem. Rev.*, **2000**, *100*, 853. (e) M.J. Zaworotko, *Chem. Commun.*, **2001**, 1. (f) B. Moulton and M.J. Zaworotko, *Chem. Rev.*, **2001**, *101*, 1629. (g) K. Biradha, *CrystEngComm*, **2003**, *5*, 374.
17. (a) R. Bishop, F. Toda and D.D. MacNicol (ed.) *Solid-State Supramolecular Chemistry: Crystal Engineering* Vol.6, in *Comprehensive Supramolecular Chemistry*, Pergamon, Chichester (UK), **1996**. (b) G.R. Desiraju, *Curr. Sci.*, **2001**, *81*, 1023. (c) D. Braga, G.R. Desiraju, J.S. Miller, A.G. Orpen and S.L.

Price, *CrystEngComm*, **2002**, *4*, 500. (d) A. Nangia, *CrystEngComm*, **2002**, *17*, 1. (e) C.B. Aakeroy, *Acta Cryst.*, **1997**, *B53*, 569. (f) D. Braga, *Chem. Commun.*, **2003**, 2751.

18. R. Pepinsky, *Phys. Rev.*, **1955**, *100*, 52.
19. G.M.J. Schmidt, *Pure Appl. Chem.*, **1971**, *27*, 647.
20. G.R. Desiraju, *Crystal Engineering: The Design of Organic Solids*, Elsevier: Amsterdam, **1989**.
21. J. Zyss and J.-F. Nicoud, *Curr. Opin. Solid State Mater. Sci.*, **1996**, *1*, 533.
22. O. Kahn, *Acc. Chem. Res.*, **2000**, *33*, 647.
23. Y. Aoyoma, *Topics Curr. Chem.*, **1998**, *198*, 131.
24. (a) M.D. Hollingsworth, *Science*, **2002**, *295*, 2410. (b) C.V.K. Sharma, *Cryst. Growth Des.*, **2002**, *2*, 465.
25. J.D. Dunitz, in *Perspectives in Supramolecular Chemistry*; (ed.) G.R. Desiraju, Wiley, NewYork, **1996**, Vol. 2.
26. P. Shuster, *Angew. Chem., Int. Ed. Engl.*, **1981**, *20*, 546.
27. E.J. Corey, *Pure Appl. Chem.*, **1967**, *14*, 19.
28. G.R. Desiraju, *Angew. Chem., Int. Ed. Engl.*, **1995**, *34*, 2311.
29. (a) M.C. Etter, *Acc. Chem. Res.*, **1990**, *23*, 120. (b) M.C. Etter, *J. Phys. Chem.*, **1991**, *95*, 4601.
30. (a) L. Leiserowitz, *Acta Cryst.*, *B32*, **1976**, 775. (b) L. Leiserowitz and G.M.J. Schimdt, *J. Chem. Soc.*, **1969**, 2372.
31. (a) G.A. Jeffery and W. Saenger, *Hydrogen Bonding in Biological Structure*, Springer, Berlin, **1991.** (b) G.A. Jeffery, *An Introduction to Hydrogen Bonding*, Oxford University Press, NewYork, **1997.**
32. (a) G.R. Desiraju, *Acc. Chem. Res.*, **1986**, *19*, 222. (b) G.R. Desiraju, *Acc. Chem. Res.*, **1990**, *24*, 290. (c) G.R. Desiraju, *Acc. Chem. Res.*, **1996**, *29*, 441. (d) G.R. Desiraju, *Acc. Chem. Res.*, **2002**, *35*, 565.

33. R. Taylor and O. Kennard, *Acc. Chem. Res.*, **1984**, *17*, 320.

34. (a) S. Scheiner, *Hydrogen Bonding: A Theoretical Perspective*, Topics in Physical Chemistry, Oxford University Press, New York.

35. M.C. Etter, Z. Urbanczyk-Lipkowska, M. Zia-Ebrahimi and T.W. Panunto, *J. Am. Chem. Soc.*, **1992**, *112*, 8415.

36. M.C. Etter and S.M. Reutzel, *J. Am. Chem. Soc.*, **1991**, *113*, 2586.

37. (a) C.T. Seto and G.M.Whitesides, *J. Am. Chem. Soc.*, **1990**, *112*, 6409. (b) C.T. Seto and G.M. Whitesides, *J. Am. Chem. Soc.*, **1991**, *113*, 712. (c) J.A. Zerkowski and G.M. Whitesides, *J. Am. Chem. Soc.*, **1994**, *116*, 4298. (d) J.C. Macdonald and G.M. Whitesides, *Chem. Rev.*, **1994**, *94*, 2383.

38. (a) A. Ranganathan, V.R. Pedireddi and C.N.R. Rao, *J. Am. Chem. Soc.*, **1999**, *121*, 1752.

39. (a) F.J. Stoddart and D. Philp, *Angew. Chem. Int. Ed. Engl.*, **1996**, *35*, 1154. (b) S.J. Cantrill, A.R. Pease and J.F. Stoddart, *J. Chem. Soc. Dalton Trans.*, **2000**, 3715.

40. R. Taylor and O. Kennard, *J. Am. Chem. Soc.*, **1982**, *104*, 5063.

41. M. Nishio, M. Hirota and Y. Umezawa, *The C–H/π Interaction*, Wiley, New York, **1988**.

42. (a) N. Ramasubbu, R. Parthasarathy and P. Murray-Rust, *J. Am. Chem. Soc.*, **1986**, *108*, 4308. (b) S.L. Price, A.J. Stone, J. Lucas, R.S. Rowland and A.E. Thornley, *J. Am. Chem. Soc.*, **1994**, *116*, 4910. (c) V. R. Vangala, A. Nangia and V.M. Lynch, *Chem. Commun.*, **2002**, 1304.

43. G.R. Desiraju and T. Stiener, *The Weak Hydrogen Bond in Structural Chemistry and Biology*, Oxford University Press, Oxford, UK, **1999.**

44. T. Steiner and G.R. Desiraju, *Chem. Commun.*, **1998**, 891.

45. (a) M.C. Etter, *Acc. Chem. Res.*, **1990**, *23*, 120. (b) M.C. Etter, J.C. MacDonald, J. Bernstein, *Acta Cryst.*, **1990**, B46, 256. (c) J. Bernstein, R.E.

Davis, L. Shimoni and C. Ning-Leh, *Angew. Chem. Int. Ed. Engl.*, **1995**, *34*, 1555.

46. S.R. Batten and R. Robson, *Angew. Chem. Int. Ed.*, **1998**, *37*, 1460.
47. M. Ohkita, M. Kawano, T. Suzuki and T. Tsuji, *Chem. Commun.*, **2002**, 3054.
48. (a) S.B. Raj, N. Stanley, P.T. Muthiah, G. Bocelli, R. Ollà and A. Cantoni, *Cryst. Growth Des.*, **2003**, *3*, 567. (b) N. Stanley, V. Sethuraman, P.T. Muthiah, P. Luger and M. Weber, *Cryst. Growth Des.*, **2002**, *2*, 631. (c) J.A. Kaduk, *Acta Cryst.*, **2000**, *B56*, 474. (d) S. Nagahama, K. Inoue, K. Sada, M. Miyata and A. Matsumoto, *Cryst. Growth Des.*, **2003**, *3*, 247. (e) M. Hernández-Molina, P.A. Lorenzo-Lewis, P. Gili and C. Ruiz-Pérez, *Cryst. Growth Des.*, **2003**, *3*, 273. (f) R.D. Willet, F. Awwadi, R. Butcher, S. Haddad and B. Twamley, *Cryst. Growth Des.*, **2003**, *3*, 301. (g) B.R. Bhogala and A. Nangia, *Cryst. Growth Des.*, **2003**, *3*, 547.
49. (a) D. Braga and F. Grepioni, *J. Chem. Soc., Dalton Trans.*, **1999**, 1. (b) C. Serbutoviez, J.-F. Nicoud, J. Fischer, I. Ledoux and J. Zyss, *Chem. Mater.*, **1990**, *6*, 1358. (c) T.W.S. Lee, S.J. Rettig, R. Stewart and J. Trotter, *Can. J. Chem.*, **1984**, *62*, 1194. (d) R. Masse, J.-F. Nicoud, M. Bagieu-Beucher and C. Bourgogne, *Chem. Phy.*, **1999**, *245*, 365. (e) R. Masse, M. Bagieu-Beucher, J. Pecaut, J.-P. Levy and J. Zyss, *Nonlinear Optics*, **1993**, *5*, 413. (f) C.C. Evans, M. Bagieu-Beucher, R. Masse and J.-F. Nicoud, *Chem. Mater.*, **1998**, *10*, 847. (g) V.A. Russell, M.C. Etter and M.D. Ward, *Chem. Mater.*, **1994**, *6*, 1206. (h) S.R. Marder, J.W. Perry and W.P. Schaefer, *Science*, 1989, *245*, 626. (i) S.R. Marder, J.W. Perry, C.P. Yakymyshyn, *Chem. Mater.*, **1994**, *6*, 1137. (j) S.R. Marder, J.W. Perry, B. Tiemann, R.E. Marsh and W.P. Schaefer, *Chem. Mater.*, 1990, *2*, 685. (k) F. Pan, M.S. Wong, V. Gramlich, C. Bosshard and P. Gunter, *Chem. Commun.*, **1996**, 1557. (l) G.R. Meridith in

Nonlinear Optical Properties of Organic and Polymeric Materials, Vol. 233. (ed.) D.J. Williams, Washington DC **1983**, p27.

50. Anwar, S. Okada, H. Oikawa and H. Nakanishi, *Chem. Mater.*, **2000**, *12*, 1162.
51. H. Koshima, M. Hamada, I. Yagi and K. Uosaki, *Cryst. Growth Des.*, **2001**, *1*, 467.
52. C. Bourgogne, Y.L. Fur, P. Juen, P. Masson, J.-F. Nicoud and R. Masse, *Chem. Mater.*, **2000**, *12*, 1025.
53. F.A. Almeida, A.D. Bond, Y.Z. Khimyak and J. Klinowski, *New J. Chem.*, **2002**, *26*, 381.
54. (a) K.T. Holman, A.M. Privovar, J.A. Swift and M.D. Ward, *Acc. Chem. Res.*, **2001**, *34*, 107. (b) A.M. Privovar, K.T. Holman and M.D. Ward, *Chem. Mater.*, **2001**, *13*, 3018. (c) K.T. Holman, S.M. Martin, D.P. Parker and M.D. Ward, *J. Am. Chem. Soc.*, **2001**, *123*, 4421.
55. V.S.S. Kumar and A. Nangia, *Chem. Commun.*, **2001**, 2392.
56. D.S. Chemla and J. Zyss, (eds.) *Nonlinear Optical Properties of Organic Molecules and Crystals*, Academic Press, Orlando, FL, USA, **1987**, vol. **1** and **2.**
57. A.I. Kitaigorodskii, *Molecular Crystals and Molecules*, Academic Press, New York, **1973**.
58. (a) J.W. Yao, J.C. Cole, E. Pidcock, F.H. Allen, J.A.K. Howard and W.D.S. Motherwell, *Acta Cryst.*, **2002**, *B58*, 640. (b) L.N. Kuleshova and M.Y. Antipin, *Russ. Chem. Rev.*, **1999**, *68*, 1. (c) A.J.C. Wilson, *Acta Cryst.*, **1993**, *A49*, 210. (d) A.D. Mighell, V.L. Himes, *Acta Cryst.*, **1983**, *A39*, 737. (e) J. Donohue, *Acta Cryst.*, **1985**, *A41*, 203. (f) N. Padmaja, S. Ramakumar and M.A. Viswamitra, *Acta Cryst.*, **1990**, *A46*, 725.
59. I.C. Paul and D.Y. Curtin, *Chem. Rev.*, **1981**, *81*, 525.

60. (a) T. Tsunekawa, T. Gotoh and M. Iwamoto, *Chem. Phys. Lett.*, **1990**, *166*, 353. (b) W. Tam, B. Guerin, J.C. Calabrese and S.H. Stevenson, *Chem. Phys. Lett.*, **1989**, *154*, 93.

61. M.D. Hollingsworth, U. Werner-Zwanzinger, M.E. Brown, J.D. Chaney, J.C. Huffman, K.D.M. Harris and S.P.J. Smart, *J. Am. Chem. Soc.*, **1999**, *121*, 9732.

62. J. Hulliger, P. Rogin, A. Quintel, P. Rechsteiner, O. König, and M. Wübbenhorst, *Adv. Mater.*, **1997**, *9*, 662.

63. (a) O.R. Evans, R.-G. Xiong, Z. Wang, G.K. Wong and W. Lin, *Angew. Chem. Int. Ed.*, **1999**, *38*, 536. (b) O.R. Ewans and W. Lin, *Chem. Mater.*, **2001**, *13*, 2705. (c) W. Lin, L. Ma and O.R. Evans, *Chem. Commun.*, **2000**, 2263. (d) O.R. Evans and W. Lin, *Acc. Chem. Res.*, **2002**, *35*, 511.

64. (a) J. Zyss and I. Ledoux, *Chem. Rev.*, **1994**, *94*, 77. (b) C. Dhenaut, I. Ledoux, I.D.W. Samuel, J. Zyss, M. Bourgault and H.L. Bozec, *Nature* (London), **1995**, *374*, 339. (c) V.R. Thalladi, S. Brasselet, H.-C. Weiss, D. Bläser, A.K. Katz, H.L. Carrell, R. Boese, J. Zyss, A. Nangia and G.R. Desiraju, *J. Am. Chem. Soc.*, **1998**, *120*, 2563. (d) B.R. Chow, S.J. Lee, S.H. Lee, K.H. Son, Y.H. Kim, J.-Y. Doo, G.J. Lee, T.I. Kang, Y.K. Lee, M. Cho and S.-J. Jeon, *Chem. Mater.*, **2001**, *13*, 1438. (e) G. Alcaraz, L. Euzenat, O. Mongin, C. Katan, I. Ledoux, J. Zyss, M. Blanchard-Desce and M. Vaultier, *Chem. Commun.*, **2003**, 2766.

65. (a) J. Zyss, J.-F. Nicoud and M. Coquillay, *J. Chem. Phys.*, **1984**, *81*, 4160. (b) T. Ueniya, N. Uenishi, Y. Shimizu, T. Yoneyama and K. Nakatsu, *Mol. Cryst. Liq. Cryst.*, **1990**, *182A*, 51. (c) T. Konda, N. Ogasawara, R. Ito, K. Whida, T. Tanase, T. Murata and M. Hidai, *Acta Cryst.*, **1988**, *44*, 102.

66. (a) A. Kálmán and L. Pàrkànyi, *Adv. Mol. Struct. Res.*, **1997**, *3*, 189. (b) A. Kálmán, L. Fábián, G. Argay, G. Bernáth and Z. Gyarmati, *Acta Cryst.*, **2002**,

B58, 855. (c) L. Fábián, A. Kálmán, G. Argay, G. Bernáth and Z. Gyarmati, *Acta. Cryst.*, **2002**, *B58*, 710.

67. (a) A. Anthony, M. Jáskolski and A. Nangia and G.R. Desiraju, *Chem. Commun.*, **1998**, 2537. (b) A. Anthony, M. Jaskolski and A. Nangia, *Acta Cryst.*, **2000**, *B56*, 512.
68. A. Kálmán, L. Párkányi and G. Argay, *Acta Cryst.*, **1993**, *B49*, 1039.
69. C.N.R. Rao, S. Natarajan, A. Choudhury, S. Neeraj and A.A. Ayi, *Acc. Chem. Res.*, **2001**, *34*, 80.
70. (a) S. George and A. Nangia, *Acta Cryst.*, **2003**, *E59*, o901. (b) S. George, A. Nangia and V.M. Lynch, *Acta Cryst.*, **2001**, *C57*, 777. (c) J. Jai-Nhuknan, A.G. Karipides, J.M. Hughes and J.S. Cantrell, *Acta Cryst.*, **1997**, *C53*, 455. (d) W. Dannecker, J. Kopf and H. Rust, *Cryst. Struct. Commun.*, **1979**, *8*, 429.
71. X. Zhao, Y.-L. Chang, F.W. Fowler and J.W. Lauher, *J. Am. Chem. Soc.*, **1990**, *112*, 6627.
72. (a) M.D. Hollingsworth, B.D. Santarsiero, H. Oumar-Mahamat and C.J. Nicholas, *Chem. Mater.*, **1991**, *3*, 23. (b) M.D. Hollingsworth, M.E. Brown, B.D. Santarsiero, J.C. Huffman and C.C. Goss, *Chem. Mater.*, **1994**, *6*, 1227.
73. J. Rebek, Jr. *Chem Commun.*, **2000**, 637.
74. L.S. Shimizu, A.D. Hughes, M.K. Smith, M.J. Davis, B.P. Zhang, L.Z. Hans-Conrad and K.D. Shimizu, *J. Am. Chem. Soc.*, **2003**, *125*, 14972. (b) L.S. Shimizu, M.K. Smith, A.D. Hughes and K.D. Shimizu, *Chem. Commun.*, **2001**, 1592.
75. (a) P.S. Chandrakala, A.K. Katz, H.L. Carrell, P.R. Sailaja, A.R. Podile, A. Nangia and G.R. Desiraju, *J. Chem. Soc., Perkin Trans 1*, **1998**, 2597. (b) A. Nangia and P.S. Chandrakala, *Tetrahedron. Lett.*, **1995**, *36*, 7771.

76. C. Schumak and J. Lex, *Eur. J. Org. Chem.*, **2001**, 1519.

CHAPTER TWO

C–H···O AND C–H···N HYDROGEN BOND SYNTHONS IN *N*-ARYLPYRIMIDINONES

2.1 Introduction

Organic molecular materials often possess interesting electronic properties, including nonlinear optical behaviour, electrical conductivity, superconductivity and ferromagnetism.[1] Current materials research relies mainly on building blocks (molecules) that are assembled into organized structures with desired properties and function. The relationship between molecular structure and supramolecular structure is yet to be understood completely and so the study of structural control at a molecular level is very important. Control of molecular orientation in supramolecular structure is difficult and is recognized as a major challenge in materials design.[2] Crystal engineering[2,3] is about directing the structure of solids through intermolecular interactions between molecules in the solid state. Control over crystal packing results in control over the properties of the resulting solids. The goal in crystal engineering is to recognize and design a recurring pattern that has transferability and reproducibility, preferably across families of structures. Such robust patterns have been termed *supramolecular synthons*[4] and the molecular building block are *tectons*.[5] The synthon approach is useful in that it offers a simplification in our understanding of crystal structures. A major difficulty in crystal engineering is the fact that the interactions which control crystal structures are numerous and weak. While in some structures it is possible to identify a particular synthon that directs self-assembly such an analysis is difficult in other structures. Closely related molecules may form widely different crystal structures and conversely very different molecules may form similar crystal structures.[6] The concept of isostructurality in steroids mentioned in Chapter 1 is an example of the latter situation. A consideration of strong O–H···O, O–H···N, N–H···N and weak C–H···O, C–H···N and C–H···π interactions[7] in crystal packing is one way

to address this problem. In general the understanding of intermolecular interactions constitutes the most important step in the control of molecular and ionic organization in solid state.

The rational design and synthesis of molecular crystals with controlled dimensionality is essential for developing molecular based materials for a variety of applications.[8] 1,2-Dihydro-*N*-aryl-4,6-dimethylpyrimidin-2-one **1** was the molecule of interest in this project. Pyrimidinones will be numbered serially from this Chapter onwards starting with 1,2-Dihydro-*N*-aryl-4,6-dimethylpyrimidin-2-one as **1**. This will continue to Chapter 6. Sakamoto and coworkers[9] reported during the writing of this thesis that racemic pyrimidinones with ortho substituted phenyl groups can be resolved by crystallization without any external chiral source to get chiral conglomerates. They have also shown that the resulting optically active isomer can be converted to other heterocycles with high enantioselectivity through synthetic reactions. The present study deals with optimizing derivatives of **1** to construct solid-state architecture *via* weak hydrogen bonds. These molecules were considered from the viewpoint of new molecules for nonlinear optics because organic molecules have fast response time and high molecular hyperpolarisability (β).[10] But the main challenge is to pack the molecules non-centrosymmetrically in the crystal. The solid state properties like SHG activity could be manipulated by the careful choice of substituents on the phenyl ring. Design of solid-state architectures through self assembly of predictable motifs directed by weak hydrogen bonding is worth mentioning, particularly in the synthesis of crystals for second harmonic generation (SHG).[11] Recently it was shown that 4-(4-ethynylphenyl)ethynylpyridine[11b] utilizes C–H···N hydrogen bonds to form linear chains that further assemble into a polar crystal in space group *Fdd*2 (Figure 1). The aim in utilizing weak interactions for self-assembly was to avoid antiparallel arrangement of large dipole moments arising from strong hydrogen bonding groups.[12]

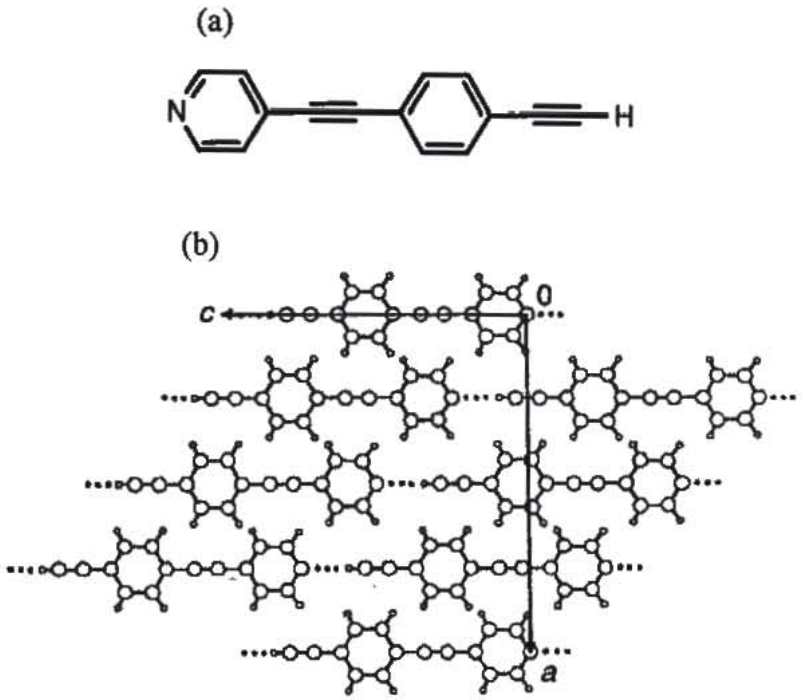

Figure 1. (a) 4-(4-ethynylphenyl)ethynylpyridine. (b) Packing arrangement in the crystal structure. Dotted lines represents C–H···N hydrogen bonds which play a role in constructing a polar crystal for useful properties in the bulk structure.[11b]

It is also important to note that the SHG signal is maximized when the molecular dipoles are oriented in a particular direction relative to the optic axis of the crystal and this value is 54.74° for point group *mm*2.[13] For example it was found that in the crystal structure of *N*-(4-nitrophenyl)-(L)-prolinol (NPP),[14] a material designed using the chirality concept, the molecular dipole is aligned within 4° of the optically ideal value of 54.7°, this value being specific to the particular space group ($P2_1$) (Figure 2). The presence of chiral handle ensures a noncentrosymmetric space group but not necessarily a high SHG efficiency.

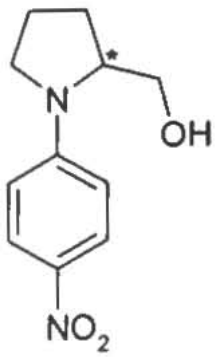

(a)

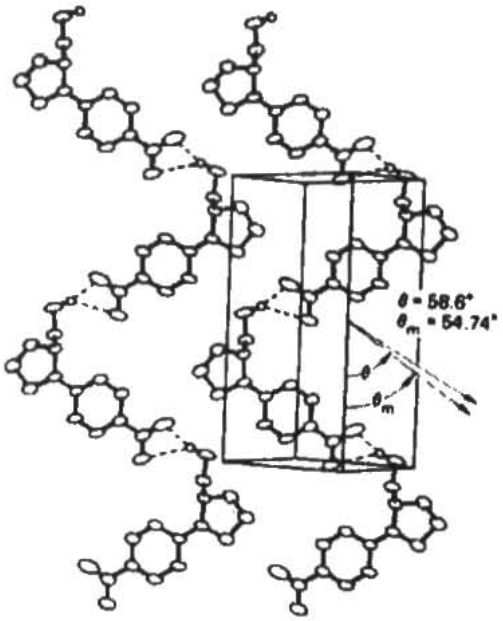

(b)

Figure 2. (a) *N*-(4-nitrophenyl)-(L)-prolinol, NPP. (b) Crystal structure of NPP. Note the angle made by the molecular dipole with the polar axis.[14]

This chapter describes the X-ray crystal structures of the initial set of 2-pyrimidinones studied. Their hydrogen bonding patterns, the alignment of the chromophore in the crystal structure and the implications of these findings for materials design are presented. The three pyrimidinone crystal structures contains the same supramolecular synthon (Figure 3), a chain of C–H···O hydrogen bond from the activated sp^2 C–H donor to the carbonyl O acceptor.

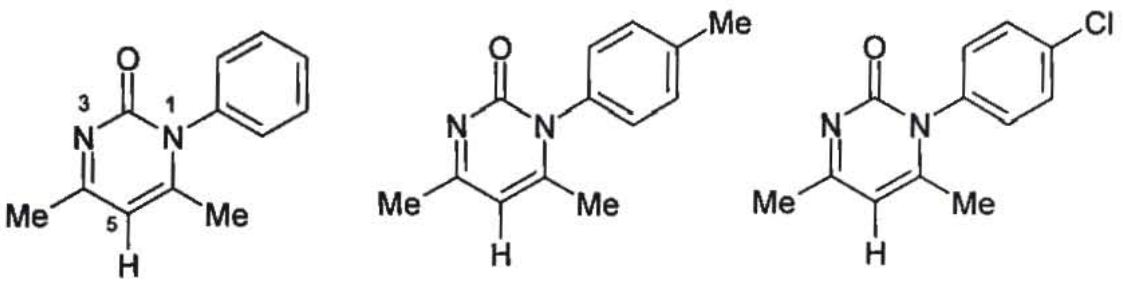

1 **2** **3**

Scheme 1. Pyrimidinone molecules discussed in this Chapter.

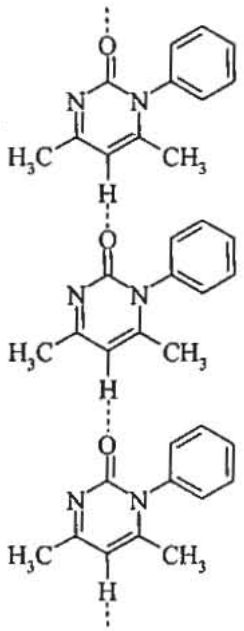

Figure 3. The linear C–H···O synthon seen in the three crystal structures **1-3.** Note the similarity with the linear C–H···N chain shown in figure 1.

2.2 Results and Discussion

The synthesis of *N*-aryl pyrimidinones **1-3** was carried out by the condensation of the corresponding *N*-aryl urea with acetyl acetone in the presence of an acid catalyst.[15] The three compounds were characterized by their satisfactory IR and NMR spectra. The compounds were crystallized from chloroform/*n*-hexane to

afford single crystals suitable for X-ray diffraction: Crystals were pale yellow for **1**, pale red for **2**, and pink for **3**. Some important interatomic distances and hydrogen bonds are summarized in Table 1.

2.3 Crystal Structure of 1,2-Dihydro-*N*–phenyl-4,6-dimethylpyrimidin-2-one, 1

Phenyl pyrimidinone **1** crystallizes in the orthorhombic space group *Pbcm* with half molecule in the asymmetric unit. The heterocyclic ring lies in the mirror plane and the *N*-phenyl ring is bisected by it (Figure 4a). Analysis of the crystal structure shows that there are infinite linear chains of C–H···O (2.11 Å, 171.5°, interaction *i*) (Table 1) hydrogen bonded molecules along the *a*-axis from the C5-H donor to the carbonyl acceptor, which connects translation-related molecules. This hydrogen bonded chain along the *a*-axis is connected to *b*-glide related neighbouring molecule by a zigzag chain of C–H···N hydrogen bond (2.42 Å, 168.5°, interaction *j*) from the *p*-phenyl H–atom to the N3 acceptor. Thus, a two-dimensional C–H···O/N hydrogen bonded planar layer parallel to the *ab*-plane containing pyrimidinone rings is produced with the *N*-phenyl rings arranged orthogonal to it. The planarity of the layers could be due to the linear hydrogen bonds within the two dimensional layers. Adjacent layers are offset such that the phenyl ring of one molecule approaches the pyrimidinone heterocycle of the next layer in an edge-to-face manner (C–H···O, 2.51 Å, 123.6°, interaction *k*) (Figure 4b). The weak hydrogen bonds formed from the activated donor hydrogen (phenyl and sp^2 C–H) and the basic acceptor (carbonyl O–atom) direct self-assembly in the crystal structure. The molecule is C–H donor rich because of methyl groups. Therefore the O–atom behaves as a trifurcated acceptor when the weak C–H···O interaction from the methyl donor (2.82 Å, 149.5°, not shown in Figure 4b) is also considered. The short C–H···O hydrogen bond (interaction *i*) is used to self associate the molecules in one-dimensional chains,

whereas the other weak hydrogen bonds complete the three dimensional hydrogen bonded structure. Since all the available good donors and acceptors in the molecule[16] are already used in the formation of the C–H···O chains any other interactions between the chains and layers are weak van der Waals interactions. The metrics of the hydrogen bonds are given in Table 1.

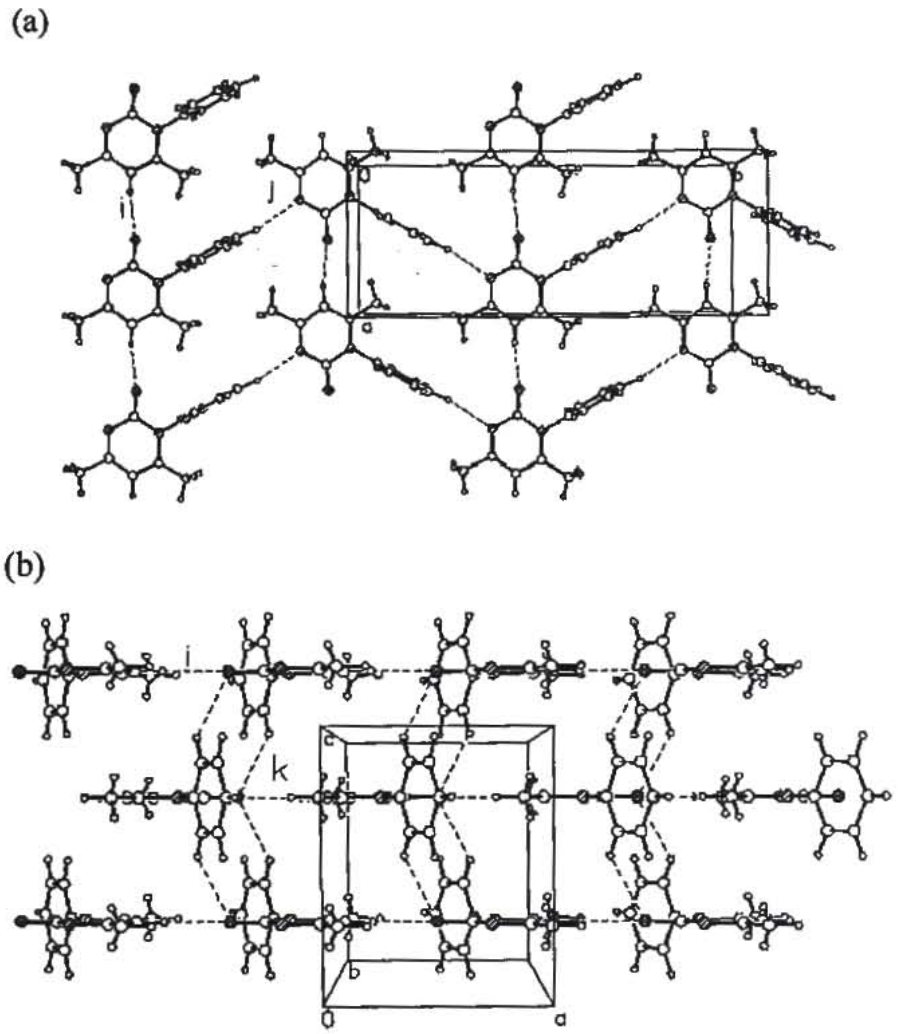

Figure 4. Crystal structure of phenyl pyrimidinone **1**. (a) View of the *ab*-layer to show the C–H···O and C–H···N hydrogen bond chains (interactions *i* and *j*). Notice that the molecules in adjacent chains run antiparallel along the *a*-axis. (b) View of interlayer interaction down the *b*-axis.

Table 1. Geometrical parameters of selected intermolecular interaction.

Pyrimidinone	Interaction	*d* (Å)	*D* (Å)	*θ* (°)
1	C(5)–H···O (*i*)	2.11	3.118(8)	171.5
	C(*p*-Ph)–H···N (*j*)	2.42	3.497(8)	168.5
	C(*o*-Ph)–H···O (*k*)	2.51	3.247(8)	123.6
	C(*m*-Ph)–H···O	2.84	3.413(9)	112.7
	C(*m*-Ph)–H···N	2.93	3.775(8)	134.4
	C(6-Ph)–H···O	2.82	3.801(9)	149.5
2	C(5)–H···O (*i*)	2.22	3.306(8)	173.9
	C(*o*-Ph)–H···O (*k*)	2.48	3.226(8)	125.0
	C(*m*-Ph)–H···O	2.73	3.319(8)	113.7
	C(*m*-Ph)–H···N	2.83	3.732(9)	140.2
3	C(5)–H···O (*i*)	2.26	3.445(7)	178.4
	C(*o*-Ph)–H···O (*k*)	2.45	3.171(8)	122.2
	C(*m*-Ph)–H···O	2.72	3.291(8)	112.5
	C(*m*-Ph)–H···N	2.77	3.657(7)	138.8

Note. All the C–H bonds are neutron-normalised to 1.083 Å

2.4 Crystal Structure of 1,2-Dihydro-*N*-tolyl-4,6-dimethylpyrimidin-2-one, 2

Tolyl derivative **2** crystallizes in the orthorhombic space group *Pnma* and here too the heterocyclic ring lies in the mirror plane while the tolyl ring is bisected by it. Translation related molecules are connected by a linear chain of C–H···O hydrogen bonds (2.22 Å, 173.9°, interaction *i*) along [100] (Figure 5a). Adjacent chains related by *a*-glide symmetry pack parallel to each other to produce a 2D polar layer. Layers of molecules are arranged parallel to the *a*-axis hence the *ac*-plane has a two dimensional polar layer structure. Such parallel layers are connected through C–H···O hydrogen bond interaction from the *o*-and *m*-phenyl H–atoms to the carbonyl O–atoms (2.48 Å, 125° interaction *k*; 2.73 Å, 113.7°, not indicated in the Figure) (Figure 5b).

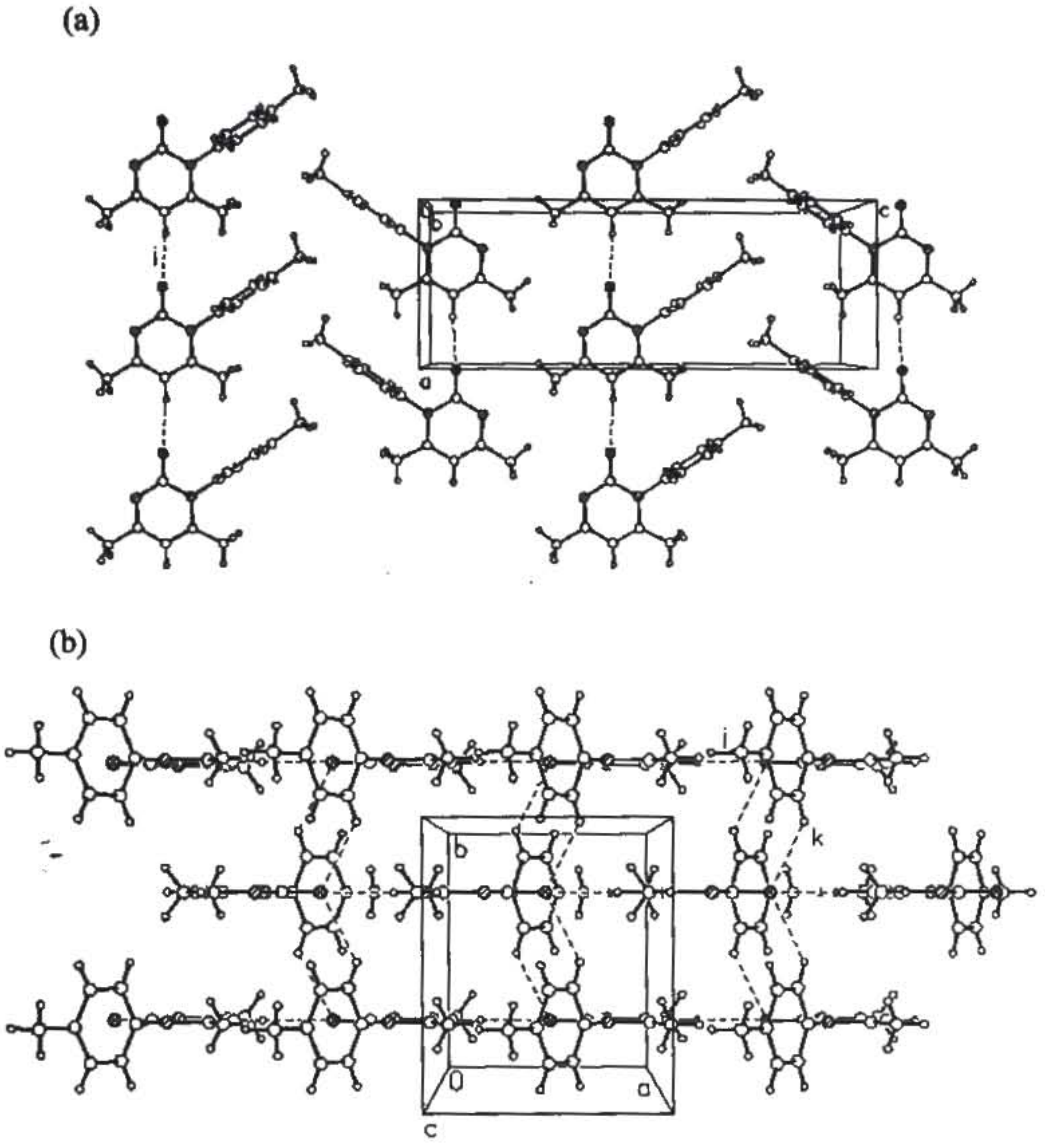

Figure 5. Crystal structure of tolyl pyrimidinone **2**. (a) View of the *ac*-layer to show the C–H···O chain (interaction *i*) and the T-shaped approach of the tolyl methyl group to the phenyl ring centroid (CH_3···π 3.78 Å). Notice the parallel arrangement of molecules along the *a*-axis. (b) Inter layer packing viewed down the *c*-axis.

The layers stack anti parallel in the third dimension and the overall structure is centrosymmetric. There are two types of methyl groups in the tolyl derivative **2**: the

C4– and C6– methyl groups in the pyrimidinone ring are close packed with van der Waals interaction while the tolyl methyl groups points toward the phenyl π-cloud centroid of an adjacent molecule (C···π 3.78 Å, interaction *j*). This latter approach geometry is suitable for electrostatic stabilization of the C–H dipole by the negatively charged surface of the phenyl ring, that is C(δ-)–H(δ+)···π(δ-). It is difficult to say whether this interaction represents a C–H···π hydrogen bond[7] for two reasons: (i) the interaction is very weak and soft, (ii) the exact location of methyl H atoms cannot be determined accurately by the X-ray diffraction. Nevertheless the role of C–H···π interactions in determining the structure and physical properties has been reported.[18a]

2.5 Crystal Structure of 1,2-Dihydro-*N*-(4-chlorophenyl)-4,6-dimethylpyrimidin-2-one, 3

To better understand the structural role of the tolyl methyl group in **2** the crystal structure of the chloro analogue **3** was analysed. The compound crystallizes in the orthorhombic space group *Pnma* with half molecule in the asymmetric unit. Translation related molecules are connected through C–H···O hydrogen bond to form a one-dimensional infinite chain along the *a*-axis. The chloro group on the phenyl ring points towards the phenyl π cloud of a molecule in the adjacent chain and thus the chains are connected through zigzag C–Cl···π (centroid) interaction (3.54 Å, 177.5°, interaction *j*) to form a 2D polar layer (Figure 6a). Adjacent layers are inversion related hence the overall packing is centrosymmetric. Inter layer region is dominated by weak C–H···O hydrogen bonds. The packing analysis of the chloro derivative **3** shows that it is having remarkable similarities with that of the tolyl derivative **2**.[17]

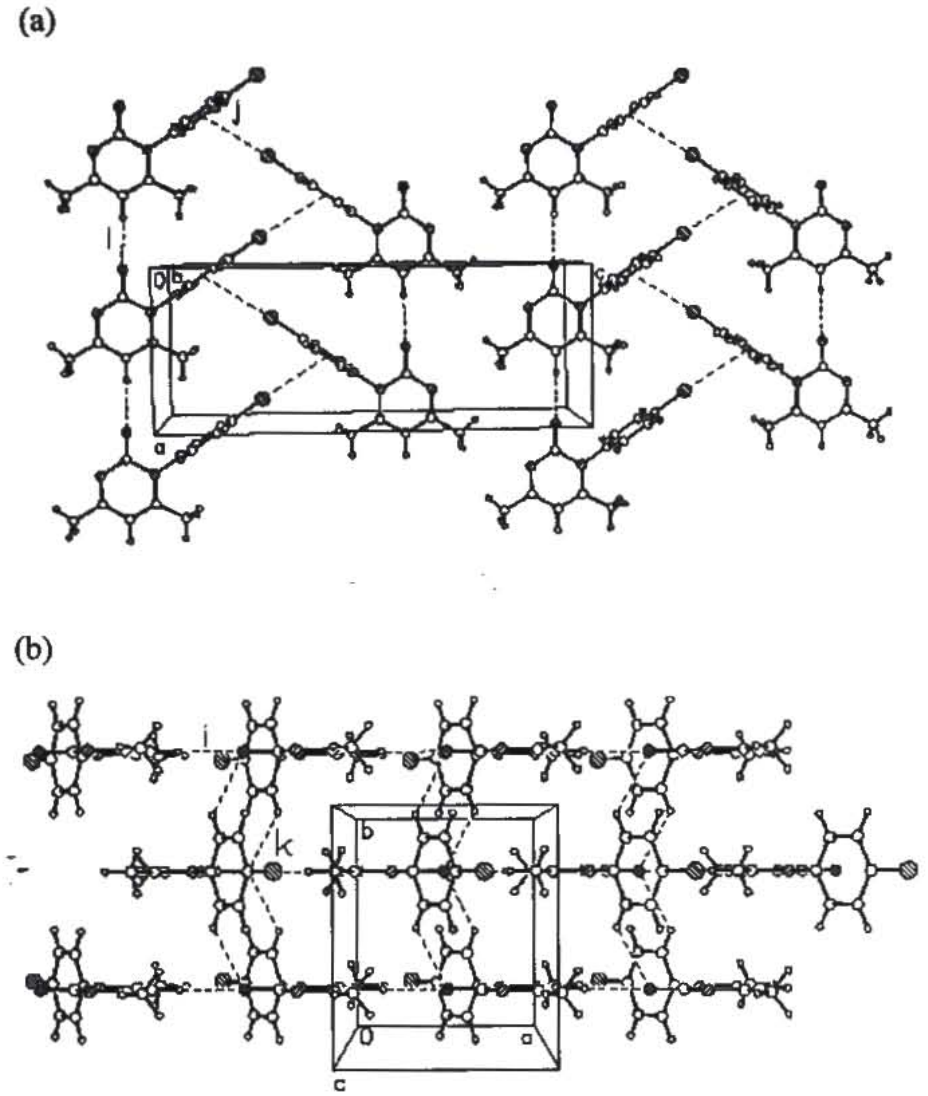

Figure 6. Crystal structure of chlorophenyl pyrimidinone **3**. (a) View of the *ac*-layer show the network of C–H···O and C–Cl···π (3.54 Å) interactions (*i* and *j*). Note the similarity with Figure 5a. (b) View of the structure down the *c*-axis. Compare with Figure 5b.

2.6 Isostructurality in 2 and 3

The C–H···O and C–H/Cl···π interactions observed in the crystal structures of pyrimidinones **2** and **3** are identical and the two crystal structures can be compared.

Compounds **2** and **3** have the same space group (*Pnma*) and the unit cell dimensions are nearly identical (see Chapter 7 for crystallographic data). Analysis of the layers in the structures shows that the hydrogen bonded motifs in the *ac* plane are identical which comprises linear C–H···O hydrogen bonded chains arranged parallel. It was noticed that the chloro and methyl groups in the molecule not only have a space filling role (chloro-methyl exchange) but also provide electrostatic stabilization with the C–H and C–Cl groups pointing towards the centre of the phenyl ring. The C–H···π[18] as well as C–Cl···π[19] contacts has been crystallographically studied and it is shown that these weak intermolecular interactions have a directional preference. The C–Cl and C–H pointing towards the centre of the phenyl ring has some bonding character stabilizing the two dimensional layers. The unit cell similarity index[20a] (Π) for the pair **2** and **3** was calculated using the formulae given below and was found to be 0.002 which indicates that both these structures are nearly identical. Details about isostructurality is explained in Chapter 1.

$$\Pi = \left| \frac{a+b+c}{a'+b'+c'} \right| - 1 \cong 0$$

The three structures **1-3** studied shows that weak hydrogen bonds reproducibly direct crystal packing in *N*-aryl pyrimidinones. In the unsubstituted aryl ring the one-dimensional chains are packed antiparallel within the layer. Two-dimensional polar layers are obtained when the para substituent is a weak hydrogen bonding functionality (Cl, CH_3), which does not interfere with the one-dimensional chain but has an influence in generating 2D layers through polarization induced interactions. These results exhibit an example where weak interactions are used to guide the molecular arrangements to a polar layer.

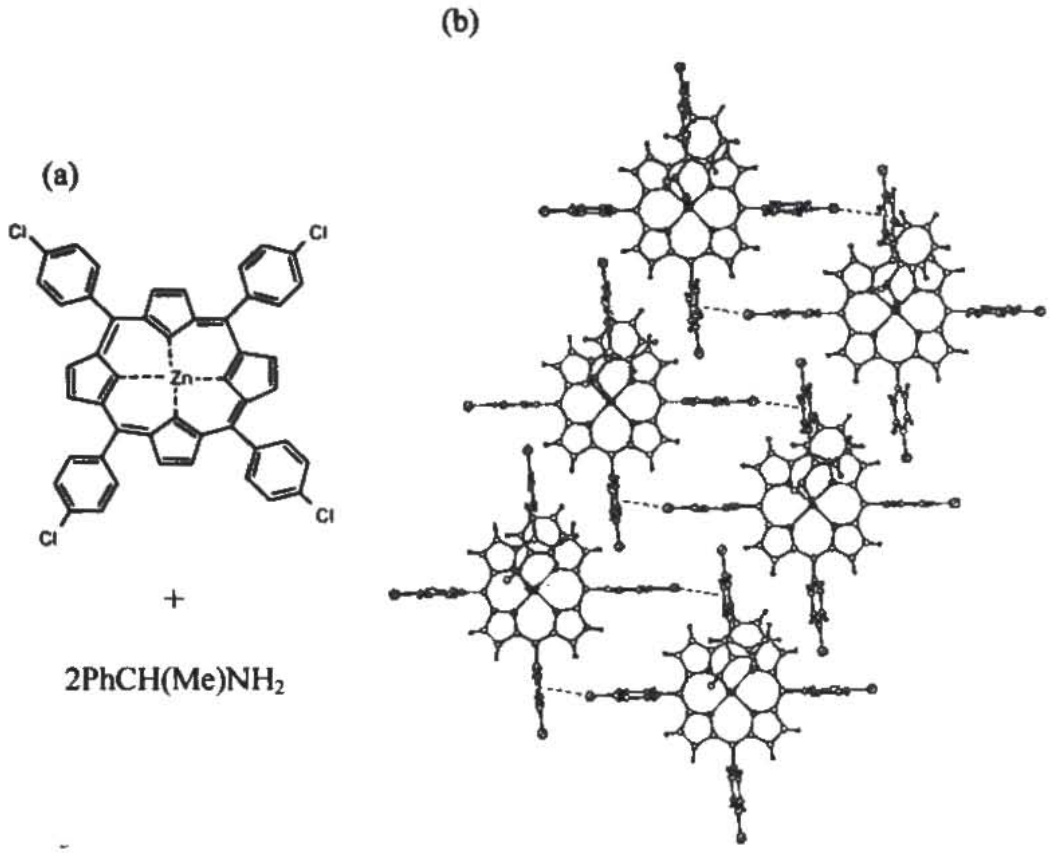

Figure 7. (a) Zn-tetra(4-chlorophenyl)porphyrin: L-α-methylbenzylamine. (b) The T-shaped interactions between the chlorophenyl rings of adjacent molecules showing the C–Cl···π interactions (3.57Å, 166.7°). For clarity some of the guest molecules (L-α-methylbenzylamine) are removed.

The isostructural[20] Me/Cl pair **2** and **3** may be contrasted with the tetraphenylporhyrin crystal structures wherein the 4-chlorophenylporphyrin[21] (Figure 7) contains the unusual C–Cl···π contact but the 4–tolyl derivative[22] (Figure 8) has a very different crystal packing. In the 4-tolylporphyrin, the major interaction along the stacks is not of the π···π type rather the methyl group of one ring is sandwiched between the phenyl fragments of neighbouring species along the stack and its C–H dipoles are oriented towards the negatively charged surface of the latter (Figure 8c).

Based on some of these examples, it appears that the polarization-type C–Cl···π (halogen···π)[23] interaction could also emerge as a useful supramolecular synthon in crystal engineering and complement the well-known steering ability of Cl···Cl interactions.[24] Nangia[23a] and Bishop[23b,c] have exploited the halogen···π interaction in the design of host-guest frameworks.

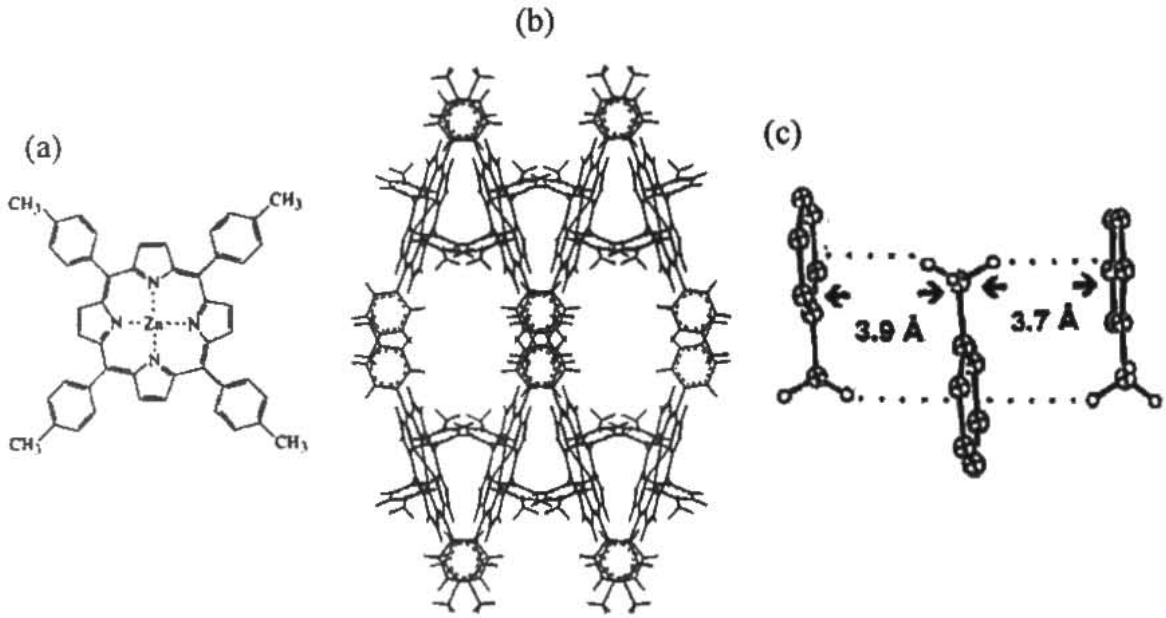

Figure 8. (a) Zinc-tetra-*p*-tolylporphyrin. (b) Porphyrin host lattice viewed down the *c*-axis. (c) The stacking geometry of tolyl residues along the *c*-axis, depicting the interplanar distances and C–H···π contacts along the stack.

2.7 Crystal Engineering and Mirror Symmetry

It is useful to analyse the present structures in crystal engineering terms. Robust supramolecular modules can reduce significantly the number of possible solid state packing motifs, a key goal in crystal engineering strategies which aims to design and synthesize molecular solids with controlled solid-state structure and properties. Three structures have been examined and all three structures have the same one-dimensional arrangement of C–H···O hydrogen bonds. These structures have two-

dimensional layers of C–H···O/N hydrogen bonds separated by regions containing aryl ring. The inter layer region is dominated by weak C–H···O and van der Waals interactions. The aryl rings penetrate into the interlayer regions maximizing hydrophobic close packing. While two-dimensional structure in pyrimidinone is controlled by hydrogen-bonding interactions, assembly in the third dimension is influenced by weak van der Waals interactions. However, it is interesting that in all three cases, the heterocyclic moieties lie on a mirror plane in the crystal, thus necessitating that the phenyl rings be either (a) in the mirror plane, (b) inclined at an arbitrary angle and disordered about the plane, or (c) perpendicular to the plane. In the present situation the last option is preferred. Generally, the rings in biphenyl-type systems are inclined because of steric hindrance. However, it is quite unusual to find cases in which the rings are exactly perpendicular (because of the location of the molecule on a special position). The two-dimensional structure follows from the substituent pattern (H, Cl, CH_3). The anticipated C–H···O chain analogous to urea N–H···O network is faithfully reproduced.

2.8 Alignment of Pyrimidinone Chromophore in Crystal Structure

The synthesis and crystal structures were studied to find the NLO potential of these materials. Even though the primary condition *i.e.* crystallization in noncentrosymmetric space group, is not satisfied here the angle at which the charge transfer axis of the aryl chromophore is oriented in the crystal was calculated. It was observed that these values are 61.3, 56.9, 56.9° for **1**, **2** and **3** respectively (Figure 9). These values are close to the optimum angle of alignment of molecular axis with the polar crystallographic axis for phase matching for the point group *mm*2, which is 54.74°. This result is encouraging and could form the basis for future experiments like substitution of suitable functional groups with appropriate electronic properties on the

phenyl ring and strategies that would favour control in the third remaining dimension and thereby crystallization in non-centrosymmetric space groups.[25, 26]

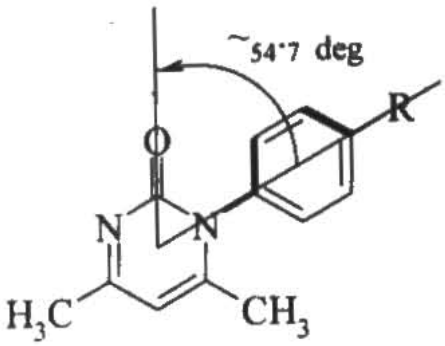

Figure 9. Orientation of a potential chromophoric aryl group with the *a*-axis in the crystal structures of the 2-pyrimidinone molecule. The values of the angles in **1**, **2** and **3** are 61.3, 56.9 and 56.9° respectively. The optically ideal value is 54.7°.

2.9 Conclusions

The present study was started to assess the NLO potential of the *N*-aryl dimethylpyrimidinones and have shown that proper combination of molecular skeleton and hydrogen bonding can lead to substantial control over crystal packing, even with weak C–H···O hydrogen bonds. Immediate implications for second-order NLO applications are not apparent in view of the centrosymmetric packing arrangement of the three compounds reported in this chapter. However, it is worth mentioning that (1) the same hydrogen bonded pattern is maintained in all the three cases and the assembly of the hydrogen bonded layers in the third dimension is controlled by weak van der Waals interactions. (2) The angle made by the phenyl ring to [100] direction is close to the optically ideal value of 54.7°. After the self-assembly of pyrimidnones into one-dimensional chains, further self assembly occurs into one of the two different motifs *i.e.* either a centrosymmetric layer or a two dimensional polar layer. Inspection of figure 5a and figure 6a shows the presence of a 2D polar layer

with a chromophoric group aligned at nearly the optical angle with respect to the polar direction.

2.10 Experimental

1,2-Dihydro-*N*-phenyl-4,6-dimethylpyrimidin-2one, 1[15]

Acetyl acetone (2.6 ml, 2.4 g, 24 mmol) and *N*-phenyl urea (2.72 g, 20 mmol) were taken in 25 ml of 95 % EtOH and concentrated HCl (5 ml) was added. The reaction mixture was refluxed for 3 h, then cooled in ice, and the precipitated solid was filtered and washed with cold EtOH to provide the hydrochloride salt of **1** (3.85 g). The salt was dissolved in 10 ml of water and neutralized with NaOH solution (0.7 g in 5 ml of water) at 0°C. Extraction of the aqueous layer with chloroform and evaporation of the solvent afforded 2.8 g of phenyl derivative **1.** M.p. 214-215°C. FT-IR (cm^{-1}): 3086, 1651, 1530, 1480, 1334, 1170, 1076, 1005, 949, 779, 634. ^1H NMR (200 MHz, $CDCl_3$): δ 7.55-7.15 (m, 5H), 6.16 (s, 1H), 2.42 (s, 3H), 1.97 (s, 3H).

A similar procedure was used to synthesize **2** and **3**.

1,2-Dihydro-*N*-tolyl-4,6-dimethylpyrimidin-2one, 2. M.p. 190-192°C. FT-IR (full, cm^{-1}): 1657. ^1H NMR (200 MHz, $CDCl_3$): δ 7.30 (d, J = 8 Hz, 2H), 7.10 (d, J = 8 Hz, 2H), 6.20 (s, 1H), 2.42 (s, 6H), 2.00 (s, 3H).

1,2-Dihydro-*N*-(4-chlorophenyl)-4,6-dimethylpyrimidin-2one, 3. M.p.: 215-216°C. FT-IR (full, cm^{-1}): 1655. ^1H NMR (200 MHz, $CDCl_3$): δ 7.52 (d, J = 7 Hz, 2H), 6.22 (s, 1H), 2,45 (s, 3h), 2.00 (s, 3H).

Data collection and Crystal Structure Determination

The cell parameters, space groups, and crystal structures were determined from single-crystal X-ray diffraction data collected at ambient temperature on Nonius-CAD4 diffractometers (Grenoble and Hyderabad) with Mo-Kα radiation (λ =

0.7101 Å). Crystal data, experimental conditions and structure refinement parameters for **1-3** are mentioned in Chapter 7. No absorption corrections were applied. The structures were solved by direct methods using the SIR92 program.[27] Full-matrix least-squares refinements were performed on F using the teXsan software.[28] Scattering factors for neutral atoms and f', $\Delta f'$, f'', $\Delta f''$ were taken from the *International Tables for X-ray Crystallography*.[29] Geometrical analysis was carried in PLATON[30] on Silicon Graphics Indigo workstation.

2.11 References

1. D.S. Chemla and J. Zyss, (ed.) *Nonlinear Optical Properties of Organic Molecules and Crystals*, Academic Press, Orlando, FL, Vol.1, **1987.**
2. G.R. Desiraju, *Crystal Engineering: The Design of Organic Solids*, Elsevier, Amsterdam, **1989.**
3. D. Braga, *Chem. Commun.*, **2003**, 2751.
4. G.R. Desiraju, *Angew. Chem., Int. Ed. Engl.*, **1995**, *34*, 2311.
5. P. Brunet, M. Simard and J.D. Wuest, *J. Am. Chem. Soc.*, **1997**, *119*, 2737.
6. V. R. Vangala, B. R. Bhogala, A. Dey, G. R. Desiraju, C. K. Broder, P. S. Smith, R. Mondal, J. A. K. Howard and C. C. Wilson, *J. Am. Chem. Soc.*, **2003**, *125*, 14495.
7. G.R. Desiraju and T. Steiner, *The Weak Hydrogen Bond in Structural Chemistry and Biology*, Oxford University Press, Oxford **1999.**
8. D. Braga, F. Grepioni and A.G. Orpen, *Crystal Engineering: from Molecules and Crystals to Materials*, Kluwer Academic Publishers, Dordrecht, **1999.**
9. M. Sakamoto, N. Utsumi, M. Ando, M. Saeki, T. Mino, T. Fujita, A. Katoh, T. Nishio and C. Kashima, *Angew. Chem., Int. Ed.*, **2003**, *42*, 4360.
10. J. Zyss and J.-F. Nicoud, *Curr. Opin. Solid State Mater. Sci.*, **1996**, *1*, 533.

11. (a) P.K. Thallapally, G.R. Desiraju, M.Bagieu-Beucher, R. Massé, C. Bourgogne and J.-F. Nicoud, *Chem. Commun.*, **2002**, 1052. (b) M. Ohkita, T. Suzuki, K. Nakatani and T. Tsuji, *Chem. Commun.*, **2001**, 1454. (c) A.D. Bond, J. Griffiths, J.M. Rawson and J. Hulliger, *Chem. Commun.*, **2001**, 2488.
12. J.K. Whitesell, R.E. Davis, L.L. Saunders, R.J. Wilson, J.P. Feagins, *J. Am. Chem. Soc.*, **1991**, *113*, 3267.
13. J. Zyss and J.L. Oudar, *Phys. Rev. A*, **1982**, *26*, 2028.
14. J. Zyss, J.-F. Nicoud and M. Coquillay, *J. Chem. Phys.*, **1984**, *81*, 4160.
15. (a) R.O. Hutchins and B.E. Maryanoff, *J. Org. Chem.*, **1972**, *37*, 1829. (b) P.S. Chandrakala, A.K. Katz, H.L. Carrell, P.R. Sailaja, A.R. Podile, A. Nangia and G.R. Desiraju, *J. Chem. Soc., Perkin Trans 1*, **1998**, 2597.
16. M.C. Etter, *J. Phys. Chem.*, **1991**, *95*, 4601.
17. (a) U. Rychlewska, B. Warzajtis, *Acta Cryst.*, **2002**, *B58*, 265. (b) A. Kálmán, G. Argáy, L. Fabian, G. Bernath, F. Fulop, *Acta Cryst.*, **2001**, *B57*, 539. (c) M.R. Edwards, W. Jones, W.D.S. Motherwell and G.P. Shields, *Mol. Cryst. Liq. Cryst.*, **2001**, *356* 331. (d) W. Jones, "Reactivity and Crystal Design in Organic Solid State Chemistry", in *Organic Molecular Solids: Properties and Applications*, Ed. W. Jones, CRC Press, Boca Raton, 1997. (e) G.R. Desiraju and J.A.R.P. Sarma, *Proc. Ind. Acad. Sci., Chem. Sci.* **1986**, *96*, 599. (f) C-K. Lam, T.C.W. Mak, *Cryst. Eng.*, **2000**, *38*, 33. (g) A. Kálman, L. Fabián, G. Argáy, *Chem. Commun.*, **2002**, 2255.
18. (a) A.D. Bond, *Chem Commun.*, **2002**, 4. (b) H. Suezawa, T. Yoshida, S. Ishihara, Y. Umezawa and M. Nishio, *CrystEngComm*, **2003**, *5*, 514. (c) E.A. Meyers, R.K. Castellano, and F. Diedrich, *Angew. Chem., Int. Ed.*, **2003**, *42*, 1210. (d) M. Nishio, M. Hirota and Y. Umezawa, *The C–H/π Interaction*, Wiley, New York, **1988**.

19. I. Csorégh, E. Weber, T. Hens and M. Czugler, *J. Chem. Soc., Perkin Trans. 2*, **1996**, 2733.

20. (a) A. Kálmán, L. Párkányi, G. Argay, *Acta Cryst.*, **1993**, *B49*, 1039. (b) A. Kálmán, L. Párkányi, *Advances in Molecular Structure Research*, **1997**, *3*, 189. (c) A. Anthony, M. Jaskólsky and A. Nangia, *Acta Cryst.*, **2000**, *B56*, 512.

21. H. Krupitsky, Z. Stein and I. Goldberg, *J. Incl. Phenom. Mol. Recognit.*, **1995**, *20*, 211.

22. P. Dastidar and I. Goldberg, *Acta Cryst.*, **1996**, *C52*, 1976.

23. (a) R.K.R. Jetti, A. Nangia, F. Xue and T.C.W. Mak, *Chem. Commun.*, **2001**, 919. (b) A.N.M.M. Rahman, R. Bishop, D.C. Craig and M.L. Scudder, *CrystEngComm*, **2002**, *4*, 510. (c) A.N.M.M. Rahman, R. Bishop, D.C. Craig and M.L. Scudder, *CrystEngComm*, **2003**, *5*, 422.

24. (a) J.A.R.P. Sarma, and G.R. Desiraju, *Acc. Chem. Res.* **1986**, *19*, 222. (b) S.L. Price, A.J. Stone, J. Lucas, R.S. Rowland and A.E. Thornley, *J. Am. Chem. Soc.*, **1994**, *116*, 4910. (c) N. Ramasubbu, R. Parthasarathy and P. Murray-Rust, *J. Am. Chem. Soc.*, **1986**, *108* 4308. (d) R. Boese, M.T. Kirchner, J.D. Dunitz, G. Filippini and A. Gavezzotti, *Helv. Chim. Acta.*, **2001**, *84*, 1561-1577. (e) M. Freytag, P.G. Jones, B. Ahrens and A.K. Fischer, *New J. Chem.*, **1999**, *23*, 1137.

25. G.R. Desiraju and T.S.R. Krishna, *Mol. Cryst. Liq. Cryst.*, **1988**, *159*, 277.

26. J.A.R.P. Sarma, F.H. Allen, V.J. Hoy, J.A.K. Howard, R. Thaimattam, K. Biradha and G.R. Desiraju, *Chem. Commun.*, **1997**, 101.

27. A. Altomare, M. Cascarano, C. Giacovazzo and A. J. Guagliardi, *J. Appl. Cryst.* **1993**, *26*, 343.

28. Molecular Structure Corp. **(1997-1998)**. teXsan for Windows version 1.03. Single Crystal Strucutre Analysis Software. Version 1.04. MSC, 3200 Research Forest Drive, Woodlands, TX 77381.

29. *International Tables for Crystallography* (A. J. C. Wilson, Ed.), Vol. C, Table 4268, pp. 6112, Kluwer Academic, Dordrecht, **1992.**

30. *PLATON.* A.L. Spek, Bijvoet Centre for Biochemical Research, Vakgroep Kristal-en Structure-Chemie, University of Utrecht, The Netherlands.

CHAPTER THREE

RECURRENCE OF C–H···O SUPRAMOLECULAR SYNTHON IN SOME *N*-ARYLPYRIMIDINONE SALTS

3.1 Introduction

The field of crystal engineering deals with the design and assembly of crystalline solids with predictable structure and properties.[1] Hydrogen bonds are key interactions that hold together supramolecular assemblies.[2] There exists a wide range of hydrogen bonds with strengths ranging from the very strong [F–H···F]$^-$, [O–H···O]$^-$ hydrogen bond having energy in the range 15-40 kcal/mol, strong O–H···O, N–H···O hydrogen bonds with energy in the range 4-15 kcal/mol, and weak C–H···O and C–H···N hydrogen bonds having energy of less than 4 kcal/mol.[3,4] Among the various classes of materials presently investigated, organic crystals are of special interest because their properties can be tuned through functional group modulations. Organic molecules exhibiting NLO properties have been intensely engineered in the previous years because of the potential applications in telecommunications.[5] The optimization of these organic crystals needs to combine two key steps: (1) To design and synthesize stable chromophore molecules with large molecular hyperpolarizabilities (molecular engineering), (2) to grow these chromophores into crystals with optimized orientation to maximize large macroscopic NLO effects (crystal engineering). Unfortunately, it is still not possible to deduce three-dimensional crystal packing from the molecular structure due to the multiplicity of possible orientation of molecules in the crystal and the interplay of strong and weak hydrogen bonds during crystallization.[6] But in addition there are several critical crystal properties that are essential to be considered in designing and developing a solid material such as high crystallinity, ease of crystal growth, good thermal and

chemical stabilities as well as high optical damage threshold especially for different applications in material science.

Despite these challenges several inorganic and organic materials have been engineered for properties like second harmonic generation (SHG): POM (3-methyl-4-nitropyridine-1-oxide), NPP [*N*-(4-nitrophenyl)-(S)-prolinol], *meta*-nitroaniline, DANS (Dimethyl amino nitro stilbene), $LiNbO_3$, KDP (KH_2PO_4). The use of enantiomerically pure derivatives ensure non-centrosymmetry in organic crystals which is attained by the introduction of chiral centres in the molecule by directed organic synthesis.[7] Some of the other methods that do not require NLO chromophore in pure enantiomeric form are molecular octupoles,[8] donor-acceptor co-crystals,[9] interpenetrated diamondoid networks,[10] and the inclusion of dipolar molecules in the constrained channel of a perhydroterphenylene host.[11] Recently it was shown that the normally centrosymmetric crystalline structure of *para*-nitroaniline is altered by recrystallization under the influence of an intense continuous electric field.[12] This electric field induced symmetry breaking is confirmed by the generation of an optical second harmonic signal which was approximately five times smaller than urea.

Meredith[13] introduced the use of strong coulombic interactions to override the weak dipole-dipole interactions and induce non-centrosymmetric packing. Marder[14] and co-workers used this strategy by varying the counterions of various stilbazolium chromophores. But the argument that centric ordering in molecular crystals is not associated with the dipole moments of the molecule is also taken into note.[15] This Chapter explains the crystal structure analysis of some salt derivatives of pyrimidinones.

3.2 Hydrogen Bonding in Neutral Pyrimidinones, Salts and their Objectives

Analysis of three crystal structures of 1,2-dihydro-*N*-aryl-4,6-dimethylpyrimidin-2-ones **1-3** (Scheme 1), in Chapter 2 was done with the motivation

of finding a crystal engineering strategy to obtain acentric structures[16] and thereby introducing NLO chromophore to it and get efficient SHG effects. These three crystal structures contain the recurring supramolecular synthon, a chain of C–H···O hydrogen bond[4] from sp^2C–H donor to the carbonyl oxygen (CO) acceptor (2.1-2.3 Å, 170-180°). This arrangement of pyrimidinone molecules in the crystal resembles the pattern common to many urea derivatives *i.e.* the α-network[17] (Figure 1) where the carbonyl oxygen atom accepts two hydrogen bonds, from the urea N–H donors of a neighbouring molecule. With the weak C–H···O chain in the former structures replacing the strong N–H···O motif in the latter[18] the compound behaves as a weak hydrogen bond equivalent of urea with respect to hydrogen bonding motif (Figure 2).

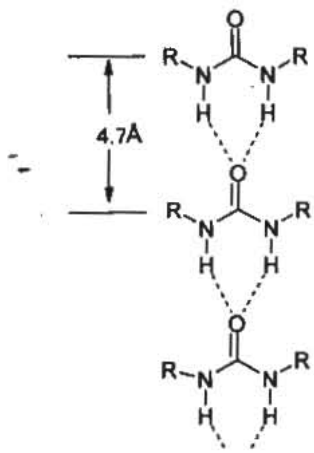

Figure 1. α-Network in urea, which is used for reliable molecular assembly with repeat distance of 4.7 Å

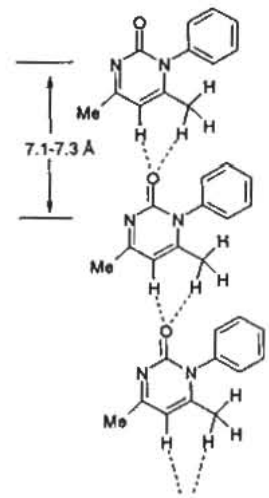

Figure 2. The most prominent synthon in the crystal structures discussed in this chapter. Note the similarity of weak C–H···O hydrogen bonded synthon in assembling the molecules with that of the strong N–H···O α-network shown in Figure 1. Repeat distance is 7.1-7.3 Å in pyrimidinones

Nevertheless, neutral pyrimidinones **1-3** are not of direct SHG relevance because they adopt centrosymmetric packing (R=H: *Pbcm*, R=Me and R=Cl: *Pnma*). Finally even though these crystal structures are centrosymmetric, the layers have polar arrangement of molecules in two of the neutral structures analysed in Chapter 2.

In extension of our studies on the pyrimidinone heterocycle, HCl and HNO_3 crystalline salt adducts were prepared and their structures were determined. In this Chapter, hydrogen bonding pattern in the crystal structures of **4** (H·HCl), **6** (Me·HCl), **7** (Cl·HCl), **8** (Cl·HNO_3) and **9** (Me·HNO_3) salts are presented (Scheme 1). The salt adduct structure are analysed on the basis of C–H···O and N–H···Cl^-/O^- interactions. Marchewka *et. al.*[19] have discussed recently the presence of hydrogen bonds in the crystals and its potential role in the second harmonic generation phenomena using vibrational spectroscopy.

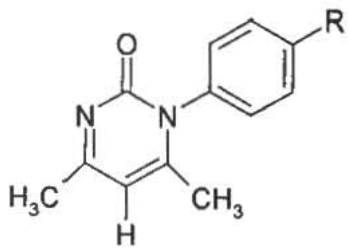

1. R=H

2. R=CH_3

3. R=Cl

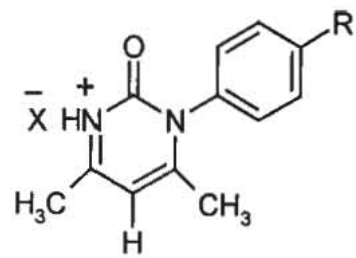

4. R = H, X = Cl^-(H·HCl)

5. R = H, X = NO_3 (H·HNO_3)

6. R = CH_3, X = Cl^-(Me·HCl)

7. R = Cl, X= Cl^-(Cl·HCl)

8. R= Cl, X = NO_3^-(Cl·HNO_3)

9. R = CH_3, X = NO_3^-(Me·HNO_3)

10. R = Ph

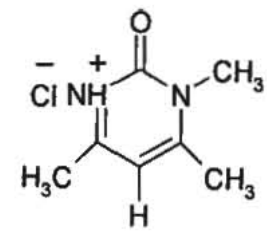

11.·HCl

Scheme 1. Compounds **1-3, 11** are referred and **4-10** studied in this Chapter.

3.3 Results and Discussions

Pyrimidinones **1-3** were synthesized as described in Chapter 2. Recrystallization of **1-3** from acidified aqueous solution of HCl or HNO_3 furnished the corresponding *N*-protonated salts as diffraction quality crystals at room temperature. Reflections were collected on crystals of **5** ($H{\cdot}HNO_3$) but the data could not be solved and refined because of heavy distortions of the phenyl ring. Crystals of neutral 4-biphenylylpyrimidinone **10** (R = Ph) were obtained from ethyl acetate.

3.4 Crystal Structure of 1,2-Dihydro-*N*–phenyl-4,6-dimethylpyrimidin-2-one hydrochloride, 4

Hydrochloride salt **4** ($H{\cdot}HCl$) crystallizes in the space group $Pmn2_1$ with half molecule in the asymmetric unit. Crystallographic analysis shows that the heterocyclic pyrimdinone moiety is protonated at one of the imine nitrogen and the ring lies on the mirror plane with the *N*-phenyl ring orthogonal to the mirror plane and bisected by it (Figure 4a). The molecules self organize to hydrogen bonded chains through a V-shaped bifurcated motif of C–H···O hydrogen bond from vinyl and methyl donors (2.77 Å, 146°; 2.31 Å, 169°; Table 1) which connect translation-related molecules along [001] (Figure 4b). Such chains further interact with the Cl^- ion *via* N^+–H···Cl^- (2.01 Å, 158°) and C–H···Cl^- (3.03 Å, 168°) hydrogen bonds to produce a lamellar motif in the (100) plane (Figure 4c). The layered structure is stabilized by the synthonic interactions between the pyrimidinone cations and the chloride anions in the layers. The polar layers of phenylpyrimidinone molecules pack in a non-centrosymmetric fashion such that the phenyl ring projects out of the *bc* plane above and below the pyrimidinone ring of adjacent 2_1 related molecules (Figure 4d). The inter-layer region is stabilized by a combination of C–H···O, C–H···Cl^- and van der Waals interaction (2.6-2.8 Å). Both strong ionic and weak hydrogen bonds[4]

play a crucial role in aggregating molecules in the crystal. The C–H···O hydrogen bond formed between the sp^2C–H and carbonyl oxygen is intact in the salt which shows that the recognition process can tolerate the presence of several other strong hydrogen bond donors in this family. This makes the C–H···O chain in this structures a reliable structure directing tool. The layers stack one over the other with the phenyl rings filling space between them (Figure 4d).

Pertaining to the hydrogen bonds with Cl atom as the acceptor in hydrochloride salts, it was shown in a database study[20] that metal-bound chlorine and chloride ions accept hydrogen bonds from O–H and N–H donors. The N–H···Cl^- hydrogen bond at 2.01 Å in this structure is in the short distance range of the H···Cl^- histogram shown in figure 3a. C–H···Cl^- hydrogen bonds too have been analysed using the database approach.[20b,c] The distances of these interactions (Table 1) may be compared to the histogram shown in figure 3.[20]

Table 1. Geometry of Intermolecular Interactions

Compound	Interaction[a] D–H···A	H···A/Å	D···A/Å	D–H···A/°
4(H·HCl)[b]	C3–H4···O1(i)	2.77(4)	3.555(3)	146(3)
	C5–H5···O1(ii)	2.31(6)	3.216(4)	169(4)
	N2–H1···Cl1(iii)	2.01(6)	3.029(2)	158(4)
	C10–H9···Cl1(iv)	3.03(4)	3.961(3)	168(4)
	C8–H7···Cl1(v)	2.68(3)	3.595(2)	146(2)
	C6–H1···O1(vi)	2.75(5)	3.429(1)	136(2)
6(Me·HCl)[b]	C3–H1···O1(i)	2.75(2)	3.547(3)	146(2)
	C5–H2···O1(ii)	2.39(3)	3.221(3)	170(2)
	N2–H10···Cl1(iii)	2.15(3)	3.030(2)	176(2)
7(Cl·HCl)[b]	C3–H4···O1(i)	2.82(2)	3.560(2)	140(1)
	C6–H5···O1(ii)	2.34(3)	3.217(3)	165(2)
	N1–H1···Cl2(iii)	2.11(3)	3.010(2)	177(2)
9(Me·HNO_3)[c]	C5–H2···O1(i)	2.59	3.389(7)	142
	N2–H10···O4(ii)	1.89	2.845(5)	166

	C3–H1···O4(iii)	2.38	3.500(6)	172
	C6–H4···O2(iv)	2.22	3.173(7)	177
8($Cl{\cdot}HNO_3$)[c]	C5–H3···O1(i)	2.61	3.419(10)	143
	N2–H1···O3(ii)	1.90	2.812(7)	163
	C3–H2···O3(iii)	2.54	3.489(9)	174
	C6–H5···O2(iv)	2.15	3.080(9)	174
10(Ph)[c]	C3–H1···O1(i)	2.19	3.20(2)	155
	C5–H4···O1(ii)	2.64	3.58(1)	145
	C2–H17···O2(iii)	2.21	3.24(2)	155
11(·HCl)[d]	C7–H13···O2(i)	2.63(2)	3.405(2)	146(2)
	C10–H11···O2(ii)	2.65(3)	3.446(3)	161(2)
	N4–H12···Cl1(iii)	2.13(2)	3.034(1)	175(2)

[a]The roman numbers after each interaction refer to the interaction number in its figures. [b]H atom refined experimentally. [c]H atom rides on the C/N carrier. [d]Reference 29.

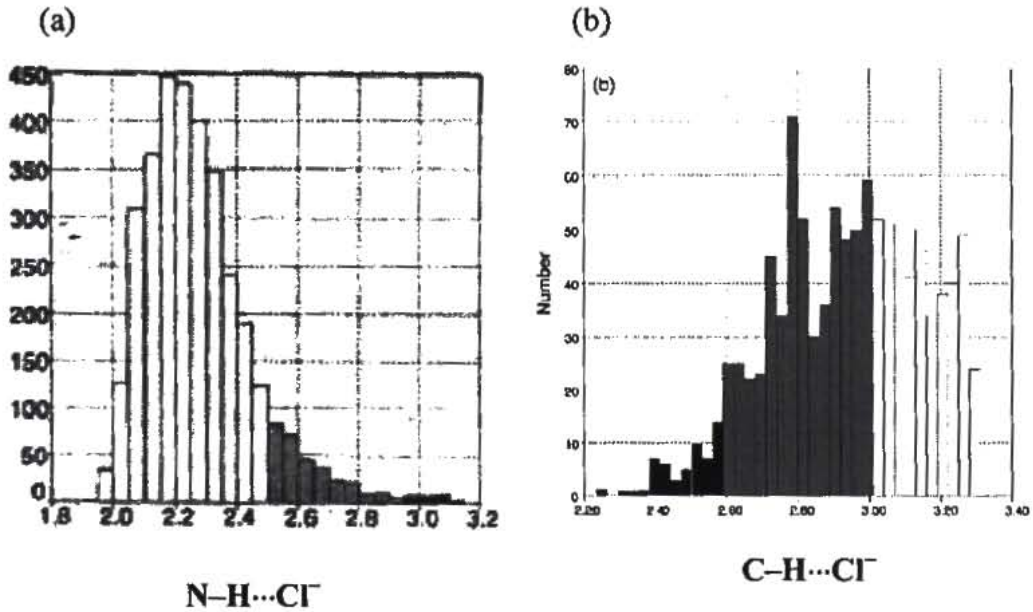

Figure 3. (a) Histogram of N–H···Cl^- distances. Short distances are in light grey, intermediate in grey and long in black. The N–H···Cl^- intermolecular interactions seen in molecules present in this Chapter belong to the light grey area. (b) Histogram of C–H···Cl^- distances. Short distances are in light black, intermediate in grey and long in white. The C–H···Cl^- intermolecular interactions seen in molecules present in this chapter belong to the grey and white area.

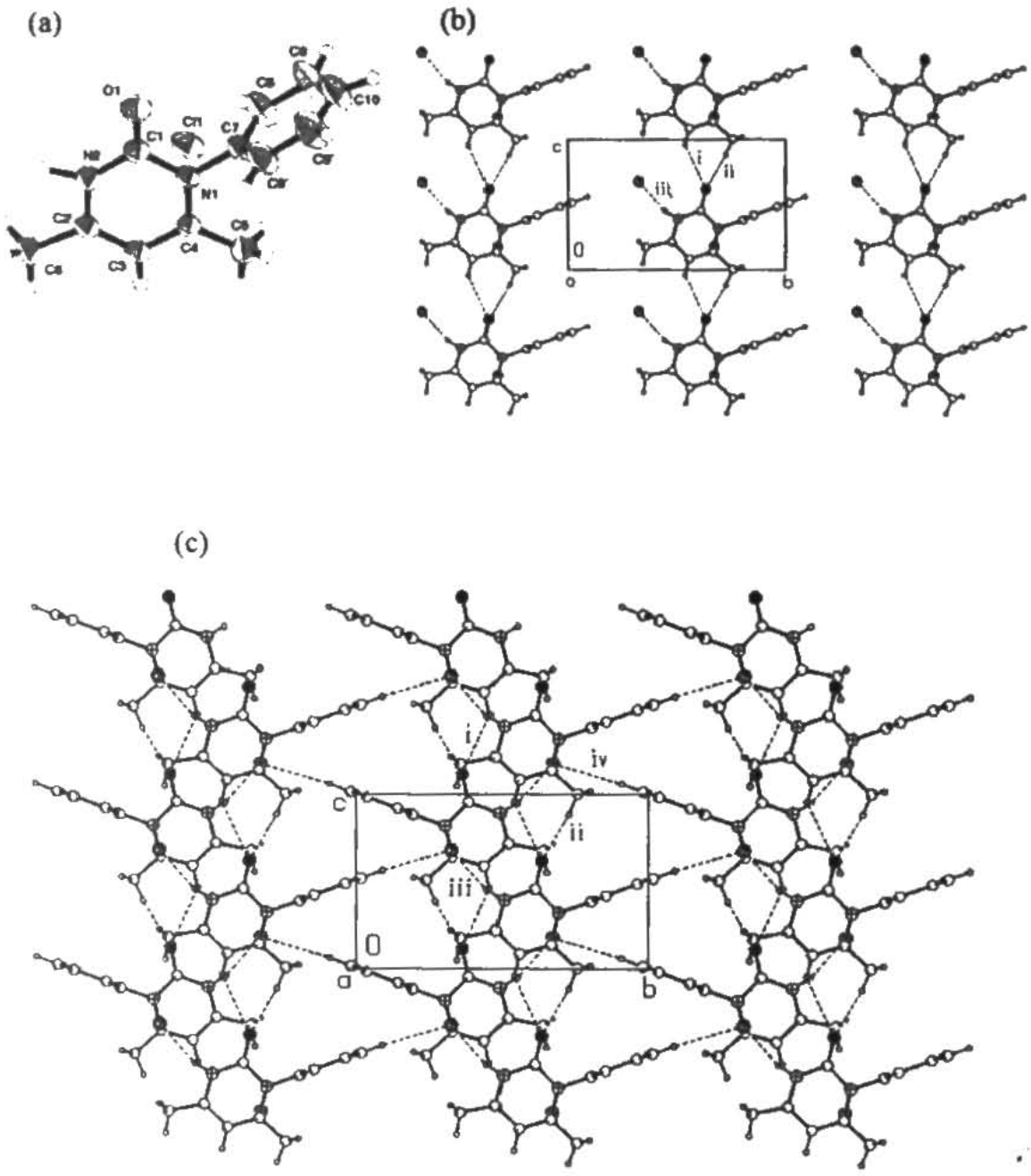
(a)
(b)
(c)
O1
C1
C5
C7
C8
C9
C10
N1
C2
C3
C4
C6
c
i
ii
iii
0
o
b
iv
a

(d)

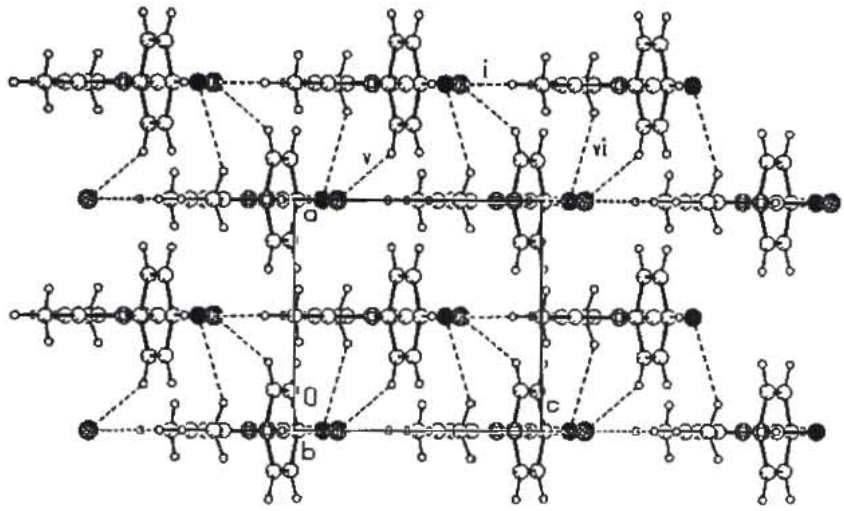

Figure 4. (a) ORTEP plot of **4** (H·HCl) showing the bisected phenyl conformation in the molecule drawn at 50% probability for non-H atom in this and subsequent diagrams. (b) Linear array of phenylpyrimidinone molecules in the crystal structure of **4** (H·HCl) mediated by the V-shaped C–H···O synthon. (c) N^+–H···Cl^-, C–H···O and C–H···Cl^- hydrogen bonds stabilise the *bc* layer. Note the parallel stacking of 2D polar layers. (d) Side view showing the stacking of layers. See Table 2 for a description of the weak interaction.

3.5 Crystal Structure of 1,2-Dihydro-*N*-4-tolyl-4,6-dimethylpyrimidin-2-one hydrochloride, 6

Hydrochloride salt **6** (Me·HCl) crystallizes in the space group $P2_1/m$ with half molecule in the assymetric unit. The cation and anion associate via a finite N^+–H···Cl^- interaction. A V-shaped C–H···O synthon connects the translation related pyrimidinone cation molecules along the *a*-axis (2.75 Å, 146°; 2.39 Å, 170°). The C–H···O and N^+–H···Cl^- hydrogen bond (2.15 Å, 176°; Table 1) connect pyrimidinone molecules in the mirror plane. Although the pyrimidinone rings of **6** are aligned parallel in the *ac* layer with their carbonyl groups pointing in the same direction (2D

polarity) as shown in figure 5b, the structure is centrosymmetric because adjacent layers are inversion-related (Figure 5c). C–H···O interactions (2.6-2.7 Å) stabilize the inter layer region.

(a)

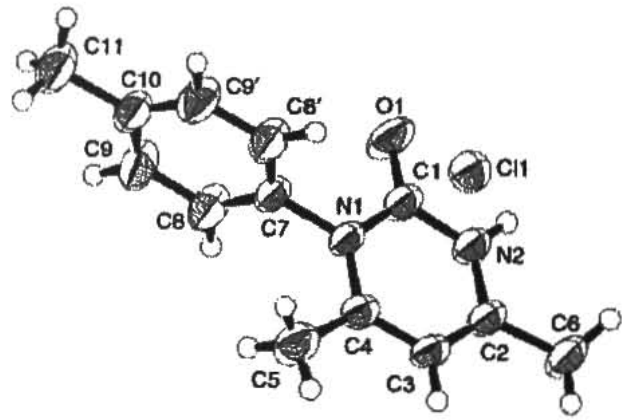

(b)

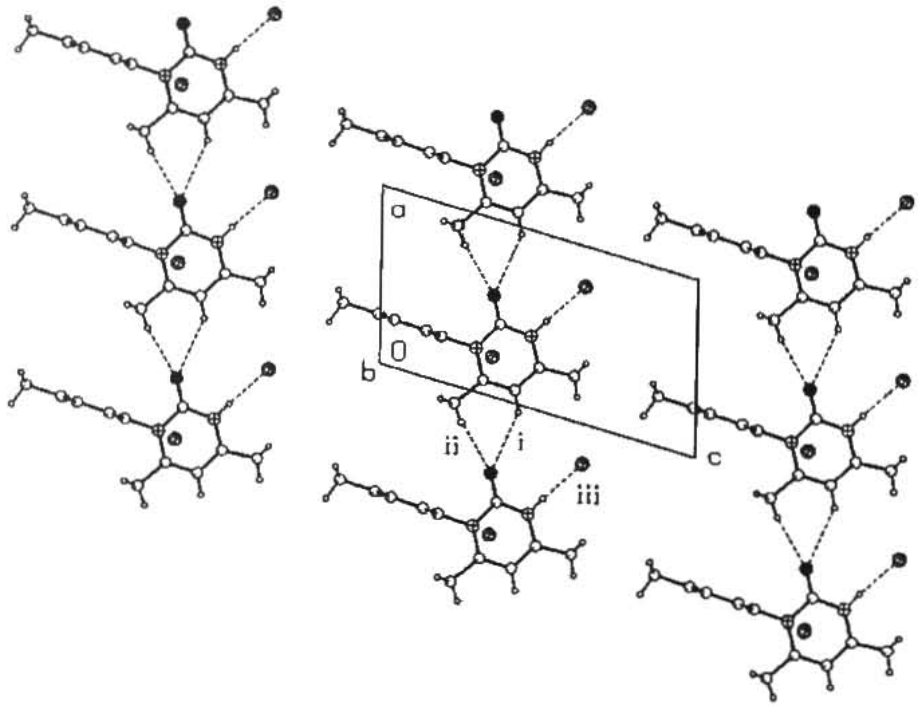

(c)

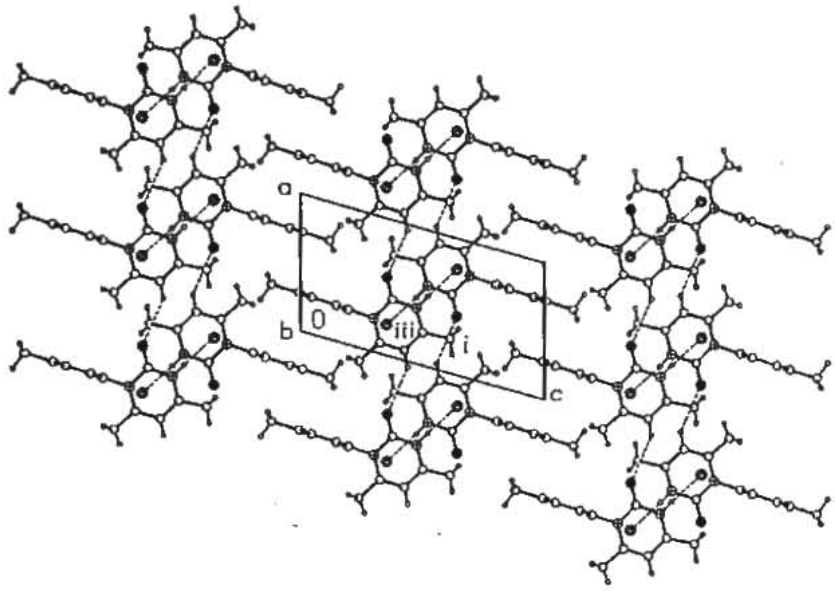

Figure 5. (a) ORTEP plots of **6** (Me·HCl) showing the bisected phenyl conformation. (b) Lamellar packing of tolylpyrimidinone molecules in **6** (Me·HCl) stabilized by V-shaped C–H···O synthon and N^+–H···Cl^- hydrogen bond. Note the 2D polar arrangement. (c) Molecules in djacent layers pack in opposite directions giving a centrosymmetric arrangement.

3.6 Crystal Structure of 1,2-Dihydro-*N*-4-chloro-phenyl-4,6-dimethylpyrimidin-2-one hydrochloride, 7

The hydrochloride salt **7** (Cl·HCl) crystallizes in the space group $P2_1/m$. The asymmetric unit contain half the molecule because the heterocyclic ring lie in the mirror plane and bisects the phenyl ring. An infinite chain of V shaped C–H···O hydrogen bond connects the translation related molecule along the *a*-axis. The anion Cl^- is connected to the nitrogen atom on the pyrimidinone ring through a strong N–H···Cl^- interaction. Adjacent chains pack parallel to each other resulting in a two dimensional polar layer (Figure 6b). Inter layer regions are dominated by weak C–H···O/Cl^- interactions. Since the adjacent layers are inversion related the crystal structure is centrosymmetric.

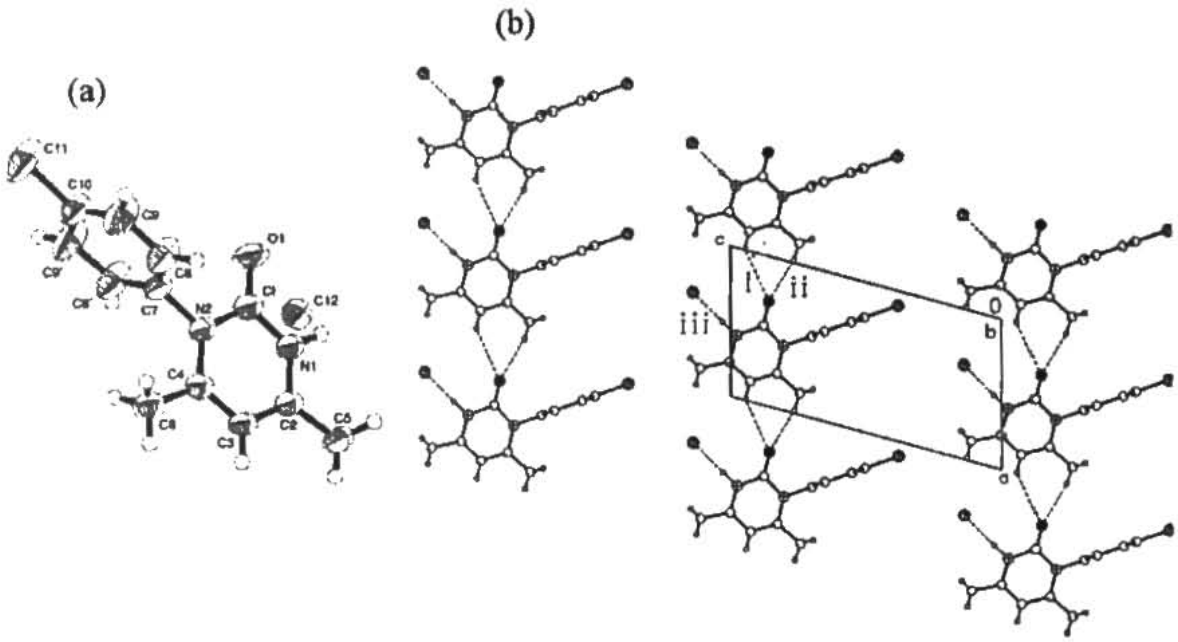

Figure 6. (a) The ORTEP diagram of hydrochloride salt **7**. (b) The packing diagram of **7** showing the polar layer containing the weak C–H···O hydrogen bonded chain along the *a*-axis.

Structures **6** and **7** are isostructural with nearly similar cell dimensions (see Chapter 7 for crystallographic Table). Isostructurality of methyl- and chloro-pyrimidinone crystals in salt structures is attributed to the robust C–H···O synthon. Notice that the tolyl groups in figure 5b can be replaced by chlorophenyl in its chloro derivative (Figure 6b) without any change in the rest of the crystal structure. This indicates that all the interactions are replaceable. There are no structure directing halogen···halogen interactions[21] (up to 4 Å) in **7** (Cl·HCl). It was shown in the context of CH_3 and CF_3 exchange[22] that crystal structure with robust supramolecular synthons are able to tolerate up to three fold increase in volume (vdW hemisphere: CH_3 17 $Å^3$, CF_3 43 $Å^3$) without perturbing the overall organization in the lattice. The 30% void space in molecular crystals can accommodate such structural adjustments without a significant change in the overall cell volume. The unit cell similarity index (Π) for the

pair **6** and **7** was calculated using the formulae given in Chapter 1 and was found to be 0.0043.

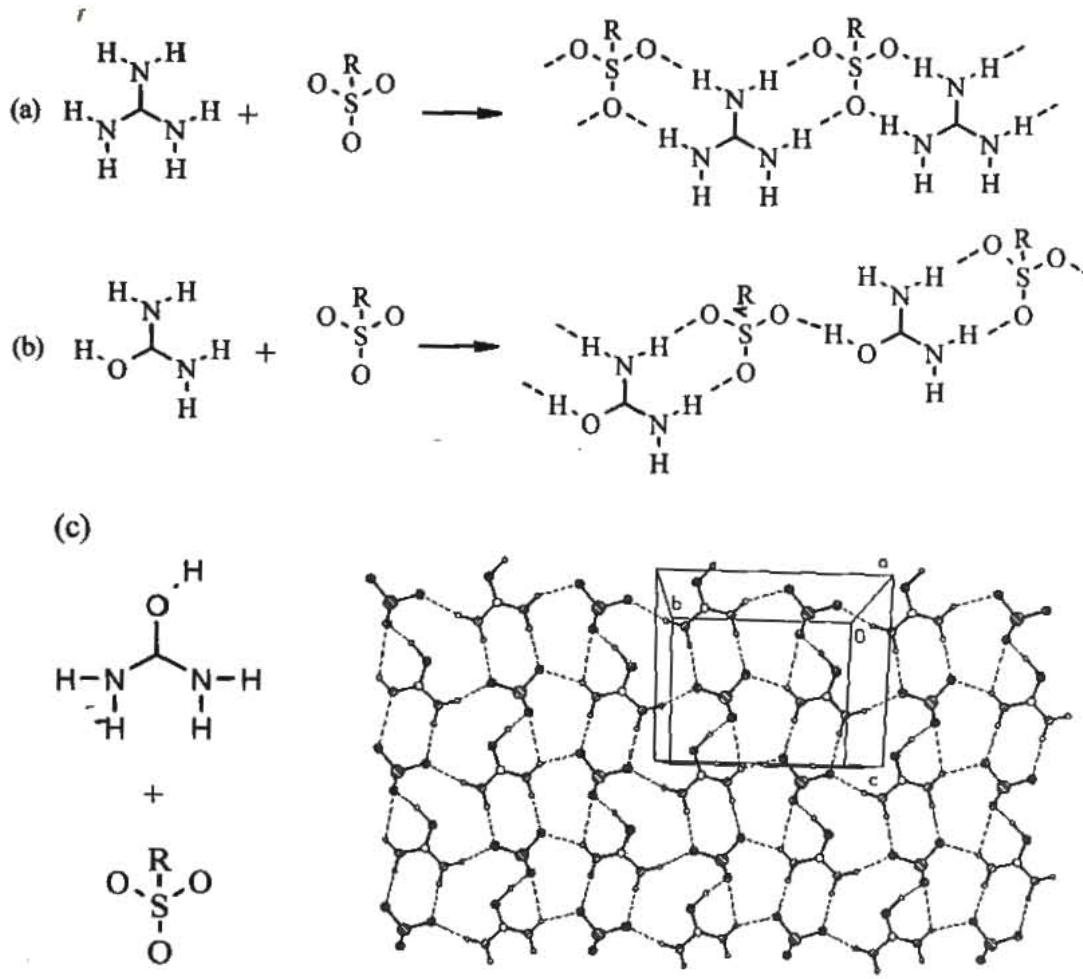

Figure 7. (a) Hydrogen bonded packing pattern observed in guanidinium sulfonate crystal structure. (b) Hydrogen bonding packing pattern seen in uronium sulfonates. (c) The 2D organization of the uronium and sulfonate ions into a polar layer. The overall structure is centrosymmetric. Note that all the uronium ions are pointing in the same direction. The phenyl rings are removed for clarity.

Two dimensional polar sheets observed in uronium sulfonate salt crystals[23] were reported (Figure 7) when our work was in progress. Uronium and sulfonate ions self assemble into two-dimensional hydrogen bonded polar sheets as shown in figure

7c. Uronium and the sulfonate moieties are mismatched in terms of the number of hydrogen bonding groups, which results in the formation of chains (Figure 7b) similar to the ribbon motif in guanidinium ion (Figure 7a). The hydrogen bonded donors and acceptors that are not used in the formation of the chain connect these chains. (Figure 7c). The van der Waals interaction controls the packing in the intralamellar space and the overall structure is centrosymmetric.

The 2D polar layers observed in the chloride structures discussed can be compared with the 2D polar layers observed in isoleucinamide hydrochloride (Cambridge Structural Database (CSD) refcode GUKMII, space group = $P2_1$) (Figure 8) and valinamide hydrochloride (refcode GUKMOO, space group = $P2_1$) (Figure 9).[24] In the crystal structures of isoleucinamide hydrochloride the translation related molecules are connected through N–H···O and C–H···O hydrogen bond along the *b*-axis where carbonyl oxygen acts as a bifurcated acceptor. The chains are in turn cross linked through N–H···Cl^- resulting in a 2D polar layer (Figure 8). Similarly figure 9 shows the 2D polar arrangement in valinamide hydrochloride.

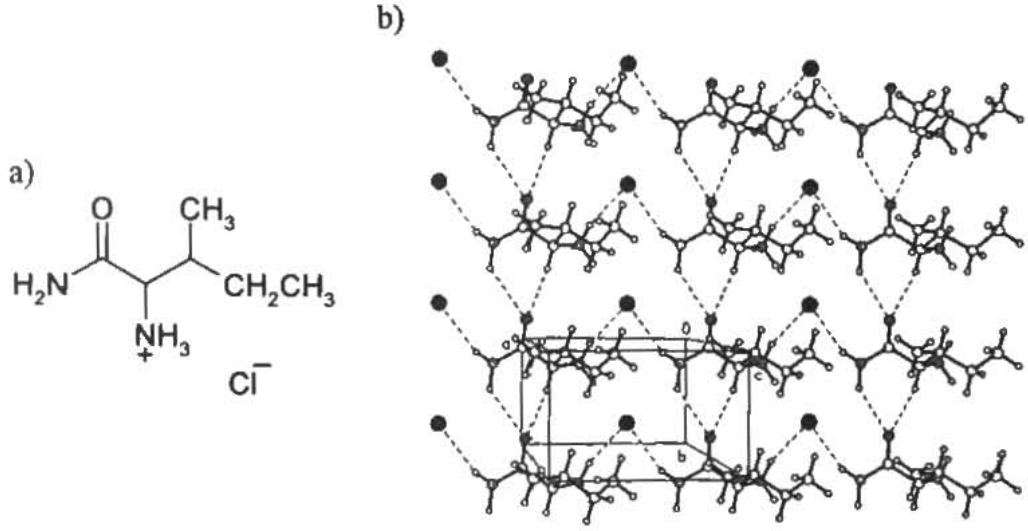

Figure 8. (a) Isoleucinamide hydrochloride. (b) Crystal structure of isoleucinamide hydrochloride showing the 2D polar layered structure. Note the similarity with the hydrochloride derivative **4** shown in figure 4.

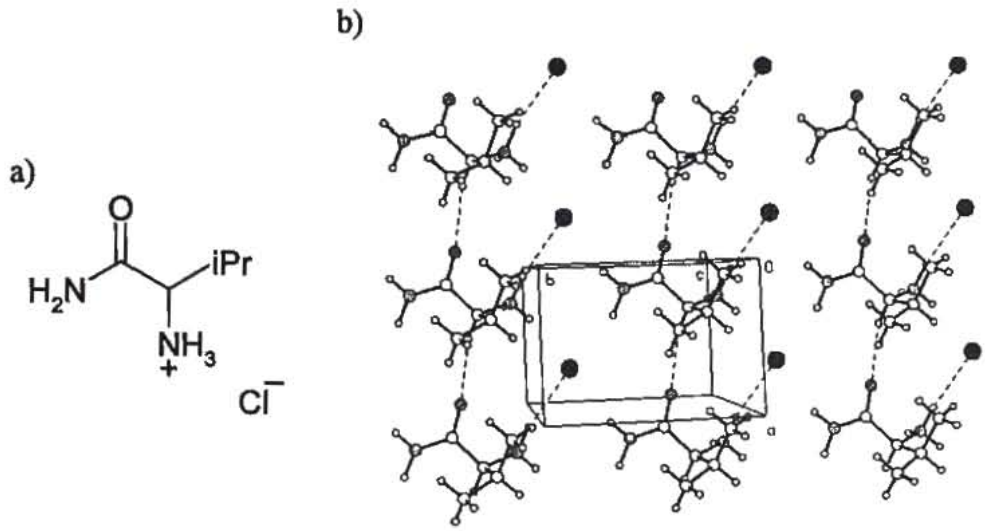

Figure 9. (a) Valinamide hydrochloride. (b) 2D polar layer stabilized by C–H···O and N–H···Cl^- interactions.

3.7 Crystal Structure of 1,2-Dihydro-*N*–4–chloro–phenyl-4,6-dimethyl pyrimidin-2-one nitrate, 8.

The nitrate salt, **8** (Cl·HNO_3) crystallizes in the space group *Pnma*. The C–H···O chain in **8** (Cl·HNO_3) (2.61 Å, 143°) originates from the methyl hydrogen donor and the acceptor is not bifurcated as observed in the chloride salt structures described before (Figure 10b). This could be to accommodate the relatively bigger counterion without much alteration in the usual structure seen in the pyrimidinone family. NO_3^- ions connect molecules along [001] through an elaborate network of N–H···O (1.90 Å, 163°) and C–H···O hydrogen bonds (2.54 Å, 174°, 2.15 Å, 174°, Table 1). Aryl rings of inversion related molecules interdigitate between hydrogen-bonded domains giving a centrosymmetric layer (Figure 10c). The close interdigitation of the aryl rings in between the chains prevents the formation of voids which otherwise could have been occupied by solvent molecules.

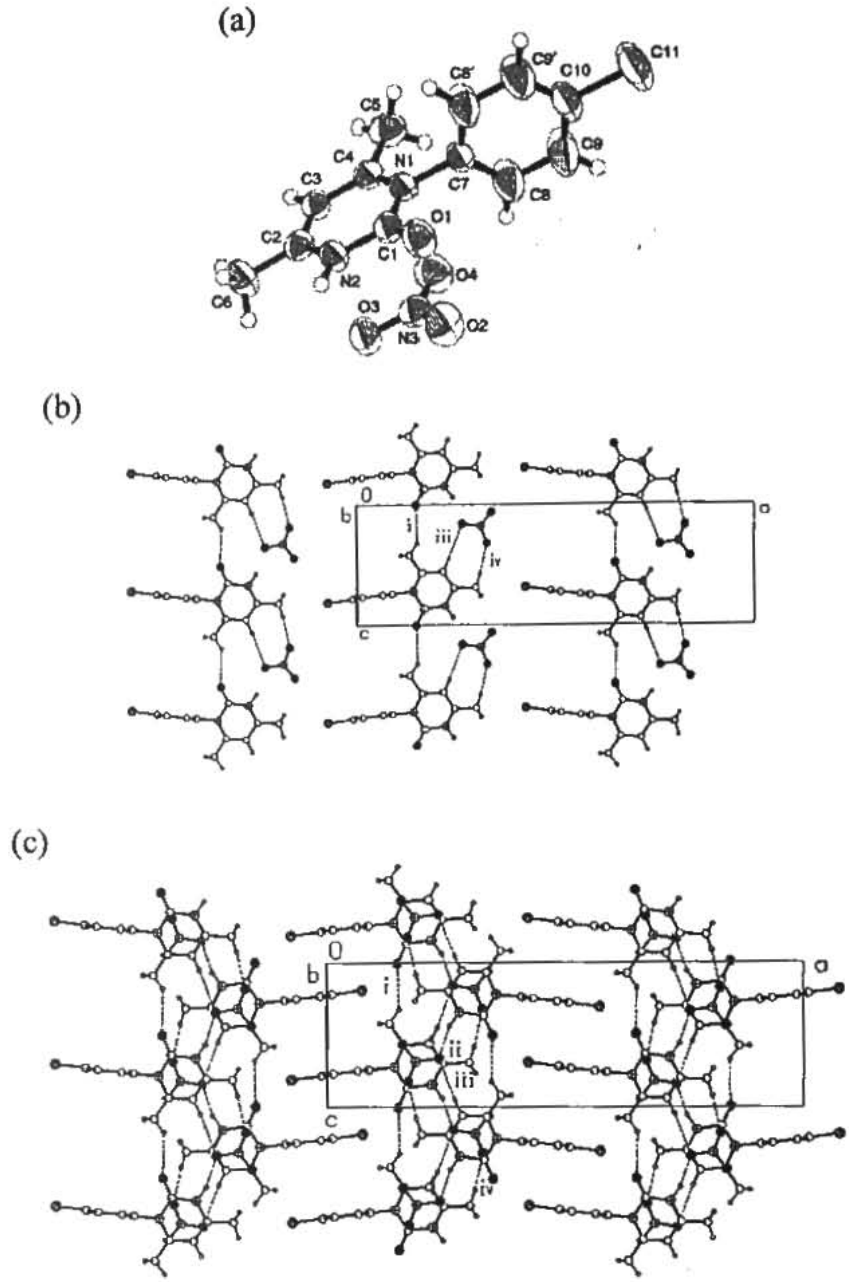

Figure 10. (a) ORTEP diagram of nitrate salt **8** ($Cl{\cdot}HNO_3$). The pyrimidinone ring and the nitrate ion occupy the mirror plane and the phenyl ring is bisected. (b) Lamellar packing of **8** ($Cl{\cdot}HNO_3$), molecules with C–H···O hydrogen bonds along the *c*-axis. Molecules are aligned antiparallel within the *ac* plane. (c) The N^+–H···O^- and C–H···O hydrogen bonds in the intra- and inter-layer region of **8** ($Cl{\cdot}HNO_3$) and the interdigitation of aryl groups between hydrogen bonded columns.

3.8 Crystal Structure of 1,2-Dihydro-*N*–4–tolyl-4,6-dimethylpyrimidin-2-one nitrate, 9

Nitrate salt **9** crystallizes in the space group *Pnma* with half molecule in the asymmetric unit. Translation related molecules are connected through a C–H···O (2.61 Å, 143°) hydrogen bond, which forms an infinite chain along the *c*-axis. The nitrate ion is connected to the pyrimidinone cation through strong and linear N–H···O (1.90 Å, 163°) and C–H···O (2.54 Å, 174°; 2.15 Å, 174°) interactions. Adjacent chains pack anti parallel to each other giving a centrosymmetric layer (Figure 11b). The almost similar cell dimensions and packing patterns shows that **8** ($Cl{\cdot}HNO_3$) and **9** ($Me{\cdot}HNO_3$) are isostructural (see Chapter 7 for crystallographic table). The unit cell similarity index (Π) for **8** and **9** is 0.008.

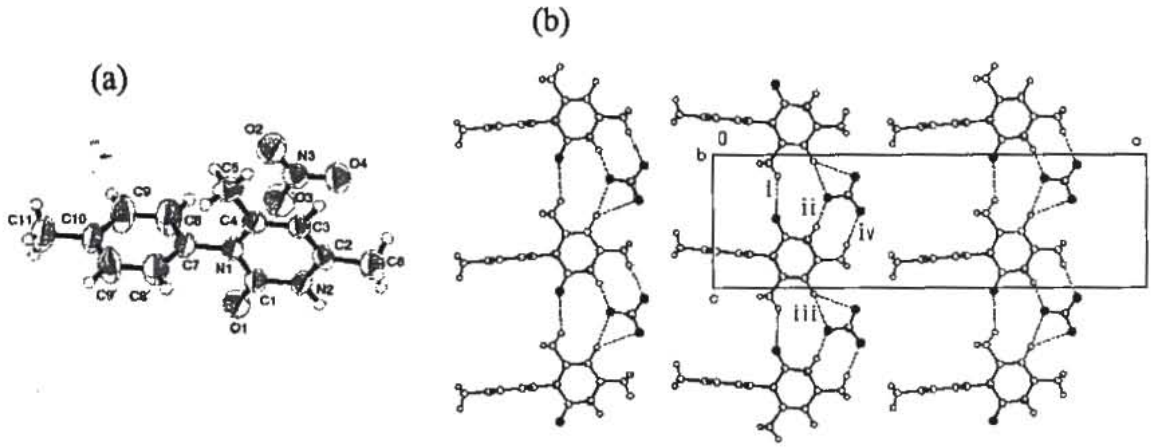

Figure 11. (a) ORTEP diagram of **9** ($Me{\cdot}HNO_3$). (b) The N^+–H···O^- and C–H···O hydrogen bonded layer showing the antiparallel packing of molecules in the *ac*-plane. Note structures **8** and **9** are isostructural.

The nitrate salt derivatives **8** and **9** can be compared with the layered structure observed in hypoxanthium nitrate monohydrate[25] (CSD refcode BONKOE01, space group = *Pnma*) (Figure 12). The unit cell contains the protonated

hypoxanthinium cation, nitrate ion and a non-protonated water molecule. In the crystal structure screw axis related molecules are connected through C–H···O hydrogen bonds forming a chain along the *a*-axis. The H-atoms of the hypoxanthinium ion are involved in bifurcated N–H···O hydrogen bonds with adjacent nitrate ions. The chains are arranged parallel within a layer.

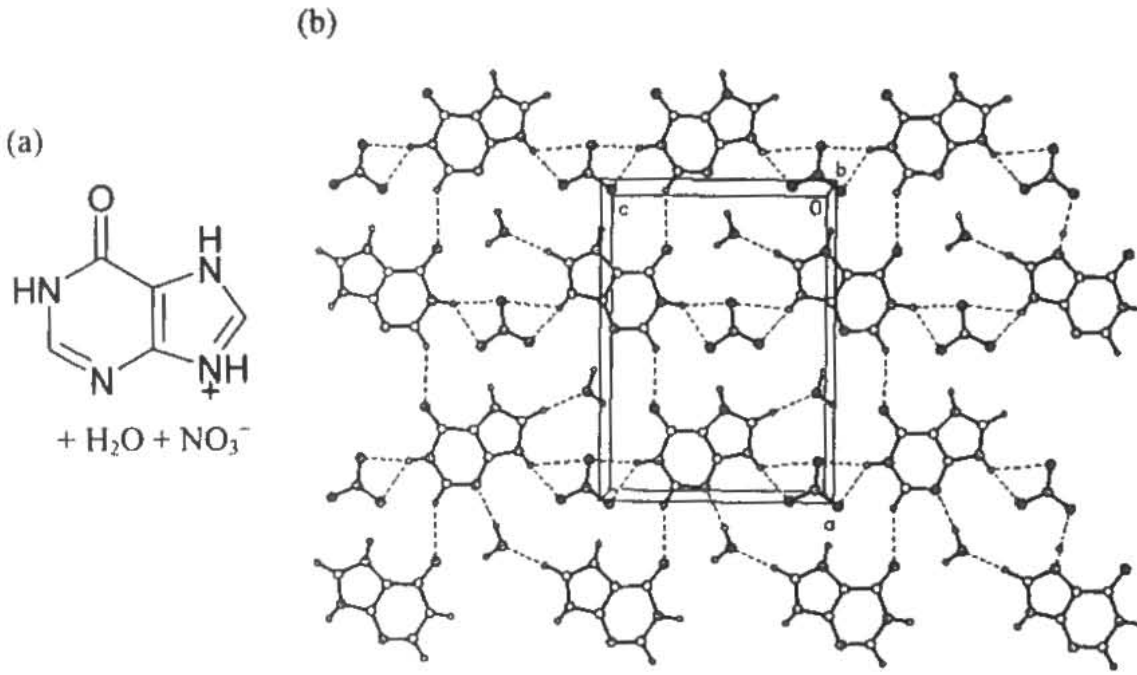

Figure 12. (a) Hypoxanthium nitrate monohydrate. (b) The layered structure in the crystal structure showing the 2D layer stabilized by an extended hydrogen bonds of the type N–H···O, O–H···O and C–H···O.

Crystal structure of 2-amino-5-butyl-4-methyl-1,3-thiazol-3-ium nitrate[26] can also (refcode GUWBEF, space group $P\,\overline{1}$) (Figure 13a) be compared with the nitrate salt derivatives **8** and **9**. The structure comprises a substituted thaizolium ring that is connected to a nitrate ion via N–H···O hydrogen bonding interaction. The crystal packing is stabilized by ionic interactions between the nitrate anions, organic cations

and N–H···O hydrogen bonds. Two of the cations are joined head-to-head by hydrogen bonds between them and the nitrate ions. These pairs of molecules from chains extending along the *a*-axis and such chains are aligned antiparallel (Figure 13b).

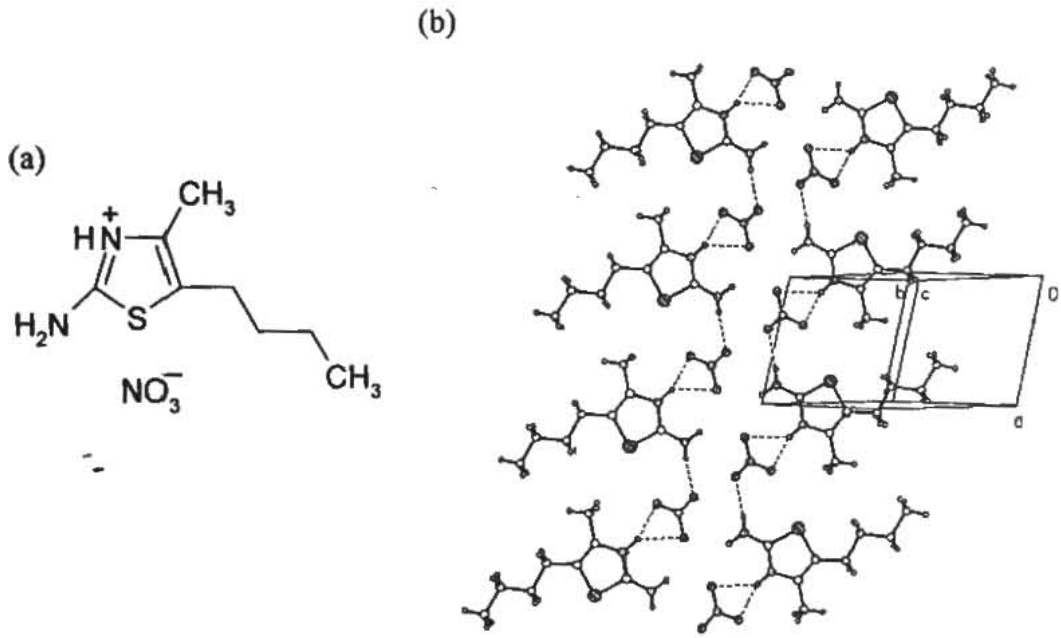

Figure 13. (a) 2-amino-5-butyl-4-methyl-1,3-thiazol-3-ium nitrate. (b) Antiparallel arrangement of adjacent chains as in nitrate salt derivatives **8** and **9**.

The hydrochloride salt **4** is the only pyrimidinone adduct that has a non-centrosymmetric crystal structure in the present series studied. When a crystalline sample of this material was subjected to the Kurtz and Perry[27] SHG powder test with laser light at 1.06 μm, no visible second harmonic signal was detected at 530 nm. In a control experiment, crystalline urea showed a highly visible green light under identical laser conditions. Examination of the crystal structure of **4** H·HCl (Figure 4)

offers an explanation for the absence of visible SHG signal. Although the phenyl ring is oriented correctly in the acentric crystal for phase matching, the chromophore bears no electron-with drawing/donating functional groups to extend the π-conjugation. Moreover, since the phenyl and pyrimidinone rings are orthogonal, there is no possibility of intramolecular charge transfer leading to a significant hyperpolarisability. The pyrimidinone ring itself is a modestly polarisable chromophore, but the SHG effect is probably too feeble to be visible to the human eye.

3.9 Mirror Symmetry and CSD Analysis

The presence of molecules on a mirror plane in crystal structures is generally avoided because it decreases packing efficiency by 0.02-0.03. Molecules in general tend to crystallize into space groups that contain inversion or translation symmetries such as glide planes and screw axes, as these symmetries favour close packing. However, retention of *m* or 2 symmetry in crystals is thermodynamically advantageous because the molecules are symmetrically arranged.[28] Unoccupied mirror planes results in like-like interactions (bump-bump) between adjacent molecules, which is unfavourable by Kitaigorodskii's close packing idea. In space groups with a mirror plane, the molecules *must* reside on the special position: otherwise, the structure is usually disordered. More over if the special position of a given site symmetry (*e.g.*, *m*) are occupied, the packing is effectively that of a lower symmetry group. Here the crystalline derivatives **1-4, 6-10** follow this rule in that the pyrimidinone ring resides on the mirror plane ($Z' = 0.5$) and the *N*-phenyl ring is orthogonal and bisected. Because *m* symmetry is not common in crystals, the recurrence of a mirror plane in pyrimidinone crystal structures was examined further.

In addition to the phenyl pyrimidinone adducts discussed in this thesis there is one structure from CSD which can be compared. A closely related molecule, *N*–

methylpyrimidinone hydrochloride **11** (·HCl) (CSD refcode COBYIB),[29] crystallizes in space group $P2_1/n$. This crystal structure has a layer motif like the chloride adducts **4, 6** and **7** but without a mirror plane (Figure 14b, Table 1). The absence of mirror symmetry in **11** (·HCl) despite its resemblance to *N*-arylpyrimidinones led us to carry out an analysis of crystal structures in CSD that have a phenyl group and are bisected by a mirror plane.

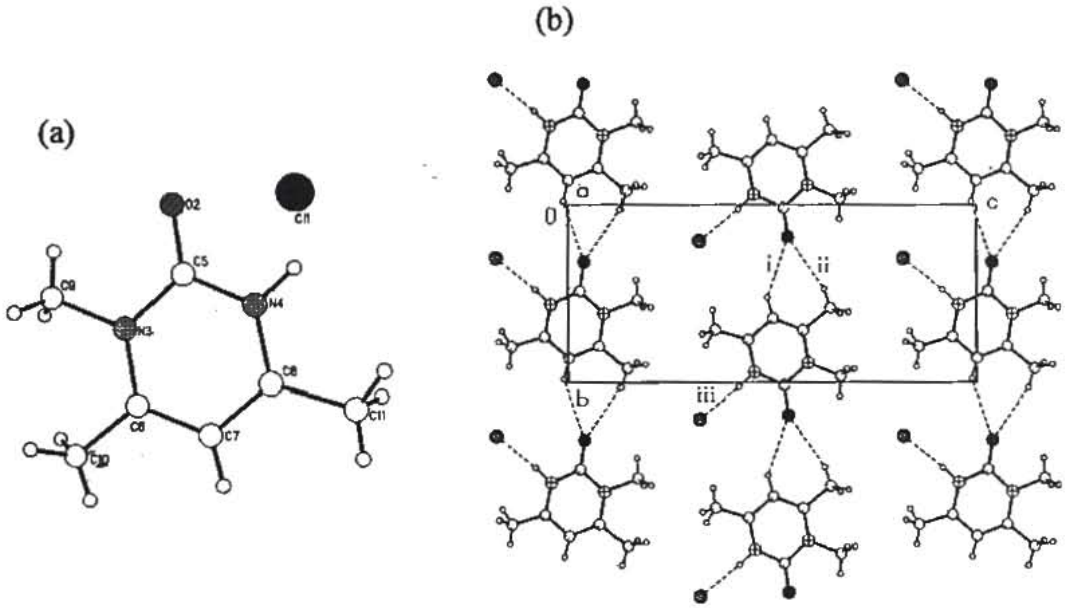

Figure 14. (a) The numbering scheme of the compound COBYIB (CSD refcode). (b) Notice the V-shaped C–H···O synthon and the N–H···Cl^- hydrogen bond in this structure, which are similar to that seen in the structures explained in this Chapter.

Table 2. CSD refcodes of organic structures in which a phenyl ring is bisected by a mirror plane in the three common space groups.

Pnma	$P2_1/m$	*C2/m*
KALKUA	JIFLIW	DADYAI
MEACAN10	KANCAD	KOSBUP
REKJUM	LINBIT	PERWUE
REKKEX	PIJXEL01	QAFXOK

RUHQOA	PMIQLO	SEQYIW
TUFQOA	TIQDIG	
YAZZOO	YILZUO	
YIZHEU	ZOMDIO	

This exercise was carried out for the top three mirror-containing space groups listed by Padmaja *et.al.*,[30] *Pnma*, $P2_1/m$ and *C2/m* (Table 2). While there are examples of phenyl rings being bisected by a mirror plane in crystal structures, these are special cases with specific reasons determining the packing in each structure. A manual examination of the refcodes in table 2 shows that there is no preference for the occurrence of mirror symmetry in a family of structures.

3.10 RHF Computations

Since crystallographic analysis did not provide a suitable explanation, we assumed that there could be a molecular feature in pyrimidinone that favours a bisected phenyl ring conformation. The RHF (Restricted Hartee Fock) energy of the neutral pyrimidinone **1** (R = H) was calculated in the PC Spartan Pro 1.0 program[31] with STO-3G, 3-21G* and 6-31G* basis sets. The energy of the molecule (*E*/au) and torsion angle about the pyrimidinone-phenyl (O)C–N–C–C(Ph) bond (τ/°) are listed in Table 3. In the minimum energy conformation of **1** calculated using 3-21G* and 6-31G* basis set, the phenyl ring is orthogonal to the pyrimidinone heterocycle. The energy profile of **1** (where R = H) as a function of phenyl group torsion about the N-C bond was calculated in the range 0 to 180° with 3-21G* (Figure 15). This basis set was selected because it gives a comparable results to 6-31G* with about a three-fold saving of computer time. The bisected conformation of **1** (R = H) (τ = 90°) is 0.030 au (18 kcal mol^{-1}; 1 au = 627 kcal) more stable than the almost planar conformation (τ = 2, 178°).

Table 3. RHF energy of **1** (R = H) calculated in PC Spartan Pro.

	E/au	E/kcal mol^{-1}	τ/°
STO-3G	-637.143	-399807.01	77.21
3-21G*	-641.580	-402591.45	90.08
6-31G*	-645.186	-404854.22	89.67

1 au = 627.5kcal/mol

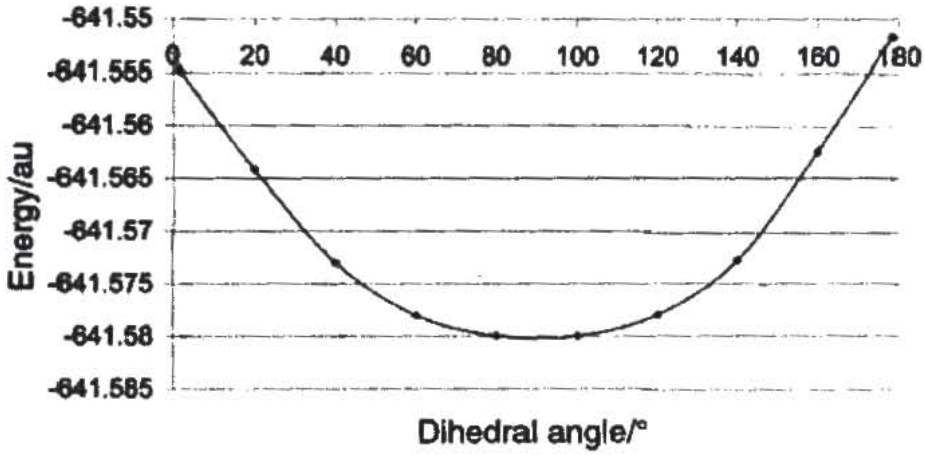

Figure 15. RHF 3-21G* energy *vs* (O)C–N–C–C– (Ph) torsion angle in phenylpyrimidinone **1**H calculated using Spartan Pro 1.0 on a Pentium PC.

The energy of the perfectly planar conformation (τ = 0, 180°) could not be calculated in the Profile run, presumably because the energy of the all-planar conformation is so high that the program starts about 2° away from the extreme values. Thus, RHF calculations explain the recurrence of the mirror symmetry in *N*-arylpyrimidinones: intermolecular interactions and close packing are optimized in the crystal with the molecule adopting the stable bisected-phenyl conformation.

3.11 Crystal Structure of 4-Biphenylylpyrimidinone, 10

The crystal structure of 4-biphenylylpyrimidinone **10** was determined to understand this issue further. In *Pbcm*, *Pnma* or $P2_1/m$ space groups observed in this

family, the pyrimidinone ring will occupy the mirror plane and the *N*-phenyl moiety will be orthogonal. The *para*-phenyl ring in biphenylyl derivative **10** can be either (1) coplanar with the *N*-phenyl ring, or (2) orthogonal to the *N*-phenyl ring, or (3) oriented at some arbitrary angle but disordered to conform to the crystallographic mirror symmetry. Alternatively, the structure may adopt other common space groups like $P2_1/c$, *Pbca* or $P\bar{1}$. In any event, this result will shed light on the interplay of factors that control the recurrence of mirror symmetry. Option (1) causes steric crowding of phenyl rings in the same plane while in (2) the steric penalty is released but there is break down of conjugation in the biphenyl chromophore.

The biphenylyl analogue **10** was synthesized by condensation of 4-biphenylylurea[32] with acetylacetone. The neutral molecule **10** crystallizes in the $P2_1/a$ space group with two molecules (Figure 16a) in the asymmetric unit ($Z' = 2$). The *N*-phenyl group is twisted by an angle of 84.8, 87.9° at the N–C bond with respect to the pyrimidinone ring and the *para*-phenyl group is twisted by 145.3°, 152.5° about the C–C bond. Significantly, the biphenyl group in both molecules is ordered. Crystallographically independent molecules are present in distinct chains. Glide related molecules are connected by a V-motif (2.19 Å, 155°, 2.64 Å, 145°) and a linear chain (2.21 Å, 155°) of C–H···O interactions (Figure 16b). It was interesting to see that the C–H···O synthon is preserved in even with the loss of mirror symmetry in the crystal and the increase of Z' from 0.5 to 2. In the hydrophobic region between hydrogen bonded synthons, aryl groups of symmetry-independent molecules interdigitate *via* the herringbone T-motif.

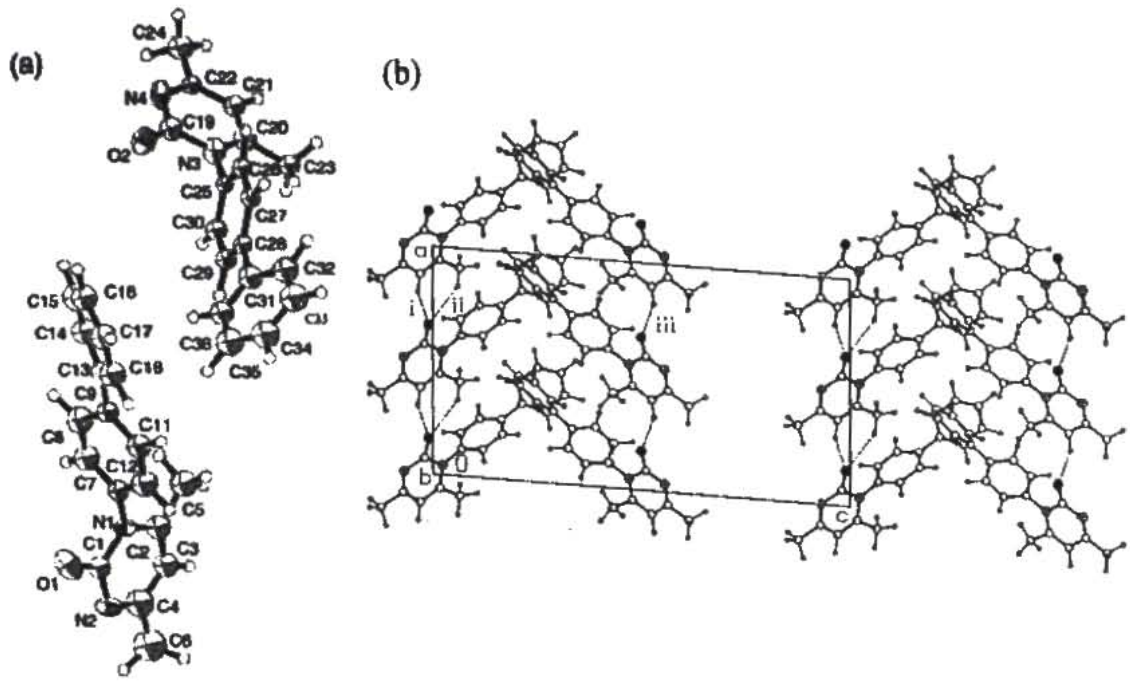

Figure 16. (a) ORTEP plot of biphenylylpyrimidinone **10**. There are two symmetry-independent molecules in the crystals. (b) Glide-related molecules are connected by V-shaped and linear chain C–H···O synthons. Phenyl rings of symmetry-independent molecules are stabilized by the herringbone T-motif. Inversion-related molecules are not shown for clarity. See Table 1 for the description of weak interactions.

To summarise, two structural types are present in the pyrimidinone family. *N*-Arylpyrimidinones (R = H, Me, Cl)[16] and their salt adducts have *m* symmetry in their crystal structure while *N*-methyl and *N*-biphenylylpyrimidinone have a 2_1 screw axis. Yet, chemical recognition is mediated by the robust C–H···O synthon, a recurring pattern in all these structures. It is possible that the repeated appearance of mirror symmetry is a result of crystal data being collected at room temperature.[33] DSC (Figure 17) were recorded on neutral molecules and salt adducts of **1** (R = H), **2** (R = Me), **3** (R = Cl) and **10** (R = Ph) show a sharp endotherm at the melting temperature.

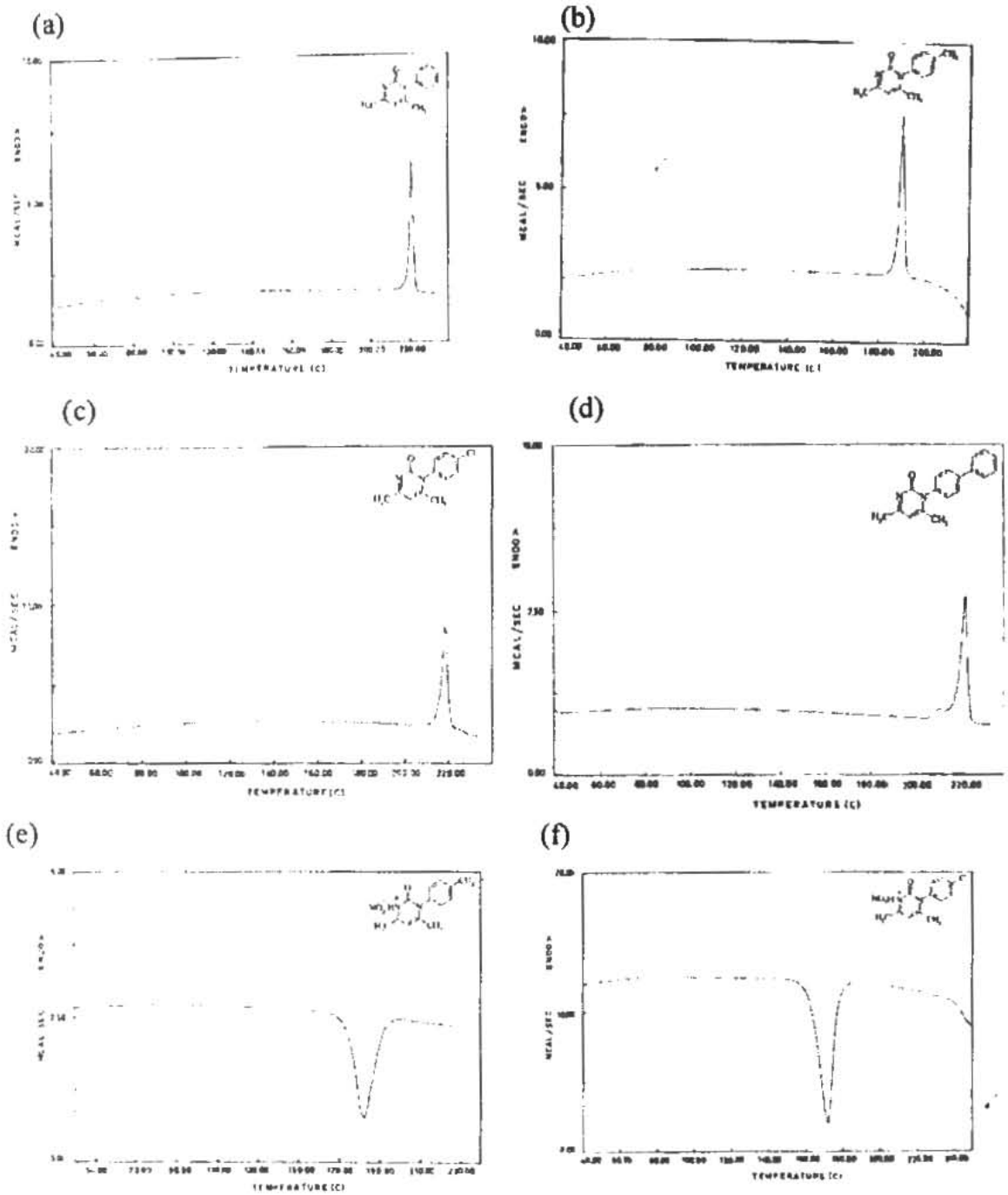

Figure 17. The DSC plots of the compounds (a) **1** (b) **2** (c) **3** (d) **10** (e) **9** (f) **8**. a-d show melting behaviour of compounds and e, f exhibit exotherm because of decomposition.

The chloride salts, **4** (H·HCl), **6** (Me·HCl) and **7** (Cl·HCl), do not exhibit a phase transition up to 240°C. The nitrate salts, **8** (Cl·HNO_3) and **9** (Me·HNO_3), decompose between 170-190°C as indicated by the sharp endotherm. Some of these DSC plots are shown in figure 17.

3.12 Conclusions

Crystal structures of neutral and salt adducts are studied and organic salts are used as molecular building blocks. These salts self assemble via ionic N^+–H···$X^-$and neutral C–H···O hydrogen bonds when crystallized. One advantage in using organic salts compared to neutral molecules is that hydrogen bonds between the ions are stronger than those between neutral molecules. Some of the salts in the present study form polar hydrogen bonded layers. These layers serve as scaffolds to control molecular packing in two dimensions for engineering the structures of crystals. The pyrimidinone cation function as multidendate proton donors by forming weak, recurring C–H···O hydrogen bonds in addition to the N^+–H···Cl^-/O^- hydrogen bonds. The recurrence of the C–H···O synthon in *N*-arylpyrimidinones provides the possibility of crystal engineering with a novel molecular scaffold in which functional groups can be manipulated to tailor the target architecture. Strong and weak hydrogen bonds define structure and connectivity within layers while weaker hydrogen bonds and van der Waals interactions dominate between layers in these salts. Pyrimidinone derivatives **12** and **13** should be interesting molecules for further study because extended conjugation of the phenyl ring with the heterocycle will increase the molecular hyperpolarisability. Crystal structure of these molecules are explained in Chapter 4. The occurrence of a crystallographic mirror plane in *N*-arylpyrimidinone is explained through *ab initio* computations as the tendency of the molecule to adopt the lowest energy conformation in the crystal. A possible reason for the ordered arrangement of molecules in the solid state, despite that structures with mirror planes

tend to be disordered, could be the intricate network of weak interactions, namely C–H···O, C–H···Cl^- and the herringbone motif.

Constraining molecules to assemble into layers limits molecular packing to just a few packing arrangements. It reduces the problem of predicting crystal packing in three dimension from that of individual molecules to that of the layers. The recurring C–H···O synthon and the occurrence of 2D polarity in these structure simplifies the task of directing self-assembly for useful crystal properties to the third dimensions.

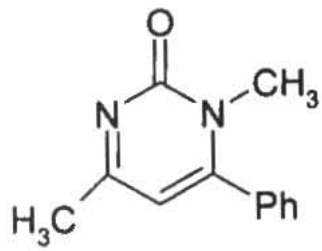

12

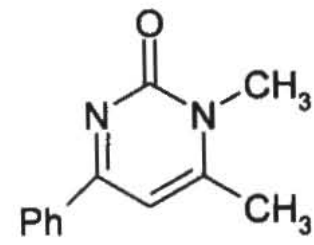

13

3.13 Experimental Section

Synthesis of *N*-arylpyrimidin-2-ones

Synthesis of the neutral phenylpyrimidinone **1** (R = H) was followed exactly as in Chapter 2. Similarly, other aryl derivatives were prepared.[16] Condensation of *para*-biphenylylurea[32] with acetyl acetone afforded crystals of **10**. ^{1}H NMR (200 MHz, $CDCl_3$): δ 7.75 (d, J = 8 Hz, 2H), 7.60 (d, J = 8 Hz, 2H), 7.50-7.20 (s, 3H). IR (KBr, cm^{-1}): 1640 (C=O group).

Preparation of salt adducts. Neutral *N*-aryl pyrimidinone derivatives **1-3** were dissolved in 10 ml water in a beaker and conc. HCl or HNO_3 was added until the mixture became acidic. The solution was heated to boil, filtered, concentrated and

then left for crystallization at ambient temperature. Diffraction quality crystals of HCl salts and HNO_3 salts were obtained after a few days.

Differential scanning calorimetry. DSC was recorded on a Perkin Elmer instrament in the temperature range 30 to 240°C at a rate of 20°C min^{-1}.

Crystallography

Single crystal X-ray data on salt samples were collected on a Nonius-CAD4 diffractometer with Mo-Kα radiation (λ = 0.71073 Å) at ambient temperature. Data on 4-biphenylylpyrimidinone were collected on a Nonius-CCD Kappa diffractometer working with Ag-Kα radiation (λ = 0.5608 Å) from 180 exposures with $\Delta\phi = 1°$, $2\theta_{max} = 35.2°$. No absorption corrections were applied. Hydrogen atoms of **4** (H·HCl), **6** (Me·HCl) and **7** (Cl·HCl) were refined experimentally and H atoms in **8** (Cl·HNO_3), **9** (Me·HNO_3) and **10** (Ph) were fixed because of the limited number of reflections. Structures were solved using direct methods with the SIR92 program.[34] Full-matrix least-squares refinement were performed on *F* using the teXsan software.[35] Scattering factors for neutral atoms and f', $\Delta f'$, f'', $\Delta f''$ were taken from the *International tables for X-ray crystallography*.[36] Details of the crystal data collection, structure solution and refinement are listed in Table given in the Chapter 7 and metrics of some important hydrogen bonds are summarised in Table 1. Crystal packing diagrams are drawn using PLATON.[37]

Cambridge Structural Database

The Cambridge structural Database (April 2000 update, version 5.19, 215 403 entries)[38] was searched for the crystal structures in the top three mirror containing space groups, namely *Pnma*, $P2_1/m$, and *C2/m*,[30] in which a phenyl ring is bisected by a mirror plane. This was done manually from the sub-set of organic structures (screen

57) that contain a phenyl ring in these three space groups. The list of refcodes is given in Table 2.

3.14 References

1. G.R. Desiraju, *J. Mol. Struct.*, **2003**, *656*, 5.
2. A. Nangia and G.R. Desiraju in *Design of Organic Solids. Topics in Current Chemsitry* 198, (ed.) E. Weber, Springer-Verlag, Berlin, **1998**, *198*, p57.
3. G.A. Jeffery, *An Introduction to Hydrogen Bonding*, Oxford University Press, NewYork, **1997**.
4. G.R. Desiraju and T. Stiener, *The Weak Hydrogen Bond in Structural Chemistry and Biology*, Oxford University Press, Oxford, UK, **1999**.
5. (a) P. Gunter, *Nonlinear Optical Effects and Materials*, Springer-Verlag, Heidelberg, **2000**. (b) Ch. Bossard, K. Sutter, Ph. Prétre, J. Hulliger, M. Flörscheimer, P. Kaatz and P. Günter, *Organic Nonlinear Optical Materials* (*Advances in Nonlinear Optics*), Gordon and Breach, Amsterdam, **1995**, vol. 1. (c) J. Zyss and J.-F. Nicoud, *Curr. Opin. Solid State Mater. Sci.*, **1996**, *1*, 533. (d) *Non-linear Optics of Organic Molecules and Polymers*, ed. H.S. Nalwa and S. Miyata, CRC Press, Boca Raton, FL, USA, **1997**. (e) R.G. Denning, *J. Mater. Chem.*, **2001**, *11*, 19.
6. V.A. Russell and M.D. Ward, *Chem. Mater.*, **1996**, *8*, 1654.
7. (a) M. Muthuraman, M. Bagieu-Beucher, R. Masse, J.-F. Nicoud and G.R. Desiraju, *J. Mater. Chem.*, **1999**, *9*, 2233. (b) P.J. Langley, R.T. Bailey, F.R. Cruickshank, A.R. Kennedy, S. Lochran, D. Pugh, J.N. Sherwood, A. Vikki and J.D. Wallis, *J. Mater. Chem.*, **2001**, *11*, 1047. (c) A. Jouaiti, M.W. Hosseini and N. Kyritsakas, *Chem. Commun.*, **2002**, 1898. (d) S. Ferlay, O. Felix, M.W. Hosseini, J.-M. Planeix and N. Kyritsakas, *Chem. Commun.*,

2002, 702. (e) P. Grosshans, A. Jouaiti, V. Bulach, J.-M. Planeix, M.W. Hosseini, *Chem. Commun.*, **2003**, 1336.

8. (a) T. Renouard, H.L. Bozec, S. Brasselet, I. Ledoux and J. Zyss, *Chem. Commun.*, **1999**, 871. (b) V.R. Thalladi, R. Boese, S. Brasselet, I. Ledoux, J. Zyss, R.K.R. Jetti and G.R. Desiraju, *Chem. Commun.*, **1999**, 1639. (c) F. Cherioux, H. Maillotte, P. Audebert and J. Zyss, *Chem. Commun.*, **1999**, 2083. (d) S. Brasselet, F. Cherioux, P. Audebert and J. Zyss, *Chem. Mater.*, **1999**, *11*, 1915. (e) W. Lin, Z. Wang and L. Ma, *J. Am. Chem. Soc.*, **1999**, *121*, 11249. (f) C. Bourgogne, Y. L. Fur, P. Juen, P. Masson, J.-F. Nicoud and R. Masse, *Chem. Mater.*, **2000**, *12*, 1025. (g) K. Senechal, O. Maury, H.L. Bozec, I. Ledoux and J. Zyss, *J. Am. Chem. Soc.*, **2002**, *124*, 4560. (h) G.P. Bartholomew, I. Ledoux, S. Mukamel, G.C. Bazan and J. Zyss., *J. Am. Chem. Soc.*, **2002** *124*, 13480. (i) J. Zyss, I. Ledoux-Rak, H.-C. Weiss, D. Blaser, P.K.Thallapally, V.R. Thalladi and G.R. Desiraju., *Chem. Mater.*, **2003**, *15*, 3063.

9. (a) C.C. Evans, M. Bagieu-Beucher, R. Masse and J.-F. Nicoud, *Chem. Mater.*, **1998**, *10*, 847. (b) M. Malaun, Z.R. Reeves, R.L. Paul, J.C. Jeffrey, J.A. McCleverty, M.D. Ward, I. Asselberghs, K. Clays and A. Persoons, *Chem. Commun.*, **2001**, 49. (c) M. Muthuraman, R. Masse, J.-F. Nicoud and G.R. Desiraju, *Chem. Mater.*, **2001**, *13*, 1473.

10. (a) O.R. Evans, R.-G. Xiong, Z. Wang, G.K. Wong and W. Lin, *Angew. Chem., Int. Ed.*, **1999**, *38*, 536. (b) W. Lin, L. Ma and O. R. Evans, *Chem. Commun.*, **2000**, 2263. (c) R. Thaimattam, C.V.K. Sharma, A. Clearfield and G.R. Desiraju, *Cryst. Growth Des.*, **2001**, *1*, 103. (d) O. R. Evans and W. Lin, *Chem. Mater.*, **2001**, *13*, 2705. (e) O. R. Evans and W. Lin, *Acc. Chem. Res.*, **2002**, *35*, 511.

11. (a) P.J. Langely and J. Hulliger, *Chem. Soc. Rev.*, **1999**, *28*, 279. (b) J. Hulliger, S. W. Roth and A. Quintel, *J. Solid State Chem.*, **2000**, *152*, 49.
12. E.M. Gomes and M. Belsley, *Cryst. Growth Des.*, **2003**, *3*, 445.
13. G.R. Meredith in *Nonlinear Optical Properties of Organic and Polymeric Materials*, Vol. 233, ed. D. J. Williams Washington, DC **1983**, p27.
14. (a) S.R. Marder, J.W. Perry and W.P. Schaeffer, *Science*, **1989**, *245*, 626. (b) S.R. Marder, J.W. Perry, B.G. Tiemann, R.E. Marsh and W.P. Schaefer, *Chem. Mater.*, **1990**, *2*, 685.
15. J.K. Whitesell, R.E. Davis, L.L. Saunders, R.J. Wilson and J.P. Feagins, *J. Am. Chem. Soc.*, **1991**, *113*, 3267.
16. (a) M. Muthuraman, Y. L. Fur, M. Bagieu-Beucher, R. Masse, J.-F. Nicoud, S. George, A. Nangia and G.R. Desiraju, *J. Solid State Chem.*, **2000**, *152*, 221. (b) P.S. Chandrakala, A.K. Katz, H.L. Carrell, P.R. Sailaja, A.R. Podile, A. Nangia and G.R. Desiraju, *J. Chem. Soc., Perkin Trans. 1*, **1998**, 2597.
17. (a) M.D. Hollingsworth and K.D.M. Harris, *in Comprehensive Supramolecular Chemsitry. Solid –State Supramolecular Chemistry: Crystal Engineering*, (eds.) D. D. MacNicol, F. Toda and R. Bishop, Pergamon, Oxford, UK, 1996, vol. **6**, pp. 177. (b) S. Boileau, L. Bouteiller, F. Lauprêtre and F. Lortie, *New J. Chem.*, **2000**, *24*, 845. (c) H.-Y. Liao, S.-Y. Chu, *New J. Chem.*, **2003**, *27*, 421. (d) J. Jai-Nhuknan, A.G. Karipides, J.M. Hughes and J.S. Cantrell, *Acta. Cryst.*, **1997**, *C53*, 455. (e) S. George and A. Nangia, *Acta. Cryst.*, **2003**, *E59*, o901.
18. Examples of the mimicry of strong and weak hydrogen bond synthons: (a) A. Anthony, M. Jaskólski, A. Nangia and G.R. Desiraju, *Chem. Commun.*, **1998**, 2537. (b) A. Anthony, M. Jaskolski and A. Nangia, *Acta Cryst.*, **2000**, *B56*, 512. (c) C. Schmuck and J. Lex, *Eur. J. Org. Chem.*, **2001**, 1519.

19. M.K. Marchewka, S. Debrus and H. Ratajczak, *Cryst. Growth Des.*, **2003**, *3*, 587.

20. (a) G. Aullón, D. Bellamy, L. Brammer, E.A. Bruton and A.G. Orpen, *Chem. Commun.*, **1998**, 653. (b) P.K. Thallapally and A. Nangia *CrystEngComm*, **2001**, 27. (c) L. Brammer, E.A. Bruton and P. Sherwood, *Cryst. Growth Des.*, **2001**, *1*, 277.

21. (a) V.R. Pedireddi, D.S. Reddy, B.S. Goud, D.C. Craig, A.D. Rae and G.R. Desiraju, *J. Chem. Soc., Perkin Trans. 2*, **1994**, 2353. (b) V.R. Vangala, A. Nangia and V.M. Lynch, *Chem. Commun.*, **2002**, 1304. (c) O. Navon, J. Bernstien and V. Khodorkovsky, *Angew. Chem., Int. Ed.*, **1997**, *36*, 601. (d) S.L. Price, A.J. Stone, J. Lucas, R.S. Rowland and A.E. Thornley, *J. Am. Chem. Soc.*, **1994**, *116*, 4910. (e) R. Boese, M.T. Kirchner, J.D. Dunitz, G. Filippini and A. Gavezzotti, *Helv. Chim. Acta.*, **2001**, *84*, 1561.(f) E. Bosch and C.L. Barnes, *Cryst. Growth Des.*, **2002**, *2*, 3234. (g) R.K.R. Jetti, P.K. Thallapally, T.C.W. Mak and A. Nangia, *Tetrahedron*, **2000**, *56*, 6707.

22. A. Nangia, *New J. Chem.*, **2000**, *24*, 1049.

23. V. Vedenova-Adrabinska and E. Janéczko, *J. Mater. Chem.*, **2000**, *10*, 555.

24. Y. In, M. Fujii, Y. Sasada and T. Ishida, *Acta Cryst.*, **2001**, *B57*, 72.

25. H. Schmalle, G. Hänggi and E. Dubler, *Acta Cryst.*, **1990**, *C46*, 340.

26. B. Zarychta, G. Spaleniak and J. Zaleski, *Acta Cryst.*, **2003**, *E59*, o304.

27. S.K. Kurtz and T.T. Perry, *J. Appl. Phys.*, **1968**, *39*, 3798.

28. (a) A.I. Kitaigorodski, *Molecular Crystals and Molecules*, Academic Press, New York, **1973**. (b) C.P. Brock and J.D. Dunitz, *Chem. Mater.*, **1994**, *6*, 1118.

29. T.W.S. Lee, S.J. Rettig, R. Stewart and J. Trotter, *Can. J. Chem.*, **1984**, *62*, 1194.

30. N. Padmaja, S. Ramkumar and M.A. Viswamitra, *Acta Cryst.*, **1990**, *A46*, 725.
31. *PC Spartan Pro 1.0*, Wavefunction Inc., Irvine, **CA USA**, 1999.
32. S. George, A. Nangia and V.M. Lynch, *Acta Cryst.*, **2001**, *C57*, 777.
33. J.A.R.P. Sarma and J.D. Dunitz, *Acta Cryst.*, **1990**, *B46*, 784.
34. A. Altomare, M. Cascarano, C. Giacovazzo and A.J. Guagliardi, J. *Appl. Crystallogr.*, **1993**, *26*, 343.
35. Molecular Structure Corp. (1997-98) teXsan for Windows, v. 1.03, Single Crystal Structure Analysis Software Corp., Woodlands, TX 77381, USA,
36. *International Tables for Crystallography*, ed. A.J.C. Wilson, Kluwer Academic , Dordrecht, **1992**, vol. C, table 4268, pp. 6111-6112;
37. A.L. Spek, Platon97, University of Utrecht, The Netherlands, **1997**.
38. F.H. Allen and O. Kennard, *Chem. Des. Autom. News*, **1993**, *8*, 31.

CHAPTER FOUR

TWO DIMENSIONAL POLAR LAYERS IN SOME *N-meta*-ARYLPYRIMIDINONES

4.1 Introduction

The design of molecular solids with certain desired physical and chemical properties is a difficult challenge in organic solid state chemistry today.[1] The division of organic molecular crystals into two categories, centrosymmetric and non-centrosymmetric, is of primary significance, because the close-packing principle states that crystal structures with an inversion centre pack more efficiently than those which lack this symmetry element.[2] The inversion centre is the only molecular symmetry element that is routinely carried over into the crystal. Crystal engineering[3] is the design of organic solid-state structures with hydrogen bonds and intermolecular interactions. Crystallization of achiral molecules in non-centrosymmetric space groups, is one of the current challenges. The specific solid-state properties often depend on the relative arrangement and orientation of the constituent molecules in the crystal structure. One of the widely exploited crystal engineering approaches is to design and synthesize reliable one- or two-dimensional predefined aggregates. This reduces the task to controlling molecular organization in the remaining third dimension.[4]

The problem of predicting[5] or controlling crystallization of organic molecules to obtain crystals of a desired symmetry is still mostly unsolved. Despite the enormous potential of chiral or polar hydrogen-bonded solids in materials science (*e.g.* ferroelectric, nonlinear optics),[6] there are no general solutions for inducing the self-assembly of achiral molecules into space groups that lack an inversion centre. Using chiral molecules is an obvious approach because the absence of crystallographic inversion center is guaranteed. But due to difficulty in synthesizing chiral molecules materials scientists rely on achiral

molecules to get the desired properties. Moreover issues such as phase matching and the distance of chiral center from the chromophore still have to be addressed. The most preferred noncentrosymmetric space group for chiral molecules is $P2_12_12_1$ but this packing is of no utility in inducing SHG effects because the three polar axes are mutually orthogonal and cancel each other. Although the presence of a chiral handle guarantees a noncentrosymmetric space group it may not necessarily give high SHG efficiency.[3a] In the context of rational approaches to engineering polar materials, Hollingsworth[7] and Hulliger[8] have shown that channel-type inclusion compounds have considerable promise for the parallel alignment of dipolar molecules. Two-dimensional host frameworks have been used to produce polar crystallographic symmetries through crystal engineering of the flexible hydrogen-bonded sheets with banana-shaped pillars.[9] Lin's group has shown that diamondoid networks couple high thermal stability with second harmonic generation (SHG) activity.[6b,10] Diamondoid networks characterize an interesting structural motif for the construction of acentric solids because they are not inclined to pack in centrosymmetric space groups due to the lack of inversion center on each tetrahedral connecting point. In the area of coordination polymers the helix[11,6] is of added interest. Helices have a chiral network irrespective of what the molecular components might be. The inherent chirality in this construction comes from the spatial arrangement rather than the presence of chiral atoms. This illustrates that it is possible to generate chiral crystals (polar) from achiral molecules. Our approach to the problem of polar self-assembly is modular: the 3D polar structure is dissected into 2D polar layers that must stack in a parallel fashion. This simplifies the difficult task of steering the parallel alignment of dipoles to the third dimension. Such a modular build-up of 3D architectures (= 2D + 1D) from functionalized molecules has been successfully implemented in hydrogen bonded solids, *e.g.* lamellar clay-type intercalates with

guanidinium cations and sulfonate anion organic pillars.[9] However, for materials applications single component crystals offer certain advantages compared to inclusion adducts, such as mechanical stability and ease of crystal growth, and hence the motivation to continue the present study.

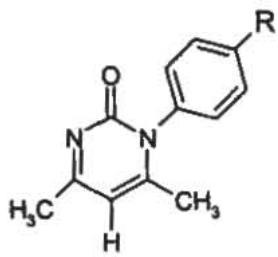

1 = R = H
2 = R = CH_3
3 = R = Cl
10 = R = Ph

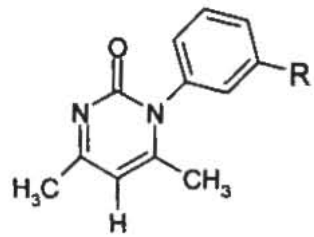

14 = R = Br
15 = R = I
16 = R = NO_2
17 = R = CH_3
18 = R = OCH_3
19 = R = F
20 = R = Cl

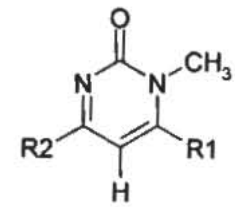

21 = R1 = Me, R2 = Ph
22 = R1 = Ph, R2 = Me

Scheme 1. The compounds referred (**1-3, 10**) as well as studied (**14-22**) in this Chapter.

Even though the problem of predicting or controlling the crystallization of organic molecules to obtain crystals of a desired structure is still unsolved, certain crystal symmetries seem to be favoured by certain types of molecular structures. For example it has long been recognized that *meta*-disubstituted benzenes are more likely to crystallize in polar space groups than are the *ortho* or *para* derivatives.[12] 3-Methyl-4-nitropyridine-1-oxide[13] and *meta*-nitroaniline[14] are two simple molecules where this strategy is successful.

4.2 Objective of the Study

X-ray crystal structures of *N*-arylpyrimidinone **1-3** (aryl = phenyl, tolyl, halophenyl) and their HCl and HNO_3 salts (six compounds studied in Chapter 3) were reported in the previous chapters.[15] Initial experiments with these nine derivatives of phenyl pyrimidinone was to rationally design noncentrosymmetric crystals.[16] Preliminary studies showed that: (1) the recurrence of a C–H···O hydrogen bond chain in these crystals, and its topological resemblance to the α-network in urea compounds (2) the occurrence of mirror plane *m* in eight out of nine structures (3) six of the nine structures have a 2D polar layer arrangement, *i.e.*, the dipoles are associated parallel within a hydrogen bonded layer (4) the charge transfer axis of the chromophore is tilted with the main symmetry operator in point groups 2 or *m* at an angle of ca. 57° (ideal value is 54.74°), a requirement in NLO materials. The X-ray crystal structures of *meta*-phenyl pyrimidinones **14-19** and *N*-methyl pyrimidinones **21** and **22** (Scheme 1) are discussed in this Chapter. A model is proposed to rationalize the recurrence of 2D polar layer assembly in these structures. The polar layers in these structures stack in an anti-parallel fashion and the overall crystal structures are centrosymmetric, *i.e.* adjacent layers are inversion related. Lin's group has reported a structure in which the 2-D sheet lacks a centre of symmetry.[17] This structure is based upon the $Cd_2L^1{}_4(\mu\text{-}H_2O)$ building block. Each unit is connected to four neighbouring units in the *ab* plane to form a 2D-sheet structure (Figure 1). Neighbouring chains are related by the screw axis. However adjacent 2-D sheets are related by inversion and the compound crystallizes in the centrosymmetric space group $P2_1/c$.

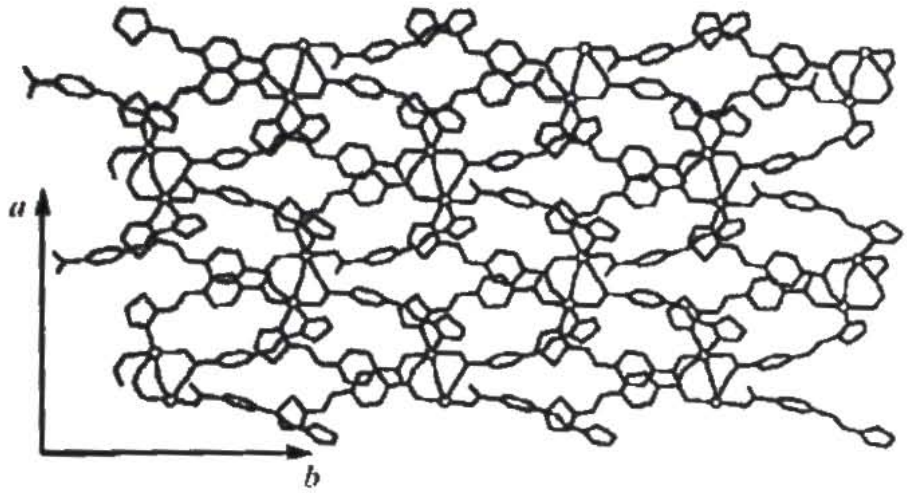

Figure 1. 2-D sheet of $Cd_2L^1_4(\mu\text{-}H_2O)$ which lacks an inversion centre viewed down the *c*-axis. Open circles represent Cd atoms. Hydrogen atoms are not shown for clarity.[17]

Despite getting centrosymmetric strucutres, we have continued our studies because a proper understanding of the factors that control the parallel *vs.* anti-parallel alignment of layers is important for the crystal engineering of polar, non-centrosymmetric solids.[4,18] MacDonald and coworkers[4] has reported the crystal structures of salts of imidazole with a variety of monocarboxylic acids. The crystal structures showed that these salts serve as building block that self assemble *via* ionic O–H···O and N–H···O hydrogen bonds. These strong hydrogen bonds generate polar hydrogen bonded layers. But adjacent layers are inversion related and hence the overall structure is centrosymmetric. But these polar layers could serve as polar scaffolds from which polar crystalline materials can be generated if there is a strategy for alignment of the parallel layers during crystallization. Polar alignment is possible in polymers and electric field,[19] but this thesis is about non-centrosymmetric crystallization through self-assembly. Due to space limit one example of polar layer structure reported by MacDonald and coworkers[4] is shown in figure 2.

(a)

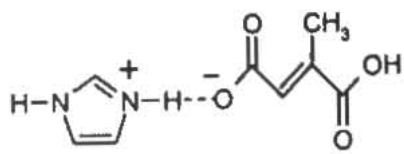

(b)

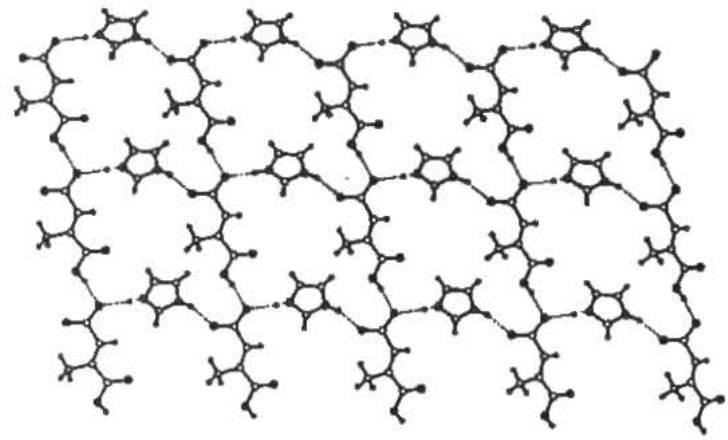

Figure 2. (a) The structure of Imidazolium hydrogen mesaconate. (b) Crystal structure showing 2D polar layer maintained by strong N–H···O hydrogen bonds. Adjacent layers are inversion related.

(a)

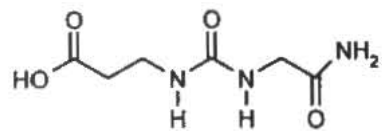

(b)

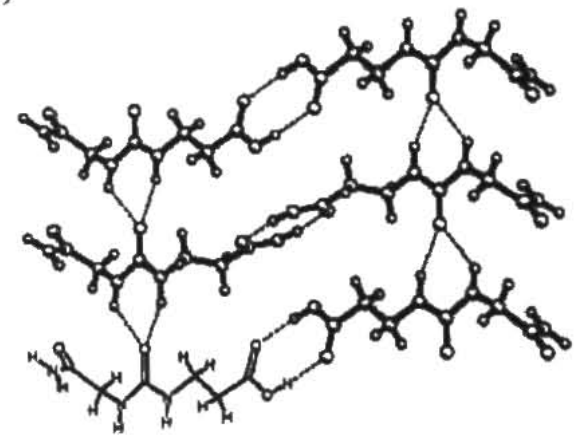

Figure 3. (a) *N*-(Carbamoylmethyl)-*N'*-(2-carboxethyl)urea and (b) the layered structure formed by the molecule through the N–H···O α-network and O–H···O acid dimer.

The goal of the present study is to analyze and understand the parallel alignment of dipolar molecules within a hydrogen-bonded layer. Fowler and Lauher have shown that two-dimensional layered structures can been assembled using strong O–H···O and N–H···O hydrogen bond networks with urea-based building blocks

(Figure 3).[20] We show in this Chapter that the pyrimidinone molecule, which may be viewed as a C–H···O surrogate of urea, results in 2D layered motifs stabilized by weak C–H···O and C–H···halogen interactions (Figure 4).

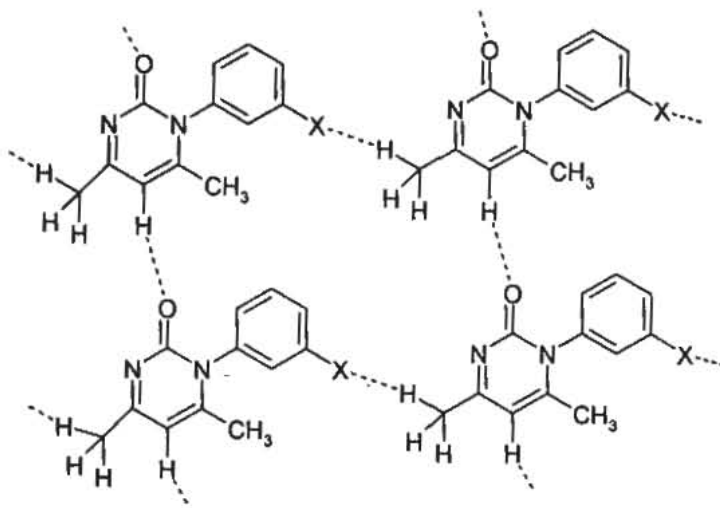

X = Br, I, NO_2, CH_3, OMe, F

Figure 4. The common hydrogen bonded pattern seen in structures discussed in this Chapter.

4.3 Results and Discussion

Phenylpyrimidinone **14-20** was synthesized as described previously.[15] Pyrimidinone **21** and **22** was synthesized by the condensation of *N*-methylurea with benzoyl acetone, followed by the separation of isomers **21** and **22** by column chromatography (see Experimental). Crystallization of these pyrimidinones from different solvents (*e.g.* ethanol, benzene, ethyl acetate, *n*-hexane, and their mixtures) afforded diffraction quality crystals (see Chapter 7). The arrangement of molecules in the eight crystal structures discussed here is mediated by weak hydrogen bonds[21] (C–H···O, C–H···halogen) and van der Waals interactions. The structures are analysed in this sequence: **14***m*-Br, **15***m*-I, **16***m*-NO_2, **17***m*-Me, **18***m*-OMe, **19***m*-F, **21** and **22**. A proper understanding of the significance and hierarchy of different

hydrogen bonds in steering crystal packing is an important theme in contemporary chemical research.[22] The *m*-Cl derivative (**20**) was synthesized but despite our best efforts diffraction quality crystals could not be obtained.

4.4 Crystal Structure of 1,2-Dihydro-*N*-*meta*-bromo-phenyl-4,6-dimethyl-pyrimidin-2-one, 14

In the crystal structure of *m*-Br (**14**) (space group $P\bar{1}$), translation-related molecule are connected by a chain of C–H···O hydrogen bonds (*d*, *θ*: 2.47(4) Å, 154(3)°) along the *a*-axis. These chains are connected by a C–H···Br interaction[23] (3.12(5) Å, 121(3)°) in the lateral direction to produce a rectangular grid network in the (0 1 $\bar{1}$) plane (Figure 5a). It may be noted that the carbonyl groups of *m*-Br (**14**) point in the same direction within a layer, referred to as 2D-polarity in this thesis. In effect, linear chains of C–H···O and C–H···Br interactions run across to produce a polar sheet structure. The interlayer region has an abundance of C–H···O/C–H···Br interactions (Table 1) and an overall van der Waals close packing. The crystal structure is centrosymmetric because adjacent layers are inversion-related (Figure 5b).

The *N*-phenyl ring in *m*-Br (**14**) is tilted with respect to the pyrimidinone ring at an angle of 74.8(5)°. In symmetrical phenyl derivatives **1-3** (*e.g*, Ph, *para*-tolyl, *para*-chlorophenyl), the aryl and heterocyclic ring are exactly perpendicular to each other such that the pyrimidinone ring lies on the mirror plane and the *m* plane bisects the phenyl ring. The orthogonal orientation of aryl and pyrimidinone rings in symmetrical derivatives of pyrimidinone was explained by calculating the energy of the isolated molecule as a function of the interplanar dihedral angle (τ/°) in RHF 3-21G* basis set.[15b]

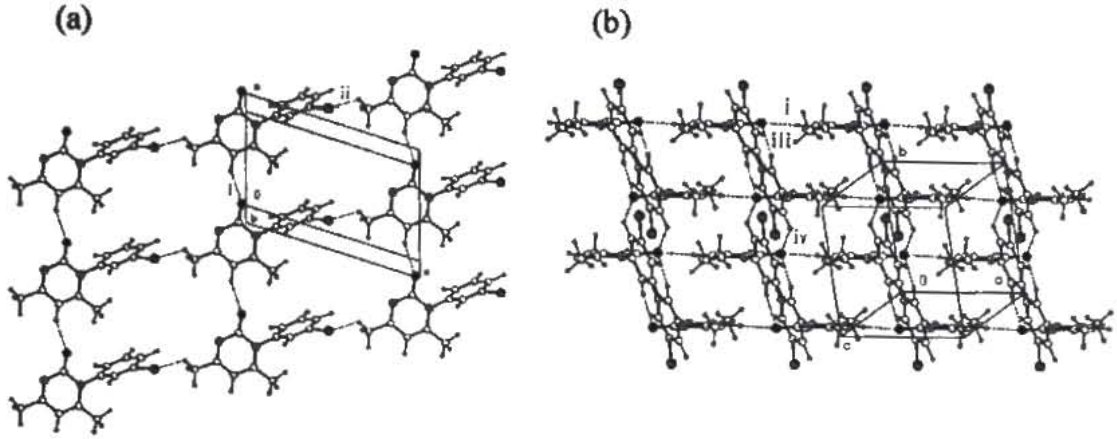

Figure 5. Crystal structure of *m*-Br (**14**). (a) C–H···O hydrogen-bonded 1D chain (interaction i) and C–H···Br interaction in the lateral direction (interaction ii). Note the parallel alignment of molecules in the 2D layer. (b) Centrosymmetric arrangement of adjacent layers mediated by interactions iii, iv.

Table 1. Hydrogen bond metrics in crystal structures

Compound	Hydrogen bond[a]	*d*/Å	*D*/Å	*θ*/deg
14(*meta*-Br)	C3–H1···O1(i)	2.47(4)	3.230(5)	154(3)
	C6–H7···Br1(ii)	3.12(5)	3.723(5)	121(3)
	C12–H11···O1(iii)	2.67(4)	3.472(7)	167(4)
	C8–H8···O1(iv)	2.87(4)	3.477(6)	135(3)
	C6–H7···Br1(v)	3.28(5)	3.993(6)	131(3)
15(*meta*-I)	C3–H1···O(i)	2.43(5)	3.267(7)	154(4)
	C6–H6···I(ii)	3.01	3.882(9)	154
	C5–H4···O(iii)	2.58(6)	3.459(7)	154(4)
	C12–H11···O(iv)	2.52(6)	3.41(1)	165(5)
	C8–H8···O(v)	2.79(6)	3.43(1)	124(4)
16(*meta*-NO_2)	C3–H1···O1(i)	2.20	3.222(6)	156
	C6–H6···O3(ii)	2.55	3.538(6)	152
	C5–H4···O1(iii)	2.60	3.511(6)	142
	C6–H5···N3(iv)	2.70	3.730(8)	159
	C6–H5···O3(v)	2.61	3.677(8)	172
	C8–H8···O1(vi)	2.56	3.347(6)	129
	C12–H11···O1(vii)	2.39	3.423(6)	158
17(*meta*-Me)	C3–H1···O1(i)	2.40	3.272(3)	156
	C5–H2···O1(ii)	2.81	3.655(3)	144

	C12–H11···N2(iii)	2.69	3.560(4)	140
	C8–H8···O1(iv)	2.98	3.900(4)	170
	C11–H10···O1(v)	2.90	3.581(5)	123
18(*meta*-Ome)	C3–H1···O1(i)	2.45	3.366(3)	161
	C8–H3···O2(ii)	2.70	3.455(4)	137
	C6–H2···N2(iii)	2.46	3.391(4)	165
	C10–H5···O1(iv)	2.61	3.267(4)	126
19(*meta*-F)	C3–H1···O1(i)	2.30	3.166(6)	154
	C6–H2···O1(ii)	2.66	3.536(5)	151
	C9–H5···F1(iii)	2.59	3.194(7)	125
4-Me,6-Ph	C3–H10···O1(i)	2.50(2)	3.409(4)	168(1)
(**21**)	C12–H15···O1(ii)	2.48(3)	3.42(1)	164(1)
	C5–H3···N2(iii)	2.75(3)	3.691(2)	174(1)
	C6–H4···O1(iv)	2.51	3.392(3)	154
	C6–H9···O1(v)	2.57	3.392(3)	135
	C5–H2···O1(vi)	2.53(3)	3.512(9)	161(1)
4-Ph,6-Me	C3–H1···O1(i)	2.38	3.368(4)	149
(**22**)	C8–H8···N1(ii)	2.75	3.648(4)	156
	C6–H6···O1(iii)	2.74	3.655(5)	158

[a]For illustration of interactions (i), (ii), (iii), *etc.*, see the figures

The energy *vs.* dihedral angle curve, with a minimum at $\tau = 90°$, is very shallow in the region $80 < \tau < 100°$ (refer Figure 11 in Chapter 3). A slight deviation from the perpendicular conformation is tolerated if such a tilt results in favourable interactions elsewhere in the crystal. The weak C–H···Br interaction in the [0 1 $\bar{1}$] direction (Figure 5a, Table 1, interaction (ii)) is optimized as a result of the slight tilt of phenyl ring in *m*-Br (**14**). This ability to preserve architectural control when making a change to the molecular components is relevant in crystal engineering while designing robust molecular framework. In the unsymmetrical *m*-Br (**14**) derivative, both the molecular and the crystal symmetry are lower (space group $P\bar{1}$) compared to *p*-Cl (**3**), *p*-Cl·HCl (**7**) and *p*-Cl·HNO_3 (**8**) (*Pnma*, $P2_1/m$ and *Pnma*).[15] Thus, the *meta* derivatives crystallizes in the triclinic system while the symmetrical *para* analogues crystallize in monoclinic and orthorhombic systems with a mirror plane.

4.5 Crystal Structure of 1,2-Dihydro-*N*-*meta*-iodo-phenyl-4,6-dimethylpyrimidin-2-one, 15

The compound crystallizes in the space group $P\bar{1}$. The translation related molecules are connected through an infinite chain of C–H···O hydrogen bond (2.43 Å, 154°) along the *c*-axis. The parallel chains are in turn connected through a lateral C–H···I interaction resulting in a two dimensional polar layer in the (1 1 0) plane (Figure 6). Adjacent layers are inversion related and they are stabilized by C–H···O hydrogen bonds (interactions iii and iv). The (O)C–N–C–C(Ph) torsion angle (τ) is 74.0(11)°. Crystal structure of *m*-I (**15**) is isostructural with that of *m*-Br (**14**) and *m*-NO_2 (**16**) having the same space group but different cell axes and angles (see Chapter 7).

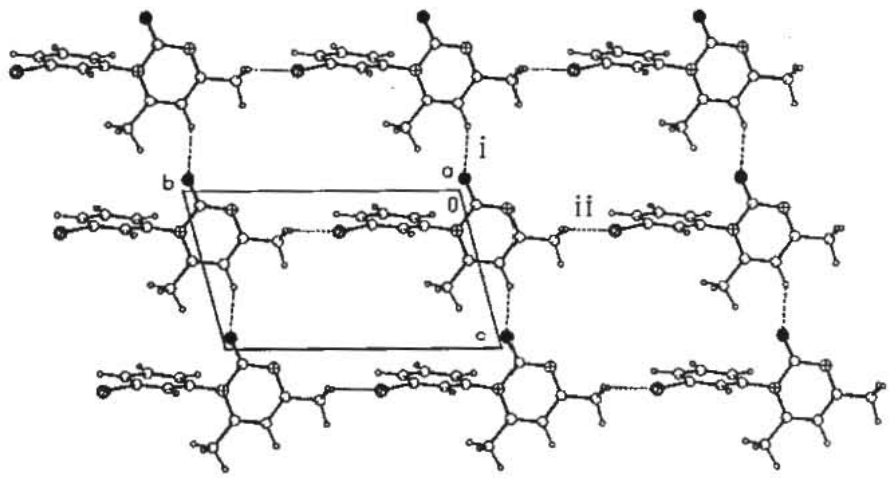

Figure 6. The 2D polar layer arrangement in *m*-**I** (**15**) mediated by C–H···O and C–H···I interactions in the *bc*-plane.

4.6 Crystal Structure of 1,2-Dihydro-*N*-*meta*-nitro-phenyl-4,6-dimethylpyrimidin-2-one, 16

The compound crystallizes in the space group $P\bar{1}$. A linear chain of C–H···O hydrogen bond (2.20 Å, 156°) connects the translation related molecules along the *a*-axis. The phenyl ring is inclined at an angle of 78.0(4)° with the heterocyclic

ring. The one dimensional chains are connected laterally by a C–H···O hydrogen bond formed between the oxygen atom of the nitro group and hydrogen atom from the methyl group in the heterocyclic ring to form a 2-dimensional polar layer (Figure 7). Inter layer regions are dominated by C–H···O hydrogen bonds formed between the hydrogen atoms in the *ortho* position in the aryl and the carbonyl oxygen in the heterocyclic ring. The above analyzed structures illustrates that the basic building block of the three dimensional frame work should be the 2D polar layer. The layered structures are explained as 1D polar chains fused along the edges by lateral C–H···O/Hal interactions.

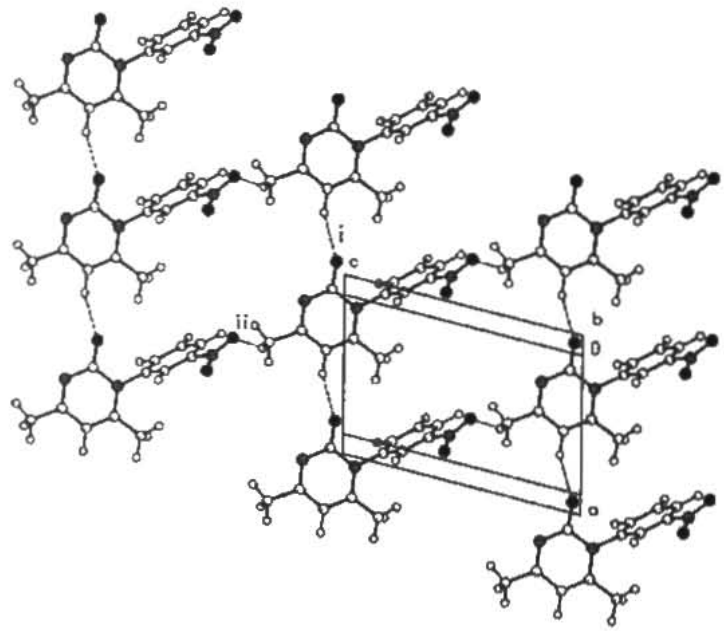

Figure 7. The 2D polar network in *m*-NO_2 **(16)**. Note the similarity with *m*-Br **(14)** and *m*-I **(15)** structures.

Uniqueness in the networks of lateral C–H···halogen and C–H···O(nitro) interactions highlights the importance of weak hydrogen bonds in controlling the self-assembly in these crystal structures. The structures explained (in Chapter 2 and Chapter 3) and those that follows illustrate that the inherent dimensionality and

supramolecular connectivity in the family of pyrimidinones. The weak hydrogen bonds involved in the assembly are flexible enough to permit the puckering of the layers without an appreciable change in the near-linear geometries of the H bonds. The calculated volume of Br, I and NO_2 groups is nearly similar (26, 32, 29 $Å^3$),[24] and so is the arrangement of molecules in the crystal. This also signifies the robustness of the recurring C–H···O hydrogen-bonded chain synthon (Figures 5–7) in directing the arrangement of molecules. While the individual C–H···O interactions are weak (2–3 kcal/mol), the chain synthon constructed with these weak hydrogen bonds is robust enough to sustain self-assembly in a number of structures.

4.7 Crystal Structure of 1,2-Dihydro-*N*-*meta*-tolyl-4,6-dimethylpyrimidin-2-one, 17

The compound *m*-Me (**17**) crystallizes in the space group group $P2_1/n$. The crystal structure contains the C–H···O hydrogen bond chain along the *a*-axis, further stabilized by a (Me)C–H···O interaction (2.40 Å, 156°; 2.81 Å, 144°) which connects the translation related molecules as shown in figure 8. The tolyl ring in *m*-Me rotates about the C–N bond such that its Me group moves away from the Me group on the pyrimidinone ring of an adjacent molecule. Thus it is the Me···Me repulsion and not the C–H···O/halogen attraction that determines the conformation in this crystal structure. Although the conformation of the *N*-tolyl moiety is different from the Br-Ph (**14**), I-Ph (**15**) and NO_2-Ph (**16**) groups, the 2D polar layer arrangement is a recurring pattern in all these structures. The details of crystal packing in *m*-Me are different from *m*-Br and *m*-I structures although methyl–halogen mimicry[25] is common phenomenon in crystal structures where their groups are exchanged. If the methyl and halogen structures are different, as in this case, it is usually a result of specific, directional interactions controlling the crystal packing and not mere space filling of hydrophobic groups. It is likely that the weak C–H···halogen interaction and Me···Me repulsion are responsible for the differences in crystal packing of

halogen and methyl substituted analogues. It has been possible to probe the role of such subtle effects in crystal packing because a series of molecules with minor substituent variations are synthesized, and their crystal packing analyzed systematically.

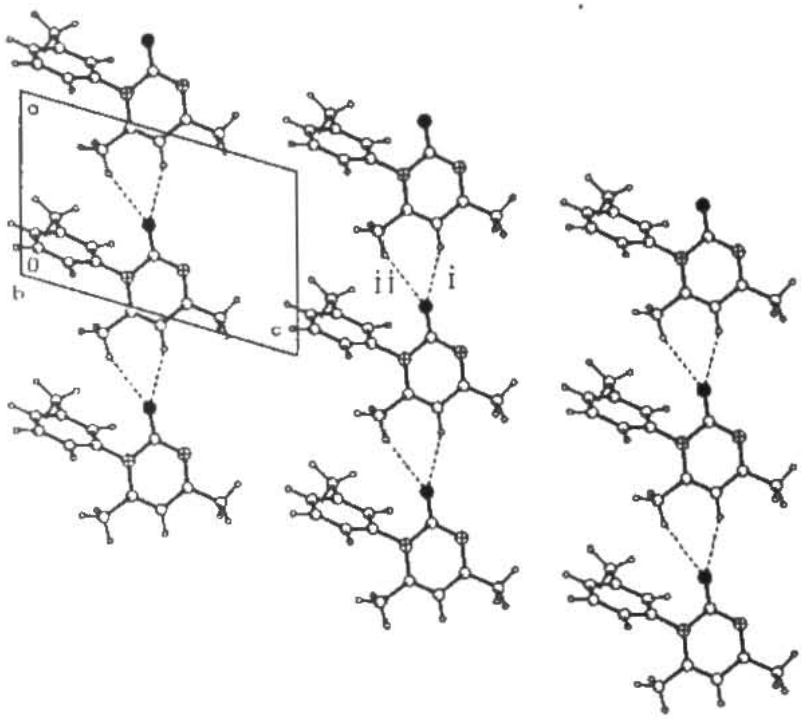

Figure 8. 2D polar layer in *m*-Me (**17**). The conformation of the *m*-tolyl ring is different compared to the orientation of the phenyl ring in Figures 5 and 6

4.8 Crystal Structure of 1,2-Dihydro-*N*-*meta*-anisyl-4,6-dimethylpyrimidin-2-one, 18

The compound *m*-OMe (**18**) crystallizes in the space group *C*2/*c*. Translation-related molecules are connected *via* the C–H···O chain synthon (2.45 Å, 161°) (Figure 9a) and the OMe group is involved in forming (Ph)C–H···O dimers between inversion-related molecules (2.70 Å, 137°) (Figure 9b). All this suggests that the C–H···O chain supramolecular synthon is an invariant structural motif in the 2D-polar layer pattern. Other weak hydrogen bonds in the lateral direction, such as

C–H···O and C–H···halogen, determine the overall 3D structure. There is thus a hierarchy of interactions even within the weak hydrogen bond category. The 1D chain and the 2D layer interactions are predictable, but the factors that control the stacking of layers are not fully understood.[6b]

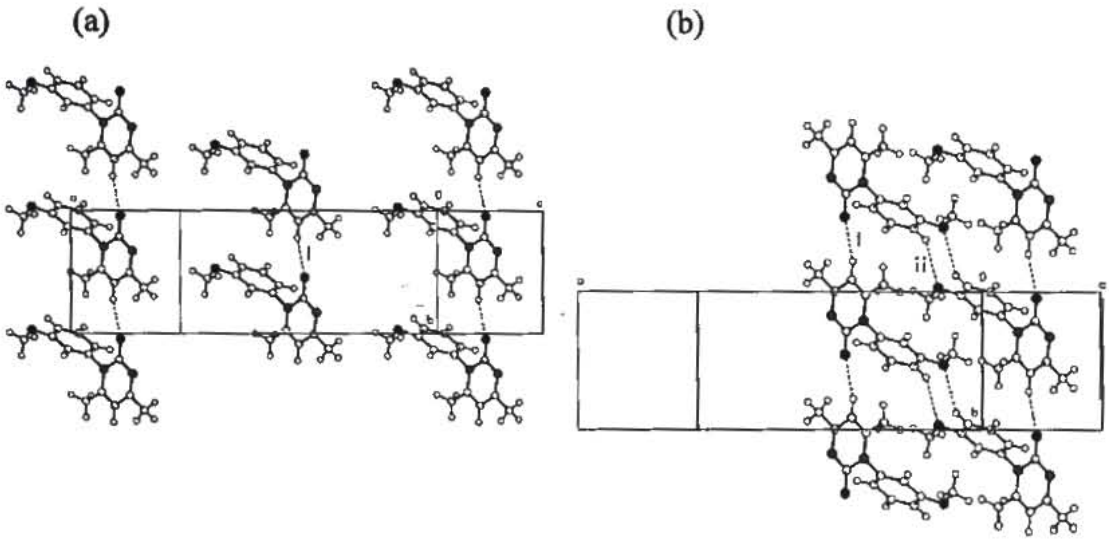

Figure 9. (a) 2D polar layer in *m*-OMe (**18**) with 1D chains oriented in the same direction. (b) C–H···O interactions between the anisyl rings of inversion related molecules.

4.9. Crystal Structure of 1,2-Dihydro-*N*-*meta*-fluorophenyl-4,6-dimethyl-pyrimidin-2-one, 19

Crystallization of *m*-F (**19**) from benzene/ethyl acetate afforded diffraction quality single crystals that solved and refined in the space group *Pnma*. The *meta*-fluoro derivative shows structural features that serve as a bridge between the unsymmetrical *meta* compounds and the symmetrical *para* series. Although the molecule has an unsymmetrical phenyl substitution, the crystal system has a mirror plane *m*, similar to the unsubstituted and *para* compounds (H (**1**), *p*-Me (**2**), *p*-Cl

(**3**)).[15] The pyrimidinone molecule resides on the mirror plane and this plane bisects the *N*-*m*-fluorophenyl ring (Figure 10a). This structure is isomorphous with *p*-Me (**2**), *p*-Cl (**3**) (*Pnma*) in that the 1D chains are oriented parallel within the 2D-polar layer. However, it is different from the structure of H (**1**) (*Pbcm*) in which 1D chains are aligned anti-parallel in the layer. Normally, replacement of H with F in a molecule does not result in significant structural differences[26] because the van der Waals radius of these atoms is similar (H_{vdW} 1.20, F_{vdW} 1.47 Å). However, when the H and F structures are different, specific C–H···F interactions may be involved. Analysis of the inter-layer packing in *m*-F (**19**) shows that there is a (Me)C–H···F[27] interaction (2.59 Å, 125°) (Figure 10b) between inversion-related molecules. The F atom is refined with a site-occupancy of 0.5. The pyrimidinone ring atoms reside on the mirror plane and are fully ordered. A possible reason for the 50% occupancy of fluorine could be that in this way the unsymmetrical phenyl ring conforms to the higher mirror symmetry in the crystal. This suggests that the presence of mirror plane *m* in the crystal is an important steering factor. This may be traced to the pyrimidinone molecule having the stable bisected-phenyl conformation.[15b] Normally, molecules do not reside on the *m* special position because this arrangement decreases packing efficiency by 2–3%.[2a,24] However, retention of *m* or 2 symmetry is thermodynamically advantageous because the molecules are symmetrically arranged. On the whole, a number of factors such as molecular symmetry, energy of the conformation in the crystal, and weak intermolecular interactions (C–H···O, C–H···halogen) determine the final packing motif in the crystal structure. Regarding the nature of fluorine disorder in the crystal, *i.e.* whether it is static or dynamic,[28] this issue can be answered only with variable low-temperature X-ray diffraction. The present X-ray data were collected at around room temperature.

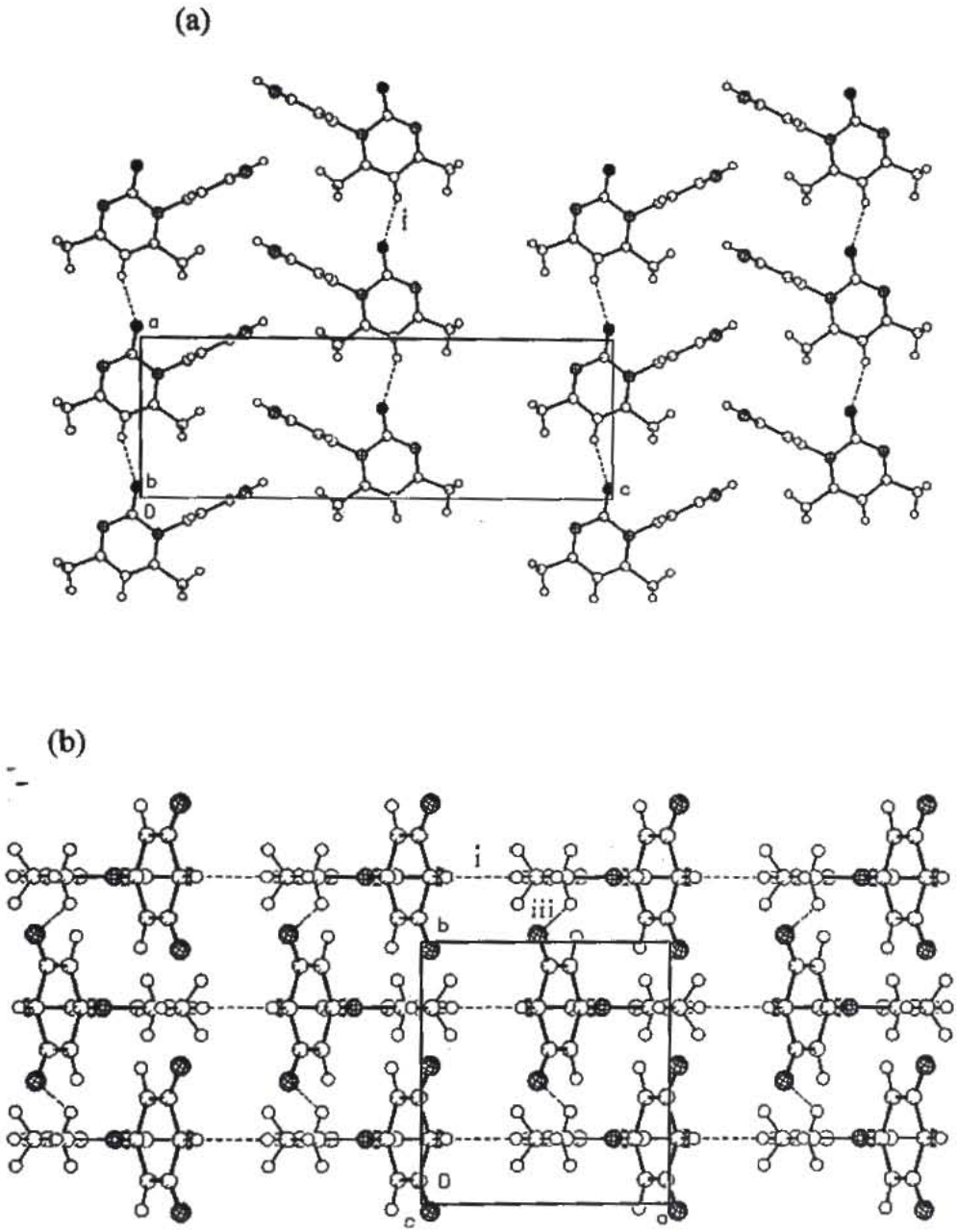

Figure 10. Crystal structure of *m*-F (**19**). (a) Parallel alignment of 1D chains sustained by C–H···O interactions i. (b) Interlayer C–H···F interaction iii. The F atom has 0.5 occupancy in each location.

4.10 Crystal Structure of 1,2-Dihydro-*N*-methyl-4-methyl-6-phenylpyrimidin-2-one, 21

The unsymmetrical molecules, 4-Me-6-Ph analogue **21** and 4-Ph-6-Me analogue **22**, were synthesized to extend conjugation of the phenyl ring with the pyrimidinone heterocycle to enhance the molecular hyperpolarizability. Since the structures of these two isomers could not be clearly ascertained by NMR spectroscopy (see experimental), the final assignment was made after X-ray diffraction. The structures **21** and **22** was confirmed from the ORTEP plots (Figure 11a). In **21** (*Pbca*), the molecules are organized in a zigzag array. The C–H···O hydrogen bonds connect the screw related molecules along the *c*-axis that extend into corrugated sheets (Figure 11b). The *N*-Me group is disordered.

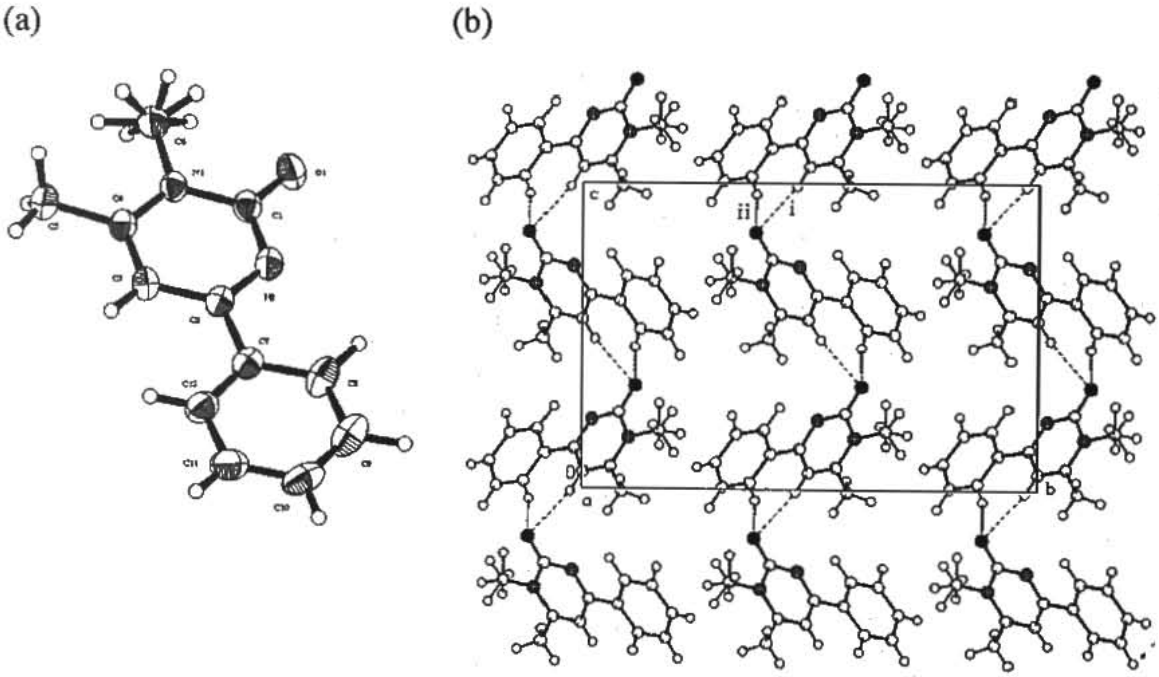

Figure 11. (a) ORTEP plot of *N*-methyl-4-methyl-6-phenylpyrimidin-2-one **21**. *N*-Me group is disordered. (b) 2D polar corrugated layer in **21**.

The corrugation of the layer is mainly because of the steric requirements of the molecule. The phenyl ring on the C-4 position does not permit coplanar arrangement of the C–H···O chains along the *c*-axis because of steric crowding (ORTEP numbering is followed in the diagram **11a**). This increase in dimensionality through corrugation with retention of supramolecular connectivity can be exploited in crystal engineering. By substituting appropriate functionalities on the molecule the control on the crystal packing can be increased

4.11 Crystal Structure of 1,2-Dihydro-*N*-methyl-4-phenyl-6-methylpyrimidin-2-one, 22

In the crystal structure of **22** the molecule crystallizes in the space group *C2/c* with one molecule in the asymmetric unit. ORTEP diagram of **22** is shown in figure 12a. Translation related molecules are connected through a chain of C–H···O hydrogen bond (2.38 Å, 149°). The C–H···O chain is preserved in this structure too (Figure 12b). The hydrogen-bonded layers are 2D polar in both crystal structures (**21** and **22**), suggesting that the parallel alignment of 1D chains in a 2D-layer motif is a characteristic feature of the pyrimidinone family. To summarise, variation in the position of alkyl and aryl residues on the molecular skeleton does not disturb the main C–H···O hydrogen bond synthon and the 2D polar layer organization in these crystal structures.

Crystals are build from molecules and one might expect that the crystal structures can be predicted from its molecular structure. A particular molecular structure can yield more than one crystal structure. Therefore the prediction of crystal structure becomes difficult. Further a change in the molecular structure or inclusion of other molecular species or a change in the functional group may result in a different crystal structure. A study of several compounds with varied structures

in a family of pyrimidinones reveals that the weak C–H···O hydrogen bonds which templates molecular assembly is robust enough to maintain the architecture.

The main idea behind synthesizing molecules **21** and **22** was to extend the conjugated chromophore compared to *N*-arylpyrimidinone. While 2D polarity is routinely achieved, the absence of 3D non-centrosymmetry in these crystals makes further attempts to optimize the molecular hyperpolarizability for inducing SHG effects a future goal.

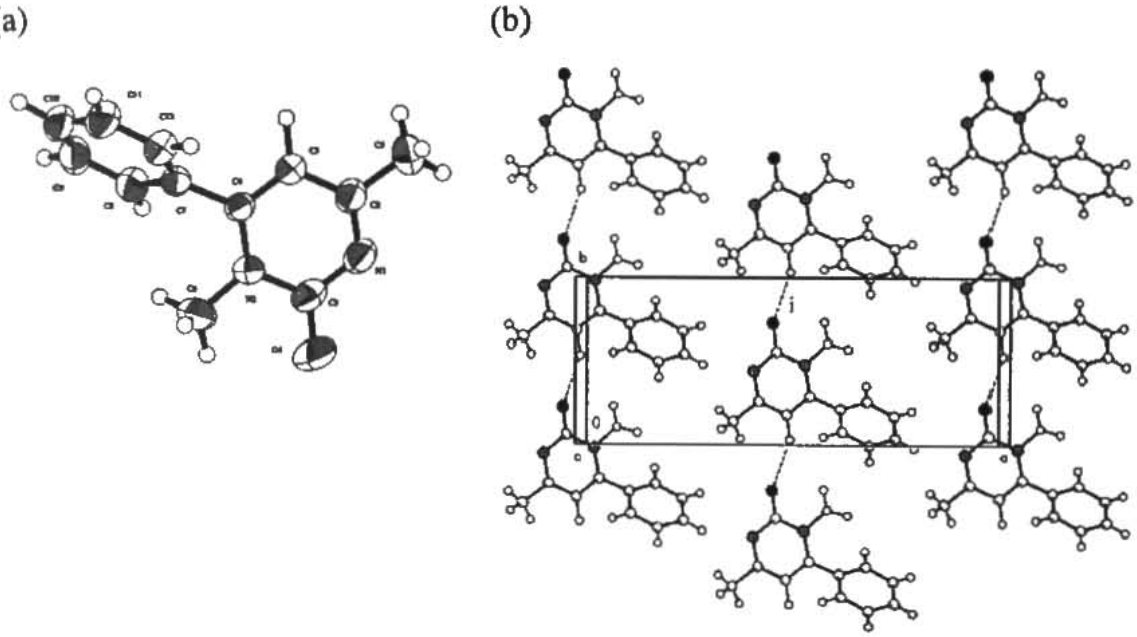

Figure 12. (a) ORTEP plot of *N*-methyl-4-phenyl-6-methylpyrimidinone **22**. (b) 2D polar assembly in **22**.

The task of controlling the parallel alignment of 1D dipoles or 2D polar layers in non-centrosymmetric space groups (*e.g.* $P2_1$, *Fdd*2, $Pna2_1$, *Imm*2), namely crystals that lack an inversion centre, is still a difficult challenge with no general solution to the problem.

4.12 Model for 2D Polar Layer

The occurrence of 2D polar layers is a repeating pattern in the pyrimidinone family of crystal structures. The changes in substitution range from simple exchange of groups on the *N*-aryl moiety to the replacement of phenyl with methyl groups on the pyrimidinone ring. While the space groups and detailed packing motifs vary from crystal to crystal, the 1D chain of C–H···O hydrogen bonds and the 2D polar layer assembly are invariant structural features. This encouraged us to understand the phenomenon of 2D polarity in terms of the molecular structure in pyrimidinones (molecules discussed in Chapter **2** to Chapter **4**) and the robust C–H···O hydrogen bond synthon in these crystals. This model is based on the fact that molecules of pyrimidinones studied so far form a linear array of C–H···O hydrogen bonds. Such chains may then align either in a parallel fashion (2D-polarity) or in an anti-parallel arrangement (a common layer motif). Four possible arrangements of hydrogen bonded chains of pyrimidinone molecules seen in a 2D layer are shown in figure 13. Motifs (a, b) are 2D polar while the chains are aligned anti-parallel in (c, d). The most common pattern in pyrimidinone crystals is depicted in (a). Translation-related molecules form the C–H···O hydrogen bonded chain (in the direction of the arrow) and such chains are further connected through weak hydrogen bonds or van der Waals interactions involving the phenyl ring. This 2D-polar motif is present in eight structures, three structures are discussed in Chapter 3 (H·HCl (**4**), *p*-Me·HCl (**6**), *p*-Cl·HCl (**7**)),[15b] and five in this Chapter (*m*-Br (**14**), *m*-I (**15**), *m*-NO_2 (**16**), *m*-Me (**17**), *m*-Ome (**18**)). In motif (b), a two-fold screw axis or a glide plane parallel to the polar (arrow) direction relates molecules in adjacent chains. This results in the stable herringbone geometry between phenyl rings and methyl groups close-pack on the other side. The 2D-polar motif (b) is present in four structures (*p*-Me (**2**), *p*-Cl (**3**), *p*-Ph (**10**) and *m*-F (**19**)) (two from Chapter 2, one from Chapter 3 and one from this Chapter). In the anti-parallel arrangement (c), the interactions are similar to (a) but

the symmetry operation that relates the hydrogen-bonded molecules is different. A 2_1-screw axis or a glide-plane perpendicular to the polar (arrow) direction relates adjacent chains that run in opposite directions within a layer. Only three structures

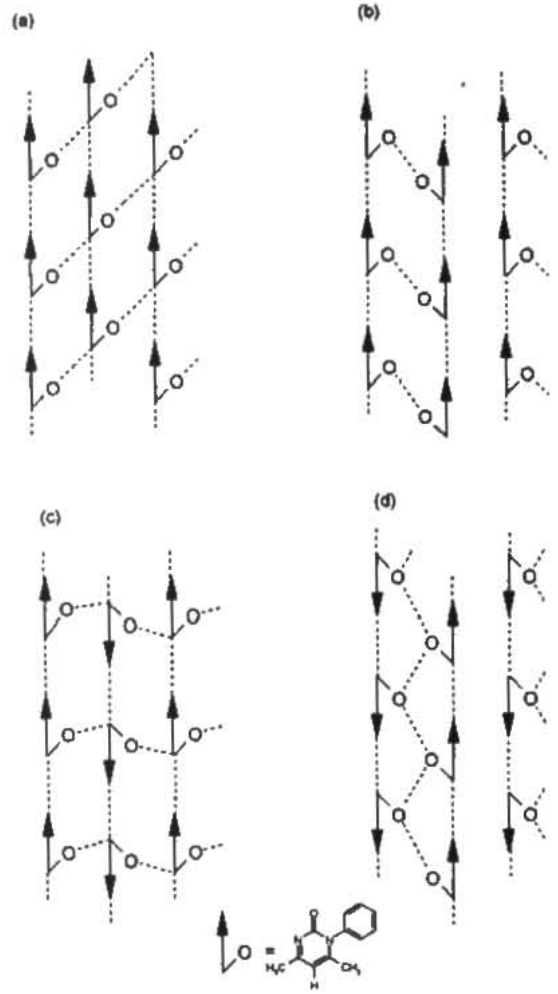

Figure 13. Model to explain the recurrence of the 2D polar layer arrangement in arylpyrimidinones studied in Chapters **2-4**. The 1D chain is constructed with C–H···O interactions in all the cases while the lateral interactions in the layer are different. (a) Parallel alignment of 1D chains and the lateral C–H···X interactions are simultaneously optimized. (b) Parallel alignment of 1D chains and herringbone motif between phenyl groups. (c) Anti-parallel alignment of 1D chains, the lateral C–H···X interactions is bent. (d) Anti-parallel alignment of 1D chains with neighbouring phenyl groups being inversion-related. Motif a is present in over half the structures studied (8/15), motif b in 4 structures and motif c in 3 structure. Motif d is not found in any structure.

(H (**1**), *p*-Me·HNO_3 (**9**), *p*-Cl·HNO_3 (**8**)) (one from Chapter two and two from Chapter three) belong to this category. Motif (c) is not preferred, despite having similar interactions and void size compared to motif (a), because the methyl group in pyrimidinones is not correctly placed within the molecular tapes for lateral interaction with a substituent on the phenyl group (dotted lines), as depicted in (c). A hydrogen bond between the phenyl ring and pyrimidinone heterocycle in the lateral direction would be bent in (c). The centrosymmetric layer (d), with adjacent chains related by an inversion centre, is not observed in any structure. This is because inversion symmetry is not compatible with the ubiquitous herringbone T-geometry between phenyl rings in the solid state.[29] Even though inversion-related phenyl rings can engage in π–π stacking, this motif may not be favoured in the present case because quadrupole–quadrupole interaction (charge-transfer component) between like phenyl rings may be minimal. Thus the dominant 2D polar layer arrangement is rationalized through motifs (a) and (b) that account for 12 of the 15 crystal structures studied. The proposed model is specific to the molecular structure of *N*-aryl pyrimidinones.

4.13 Conclusions

This study demonstrates the feasibility of crystal engineering noncentrosymmetric solids based on 2-dimensional polar layers. However control of parallel arrangement of 2D polar layers in the third dimension is still a challenge and has to be tackled in future studies. It has been shown that non-centrosymmetric crystal packing may be achieved with 1D chains sustained by C–H···N interactions[30] and in 2D layers connected via C–H···O interactions.[31] The parallel alignment of dipoles in these crystal structures is explained through the weak hydrogen bonds.

Two-dimensional layered structures assembled with O–H···O and N–H···O hydrogen bonds in crystals of uronium salts,[18] imidazole carboxylates[4] and urea

derivatives[20] have been reported. We have shown in this Chapter the recurrence of 2D polar networks in *N*-aryl pyrimidinone crystals, thereby emphasizing that robust and reliable C–H···O synthons offer an equally effective crystal design theme[32] as the strong hydrogen bonds. The role of steric and/or electronic effects in hydrogen bonding and crystal packing has been examined by the systematic variation of functional groups in a family of structures.

4.14 Experimental

Synthesis

The appropriate *N*-aryl urea used in the following reactions was prepared using Vogel's procedure.[33] A general procedure for the synthesis of *N*-arylpyrimidinone is given below. Yields are unoptimized and reported for purified products isolated after column chromatography. NMR spectra were recorded on Bruker 200 MHz spectrometer in $CDCl_3$ solvent. Peaks are reported in δ (ppm) and *J* coupling in Hz, followed by proton integration. IR spectra were recorded as KBr wafer, peaks are reported in cm^{-1}.

1. 1,2-Dihydro-*N*-*meta*-bromo-phenyl-4,6-dimethylpyrimidin-2-one, 14

Acetyl acetone (900 mg, 0.92 ml, 9 mmol) and *N*-*meta*-bromophenyl urea (500 mg, 3 mmol) were taken in 10 ml of EtOH and 1.8 ml of conc. HCl was added. The reaction mixture was refluxed for 4 h, and then cooled in ice, and the precipitated solid was filtered and washed with cold EtOH to obtain the hydrochloride salt. The salt was dissolved in 10 ml of water and neutralized with NaOH solution (0.7 g in 5 ml of water) at 0 °C. Extraction of the aqueous layer with chloroform and evaporation of the solvent afforded the product (17% yield) that was crystallized from ethyl acetate/hexane mixture. M.p. 179–183 °C. ^{1}H-NMR ($CDCl_3$):

δ 7.65 (d, J = 8, 1H), 7.40 (s, 1H), 7.34 (t, J = 8, 1H), 7.18 (d, J = 8, 1H), 6.19 (s, 1H), 2.41 (s, 3H), 2.05 (s, 3H). IR (KBr): 3053, 1653, 1527 cm^{-1}.

A similar procedure was followed for other derivatives **15-19**.

2. 1,2-Dihydro-*N-meta*-iodo-phenyl-4,6-dimethylpyrimidin-2-one, 15

Crystallized from ethyl acetate/hexane mixture, m.p. 168–170 °C, yield 26%. ^{1}H-NMR ($CDCl_3$): δ 7.85 (d, J = 8, 1H), 7.65 (s, 1H), 7.29 (d, J = 8, 1H), 7.25 (t, J = 8, 1H), 6.19 (s, 1H), 2.43 (s, 3H), 2.05 (s, 3H). IR (KBr): 3232, 1643, 1531 cm^{-1}.

3. 1,2-Dihydro-*N-meta*-nitro-phenyl-4,6-dimethylpyrimidin-2-one, 16

Crystallized from methanol, m.p. 236–240 °C, yield 34%. ^{1}H-NMR ($CDCl_3$): δ 8.37 (d, J = 8, 1H), 8.15 (s, 1H), 7.75 (t, J = 8, 1H), 7.65 (d, J = 8, 1H), 6.25 (s, 1H), 2.42 (s, 3H), 2.09 (s, 3H). IR (KBr): 3082, 1649, 1525, 1346 cm^{-1}.

4. 1,2-Dihydro-*N-meta*-tolyl-4,6-dimethylpyrimidin-2-one, 17

Crystallized from benzene/ethyl acetate mixture, m.p. 186–189 °C, yield 25%. ^{1}H-NMR ($CDCl_3$): δ 7.41 (t, J = 8, 1H), 7.30 (d, J = 8, 1H), 7.05 (d, J = 8, 1H), 7.10 (s, 1H), 6.20 (s, 1H), 2.45 (s, 6H), 2.05 (s, 3H). IR (KBr): 3049, 1651, 1531 cm^{-1}.

5. 1,2-Dihydro-*N-meta*-anisyl-4,6-dimethylpyrimidin-2-one, 18

Crystallized from benzene/ethyl acetate mixture, m.p. 137–141°C, yield 23%. ^{1}H-NMR ($CDCl_3$): δ 7.40 (t , J = 8, 1H), 7.05 (d, J = 8, 1H), 6.80 (d, J = 8, 1H), 6.79 (s, 1H), 6.18 (s, 1H), 3.85 (s, 3H), 2.40 (s, 3H), 2.05 (s, 3H). IR (KBr): 3053, 1668, 1535 cm^{-1}.

6. 1,2-Dihydro-*N-meta*-flouro-phenyl-4,6-dimethylpyrimidin-2-one, 19

Crystallized from benzene/ethyl acetate mixture, m.p. 175–183 °C, yield 26%. ^{1}H NMR ($CDCl_3$): δ 7.50 (dd, J = 8,7, 1H), 7.20 (dd, J = 8,7, 1H), 6.97 (d, J =

8, 1H), 6.91 (d, J = 8, 1H), 6.19 (s, 1H), 2.45 (s, 3H), 2.01 (s, 3H). IR (KBr):3065, 1651, 1533 cm^{-1}.

7. 1,2-Dihydro-*N*-methyl-4-methyl-6-phenylpyrimidin-2-one and 1,2-Dihydro-*N*-methyl-4-phenyl-6-methylpyrimidin-2-one (21 and 22)

Benzoyl acetone (1.42 g, 9 mmol) and *N*-methyl urea (500 mg, 7 mmol) were taken in 10 ml of EtOH and 1.65 ml of conc. HCl was added. The reaction mixture was refluxed for 4 h, and then cooled in ice, and the precipitated solid was filtered and washed with cold EtOH to obtain the hydrochloride salt. The salt was dissolved in 10 mL of water and neutralised with NaOH solution (0.7 g in 5 ml of water) at 0 °C. Extraction of the aqueous layer with chloroform and evaporation of the solvent afforded the product as a mixture of isomers in 22% yield. Isomers **21** and **22** were separated by column chromatography using neutral silica with 80:20 ethyl acetate/*n*-hexane eluent. The characterisation of **21** and **22** based on NMR and IR spectra is tentative at this stage. A final proof of the structure was postponed to single crystal X-ray diffraction.

21: Crystallized from ethyl acetate/hexane, m.p. 169–171 °C. ^{1}H-NMR ($CDCl_3$): δ 8.11 (d, J = 8, 2H), 7.40–7.50 (m, 3H), 6.71 (s, 1H), 3.62 (s, 3H), 2.44 (s, 3H). IR (KBr): 3057, 1630, 1579, 1535, 1494, 1354 cm^{-1}.

22: Crystallized from ethyl acetate/hexane, m.p. 186–188 °C. ^{1}H NMR ($CDCl_3$): δ 7.40–7.60 (m, 3H), 7.30 (d, J = 8, 2H), 6.15 (s, 1H), 3.39 (s, 3H), 2.35 (s, 3H). IR (KBr): 1651, 1539, 1489, 1072, 1026, 958 cm^{-1}.

X-ray Crystallography

Single crystal X-ray data was collected on Nonius-CAD4 diffractometer with Mo-Kα radiation (λ = 0.7107 Å) and on Nonius-CCD Kappa diffractometer working at Ag-Kα radiation (λ = 0.5608 Å) from 180 exposures with Δϕ scans, Δϕ = 1°. θ_{max} =

35.2° (CAD4) and 21.5° (or 27.9° exceptionally) on the CCD. Absorption correction was applied for Br and I atoms. Hydrogen atoms were refined in such a way that the ratio of reflections to parameters for each crystal structure is favourable, *i.e.*, about 10. Structures were solved using direct methods with SIR92 program.[34a] Full-matrix least-squares refinement were performed on F using the teXsan software.[34b] Scattering factors for neutral atoms and f', $\Delta f'$, f'', $\Delta f''$ were taken from the *International Tables for X-ray Crystallography*.[34c] Details of crystal data collection, structure solution and refinement are listed in the Chapter 7 and metrics of some important hydrogen bonds are summarised in Table 1. Crystal packing diagrams are drawn using PLATON.[34d]

4.15 References

1. (a) J.A.K. Howard, F.H. Allen, G.P. Shields, (ed.), *Implications of Molecular and Materials Structure for New Technologies*, Kluwer Academic Publishers, Netherlands, **1999**. (b) C.V.K. Sharma, *Cryst. Growth Des.*, **2002**, *2*, 465. (b) M.D. Hollingsworth, *Science*, **2002**, *295*, 2410.
2. (a) C.P. Brock and J.D. Dunitz, *Chem. Mater.*, **1994**, *6*, 1118. (b) A.D. Mighell and V.L. Himes, *Acta Cryst.*, **1983**, *A39*, 737.
3. (a) G.R. Desiraju, *Crystal Engineering. The Design of Organic Solids*, Elsevier, Amsterdam, **1989**. (b) M.S. Wong, C. Bosshard and P. Gunter, *Adv. Mater.*, **1997**, *9*, 837. (c) A. Nangia, *CrystEngComm*, **2002**, *17*, 1. (d) D. Braga, G.R. Desiraju, J.S. Miller, A.G. Orpen and S.L. Price, *CrystEngComm*, **2002**, *4*, 500. (e) D. Braga, *Chem. Commun.*, **2003**, 2751.
4. J.C. MacDonald, P.C. Dorrestein and M.M. Pilley, *Cryst. Growth Des.*, **2001**, *1*, 29.

5. (a) S.W. Gordon-Wylie and G.R. Clark, *Cryst. Growth Des.*, **2003**, *3*, 453. (b) G.R. Desiraju, *Nature Materials*, **2002**, *1*, 77. (c) J.D. Dunitz, *Chem. Commun.*, **2003**, 545.
6. (a) B. Moultan and M.J. Zaworotko, *Chem. Rev.*, **2001**, *101*, 1629. (b) O.R. Evans and W. Lin, *Acc. Chem. Res.*, **2002**, *35*, 511.
7. M.D. Hollingsworth, *Curr. Opin. Solid State Mater. Sci.*, **1996**, *1*, 514.
8. P.J. Langley and J. Hulliger, *Chem. Soc. Rev.*, **1999**, *28*, 279.
9. (a) K.T. Holman, A.M. Privovar and M.D. Ward, *Science*, **2001**, *294*, 1907. (b) K.T. Holman, A.M. Privovar, J.M. Swift and M.D. Ward, *Acc. Chem. Res.*, **2001**, *34*, 107.
10. (a) O.R. Ewans and W. Lin, *Chem. Mater.*, **2001**, *13*, 2705. (b) W. Lin, L. Ma and O.R. Evans, *Chem. Commun.*, **2000**, 2263.
11. (a) M.C. Hong, W.P. Su, M. Fujita, J.X. Lu, *Chem. Eur. J.*, **2000**, *6*, 427. (b) C. Piguet, G. Bernardelli and G. Hopfgartner, *Chem. Rev.*, **1997**, *97*, 2005. (c) O. Mamula, A.V. Zelewsky, T. Bark, G. Bernardinalli, *Angew. Chem., Int. Ed.*, **1999**, *38*, 2945. (d) K. Biradha, C. Seward and M.J. Zaworotko, *Angew. Chem., Int. Ed.*, **1999**, *38*, 492. (e) T. Ezuhara, K. Endo and Y. Aoyama, *J. Am. Chem. Soc.*, **1999**, *121*, 3279.
12. (a) G.R. Desiraju and T.S.R. Krishna, *Mol. Cryst. Liq. Cryst.*, **1988**, *159*, 277. (b) D.Y. Curtin, I.C. Paul, *Chem. Rev.*, **1981**, *81*, 525. (c) W. Tam, B. Guerin, J.C. Calabrese and S.H. Stevenson, *Chem. Phys. Lett.*, **1989**, *154*, 93. (d) T. Tsunekawa, T. Gotoh and M. Iwamoto, *Chem. Phys. Lett.*, **1990**, *166*, 353. (e) G.F. Lipscomb, A.F. Garito and R.S. Narang, *Appl. Phys. Lett.*, **1981**, *38*, 663.
13. J. Zyss, D.S. Chemla and J.-F. Nicoud, *J. Chem. Phys.*, **1981**, *74*, 4800.
14. A. C. Skapski and J.L. Stevenson, *J. Chem. Soc., Perkin 2*, **1973**, 1197.

15. (a) M. Muthuraman, Y.L. Fur, M. Bagieu-Beucher, R. Masse, J.-F. Nicoud, S.George, A. Nangia and G.R. Desiraju, *J. Solid State Chem.*, **2000**, *152*, 221. (b) S. George, A. Nangia, M. Muthuraman, M. Bagieu. Beucher, R. Masse and J.-F. Nicoud, *New. J. Chem.*, **2001**, *25*, 1520.

16. (a) J. Messier, K. Kajzar and P. Prasad (eds.), *Organic Molecules for Nonlinear Optics and Photonics*, Kluwer Academic Publishers, Dordrecht, **1990**. (b) T. Verbiest, S. Houbrechts, M. Kauranen, K. Clays and A. Persoons, *J. Mater. Chem.*, **1997**, *7*, 2175. (c) D.S. Chemla and J. Zyss (eds.), *Nonlinear Optical Properties of Organic Molecules and Crystals*, Academic Press , Orlando, Fl, USA, vol. **1** and **2**, **1987**.

17. O.R. Evans and W. Lin, *J. Chem. Soc., Dalton Trans.*, **2000**, 3949.

18. V. Vedenova-Adrabinska and C. Janéczko, *J. Mater. Chem.*, **2000**, *10*, 555.

19. S. Miyata and H. Sasabe, (eds.), *Poled Polymers and their Application to SHG and EO Devices*, Gordan and Breach Science Publishers, Amsterdam, **1997**.

20. (a) Y.-L. Chang, M.-A. West, F. W. Fowler and J. W. Lauher, *J. Am. Chem. Soc.*, **1993**, *115*, 5991. (b) L. M. Toledo, J. W. Lauher and F. W. Fowler, *Chem. Mater.*, **1994**, *6*, 1222. (c) B. Gong, C. Zheng, E. Skrzypczak-Jankun, Y. Yan and J. Zhang, *J. Am. Chem. Soc.*, **1998**, *120*, 11194. (d) F.W. Fowler and J.W. Lauher, *J. Phys. Org. Chem.*, **2000**, *13*, 850.

21. G.R. Desiraju and T. Steiner, *The Weak Hydrogen Bond in Structural Chemistry and Biology*, Oxford University Press, Oxford, **1999**.

22. (a) T. Steiner, *Angew. Chem., Int. Ed.*, **2002**, *41*, 48. (b) G. R. Desiraju, *Acc. Chem. Res.*, **2002**, *35*, 565.

23. Some papers on C–H···halogen interactions: (a) P.K. Thallapally and A. Nangia, *CrystEngComm*, **2001**, 27. (b) L. Brammer, E.A. Bruton and P. Sherwood, *Cryst. Growth Des.*, **2001**, *1*, 277. (c) F. Neve and A. Crispini,

Cryst. Growth Des., **2001**, *1*, 387. (d) S. Haddad, F. Awwadi and R. Willet, *Cryst. Growth Des.*, **2003**, *3*, 501. (e) J.N. Moorthy, P. Venkatakrishnan, P. Mal, S. Dixit and P. Venugopalan, *Cryst. Growth Des.*, **2003**, *3*, 581. (f) H.F. Liberman, R.J. Davey and D.M.T. Newsham, *Chem. Mater.*, **2000**, *12*, 490.

24. A.I. Kitaigorodsky, *Molecular Crystals and Molecules*, Academic Press, New York, **1973**.
25. (a) M.R. Edwards, W. Jones, W.D.S. Motherwell and G.P. Shields, *Mol. Cryst. Liq. Cryst.*, **2001**, *356*, 337. (b) U. Rychlewska, and B. Warzajtis, *Acta Cryst.*, **2002**, *B58*, 265.
26. A. Nangia, *New J. Chem.*, **2000**, *24*, 1049.
27. V.R. Vangala, A. Nangia and V.M. Lynch, *Chem. Commun.*, **2002**, 1304. (b) L.S. Reddy, A. Nangia, V.M. Lynch, *Cryst. Growth Des.*, **2004**, *4*, 89. (c) J.N. Moorthy, P. Venkatakrishnan and A.S. Singh, *CrystEngComm*, **2003**, *5*, 507. (d) V.R. Thalladi, H.-C. Weiss, D. Bläser, R. Boese, A. Nangia and G.R. Desiraju, *J. Am. Chem. Soc.*, **1998**, *120*, 8702. (e) J.D. Dunitz and R. Taylor, *Chem. Eur. J.*, **1997**, *3*, 89.
28. R. Boese, M.Y. Antipin, D. Bläser and K.A. Lyssenko, *J. Phys. Chem. B.*, **1998**, *102*, 8654.
29. (a) C. Janiak, *J. Chem. Soc., Dalton Trans.*, **2000**, 3885. (b) W. B. Jennings, B.M. Farrell and J.F. Malone, *Acc. Chem. Res.*, **2001**, *34*, 885.
30. M. Ohkita, T. Suzuki, K. Nakatani and T. Tsuji, *Chem. Commun.*, **2001**, 1454.
31. P.K. Thallapally, G.R. Desiraju, M. Bagieu-Beucher, R. Masse, C. Bourgogne and J.-F. Nicoud, *Chem. Commun.*, **2002**, 1052.
32. C.K. Broder, M.G. Davidson, V.T. Forsyth, J.A.K. Howard, S. Lamb and S.A. Mason, *Cryst. Growth Des.*, **2002**, *2*, 163.

33. *Vogel's Text book of Practical Organic Chemistry*, Revised by B. S. Furniss, A. J. Hannaford, P.W.G. Smith and A.R. Tatchell, 5th ed., ELBS Longman, Essex, p 964, **1989**.

34. (a) A. Altomare, M. Cascarano, C. Giacovazzo and A.J. Guagliardi, *J. Appl. Cryst.*, **1993**, *26*, 343. (b) Molecular Structure Corp., *teXsan for Windows version 1.03*, Single Crystal Structure Analysis Software, version 1.04, **1997-98**, MSC, 3200 Research Forest Drive, Woodlands, TX 77381, USA. http://www.msc.com (c) A. J. C. Wilson (ed.), *International Tables for Crystallography*, Vol. C, Table 4268, pp 6111-2, Kluwer Academic, Dordrecht, 1992. (d) *Platon97*: A. L. Spek, Bijvoet Centre for Biomolecular Research, University of Utrecht, The Netherlands.

CHAPTER FIVE

C–H···O AND C–H···N HYDROGEN BONDS IN SOME *N*-ARYLPYRIMIDINONE DERIVATIVES

5.1 Introduction

In previous chapters packing motifs in some *N*-arylpyrimidinone molecules were explained.[1] These crystal structures have layers with antiparallel chains of molecules or polar layers in a centrosymmetric structure. In the seventeen structures analyzed in the family of pyrimidinone, it was found there is a repetition of C–H···O hydrogen bond chain involving a C–H donor and carbonyl acceptor. Different hydrogen bonding and close packing arrangements were obtained depending on the position of functional groups in the molecule. This Chapter discusses hydrogen bonding patterns in three miscellaneous pyrimidinone structures: one neutral molecule and two salts.

5.2 Results and Discussion

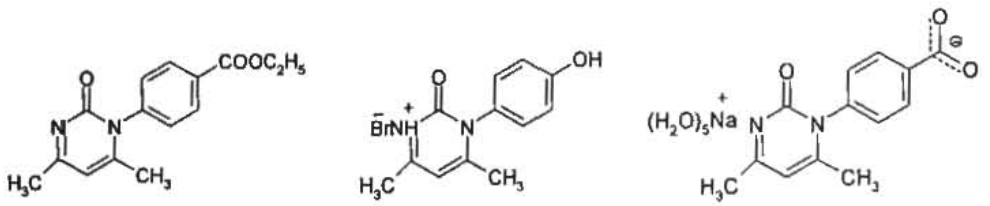

23 **24** **25**

Scheme 1. Compounds whose crystal structure will be discussed in this Chapter.

Pyrimidinones **23-25** were synthesized using reported procedures[2] and characterized by their NMR and IR spectra. Compound **23** crystallized from ethylacetate/*n*-hexane mixture, **24** crystallized from water after workup and **25** crystallized from water after neutralization of reaction mixture at room temperature to afford single crystals suitable for X-ray diffraction. Some important interatomic

distances and hydrogen bonds are given in Table 1. For crystallographic data see Chapter 7.

Table 1. Interaction Table

	Hydrogen bond	D–H···A(Å)	D···A	D–H···O(°)
23	C6–H10···N2(i)	2.60(2)	3.4811(18)	150.4(16)
	C8–H2···O1(ii)	2.59(2)	3.3122(16)	133.3(14)
	C12–H5···O1(iii)	2.59(2)	3.4093(16)	144.0(13)
24	C–H···O(i)	2.54(3)	3.160(4)	123.9(2)
	C–H···O(ii)	2.78(3)	3.832(4)	170.8(2)
	C–H···O(iii)	2.68(2)	3.185(4)	111.7(19)
	C–H···Br(iv)	3.05(3)	3.993(4)	156.3(18)
	O–H···Br(v)	2.38(3)	3.194(2)	168.6(3)
	N–H···Br(vi)	2.61(3)	3.322(2)	175.9(3)
25	C–H···O(i)	2.527(12)	3.4205(17)	178.7(11)
	O–H···O(ii)	2.184(17)	2.9260(14)	160.3(15)
	O–H···O(iii)	1.975(18)	2.7894(15)	178.7(18)
	O–H···O(iv)	2.057(16)	2.8679(15)	175.7(15)
	O–H···O(v)	2.121(17)	2.8836(14)	176.1(16)
	O–H···O(vi)	1.889(17)	2.7121(15)	175.8(12)

5.3 Crystal Structure of 1,2-Dihydro-*N*-(4-carboxyethyl)phenyl-4,6-dimethylpyrimidin-2-one, 23

Compound **23** crystallizes in space group $P2_1/a$. The *N*-phenyl group is inclined at an angle of 91.3° with the heterocyclic ring (Figure 1a). A C–H···N hydrogen bond[3] formed between the methyl group and the nitrogen atom on the heterocyclic ring connects screw related molecules in a chain along the *b*-axis (Figure 1b). The ID chains thus formed are arranged parallel within the same layer producing a polar corrugated sheet. The aryl rings interdigitate within the layer between the hydrogen bonded chains. Adjacent 2D layers pack in antiparallel fashion thus giving a centrosymmetric packing. Inter layer region is stabilized by C–H···O hydrogen bonds.[3a]

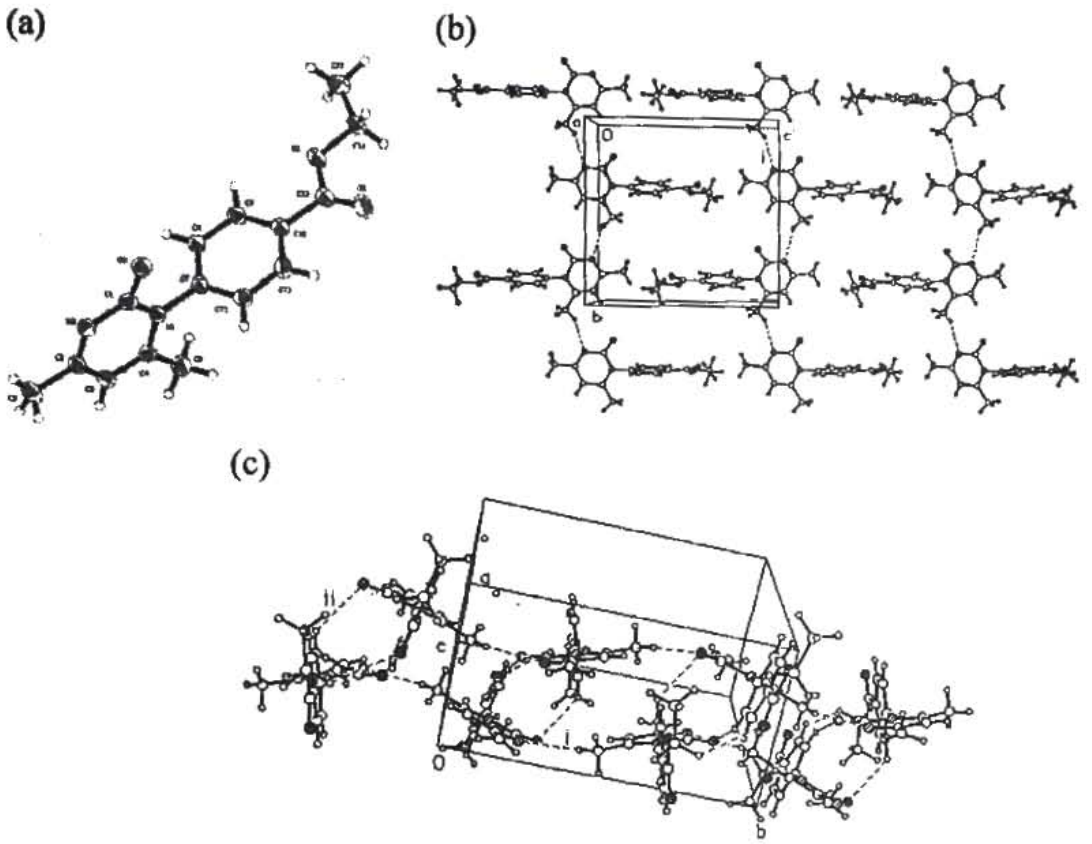

Figure 1. (a) ORTEP diagram of **23**. (b) Crystal structure of compound **23**. The C–H···N hydrogen bonded 1D chain. 1D chains are arranged parallel within the layers. (c) Antiparallel arrangement of adjacent corrugated layers connected through C–H···O hydrogen bond (interaction ii).

5.4 Crystal Structure of 1,2-Dihydro-*N*-(4-hydroxyphenyl)-4,6-dimethyl-pyrimidin-2-onehydrobromide, 24

Compound **24** crystallizes in the space group $P2_1/a$. The *N*-phenyl ring is inclined at an angle of 82.5° with the heterocyclic ring (Figure 2a). X-ray structure analysis shows that there are chains formed by cations and anions that are cross-linked via O–H···Br^- interaction[4] resulting in a layered structure. The hydroxyl group forms a strong hydrogen bond with the bromide ion (2.383 Å, 168.6°). The pyrimidinone cation and bromide anion alternate along the *c*-axis. The presence of

bromide ion has affected the packing pattern in this layered structure compared to structures analyzed in previous Chapters. The usually observed packing in the crystal structures of pyrimidinones contain a C–H···O hydrogen bond where the sp^2 C–H donates its proton to the carbonyl oxygen.[1] In the structure of **24** there is a C–H···O hydrogen bond[3a] between the allylic C–H(C5) and carbonyl oxygen, which connects glide related molecules along the *a*-axis (Figure 2b). Such chains are connected via N–H···Br^-,[5] O–H···Br^- and weak C–H···O hydrogen bonds (see Table 1 for hydrogen bond distances and angles) resulting in a polar layer. The layer is corrugated and one of the reasons probably is to accommodate the anion.[6] Intercalation of anions between the chains minimizes undesirable dipole-dipole interaction and this could be a reason for forming 2D polar layer.[7] The alternate hydroxyl groups point in opposite directions along the *a*-axis. Layers pack antiparallel. Such antiparallel layers are connected by O–H···Br^- and C–H···Br^- interactions.[8] Thus the packing is dominated by ionic interactions and stabilized by a network of O–H···Br^-, N–H···Br^- and C–H···O interactions.

(a)

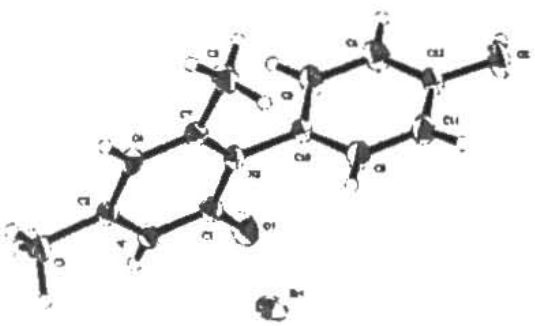

(b)

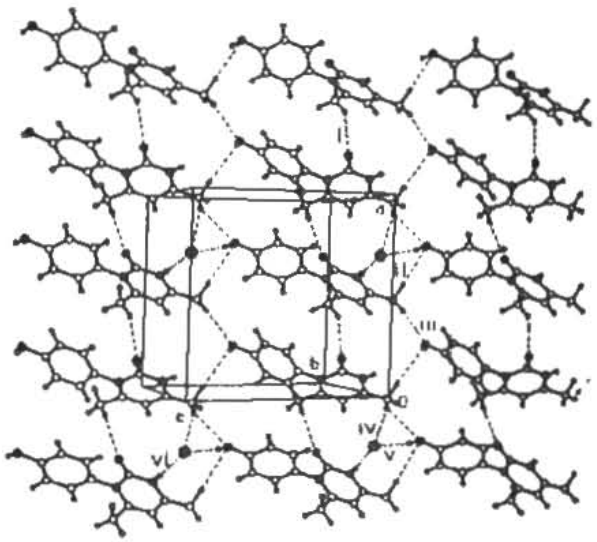

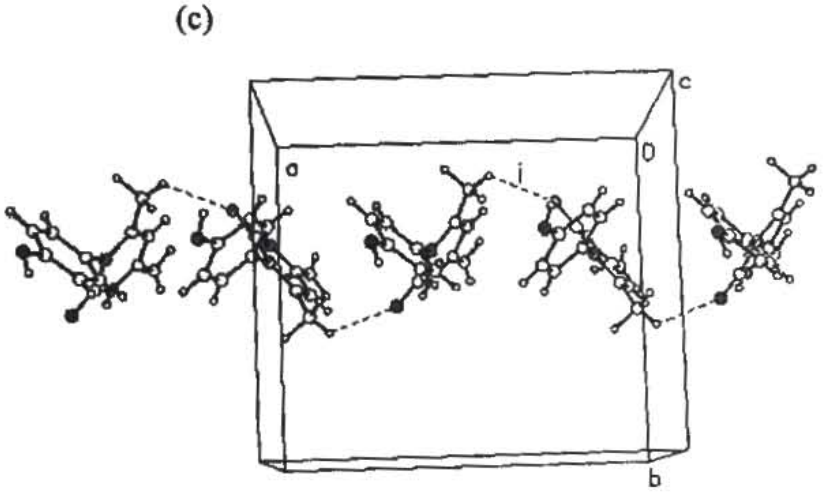

Figure 2. (a) ORTEP diagram of **24**. (b) 2D polar arrangement in **24** mediated by C–H···O (interactions i, ii and iii), C–H···Br (iv), O–H···Br (v) and N–H···Br (vi) interactions. All the bromine anions are not shown here for clarity. (c) The corrugated 1D chain.

5.5 Hydrated Sodium Salt of 1,2-Dihydro-*N*-(4-carboxyphenyl)-4,6-dimethylpyrimidin-2-one, 25

Compound **25** crystallizes in space group *Pbcn*. The Assymetric unit contains pyrimidinone anion, sodium cation and five water molecules. Figure 3a shows the ORTEP diagram of the molecule with numbering scheme. Out of five water molecules four are coordinated to sodium atom and one exists as water of crystallization. The aryl ring is inclined at an angle of 88° with the heterocyclic ring. There are two bridging water molecules (O_w^5, O_w^7) between adjacent sodium cations (Figure 4). Selected bond distances and angles are given in the Table 1. The environment of sodium can be described as a six coordinated distorted octahedron (Figure 4), by analyzing the molecular dimensions given in Table 2.[9] The coordination sphere of sodium include six water molecules. Two water molecules (O_w^4, O_w^6) are axial and the four are in equatorial plane. Na^+ ions are well packed in

between the anions in the lattice resulting in an infinite [Na $(H_2O)_5$]+[anion] chain aggregate. The arrangement of various ions and water molecule along with hydrogen bonding interactions is shown in figure 3b. The sp^2 C–H of the pyrimidinone anion donates hydrogen to the water of crystallization which form part of a one-dimensional chain along the *c*-axis (interaction i in Figure 3b). The carbonyl group accepts hydrogen from the bridging water molecule to form an O–H···O hydrogen bond to complete the chain (interaction ii in Figure 3b). Adjacent chains pack in antiparalell manner to produce a layered structure. Several O–H···O hydrogen bonds (1.8-2.1 Å, 170-177 °) formed between the carboxylate group and the water molecules links the linear chains. Even though the Na^+ ion and the water molecules insulate the molecules in a chain from one another, the information about the orientation of molecule is relayed through out the chain. The degree of corrugation in the layer is less here compared to **23** and **24**.

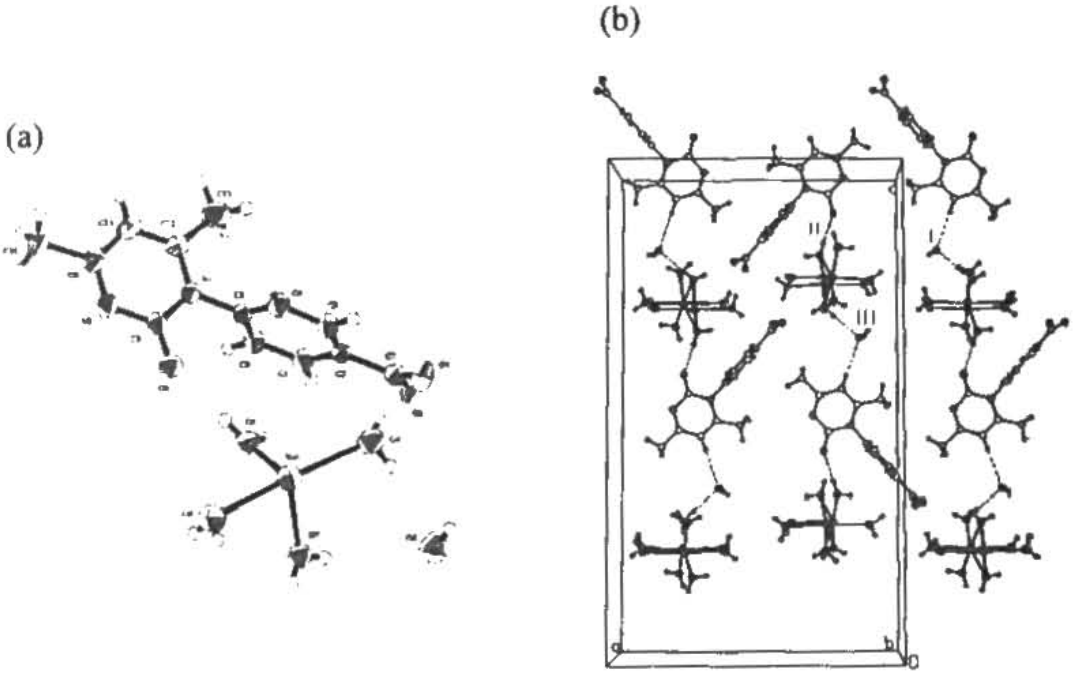

Figure 3. (a) ORTEP diagram of **25.** (b)The layered structure mediated by C–H···O (interaction i) and O–H···O interactions (ii and iii).

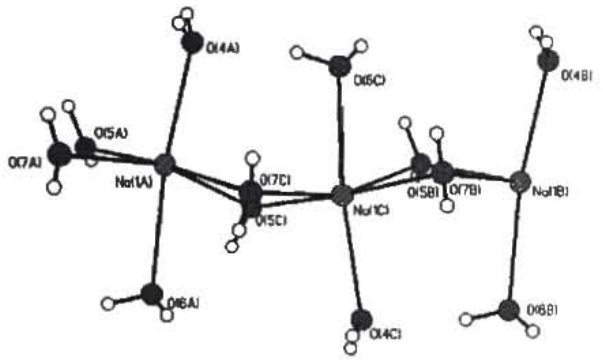

Figure 4. The distorted octahedral geometry of sodium cation in the crystal. Six water molecules coordinate to the sodium atom.

Table 2. Bond Distances and Angles of the Six Coordinated Sodium Cation.

Bond Distances	(Å)
Na1C-O5B	2.397
Na1C-O7B	2.438
Na1C-O4C	2.393
Na1C-O5C	2.390
Na1C-O6C	2.463
Na1C-O7C	2.392
Bond Angles	(°)
O6C-Na1C-O4C	171.7
O5C-Na1C-O7B	175.7
O7C-Na1C-O5B	163.3
O4C-Na1C-O5B	101.7
O4C-Na1C-O7B	91.3
O4C-Na1C-O7C	94.6
O4C-Na1C-O5C	92.3
O6C-Na1C-O5B	75.4
O6C-Na1C-O7B	80.7
O6C-Na1C-O7C	88.0
O6C-Na1C-O5C	95.8
O5C-Na1C-O7C	85.2
O7B-Na1C-O7C	92.2
O7B-Na1C-O5B	84.1
O5B-Na1C-O5C	97.5

5.6 Conclusion

We have discussed three structures of pyrimidinones having different substituents and counter ions. All the three structures follows the usual layered structure seen in the pyrimidinone family. The molecules form one dimensional chains which in turn form two dimensional layers. The layers are corrugated to accommodate counter ions and bulky groups. It is clear that pyrimidinone architecture sustained by weak C–H···O/N hydrogen bonds can tolerate structural changes.

5.7 Experimental

Synthesis

For the preparation of the compounds **23-25** the appropriate *N*-aryl urea used in the following reactions was prepared by using Vogel's procedure.[10] NMR spectra were recorded on Bruker 200 MHz spectrometer in $CDCl_3$/DMSO(d_6). Peaks are given in δ (ppm). IR spectra were recorded as KBr wafer, peaks are reported in cm^{-1}. *N*-arylpyrimidinone was prepared as before.[1,2] Compound **24** was prepared by deprotection of methoxy group in the corresponding *N*-arylpyrimidinone using boron tribromide (BBr_3) reagent in dichloromethane.[11]

1. 1,2-Dihydro-*N*-(4-carboxyethyl)-4,6-dimethylpyrimidin-2-one, 23

The product was crystallized from ethylacetate/*n*-hexane mixture. M.p. 180-182°C. ^{1}H-NMR ($CDCl_3$): δ 8.22 (d, J = 8, 2H), 7.33 (d, J = 8, 2H), 6.21 (s, 1H), 4.4 (q, 2H), 2.42 (s, 3H), 1.97 (s, 3H), 1.4 (t, 3H). IR (KBr): 2989, 1722, 1664, 1273 cm^{-1}.

2. 1,2-dihydro-*N*–(4-hydroxyphenyl)-4,6-dimethylpyrimidin-2onehydrobromide, 24

The 1,2-dihydro-*N*–(4-anisyl)-4,6-dimethylpyrimidin-2-one was prepared and characterized m.p.151-153°C. ^{1}H-NMR ($CDCl_3$): δ 7.2 (d, J = 8, 2H), 7 (d, J = 8, 2H), 6.1 (s, 1H), 3.9 (s, 3H), 2.4 (s, 3H), 1.95 (s, 3H). IR (KBr): 3056, 1666, 1537 cm^{-1}. To a stirred solution of 10 ml dichloromethane (DCM) and 1ml BBr_3 (1.5 gm, 6 mmol) at –78 °C 460 mg (2 mmol) of 4-anisyl pyrimidinone in DCM was added slowly under nitrogen atmosphere. This reaction condition was maintained for 3 h and was allowed to stir at room temperature for next 24 h. The reaction mixture was extracted with water and aq. $NaHCO_3$ solution. Product **24** crystallized from water. M.p. 272-275°C. ^{1}H-NMR ($DMSOd_6$): δ 7.7 (s, 1H), 7.2 (d, J = 8, 2H), 7.1 (d, J = 8, 2H), 6.9 (s, 1H), 2.6 (s, 3H), 2.35 (s, 3H). IR (KBr): 3132, 1745, 1610 cm^{-1}.

3. 1,2-dihydro-*N*–(4-carboxyphenyl)-4,6-dimethylpyrimidin-2-one, 25

A similar procedure was followed for compound **25** with only change in solvent used for reaction. Tetrahydrofuran was used instead of EtOH as solvent to avoid esterification. Column chromatography with ethylacetate was avoided to prevent transesterification. The hydrochloride salt was neutralized with NaOH and the compound crystallized from neutralized mixture m.p. above 285°C. ^{1}H-NMR ($DMSOd_6$): δ 8 (d, J = 8, 2H), 7.15 (d, J = 8, 2H), 6.41(s, 1H), 2.28 (s, 3H), 1.91(s, 3H). IR (KBr): 3429, 1687, 1601, 1383 cm^{-1}.

5.8 Data Collection and Crystal Structure Determination

The cell parameters, space groups, and crystal structures were determined from single-crystal X-ray diffraction data collected at ambient temperature on CCD kappa and Nonius-CAD4 diffractometers at Grenoble with Ag-Kα and Mo-Kα radiations (λ = 0.5608, 0.71073 Å). Crystal data, experimental conditions and

structure refinement parameters for **23-25** are mentioned in Chapter 7. The structures were solved by direct methods using the SIR92 program.[12] Full-matrix least-squares refinements were performed on F using the teXsan software.[13] Scattering factors for neutral atoms and f', $\Delta f'$, f'', $\Delta f''$ were taken from the *International Tables for X-ray Crystallography*.[14] ORTEP diagrams are drawn at 50% probability and crystallographic numbering is followed in the ORTEP diagram. Geometrical analysis was carried in PLATON[15] on Silicon Graphics Indigo workstation.

5.9 References

1. (a) M. Muthuraman, M. Bagieu-Beucher, R. Masse, J.-F. Nicoud, S.George, A. Nangia and G.R. Desiraju, *J. Solid State Chem.*, **2000**, *152*, 221. (b) S. George, A. Nangia, M. Muthuraman, M. Bagieu-Beucher, R. Masse, J.-F. Nicoud., *New J. Chem.*, **2001**, *25*, 1520. (c) S. George, A. Nangia, M. Muthuraman, M. Bagieu-Beucher, R. Masse, J.-F. Nicoud., *New J. Chem.*, **2003**, *27*, 568.
2. (a) R.O. Hutchins and B.E. Maryanoff, *J. Org. Chem.*, **1972**, *37*, 1829. (b) P.S. Chandrakala, A.K. Katz, H.L. Carrell, P.R. Sailaja, A.R. Podile, A. Nangia and G.R. Desiraju, *J. Chem. Soc., Perkin Trans 1*, **1998**, 2597.
3. (a) G.R. Desiraju and T. Steiner, *The Weak Hydrogen Bond in Structural Chemistry and Biology*, Oxford University Press, Oxford, **1999**. (b) M. Ohkita, T. Suzuki, K. Nakatani and T. Tsuji, *Chem. Commun.*, **2001**, 1454. (c) M. Mascal, *Chem. Commun.*, **1998**, 303.
4. H.O.N. Reid, I.A. Kahwa, A.J.P. White and D.J. Williams, *Chem. Commun.*, **1999**, 1565.
5. (a) Y.-J. Chang, Z.-M. Wang, C.-S. Liao and C.-H. Yan, *New J. Chem.*, **2002**, *26*, 1360. (b) S. Subramanian and M.J. Zaworotko, *Can. J. Chem.*, **1995**, *75*, 414. (c) M.D. Walkinshaw, A.H. Cowley and S.K. Mehrotra, *Acta*

Cryst., **1984**, *40*, 129. For some recent papers on halogen as hydrogen bond acceptor see (d) P.K. Thallapally and A. Nangia *CrystEngComm*, **2001**, *27*. (e) L. Brammer, E.A. Bruton and P. Sherwood, *Cryst. Growth Des.*, **2001**, *1*, 277.

6. (a) K.A. Hirsch, S.R.Wilson, J.S. Moore, *Chem. Eur. J.*, **1997**, *3*, 765. (b) D.M.P. Mingos, A.L. Rohl, *Inorg. Chem.*, **1991**, *30*, 3769. (c) D.M.P. Mingos, A.L. Rohl, *J. Chem. Soc. Dalton Trans.*, **1991**, 3419.
7. S.R. Marder, J.W. Perry, W.P. Schaeffer, *Science*, **1989**, *245*, 626.
8. (a) S. Shinoda, M. Tadokoro, H. Tsukuba and Arakawa, *Chem. Commun.*, **1998,** 181. (b) O.J. Dautel, M. Fourmigue and E. Canadell, *Chem. Eur. J.*, **2001**, *7*, 2635.
9. (a) C.-D. Wu, D.M. Wu, C.-Z. Lu and J.-S. Huang, *Acta Cryst.*, **2001**, *E57*, m253. (b) P. Machnitzki, T. Nickel, O. Stelzer and C. Landgrafe, *Eur. J. Inorg. Chem.*, **1998**, 1029.
10. *Vogel's Textbook of Practical Organic Chemistry*, revised by B.S. Furniss, A.J. Hannaford, P.W.G. Smith and A.R. Tatchell, ELBS Longman, Essex, 5th edn., **1989**, pp 964.
11. J.F.W. McOmie, M.L. Watts and D.E. West, *Tertrahedron*, **1968**, *24*, 2289.
12. A. Altomare, M. Cascarano, C. Giacovazzo and A. J. Guagliardi, *J. Appl. Cryst.* **1993**, *26*, 343.
13. Molecular Structure Corp. (**1997-1998**). teXsan for Windows version 1.03. Single Crystal Strucutre Analysis Software. Version 1.04. MSC, 3200 Research Forest Drive, Woodlands, TX 77381.
14. *International Tables for Crystallography* (A. J. C. Wilson, ed.), Vol. C, Table 4268, pp 6112, Kluwer Academic, Dordrecht, **1992**.
15. *PLATON*. A.L. Spek, Bijvoet Centre for Biochemical Research, Vakgroep Kristal-en Structure-Chemie, University of Utrecht, The Netherlands.

CHAPTER SIX

CRYSTAL ENGINEERING OF SOME UNSYMMETRICAL UREAS

6.1 Introduction

A family of molecules that would form predictable two-dimensional array in the crystalline state was sought by choosing molecules that would form two dependable independent sets of one-dimensional self-complementary hydrogen bonded arrays in orthogonal directions. Halogen···nitro[1] and urea[2] are well known self complementary functional groups that form one-dimensional hydrogen-bonded polymeric structures and have been used to create highly organized molecular structures in the solid state (Scheme 1). If these two functionalities are present in the same molecule and if the self complementary hydrogen bonding patterns occur as planned then a two-dimensional molecular network will result. A survey of the Cambridge Structural Database (CSD)[3] showed that not only N–H···O_{urea} and Hal···O_2N interaction but N–H···O_{nitro} and C–H···$O_{carbonyl}$ can also be formed. These include hard hydrogen bonds of both N–H···$O_{carbonyl}$, N–H···O_{nitro} type possible recognition motifs (Scheme 1), soft hydrogen bonds of C–H···$O_{carbonyl}$ and Hal···O types in which oxygen belong to nitro group. With this background we study the series of substituted nitro diphenyl ureas.

So far we used pyrimidinones, which are masked ureas, to construct supramolecular architecture. The urea scaffold is used to assemble chains and layered hydrogen bond networks in this Chapter. Lauher and Fowler have used urea tape motif and COOH/COOH[2a] and $CONH_2$/$CONH_2$[2c] hydrogen bonding in lateral direction to build 2D sheets. We decided to use α-network of urea tape with X···NO_2 interaction in the lateral direction. A search of the CSD shows that nitrodiphenyl ureas have not been studied systematically. Urea molecules whose crystal structures will be discussed in this Chapter are given in Scheme 2.

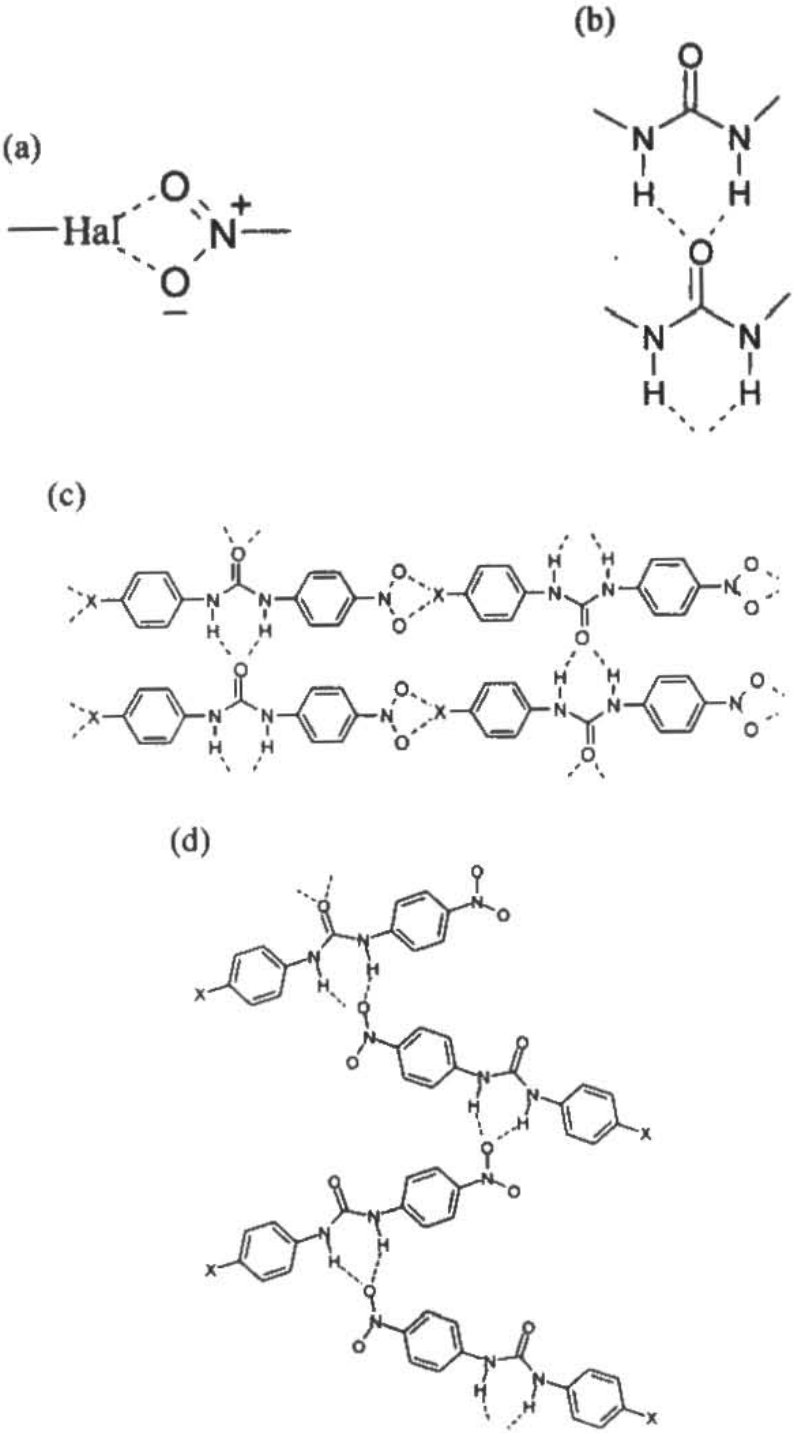

Scheme 1. Two self complementary interactions (a) Hal···Nitro and (b) urea α-network used for controlling molecular alignment. (c) and (d) shows the possible and expected patterns in the crystal structure of these molecules.

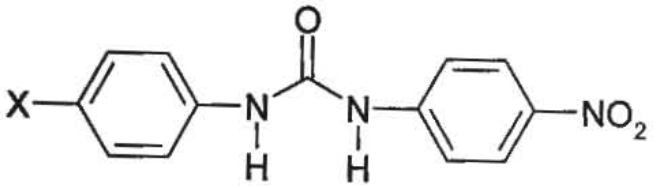

26: X = I	**32:X = CN**
27: X = ethynyl	**33:X = I(m-isomer)**
28: X = N(Me)$_2$	**34:X = I(DMSO)**
29: X = Br	**35: X = H(DMF)**
30: X = Cl	**36: X = Me(DMSO)**
31: X = F	**37: X = Ac(DMSO)**

Scheme 2. Urea molecules studied in this Chapter. **34-37** are solvates.

6.2 Aims and Objectives of the Study

We also noticed from the literature survey some closely related nitro substituted diphenyl urea compounds. The β-polymorph of *N*-3-nitrophenyl-*N'*-3'-nitrophenylurea[4] (Figure 1) (CSD version 5.24, 272066 refcode SILTOW01) and *N*-4-nitrophenyl-*N'*-4'-nitrophenylurea[5] (crystal structure of *N*-4-nitrophenyl-*N'*-4'-nitrophenylurea molecule is not reported so far) have powder SHG efficiency of 1.5 and 8.8 times that of urea respectively. Two polymorphic form of *N*-3-nitrophenyl-*N'*-3'-nitrophenylurea has been reported: α-polymorph[2b] (refcode SILTOW) and β-polymorph. The α-form crystallizes in centrosymmetric space group $P2_1/c$ while the β-form crystallizes in *C*2 noncentrosymmetric space group. Hence the motivation to reexamine the nitrosubstituted urea molecules with the aim of inducing their crystallization in non-centrosymmetric space group. We have prepared and determined the crystal structures of *para/meta* substituted diphenyl ureas. The X-group variation is quite wide including halogens, C≡C–H, $N(CH_3)_2$, CH_3, $COCH_3$, and H, on one side of the molecule and with NO_2 group on the other side.

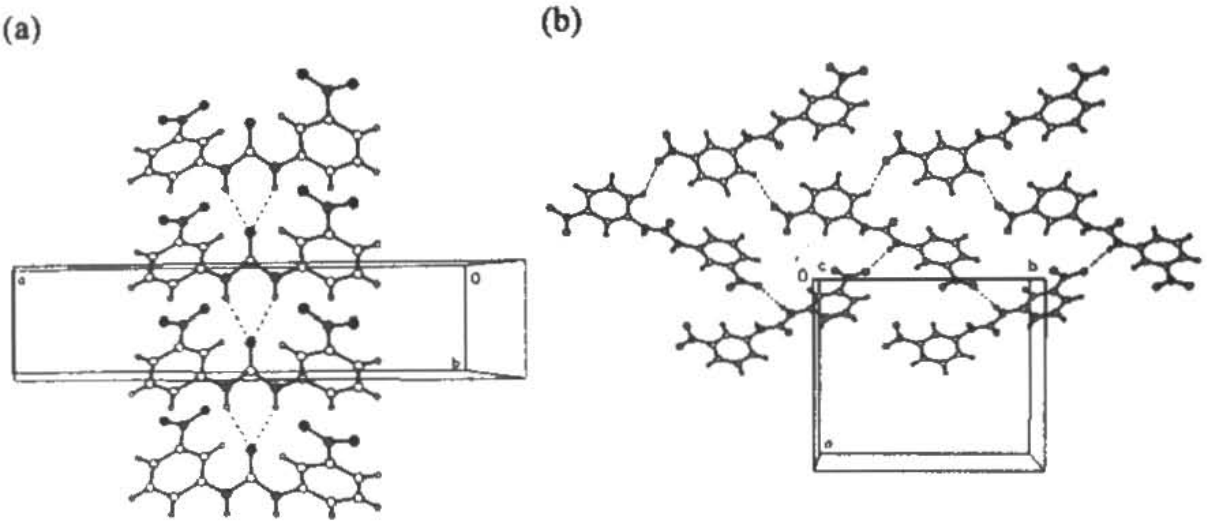

Figure 1. (a) The hydrogen bonding interaction (α-network) in the β-polymorph of *N*-3-nitrophenyl-*N'*-3'-nitrophenylurea (space group = *C*2). The phenyl rings form an angle 46.8° with the amide plane. (b) α-Polymorph of *N*-3-nitrophenyl-*N'*-3'-nitrophenylurea with different hydrogen bonding pattern (space group = $P2_1/c$).

6.3 Results and Discussion

Diphenyl ureas **26-37** were synthesized by the cognate condensation of *p*-nitrophenyl isocyanate with the corresponding *p*-X-aniline. Compounds were characterized by their NMR and IR spectra. Crystallization from different solvents like THF, ethanol, ethyl acetate, benzene, DMSO and their mixture afforded diffraction quality crystals at room temperature. Intermolecular interactions are listed in Table 1 and crystallographic information is given in Chapter 7. The crystal structures are analyzed in a sequence starting from compound **26**, *N*-4-iodophenyl-*N'*-4'-nitrophenylurea.

6.4 Crystal Structure of *N*-4-iodophenyl-*N'*-4'-nitrophenylurea, 26

The compound crystallizes in the polar space group *Cc*. Self assembly in **26** occurs *via* the urea tape N–H···O synthon with I···NO_2 interaction providing

auxiliary support in the lateral direction. The carbonyl group is aligned with the short *b*-axis, 4.67 Å of the unit cell (see Chapter 7). This short axis is characteristic of urea structures.[6] The linear alignment and repeat distance of the α-network of urea is due to the hydrogen bonds formed between the N–H donors of one molecule and the carbonyl lone pair acceptor of the translation related molecule (Figure 2). The aryl groups are twisted out of the urea plane (49.1, 45.6°) to adjust to the α-network. N–H···O hydrogen bonds in urea urea tape are 2.128 Å, 153.3° and 2.131 Å, 155°. All hydrogen atoms capable of hydrogen bonding are in fact, hydrogen bonded. The iodine atom in the molecule is linked to both nitro oxygen atoms by I···NO_2 (3.61, 3.28 Å; 154.3, 169.6°) interaction[1] in a bifurcated motif to produce polar chains running along the [2,0,-1] direction which connects glide related molecules. Adjacent chains are linked through N–H···O hydrogen bonds which form α-network orthogonal to it. Inter layer regions are dominated by van der Waals interactions and weak hydrogen bonds. From the perspective of crystal engineering macroscopic polarity in the crystal, although molecules of iodo derivative **26** are aligned anti-parallel along the carbonyl axis, the inclined, parallel orientation of NH–π–NO_2 chromophore will result in a net dipole moment. The iodo and nitro groups are disordered with site occupancy factor 0.9 and 0.1 and solved with an R-factor 2.88 %. The dominant orientation is shown in figure 2. The structure solved with an R-factor 3.77 % if the NO_2 and iodo group are treated as fully ordered in the refinement cycle.

In the crystal structure of **26** there are weak I···NO_2 interactions as well as strong N–H···O hydrogen bonds. When iodo group and nitro group are both present in a molecule I···NO_2 interaction can play an important role in supramolecular aggregation.

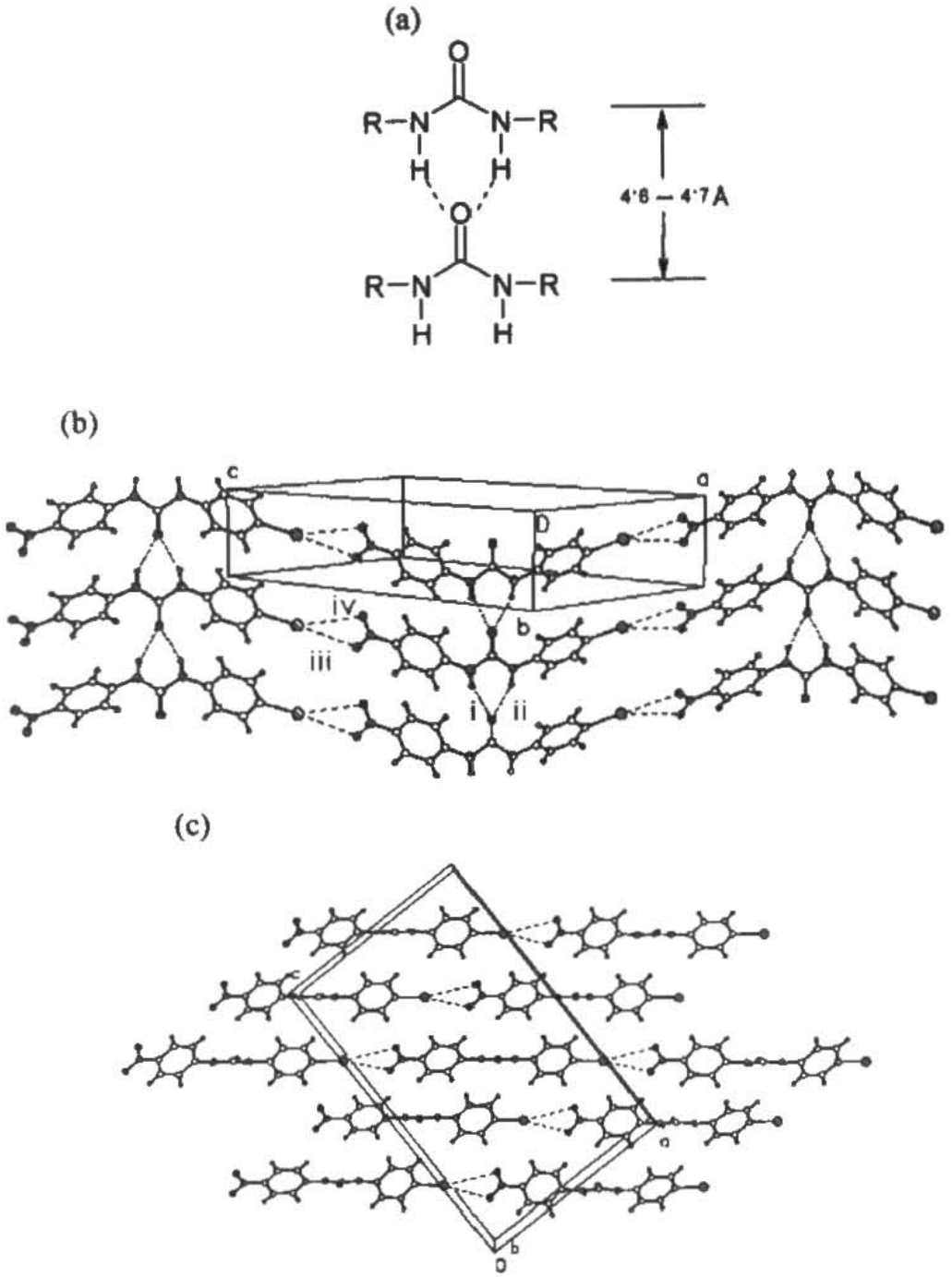

Figure 2. (a) Characteristic repeat distance of the α-network observed in urea. For the iodo derivative **26** it is 4.67 Å. (b) Packing diagram showing urea N–H···O tapes along the *b*-axis and the I···NO_2 interaction in **26**. (c) Crystal structure viewed down the *b*-axis showing the parallel arrangement of polar chains mediated via I···NO_2 synthon.

6.5 SHG Measurement on 26

Since iodo derivative **26** crystallized in a polar space group SHG measurement[7] was done on a microcrystalline sample using Nd^{3+}-YAG laser at 1064nm. The solid sample shows strong quadratic non-linear efficiency, with a green signal (530nm) equal to that of the bench mark compound 3-methyl-4-nitropyridine-1-oxide (POM).[8] The SHG activity of iodo derivative **26** is 13 times that of urea.

Table 1 Hydrogen Bonding Interaction Table

	Interaction	D-H···A(Å)	D···A	θ
26	N3–H3···O3(i)	2.128	2.931(5)	153.3
	N2–H2···O3(ii)	2.131	2.933(6)	155.0
	C11A–I1···O2(iii)	3.286	5.357	169.0
	C11A–I1···O1(iv)	3.618	5.576	154.3
27	N1–H1···O1(i)	2.107	2.914(4)	156.2
	N2–H2···O1(ii)	2.117	2.919(4)	155.1
	C14–H14···O3(iii)	2.410	3.325(7)	167.6
	C14–H14···O2(iv)	3.043	3.833(7)	143.8
28	N5–H5···O6 (i)	2.215	3.057(6)	166.5
	N8–H8···O6(ii)	2.393	3.18(6)	153.4
	N6–H6···O5(iii)	2.283	3.103(6)	159.4
	N7–H7···O5(iv)	2.294	3.104(6)	157.4
	C1–H1···O4(v)	2.737	3.463(9)	133.0
	C4–H4··O2(vi)	2.958	3.873(9)	159.7
29	N2–H2···O1(i)	2.109	2.936(5)	161.3
	N3–H3···O1(ii)	2.255	3.064(4)	157.0
	C13–H13···O2(iii)	2.742	3.638(5)	162.1
	C12–H12···O3(iv)	2.975	3.878(5)	164.1
30	N2–H2···O1(i)	2.096	2.913(2)	162.3
	N3–H3···O1(ii)	2.289	3.069(2)	155.6
	C13–H13···O2(iii)	2.764	3.658(3)	161.5
	C12–H12A···O3(iv)	2.859	3.745(2)	166.8

31	N2–H2···O1(i)	2.062	2.871(12)	165.4
	N3–H3B···O1(ii)	2.438	3.135(3)	151.5
	C13–H13···O2(iii)	2.837	3.723(3)	159.6
	C12–H12···O3(iv)	2.652	3.519(3)	170.6
32	N2–H2···O1(i)	2.073	2.907(3)	163.3
	N3–H3···O1(ii)	2.225	3.03(3)	156.1
	C12–H12···O3(iii)	2.989	3.884(3)	162
	C13–H13···O3	2.802	3.696(3)	161.2
33	N3–H13···O2(i)	2.151	3.008(6)	170.2
	N2–H2···O1(ii)	2.169	3.11(7)	165.1
	C12–H12···O3(iii)	2.738	3.5782(8)	151.1
	C13–H13···O2(iv)	2.780	3.523(8)	137.8
	C5–H5···O1(v)	2.5707	3.330(7)	139.0
	C5–H5···I1(vi)	3.364	3.93(5)	121.8
	C6–H6···I1(vii)	3.029	3.760(6)	136.5
34	N2–H7···O7(i)	1.945	2.905(10)	157.4
	N1–H1···O7(ii)	2.079	3.016(10)	153.3
	C22–H22···I2(iii)	3.428	4.246(9)	133
	C27–H27···I1(iv)	3.246	3.756(12)	109.5
	C1–H1···I1(v)	3.207	3.936(9)	126.1
	C28–H28···O5(vi)	2.465	3.417(5)	173.4
	C5–H5···O6(vii)	2.486	3.428(12)	145.6
	C29–H29b···I2(viii)	3.477	3.827(12)	104
	C29–H29a···I2(ix)	3.512	3.827(12)	101.8
	C29–H29···O6(x)	2.541	3.720(12)	165.2
	C30–H30···N3(xi)	2.920	3.858(15)	165.6
35	N1–H1···O4(i)	2.0175	2.844(4)	160.91
	N2–H1···O4(ii)	2.0353	2.853(4)	158.93
36	N2'–H2B'···O4(i)	2.007	2.818(4)	156.8
	N3'–H3B'···O4(ii)	2.100	2.902(4)	155.1
	C22–H22C···O3(iii)	3.079	3.756(7)	128.8
	C23–H23B···O3(iv)	2.884	3.542(9)	126.5
	N3–H3B···O4'(v)	2.051	2.860(4)	156.4
	N2–H2B···O4'(vi)	1.992	2.818(4)	160.4
	C23'–H23D···O3'(vii)	2.370	3.237(4)	149.9
	C22'–H22E···O3'(viii)	2.660	3.470(4)	141.5

	C2–H2A···O1(ix)	2.50	3.259(7)	139.07
37	N3–H3b···O5(SO) (i)	2.099	2.877(3)	150.1
	N2–H2B···O5(SO)(ii)	1.984	2.794(3)	156.4
	C22–H22B···O4(CO)(iii)	2.9674	3.810(4)	147.2
	C23–H23C···O4(CO)(iv)	2.495	3.438(4)	167.0
	C2–H2A···O3(CO)(v)	2.500	3.360(3)	153.9
	C23–H23A···O2(vi)	2.5418	3.393(4)	147.72

6.6 Crystal Structure of *N*-4-(ethynyl)phenyl-*N'*-4'-nitrophenylurea, 27

The ethynyl derivative **27** crystallizes in the space group *Cc* and is isostructural with iodo derivative **26,** confirming the observation that the iodo to ethynyl exchange does not generally disturb the crystal packing.[9] Figure 3 shows translation related molecules connected through N–H···O (2.11, 2.10 Å; 154.6, 156.3°) hydrogen bonds resulting in the α-network and such glide related tapes are in turn connected laterally through C≡C–H···NO_2 (2.40, 3.05 Å; 167.8, 142.9°) interactions. The C≡C–H···NO_2 chains viewed down the *b*-axis shows that all the chains are aligned in the same direction resulting in a net dipole moment, which is crucial in developing materials with useful properties.[10] The aryl rings are twisted out of the urea plane by 48.8 and 47.3°. An overlay diagram of iodo derivative **26** and ethynyl derivative **27** shows that both the molecular structures have identical conformation in the crystal (Figure 4).

(a)

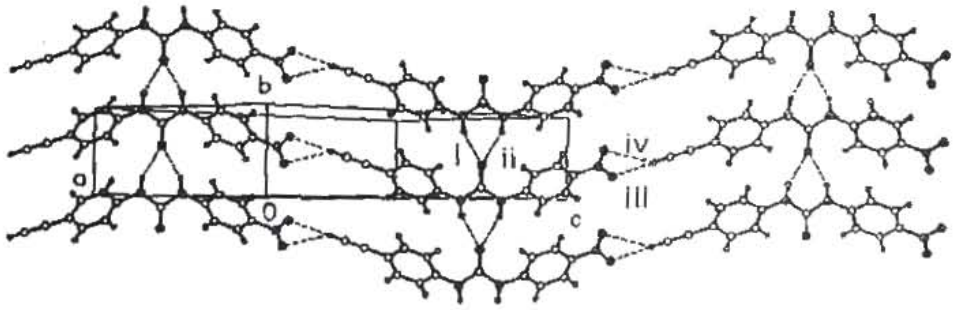

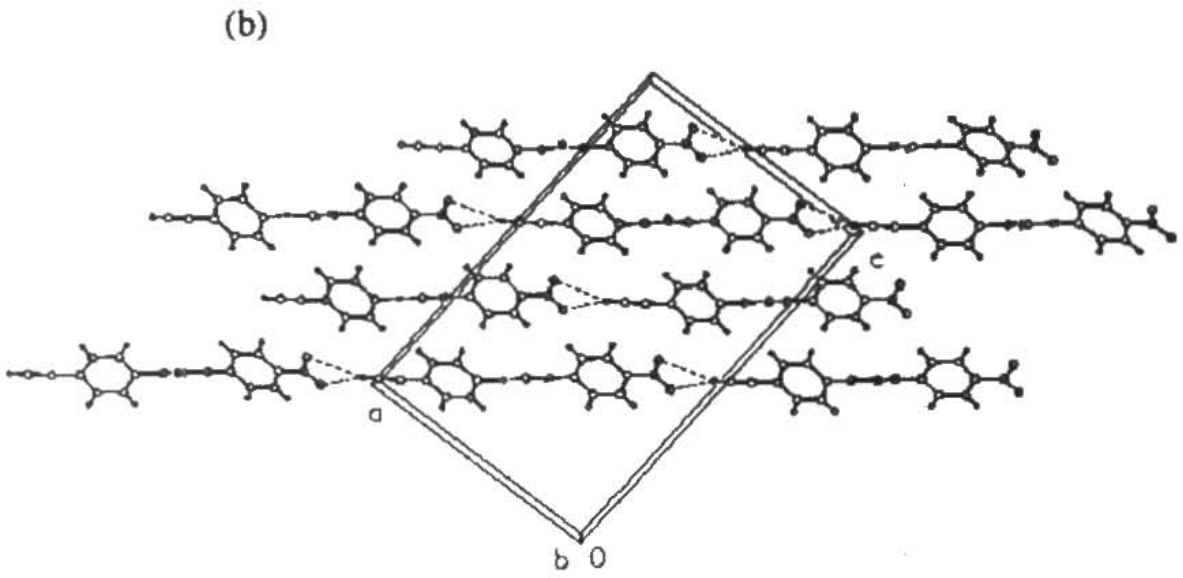

Figure 3. (a) The α-network observed in ethynyl derivative **27** which is supported by the C≡C–H···NO_2 interaction laterally, along the *b*-axis. (b) The parallel alignment of the chains formed through the C≡C–H···NO_2 interaction. See the similarity with that of **26** shown in figure 2.

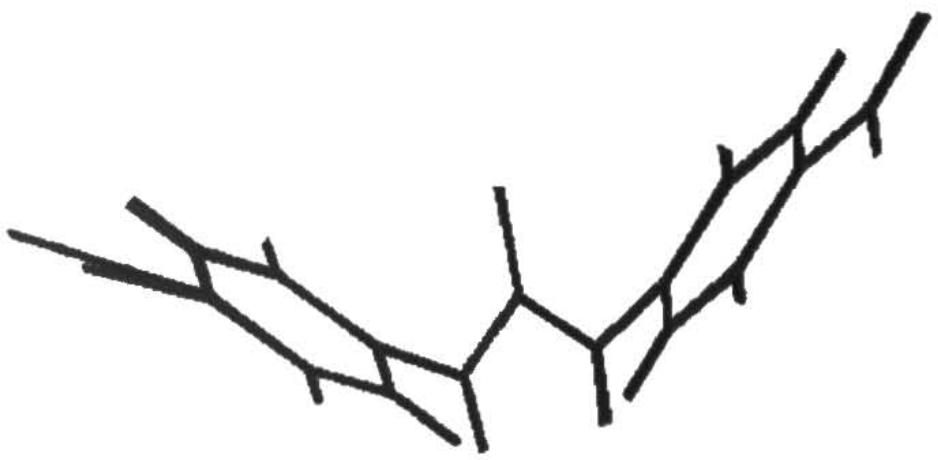

Figure 4. Overlay diagram of iodo derivative **26** and ethynyl derivative **27** shows that both molecules have identical conformations which enable them to pack in the same manner. Magenta represents the iodo derivative **26** and blue represents the ethynyl derivative **27**.

(a)

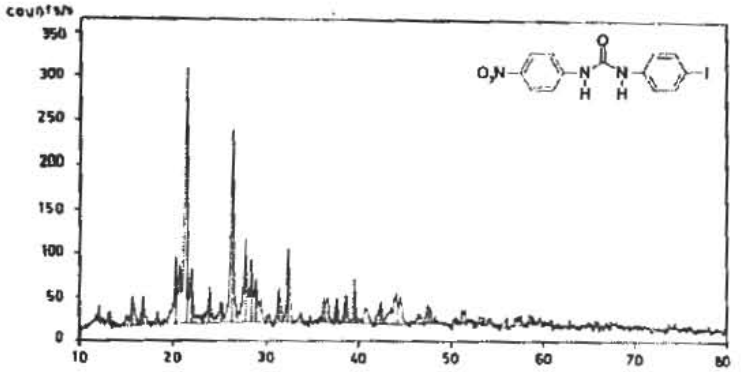

(b)

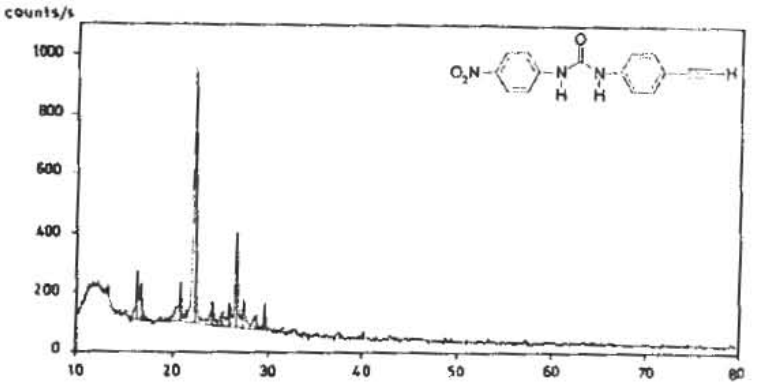

Figure 5. Experimental powder diffraction patterns for (a) iodo derivative **26** and (b) ethynyl derivative **27**. (Cu-Kα radiation, λ = 1.5405 Å)

The isostructurality[11] was further confirmed by experimental powder diffraction pattern recorded for iodo derivative **26** and ethynyl derivative **27**. Both compounds show prominent peaks at $2\theta = 21.4$ and 22.3° (Figure 5). The unit cell similarity index was also calculated for **26** and **27** and was found to be $\Pi = 0.0075$.

SHG test conducted on ethynyl derivative **27** showed efficiency of 1.2 times that of urea.

6.7 Crystal Structure of *N*-4-(*N*,*N*-dimethyl)phenyl-*N*'-4'-nitrophenylurea, 28

The crystal structure of **28** was determined to confirm the structure directing ability of the weak interactions over the strong N–H···O in this family of compounds. The *N*,*N*-dimethyl derivative **28** crystallizes in the space group $P\bar{1}$ with two molecules in the asymmetric unit. Here also the α-network (2.39, 2.21 Å, 153.2, 166.4°; 2.28, 2.29 Å, 159.4, 157.4°) is reproduced faithfully. Weak C–H···O (2.74, 2.96 Å; 133.1, 159.6°) interactions between the $N(Me)_2$ group and the oxygen atoms of the nitro group[12] gives the auxiliary support for the α-network as indicated in figure 6a. Chains along the *c*-axis are aligned antiparallel to each other. The phenyl rings are twisted out of the urea plane with an angle of 53.4, 23.9° and 98.3, 25.2°. The experimental powder pattern for **28** was recorded and the most prominent peak is at $2\theta = 20°$ (Figure 6b) which indicates that the compound has a nearly similar packing pattern to that of iodo derivative **26** and ethynyl derivative **27** explained earlier.

Iodo and ethynyl derivatives **26** and **27** crystallizes in non-centrosymmetric space group *Cc* whereas $N(Me)_2$ derivative **28** has a centrosymmetric crystal packing. Yet the hydrogen bond networks in these structures are nearly identical. Crystal engineering of 1D chains and 2D layers is possible but the final 3D arrangement in a crystal, is still very difficult (impossible) to predict particularly centrosymmetric or non-centrosymmetric.

Robust α-network, formed through recognition between strong donors and acceptors was shown to persist in the presence of functional groups like COOH and $CONH_2$ by Fowler and coworkers.[2a,c] Here the α-network observed in the crystal

structures of compounds **26-28** exhibits a good example were weak interactions play a role in directing the stronger network in the structure.[13] Many of the related derivatives **29-33** explained later in this Chapter show a different packing in centrosymmetric space group which indicates that the weaker interactions X···O_2N are the "discriminator synthon" even in the presence of strong hydrogen bonds. In compounds **26-28** we have succeeded in getting the desired urea tape structure.

(a)

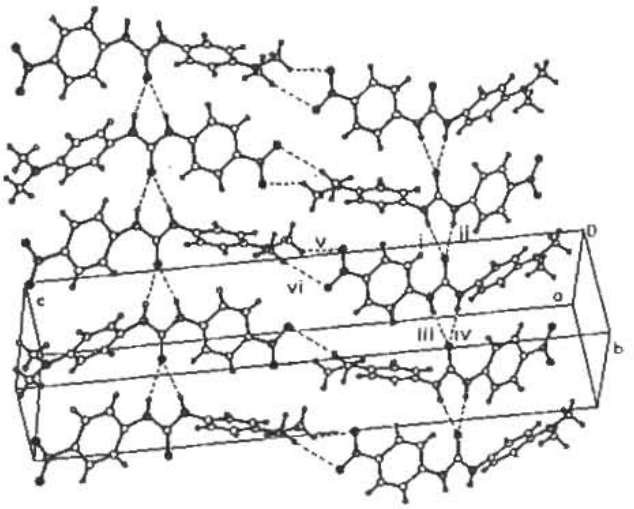

(b)

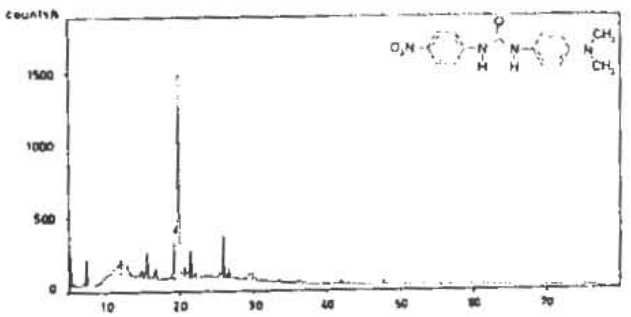

Figure 6 (a) The α-network observed in the crystal structure of *N,N*-dimethyl derivative **28** and the lateral C–H···O interaction. (b) Experimental powder diffraction pattern of **28**.

6.8 Crystal Structure of *N*-4-bromophenyl-*N'*-4'-nitrophenylurea, 29

The bromo derivative **29** crystallizes in centrosymmetric space group $P2_1/n$. This compound was synthesized and the structure was determined to evaluate the robustness of N–H···O urea tape synthon in this family of structures to find out whether the I···NO2, C≡C–H···NO_2 and $N(Me)_2$···NO_2 interactions are only a consequence of the strong hydrogen bond network or do they play a decisive structural role. Bromo derivative **29** adopts a different packing from that of compounds **26-28**. The molecule adopts a flat planar molecular conformation stabilized by intramolecular hydrogen bonds (2.3 Å, 121°; Figure 7a). Molecules pack in a herringbone fashion with respect to each other in the crystal structure. It was found that glide related urea molecules form an N–H···O (2.10, 2.25 Å; 161.3, 157°) hydrogen bond in which one of the oxygen atom in the nitro group acts as a bifurcated acceptor[2b] as shown in figure 7b. The nitro group present in the molecule can competitively act as hydrogen bond acceptor. A calculation was performed on the simple models systems like *N,N'*-dimethyl urea homo dimer and nitromethane···*N,N'*-dimethyl urea dimer (heterodimer). Synthon energies were calculated in STO-3G, 3-21G* and 6-31G* basis set by geometry optimisation in PC Spartan Pro 1.0[14] (Scheme 3). Interaction energies resulting from the N–H···O hydrogen bonds within the dimers were computed as the difference in energy between the dimer, on one hand, and the sum of isolated monomers (kcal/mol) as shown in Table 2. The urea dimer synthon has an energy –8.4 kcal/mol and the urea···NO_2 synthon energy is to –5.9 kcal/mol (6-31G* Table 2). The second oxygen of the nitro group accepts a weak C–H···O hydrogen bond from the *o*-Ph donor (2.742 Å, 162.1°) in the molecule **29**. In the absence of specific X···NO_2 interaction the 2.5 kcal/mol energy difference between the urea···urea and urea···NO_2 synthon can be made up by the three C–H···O bonds (two intramolecular

hydrogen bonds and one intermolecular bond from the *o*-Ph donor) to urea carbonyl oxygen (2.975 Å, 164.1°) which finally results in the layered structure (Figure 7). The bromine atom in the molecule is not involved in any short contacts.

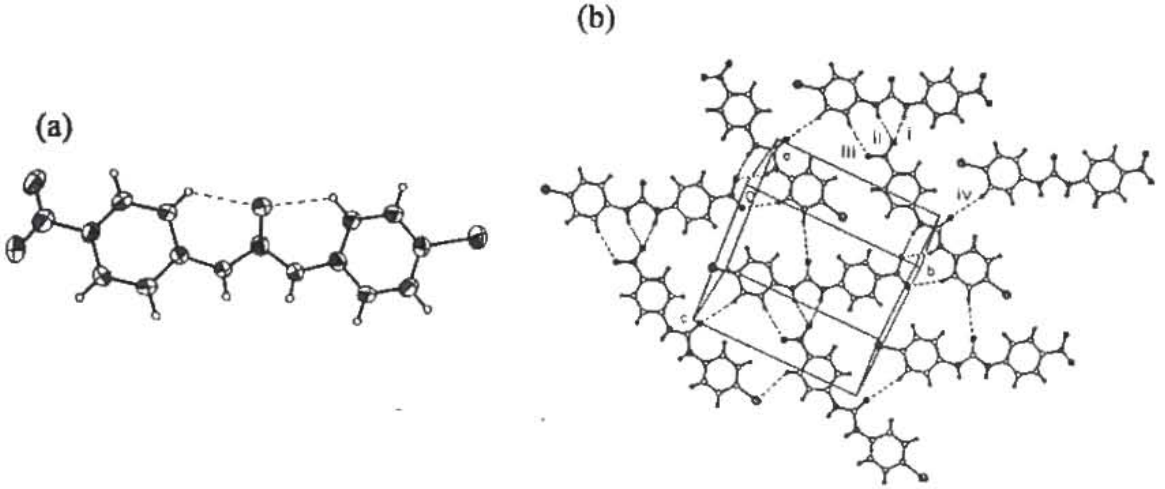

Figure 7. (a) ORTEP diagram of bromo derivative **29**. (b) Packing diagram of **29** which shows the Urea···Nitro interaction. Urea oxygen (carbonyl) is involved in the C–H···O interaction but the Br atom does not involve in any short intermolecular contact.

Table 2. Geometry optimisation energy of the model molecules (a) and (b) calculated in PC Spartan Pro. Given in bracket is value in (au).

	Urea dimer (**a**) Energy (kcal/mol)/(au)	Heterodimer(**b**) Energy (kcal/mol)/(au)	$CH_3N(H)CON(H)CH_3$ Energy (kcal/mol)/(au)	CH_3-NO_2 Energy (kcal/mol)/(au)
STO-3G	–374228.45 (–596.38)	–337984.05/ (–538.62)	–187114.23 –(298.19)	–150869.83 –(240.43)
3-21G*	–376976.9 (–600.76)	–329211.6 –(524.64)	–188482.17 –(300.37)	–152018.15 –(242.26)
6-31G*	–379071.49 (–604.098)	–432435.43 –(545.714)	–189531.64 –(302.042)	–152897.89 –(243.66)

1 au = 627.5 kcal/mol

(a) (b)

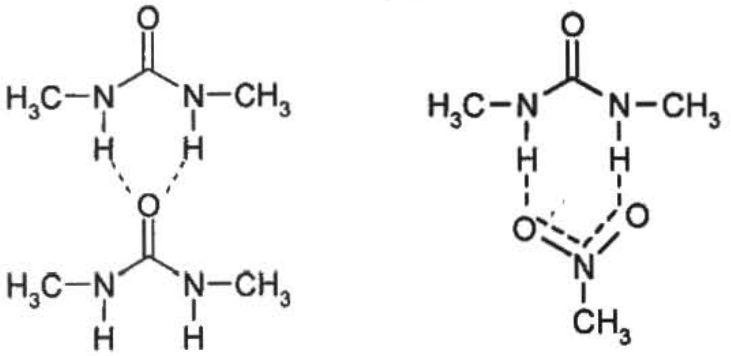

Scheme 3. The model systems on which Spartan calculations was performed (a) urea dimer (b) urea···nitro heterodimer.

6.9 Crystal Structure of *N*-4-chlorophenyl-*N*'-4'-nitrophenylurea, 30

Compounds **29-32** are isostructural and isomorphous. Hydrogen bonding and crystal packing in these structures is very similar, with only slight differences in distances and angles from structure to structure. These crystal structures are displayed in figure **8-10**. All intermolecular interactions are given in Table 1.

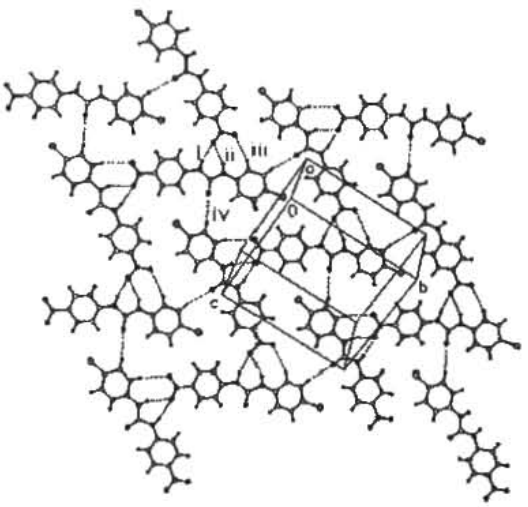

Figure 8. Packing diagram of chloro derivative **30**.

Compounds **29-32** exhibit the same packing with the same space group with nearly equal cell dimensions and angles (see Chapter 7). The unit cell similarity index (Π) was calculated for **29-32** (Table 3). An overlay diagram (Figure 11) of molecules (**29-32**) shows that they have identical conformation.

6.10 Crystal Structure of *N*-4-flourophenyl-*N'*-4'-nitrophenylurea, 31

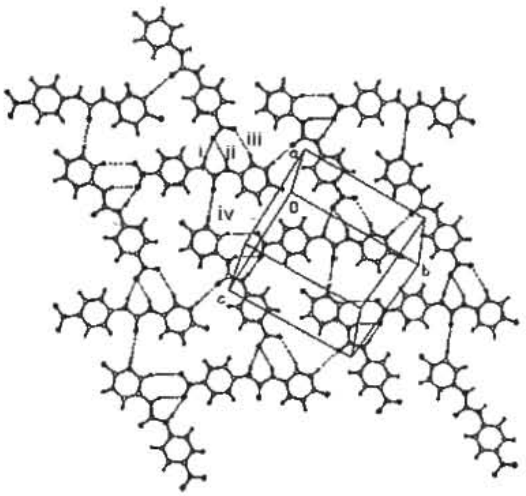

Figure 9. Crystal structure of fluoro derivative **31**.

6.11 Crystal structure of *N*-4-cyanophenyl-*N'*-4'-nitrophenylurea, 32

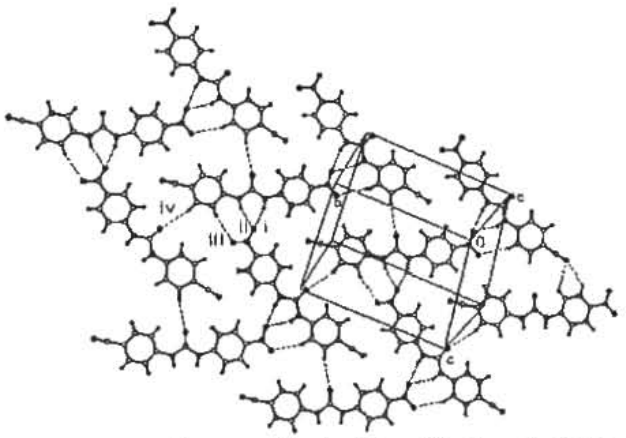

Figure 10. Crystal structure of cyano derivative **32** showing the layered structure.

Table3. Unit cell similarity index (Π) for pairs of isostructural compounds from **29-32.** Variable substituent is indicated in the bracket.

	32 (CN)	**31** (F)	**30** (Cl)	**29** (Br)
29 (Br)	0.0033979	0.0224416	0.0083439	
30 (Cl)	0.0224416	0.013981		
31 (F)	0.0189792		0.013981	0.0224416
32 (CN)			0.0224416	0.0033979

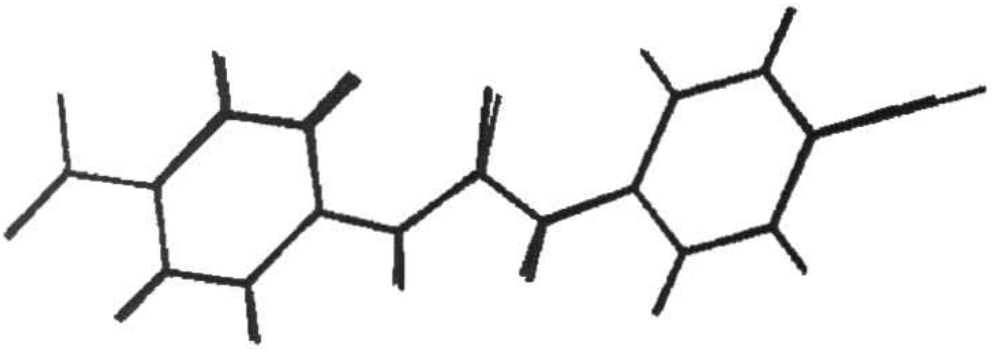

Figure 11. An overlay diagram of molecules **29-32** shows that the molecules are all having identical conformations in the crystal structure. Brown = bromo green = chloro, red = flouro and purple = cyano derivatives respectively.

Powder diffraction was recorded for samples **29-32** and they show similar pattern in terms of 2θ values and peak intensity (Figure 12).

(a)

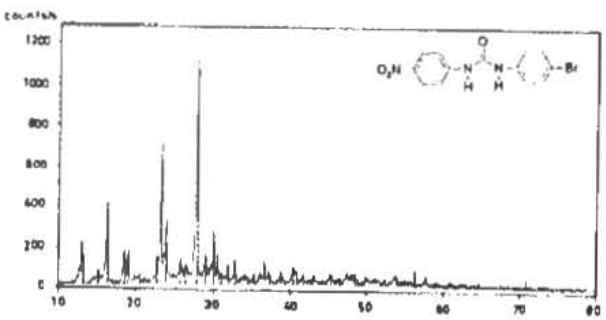

(b)

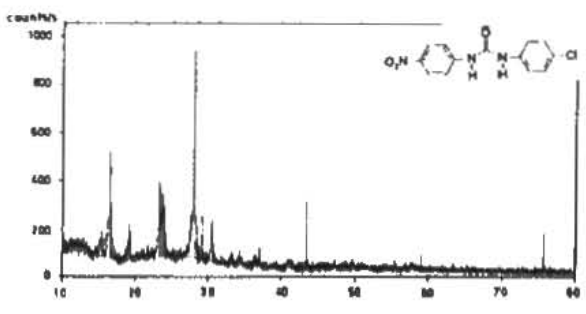

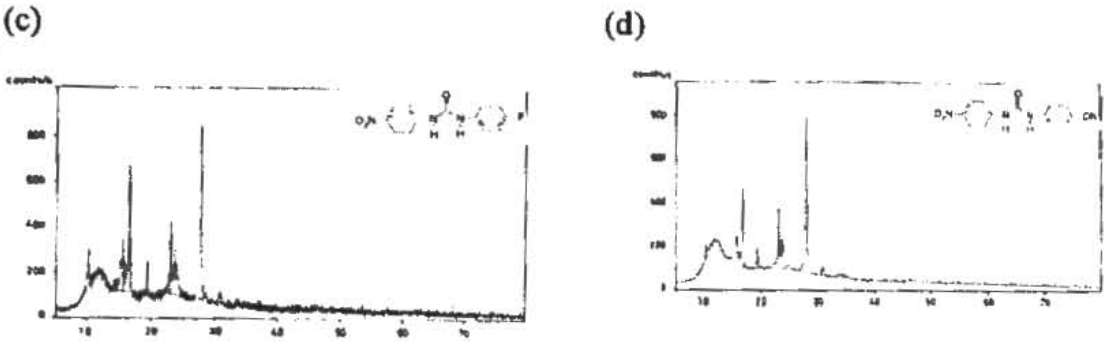

Figure 12. Experimental powder diffraction patterns of compounds (a) bromo derivative **29**, (b) chloro derivative **30**, (c) fluoro derivative **31** and (d) cyano derivative **32**. Note the similarities in the patterns. (Cu-Kα λ= 1.5405 Å.)

The structures **29-32** can be compared with the 1,3-bis(*m*-nitrophenyl)urea/2-butanone 1:1 complex (CSD refcode SILVAK) reported earlier.[2b] Here the urea N–H proton is bonded to the nitro oxygen of the neighbouring glide related molecule. In this structure the guest (2-butanone) and the host are not hydrogen bonded to each other. The butanone present in the structure is highly disordered (Figure 13).

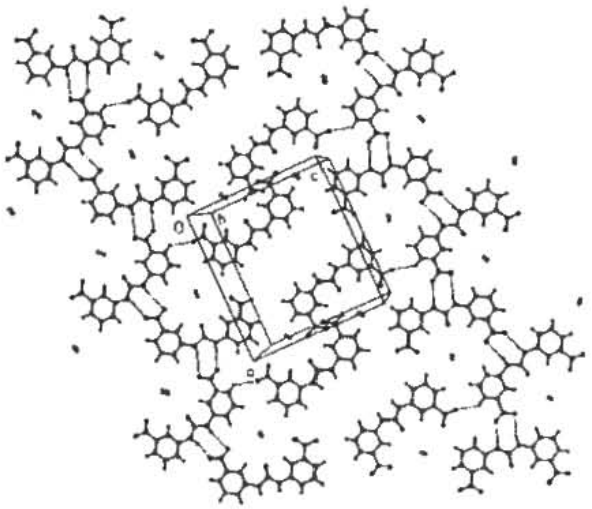

Figure 13. The crystal structure of 1,3-bis(*m*-nitrophenyl)urea/2-Butanone 1:1 complex showing the hydrogen bond formed between a urea N–H proton and oxygen of urea nitro group.

6.12 Crystal Structure of *N-meta*-iodophenyl-*N'*-4'-nitrophenylurea, 33

The compound crystallizes in the same space group as that of the isostructural molecules **29-32** explained above, $P2_1/n$. Molecules hydrogen bonded via urea···nitro synthon pack in the crystal lattice in a herringbone fashion in (Figure 14). The two N–H's of urea form N–H···O bond with the two oxygen atom of the nitro group (2.15 Å, 170.2°;2.169 Å, 165°). The hydrogen atom *ortho* to the iodo group forms a weak C–H···O with the glide related molecules thus forming a planar layer along the [101] plane. Adjacent layers are held together by weak van der Waals interaction. There is a weak C–H···I interaction between a phenyl hydrogen ortho to the nitro group (3.029 Å, 136.5°) and the iodine on the phenyl ring. It is interesting to note that crystal structure of **33** is different from that of its para analogue **26**. By comparing the structure of **33** with **26** it is clear that the position of the iodo functional group is also crucial in producing the target structure.

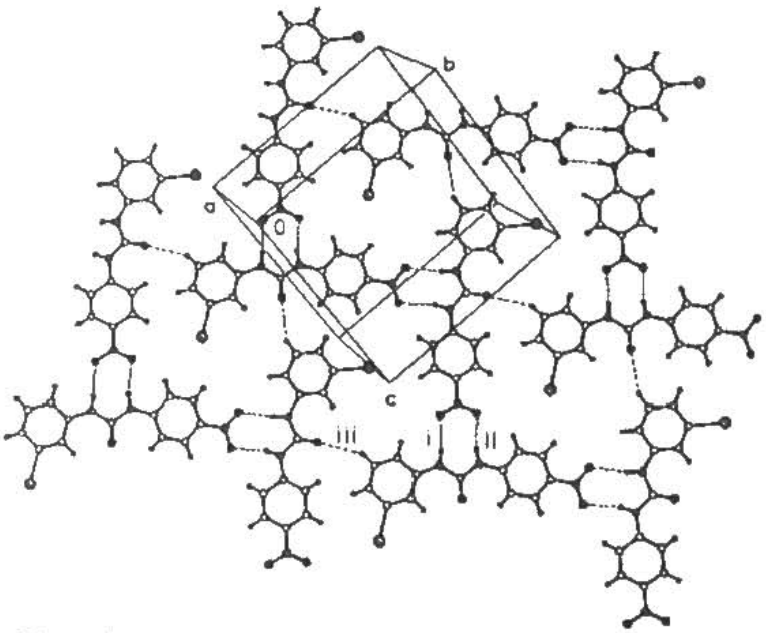

Figure 14. Packing diagram of *meta*-iodo derivative **33**. Note the similarity with the packing patterns of **29-32**.

A CSD search on the nitrodiphenylurea's show that the α-network is not so common in this family of structures. The β-polymorph of *N*-3-nitrophenyl-*N'*-3'-nitrophenylurea (CSD refcode SILTOW01) is the only structure with the α-network (Figure 1).

The above mentioned structures (**29-33**) can also be compared with the urea-carboxylate interaction reported by Hamilton and co-workers[15] (Figure 15) as a strong motif for controlling packing in the solid state. This illustrates alternative hydrogen bonding possibilities depending on the substitution and functional groups in the molecule.

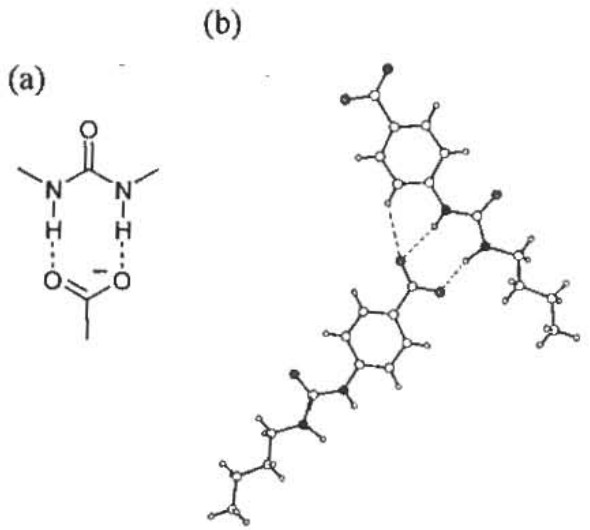

Figure 15. (a) Urea-carboxylate synthon in tetrabutyl- and tetramethyl-ammonium salts of *N*-butylureabenzoates[15] (b) the urea-carboxylate interaction in the crystal structure of tetrabutylammonium salt of 4-(3-butylureido)benzoate (CSD refcode SEPTIQ). Note the similarity with structures **29-33.**

6.13 DMSO Solvate of *N*-4-iodophenyl-*N'*-4'-nitrophenylurea, 34

The structure of four urea derivatives contain solvent of crystallization. It is possible that these solvents with multiple hydrogen bonding donors and acceptors stabilize solute (compound molecules) to crystallize. It is still not fully understood why solvent molecules are included in the crystal (solvation).

In the crystal structure of **34** DMSO solvate of iodo the compound crystallizes in the space group $P\bar{1}$. There are two molecules of the iodo derivative **34** and DMSO in the asymmetric unit (ratio 1:1). The sulfoxide oxygen in DMSO molecule acts as a bifurcated acceptor by accepting two N–H···O hydrogen bonds in the α-network fashion donated by the urea molecule (1.95, 2.079 Å; 157.4°, 153.3°) (Figure 16). The methyl groups are bonded to the iodine and oxygen of nitro group through C–H···I (3.47 Å, 104°; 3.512 Å, 101.8°) C–H···O (2.5 Å, 165.2°) and C–H···N (2.920 Å, 165.2 °) interactions (see figure 16 and table 1 for details). The role of the DMSO molecule in the crystal structure is to act as a template in self-assembly. It brings the two urea molecules together. The DMSO molecule is present in between the urea molecule and it does not have direct contacts with another DMSO molecule. The urea molecules have a nearly planar conformations.

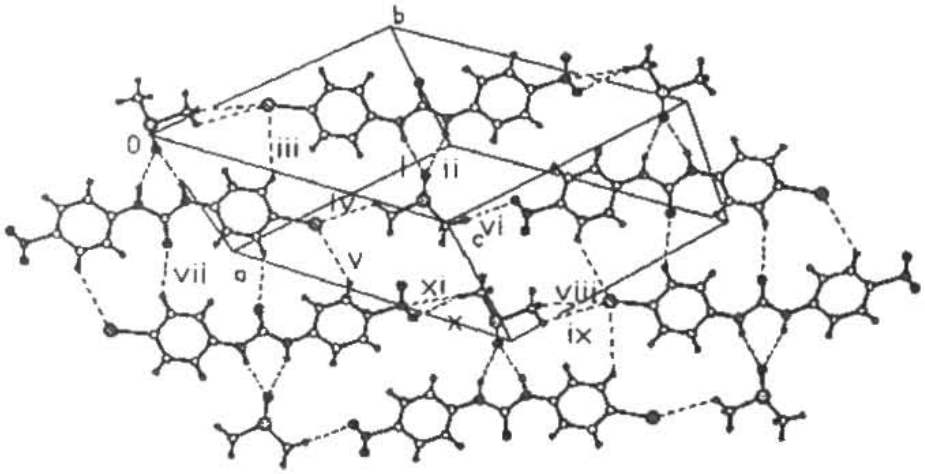

Figure16. The crystal structure of **34** showing the DMSO solvent occupying in between the urea molecule in the lattice. All the interactions are labelled.

Thermogravimetric analysis (TGA) carried out under nitrogen atmosphere from room temperature to 350°C shows weight loss steps as the temperature was increased (Figure 17). The weight loss at 120-180°C corresponds well with the loss of a DMSO molecule located in the crystal lattice. DSC was recorded on the solvate

crystal. A sharp endotherm at 170°C corresponds to the solvent loss and endotherm at 280°C corresponds to the decomposition of the iodo derivative.

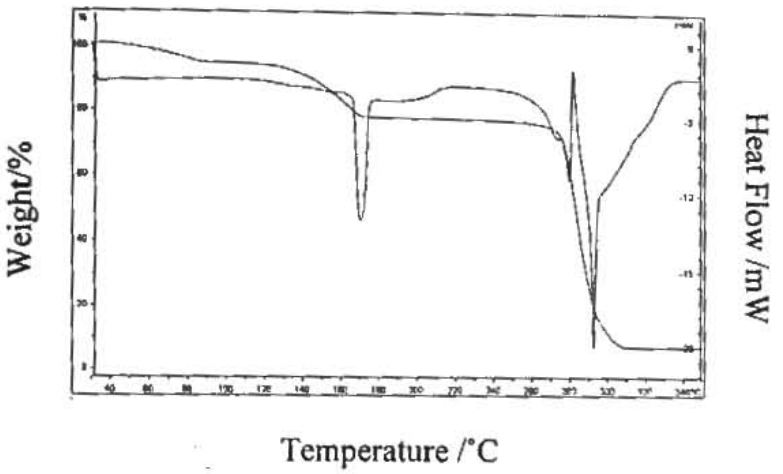

Figure 17. DSC/TGA plot recorded for DMSO solvate of *N*-4-iodophenyl-*N'*-4'-nitrophenylurea, **34**

6.14 DMF Solvate of *N*-phenyl-*N'*-4'-nitrophenylurea, 35

The tolyl derivative crystallizes in the space group $P2_1/c$ with one molecule of *N*-phenyl-*N'*-4'-nitrophenylurea and *N,N*-dimethylformamide (DMF) in the asymmetric unit (ratio 1:1). DMF accepts two N–H···O hydrogen bonds from the urea molecule forming a finite chain as shown in the figure 18. Adjacent chains are aligned parallel with respect to each other resulting in a corrugated layered structure. Adjacent layers are inversion related to produce a centrosymmetric structure. Compound **35** crystallized only from DMF despite attempting crystallization from several solvents, once again emphasizing the specific hydrogen bonding role of the solvent molecule.

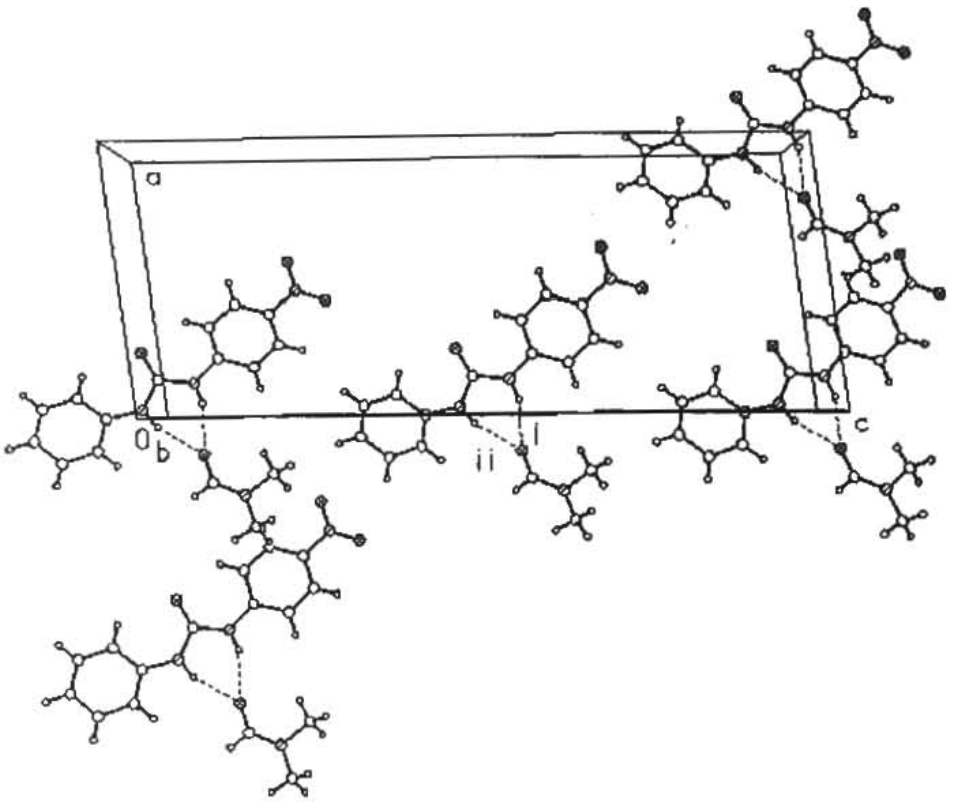

Figure 18. Packing diagram of compound **35** showing the inclusion of DMF molecule in the lattice viewed down the *b*-axis. Carbonyl oxygen in DMF accepts two N–H···O hydrogen bond from urea molecule.

TGA analysis carried out from room temperature to 350°C show evidence at 70-150°C corresponding to weight loss. The weight loss corresponds well with the loss of DMF molecule in the crystal structure (Figure 19). The sharp endotherm at 240°C in the DSC plot recorded corresponds to the melting point of *N*-phenyl-*N'*-4'-nitrophenylurea. There is evidence for two stage decomposition between 220-320°C from TGA.

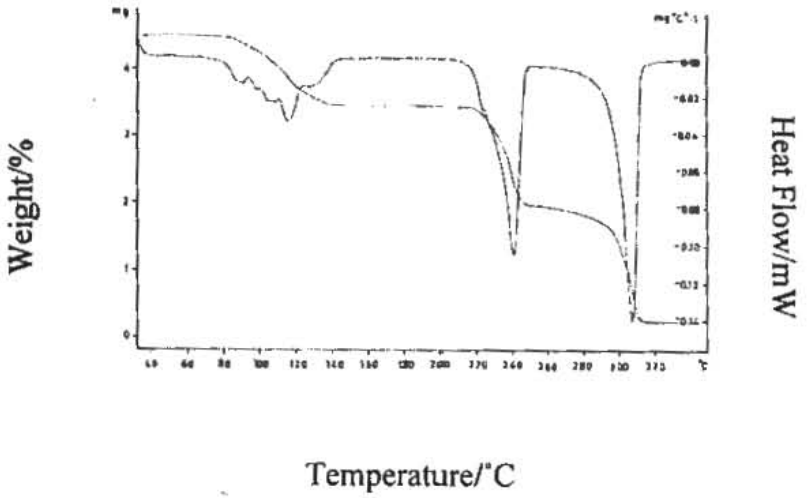

Figure 19. DSC/TGA trace of DMF solvate of *N*-phenyl-*N'*-4'-nitrophenylurea, **35**

6.15 DMSO Solvate of *N*-4-tolyl-*N'*-4'-nitrophenylurea, 36

The tolyl derivative crystallizes in the space group $P2_1/n$ with 2 molecules of urea and DMSO in the asymmetric unit (ratio 1:1). One of the DMSO molecule is partially disordered in which the sulfur atom is positionally disordered with occupancy 0.6 and 0.4. DMSO molecule links two urea molecule and forms a part of the α-network chain along the *a*-axis. The sulphoxide oxygen in both DMSO molecules accepts two N–H···O hydrogen bonds [(1.992 Å, 160.4°; 2.051Å, 156.4°), (2.001 Å, 156.8 °; 2.100, 155.1 °)] from urea NH and donates two C–H···O hydrogen bonds to the urea carbonyl oxygen [(2.666 Å, 141.5 °; 2.370 Å, 149.9 °), (3.079 Å, 128.8 °; 2.884 Å, 126.5 °)] thus completing the chain. The crucial role of DMSO solvent in forming the chain of molecules with N–H···O and C–H···O hydrogen bonds is shown in figure 20a. Adjacent chains pack parallel with respect to each other within the layer (figure 20b). The adjacent layers are antiparallel resulting in an overall centrosymmetric structure. Phenyl rings of adjacent layers

interdigitate in the inter-layer region (figure 20c). Interlayer regions are also stabilised by C–H···O hydrogen bond formed between the activated C–H group ortho to the nitro group and nitro oxygen atom (2.5 Å, 139°).

Variations in the TGA trace observed at 115-150°C corresponds to weight loss. The weight loss match in ratio well with the loss of a DMSO molecule from the lattice (Figure 21). DSC trace shows a sharp endotherm at 119°C, corresponding to the solvent loss and the exotherm at 190°C indicating decomposition.

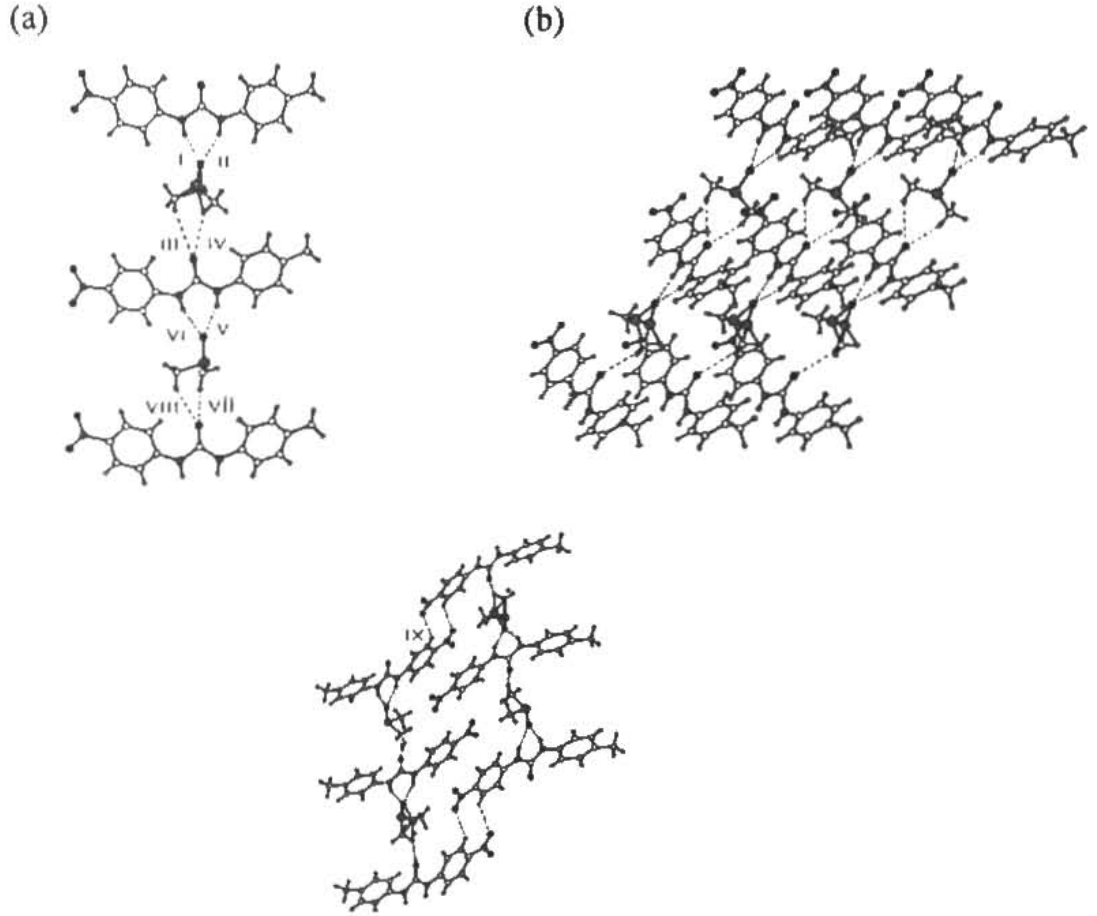

Figure 20. (a) 1D Chain containing urea molecule and DMSO packing alternatively in the crystal structure of tolyl derivative **36**. Note that the DMSO molecule sits in between the urea molecules and interrupts the α-network. (b) In a layer adjacent chains align parallel with respect to each other. (c) Centrosymmetric arrangement of adjacent layers mediated by C–H···O hydrogen bonds.

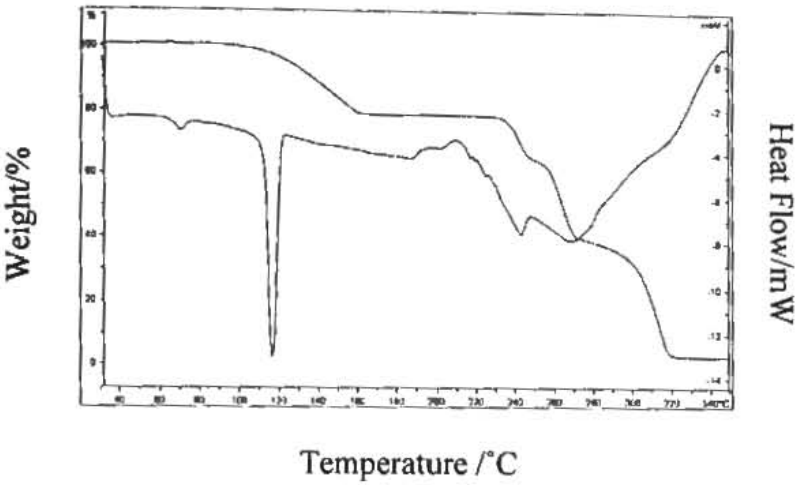

Figure 21. TGA plot of *N*-4-tolyl-*N'*-4'-nitrophenylurea, **36**

6.16 DMSO Solvate of *N*-(4-acetyl)phenyl-*N'*-4'-nitrophenylurea, 37

The acetyl derivative crystallizes in the space group $P\bar{1}$. The assymetric unit contains one molecule of acetyl derivative and one molecule of DMSO molecule. When DMSO is included in organic crystals, the main interaction is generally a strong H-bond of the O–H···O or N–H···O type where in DMSO acts as an acceptor. Further the C–H group in DMSO are sufficiently activated by the sulfoxide group so that they also donate hydrogen bonds to electronegative atoms. In this structure also the DMSO molecule is interrupting the urea tape by intervening between adjacent molecules. It can act as a template in organizing the urea molecules in the crystal. The two urea N–H's are hydrogen bonded to the oxygen of DMSO (S = O) (2.099 Å, 150.1°; 1.984 Å, 156.5°) and the C–H···O hydrogen bonds are donated (2.967 Å, 147.2°; 2.495 Å, 167°) from DMSO molecule to the carbonyl of the acetyl group which links the next molecule to complete the chain (Figure 22). The urea carbonyl is involved in a C–H···O

hydrogen bond with the activated C–H ortho to the nitro group of a neighbouring inversion related molecule (interaction v in figure 22a). Thus through a system of N–H···O and C–H···O hydrogen bonds the DMSO molecule is able to assemble urea molecules and organize them in an α-network. Thus the role of DMSO molecule in promoting crystallization is evident here. Within a layer adjacent chains pack parallel (Figure 22b) and adjacent layers are inversion related (Figure 22c). Crystallization from several other solvents was not successful.

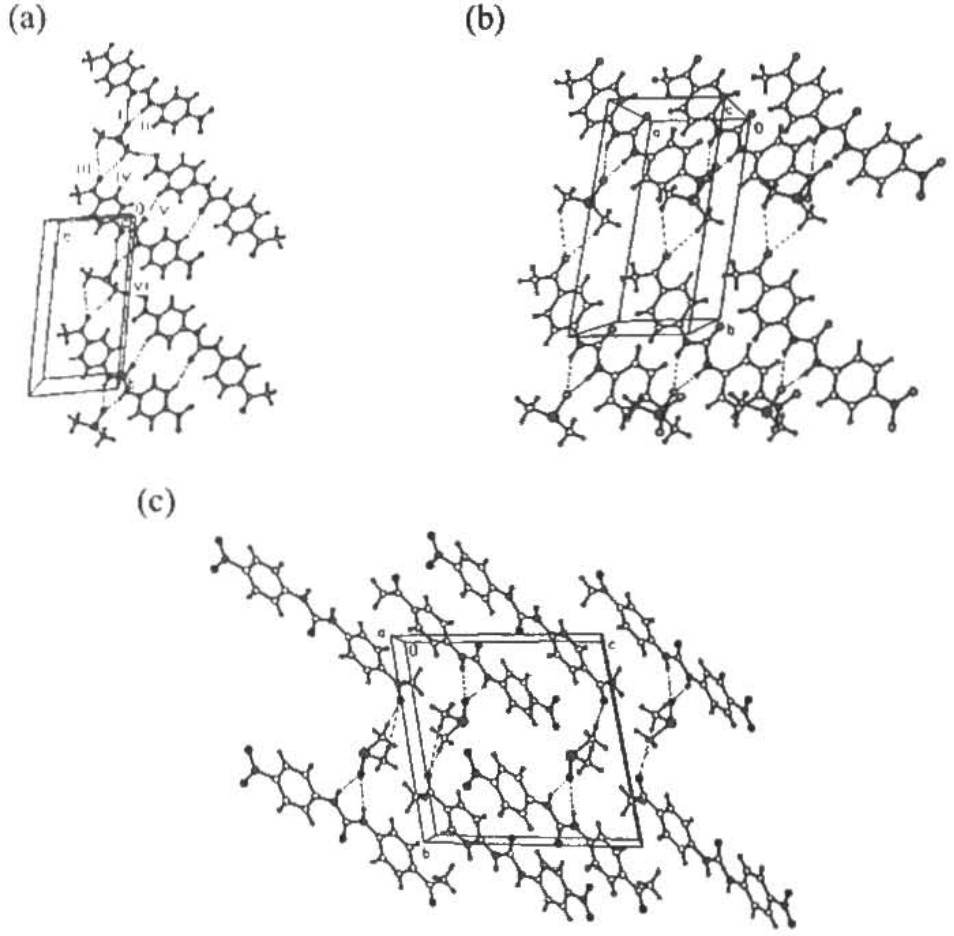

Figure 22. (a) Packing diagram of **37** showing the DMSO molecule sitting in between the urea molecule in the crystal structure in the (101) plane. (b) Parallel arrangement of the chains within a layer and c) the centrosymmetric arrangement of adjacent layers.

A TGA trace recorded on the acetyl derivative indicates solvent loss at 160°C (Figure 23). DSC was recorded on the solvate crystal and the endotherm at 179°C corresponds to the decomposition of the urea compound.

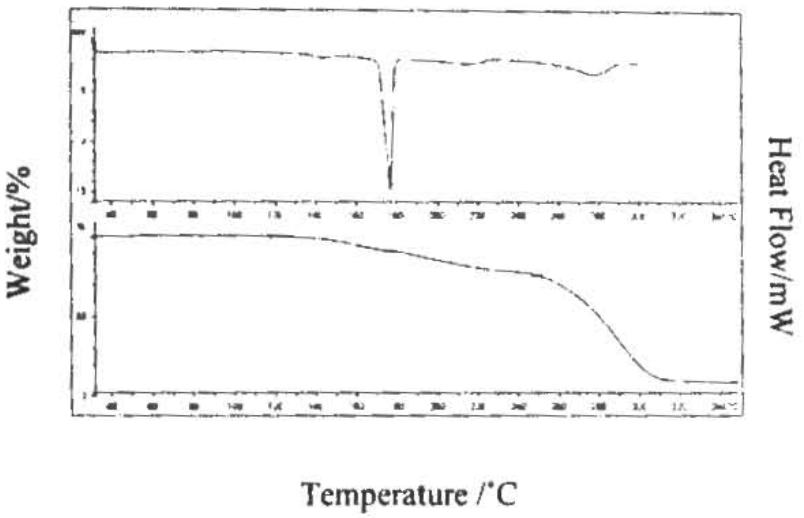

Figure 23. DSC/TGA plot of *N*-4-acetyl-*N'*-4'-nitrophenylurea, **37**

The solvates **36** and **37** can be compared with 1-(*m*-nitrophenyl)-3-(*p*-nitrophenyl)urea/DMSO 1:1 complex (CSD refcode SILVOY).[2b] Both the –NH protons from urea are donated to the oxygen of the DMSO molecule and the DMSO molecule in turn donates its methyl C–H to the urea carbonyl to complete the chain as shown in Figure 24.

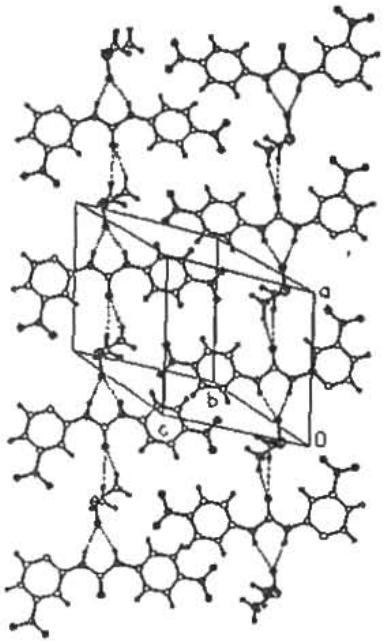

Figure 24. Crystal structure of 1-(*m*-nitrophenyl)-3-(*p*-nitrophenyl)urea/DMSO 1:1 complex showing the DMSO molecule sitting in between the urea viewed down the *b*-axis. Note the similarity with the structures of **36** and **37**.

6.17 Conclusion

This chapter discusses three different categories of crystal structures within the urea series. (a) Structures forming the α-network **26-28**; (b) structures which contain urea···NO_2 synthon **29-33**; and (c) solvates of urea molecules **34-37**. The variety of structures indicates that the aggregation pattern of one compound cannot be predicted from a knowledge of hydrogen bonding in the other structures even if they are closely related. Structure varieties of these types provide continuing challenges for predictions in crystal engineering. The cocrystallization properties of a large number of 1,3-diaryl ureas[2b] with flat planar aromatic substituents have been characterized. Diaryl ureas with *meta*-substituted electron withdrawing groups on the aryl ring were found capable of forming complexes with a wide variety of hydrogen bond acceptors. The aryl group here did not provide any steric hindrance

to hydrogen bonding by urea functional groups. The latter can thus interact with intermolecular hydrogen bond acceptors and donors. The nature of the final structure depends on the hydrogen bonding group in the molecule and the solvent of crystallization. The presence of nitro substituents in compounds discussed in this Chapter was often found to cause a significant deviation from the patterns that were expected. Cl, F, Br, CN do not form weak interaction with the NO_2 or CO (carbonyl) group. However iodo, ethynyl and *N,N*-dimethyl hydrogen bond with the nitro group and thier structures change considerably with these functional group. The N–H group of the urea preferentially form hydrogen bond with the nitro oxygen rather than the carbonyl in compounds **29-33**, thus preventing the formation of the α-network. The crystal structure illustrates both the conformational and the hydrogen bonding preferences of these nitrophenyl ureas. The energy of forming α-network with the two N–H···O's (carbonyl) can be equalled by two N–H···O (nitro) and weak C–H···O (carbonyl) bond with an alternate packing arrangement. This pattern has the feature that the carbonyl, nitro and –NH hydrogens are used in hydrogen bonding.

Solvents like DMSO, DMF plays a role in the solvated structures. They bind together the urea molecules that are unable to self assemble into a crystal lattice. There is a good donor acceptor combination of hydrogen bonds in the DMSO solvates. Majority of the organic crystals (85 %) are unsolvated. But because of multipoint recognition[16] between solute and solvent there should be an extra enthalpic gain in retaining the solvent molecule in the crystal. The multipoint recognition of certain organic solvents like DMSO, DMF and dioxane increases the probability for solvation.

6.18 Experimental

Synthesis

For the preparation of urea molecules **26-37** studied, the *p*-nitrophenyl isocyanate was condensed with the corresponding *p*-X-aniline in benzene as solvent. Yields are unoptimized. NMR spectra were recorded on Bruker 200 MHz spectrometer in DMSO (d_6). Peaks are given in δ (ppm). IR spectra were recorded as KBr wafer and peaks are reported in cm^{-1}. Compound **27** was prepared by protecting the 4-iodoaniline using trimethylsilylacetylene and condensing it with the *p*-nitrophenylisocyanate followed by deprotection to obtain the product. Melting point was recorded on Fisher Jones melting point apparatus. Powder diffraction was recorded on Philips Analytical PXRD machine.

1. *N*-4-iodophenyl-*N'*-4'-nitrophenylurea, 26

A mixture of 4-iodoaniline (500 mg, 2.28 mmol) and 4-nitrophenyl isocyanate (487.1 mg, 3 mmol) in 12 ml benzene was heated to reflux for until there was no starting material remained by TLC. The product (98% yield) was filtered from the reaction mixture and was recrystallized from THF. M.p. above 250°C. ^{1}H NMR: δ 9.45 (s, 1H), 9.03 (s, 1H), 8.2 (d, J = 8, 2H), 7.7 (d, J = 8, 2H), 7.6 (d, J = 8, 2H), 7.3 (d, J = 8, 2H). IR (KBr): 3308, 1647, 1388 cm^{-1}.

2. *N*-4-ethynylphenyl-*N'*-4'-nitrophenylurea, 27

Ethynyl derivative **27**, was prepared by protecting the 4-iodoaniline using trimethylsilylacetylene and condensing it with the *p*-nitrophenylisocyanate followed by deprotection to obtain the product.

Preparation of 4-(2-Trimethylsilyl-1-ethynyl)aniline

Trimethylsilylacetylene (3.425 mmol, 335.6 mg, 0.48 ml) was added into 4-Iodoaniline (500 mg, 2.283 mmols) taken in 7 ml Et_3N in presence of cuprous

iodide and palladium catalyst [($PdCl_2(PPh_3)$)] at 0°C under nitrogen atmosphere and the reaction mixture was allowed to stir in RT for 12 h. Et_3N was removed and the product was purified by column chromatograpy using neutral silica with hexane eluent. The product was charecterised by IR and NMR spectra, yield 52 %, M.p. 99-101°C. ^{1}H-NMR (dmso d_6): δ 0.2 (s, 9H), 5.5 (s, 2H), 6.5 (d, J = 8, 2H), 7.1 (d, J = 8, 2H). IR (KBr): 3464, 2146, 1622, 1510.

Preparation of *N*-4-(2-trimethylsilyl-1-ethynyl)phenyl-*N'*-4'-nitrophenylurea

A mixture of 4-(2-trimethylsilyl-1-ethynyl)aniline (294 mg, 1.55 mmol) and 4-nitrophenyl isocyanate (306 mg, 1.87 mmol) in 12 ml benzene was heated to reflux until there was no starting material remained by TLC. The product was filtered and charecterised, yield 98%. M.p. above 250°C. ^{1}H-NMR (dmso d_6): δ 0.2 (s, 9H), 7.2 (d, J = 8, 2H). 7.4 (d, J = 8, 2H), 7.7 (d, J = 8, 2H), 8.3 (d, J = 8, 2H), 9.2 (s, 1H), 9.5 (s, 1H). IR (KBr): 3364, 2156, 1680, 1595, 1408 cm^{-1}.

Deprotection of *N*-4-(2-trimethylsilyl-1-ethynyl)phenyl-*N'*-4'-nitrophenylurea to *N*-4-ethynylphenyl-*N'*-4'-nitrophenylurea, 27

To the protected urea derivative *N*-4-(2-trimethylsilyl-1-ethynyl)phenyl-*N'*-4'-nitrophenylurea (344 mg) taken in 15 ml MeOH was added 10 ml K_2CO_3 in MeOH. The reaction mixture was stirred for 1 h. The product ethynyl derivative was filtered and crystallized from THF/benzene mixture (yield 66%). M.p. above 250°C. ^{1}H NMR (dmso d_6): δ 9.6 (s, 1H), 8.9 (s, 1H), 8.2 (d, J = *8*, 2H), 7.75 (d, J = *8*, 2H), 7.54 (d, J = *8*, 2H), 7.45 (d, J = *8*, 2H), 4.1 (s, 1H). IR (KBr): 3260, 1647, 1585, 1502, 1408.

Procedure similar to that of **26** was followed for compounds from **28-37.**

3. *N*-4-(*N*,*N*-dimethyl)phenyl-*N'*-4'-nitrophenylurea, 28

Compound was crystallized from ethylacetate/hexane mixture (30% yield). M.p. sublimed at 246°C. ^{1}H NMR (dmso d_6): δ 9.3 (s, 1H), 8.55 (s, 1H), 8.19 (d, J = 8, 2H), 7.64 (d, J = 8, 2H), 7.25 (d, J = 8, 2H), 6.68 (d, J = 8, 2H), 2.84 (s, 6H). IR (KBr): 3310, 1643, 1612, 1406 cm^{-1}.

4. *N*-4-bromophenyl-*N'*-4'-nitrophenylurea, 29

Compound was crystallized from THF/Ethanol/Benzene mixture (97% yield). M.p. above 250°C. ^{1}H NMR (dmso d_6): δ 9.47 (s, 1H), 9.06 (s, 1H), 8.17 (d, J = 8, 2H), 7.6 (d, J = 8, 2H), 7.47 (s, 4H). IR (KBr): 3368, 1726, 1614, 1417 cm^{-1}.

5. *N*-4-chlorophenyl-*N'*-4'-nitrophenylurea, 30

Compound was crystallized from THF/Ethanol mixture (92% yield). M.p. above 250°C. ^{1}H NMR (dmso d_6): δ 9.46(s, 1H), 9.05(s, 1H), 8.17 (d, J = 8, 2H), 7.66 (d, J = 8, 2H), 7.48 (d, J = 8, 2H), 7.33 (d, J = 8, 2H). IR (KBr): 3369, 1724, 1595, 1415 cm^{-1}.

6. *N*-4-fluorophenyl-*N'*-4'-nitrophenylurea, 31

Compound was crystallized from THF/Ethanol mixture (yield 95%). M.p. above 250°C. ^{1}H NMR (dmso d_6): δ 9.417 (s, 1H), 8.93 (s, 1H), 8.16 (d, J = 8, 2H), 7.66 (s, d J = 8, 2H), 7.45 (dd , J = 5, 9, 2H), 7.10 (dd, J = 9, 8, 2H). IR (KBr): 3406, 1724, 1618, 1408 cm^{-1}.

7. *N*-4-cyanophenyl-*N'*-4'-nitrophenylurea, 32

Compound was crystallized from THF/Ethanol mixture (yield 90%). M.p. above 250°C.^{1}H NMR (dmso d_6): δ 9.62 (s, 1H), 9.42 (s, 1H), 8.2 (d, J = 8, 2H), 7.6 (m, 6H). IR (KBr): 3412, 2220, 1728, 1597, 1531, 1413 cm^{-1}

8. *N-meta*-iodophenyl-*N'*-4'-nitrophenylurea, 33

Compound was crystallized from DMSO (yield 99%). M.p. above 250°C. ^{1}H NMR (dmso d_6): δ 9.49 (s, 1H), 9.043 (s, 1H), 8.17 (d, J = 8, 2H), 8.015 (s, 1H), 7.67 (d, J = 8, 2H), 7.35 (d, J = 8, 2H), 7.1 (t, 1H). IR (KBr): 3380, 1640, 1410 cm^{-1}.

9. *N*-phenyl-*N'*-4'-nitrophenylurea, 35

Compound was crystallized from DMF (yield 98%). M.p. 226-229°C. ^{1}H NMR(dmso d_6): δ 9.42 (s, 1H), 8.91 (s, 1H), 8.17 (d, J = *8*, 2H), 7.66 (d, J = *8*, 2H), 7.45 (d, J = *8*, 2H), 7.27 (t, J = *8*, 2H), 7.018 (t, J = *6*, 1H). IR (KBr): 3298, 1649, 1698, 1562, 1446 cm^{-1}.

10. *N*-4-tolyl-*N'*-4'-nitrophenylurea, 36

Compound was crystallized from DMSO (yield 96%). M.p. 238°C. ^{1}H NMR (dmso d_6): δ 9.38 (s, 1H), 8.80 (s, 1H), 8.16 (d, J = *8*, 2H), 7.69 (d, J = *8*, 2H), 7.33 (d, J = *8*, 2H), 7.13 (d, J = *8*, 2H), 2.25 (s, 3H). IR (KBr): 3302, 1647, 1512, 1408 cm^{-1}.

11. *N*-(4-acetyl)phenyl-*N'*-4'-nitrophenylurea, 37

Compound was crystallized from DMSO (yield 50%). M.p. above 250°C. ^{1}H NMR (dmso d_6): δ 9.543 (s, 1H), 9.32 (s, 1H), 8.19 (d, J = *8*, 2H), 7.91 (d, J = *8*, 2H), 7.69 (d, J = *8*, 2H), 7.59 (d, J = *8*, 2H). IR (KBr): 3317, 1649, 1520, 1403 cm^{-1}.

Data Collection and Crystal Structure Determination

The cell parameters, space groups and crystal structures were determined from single crystal X-ray diffraction data collected at ambient temperature on Enraf-Nonius CAD-4 diffractometer and Bruker Smart CCD diffractometer at

University of Hyderabad, Hyderabad and The Chinese University, Hong Kong. The incident radiation is Mo-Kα X-ray radiation (λ = .71073 Å) on both inustraments. Data reduction was performed using the Xtal 3.5.[17] Structures were solved using the direct methods using SHELXS-97.[18] Analysis was carried out in PLATON[19] on Silicon Graphics workstation. Empirical absorption correction using SADABS[20,21,22] and semi empirical[23] was applied for **26, 29, 30, 33** and **34.** Powder pattern was collected on Philips X-ray diffractometer (Cu-Kα, λ = 1.5405 Å) in University of Hyderabad.

Thermal Analysis

Differential scanning calorimetry (DSC) was performed on a Mettler Toledo DSC 822e module and thermogravimetry (TG) was performed on a Mettler Toledo TGA/SDTA 851e module at University of Hyderabad. Crystals taken from the mother liquor were blotted dry on filter paper and placed in open alumina pans for the TG experiment and in crimped but vented aluminium sample pans for the DSC experiment. The sample size in each case was 5-7 mg. The temperature range was typically 30-300°C at a heating rate of 10°C/min. A stream of N_2 flowing at 150 mL/min for the DSC runs and 50 mL/min for the TG runs purged the samples.

6.19 References

1) (a) J.A.R.P. Sarma, F.H. Allen, V.J. Hoy, J.A.K. Howard, R. Thaimattam, K. Biradha and G.R. Desiraju, *Chem. Commun.*, **1997**, 101. (b) N. Masciocchi, M. Bergamo and A. Sironi, *Chem. Commun.*, **1997**, 1347. (c) R. Thaimattam, C.V.K. Sharma, A. Clearfield and G.R. Desiraju, *Cryst. Growth Des.*, **2001**, *1*, 103. (d) C.J. Kelly, J.M.S. Skakle, J.L. Wardell, S.M.S. Wardell, J.N. Low and C. Glidewell, *Acta Cryst.*, **2002**, *B58*, 94. (e)

P.K. Thallapally, S. Basavoju, G.R. Desiraju, M. Bagieu-Beucher, R. Masse and J.-F. Nicoud, *Current Science.*, **2003**, *85*, 995.

2) (a) X. Zhao, Y.-L. Chang, F.W. Fowler and J.W. Lauher, *J. Am.Chem. Soc.*, **1990,** *112*, 6627. (b) M.C. Etter, Z. Urbánczyk-Lipkowska, M. Zia-Ebrahimi and T.M. Panunto, *J. Am. Chem. Soc.*, **1990**, *112*, 8415. (c) Y.-L. Chang, M.-A West, F.W. Fowler and J.W. Lauher, *J. Am.Chem. Soc.*, **1993**, *115*, 5991. (d) J.S. Nowick, N.A. Powell, E.J. Martinez, E.M. Smith and G. Noronha, *J. Org. Chem.*, **1992,** *57*, 3763. (e) M.L. Loos, J.V. Esch, I. Stokroos, R.M. Kellogg and B.L. Feringa, *J. Am. Chem. Soc.*, **1997**, *119*, 12675. (f) C. Shi, Z. Huang, S. Kilic, J. Xu, R.M. Enick, E.J. Beckmen, A.J. Carr, R.E. Melendez and A.D. Hamilton, *Science*, **1999**, *286*, 1540. (g) A.J. Myles and N.R. Branda, *J. Am. Chem. Soc.*, **2001**, *123*, 177. (h) L.S. Shimizu, M.D. Smith, A.D. Hughes and K.D. Shimizu, *Chem. Commun.*, **2001**, 1592. (i) J.J.E. Moreau, L. Vellutini, M.W.C. Man and C. Bied, *Chem. Eur. J.*, **2003**, *9*, 1594. (j) J.J.E. Moreau, B.P. Pichon, M.W.C. Man, C. Bied, H. Pritzkow, J.-L. Bantignies, P. Dieudonné, J.-L. Sauvajol, *Angew. Chem. Int. Ed.*, **2004**, *43*, 134.

3) (a) F.H. Allen, and O. Kennard, *Chem. Des. Autom. News*, **1993**, *8*, 31. (b) F.H. Allen and W.D.S. Motherwell, *Acta Cryst.*, **2002**, *B58,* 407. (c) A. Nangia, *CrystEngComm*, **2002**, *17*, 1.

4) K.S. Huang, D. Britton, M.C. Etter and S.R. Byrn, *J. Mater. Chem.*, **1995**, *5*, 379.

5) (a) J.-F. Nicoud and R.J. Twieg, in *Nonlinear Optical Properties of Organic Molecules and Crystals*, D.S. Chemla and J. Zyss (eds.), Academic Press, Orlando, pp 221, **1987**. (b) K. Jain, G.H. Hewig, Y.Y. Cheng and J.I. Crowley, *IEEE J. Quantum Electron.* **1981,** QE-17 (9), 1593.

6) J. Jadżyn, M. Stockhansen and B. Zywucki, *J. Phys. Chem.*, **1987**, *91*, 754.

7) S.K. Kutz and T.T. Perry, *J. Appl. Phys.*, **1968**, *39*, 3798.

8) J. Zyss, D.S. Chemla and J.-F. Nicoud, *J. Chem. Phys.*, **1981**, *74*, 4800.

9) (a) H.-C. Weiss, R. Boese, H.L. Smith and M.H. Haley, *Chem. Commun.*, **1997**, 2403. (b) J.M.A. Robinson, B.M. Kariuki, K.D.M. Harris and D. Philp, *J. Chem. Soc., Perkin Trans. 2.*, **1998**, 2459. (c) P.J. Langley, J. Hulliger, R. Thaimattam and G.R. Desiraju, *New. J. Chem.*, **1998**, 1307. (d) J.M.A. Robinson, B.M. Kariuki and K.D.M. Harris, *Chem. Commun.*, **1999**, 329.

10) P. Gunter (ed.), *Nonlinear Optical Effects and Materials*, Springer, Heidelberg, **2000**.

11) A. Kàlmàn, L. Pàrkànyi and G. Argay, *Acta Cryst.*, **1993**, *B49*, 1039.

12) C.V.K. Sharma, K. Panneerselvam, T. Pilati and G.R. Desiraju, *Chem. Commun.*, **1992**, 832.

13) (a) S.S. Kuduva, D.C. Craig, A. Nangia and G.R. Desiraju, *J. Am. Chem. Soc.*, **1999**, 121, 1936. (b) J.N. Moorthy, R. Natarajan, P. Mal and P. Venugopalan, *J. Am. Chem. Soc.*, **2002**, *124*, 6530. (c) D. Das, R.K.R. Jetti, R. Boese and G.R. Desiraju, *Cryst. Growth Des.*, **2003**, *3*, 675. (d) F.H. Allen, V.J. Hoy, J.A.K. Howard, V.R. Thalladi, G.R. Desiraju, C.C. Wilson and G.J. McIntyre, *J. Am. Chem. Soc.*, **1997**, *119*, 3477. (e) S. Nagahama, K. Inoue, K. Sada, M. Miyata and A. Matsumoto, *Cryst. Growth Des.*, **2003**, *3*, 247. (f) E.V. García-Báez, F.J. Martínez-Martínez, H. Höpfl and I.I. Padilla-Martínez, *Cryst. Growth Des.*, **2003**, *3*, 35.

14) *PC Spartan Pro 1.0* Wavefunction Inc., Irvine, CA, USA, **1999**.

15) A. Zafar, S.J. Geib, Y. Hamuro and A.D. Hamilton, *New. J. Chem.*, **1998**, 137.

16) A. Nangia and G.R. Desiraju, *Chem. Commun.*, **1999**, 605.

17) Xtal 3.5. Manual, University of Western Australia, Australia, Geneva, Switzerland and Maryland, U.S.A., (eds.) S.R. Hall, H.D. Flack and J.M. Stewart, **1995.**

18) SHELX-97. G.M. Sheldrick, Program for the Refinement and Solution of Crystal Structures, University of Gottingen, Germany, **1997.**

19) PLATON. A. L. Spek, Bijvoet Centre for Biochemical Research, Vakgroep Kristal-en Structure-Chemie, University of Utrecht, The Netherlands.

20) T. Higashu, ABSCOR: *An Empirical Absorption Correction Based on Fourier Coefficient Fitting*; Rigaku Corporation: Tokyo, **1995.**

21) G.M. Sheldricks, SADABS: Program for Empirical Absorption of Area Detector Data; University of Göttingen, Germany, **1996.**

22) G. Kopfmann and R. Huber, *Acta Cryst.*, **1968**, *A24*, 348.

23) A.C.T. North, D.C. Phillips and F.S. Mathew, *Acta Cryst.*, **1968**, *A24*, 351.

CHAPTER SEVEN

SALIENT FEATURES OF THE CRYSTAL STRUCTURES STUDIED IN THIS THESIS

Table 1. Salient crystallograhic details of the compounds discussed in this thesis.

	Chapter 2			*Chapter 3*
	1	**2**	**3**	**4**
Empirical formula	$C_{12}H_{12}N_2O$	$C_{13}H_{14}N_2O$	$C_{12}H_{11}N_2OCl$	$C_{12}H_{13}N_2OCl$
Crystal system	Orthorhombic	Orthorhombic	Orthorhombic	Orthorhombic
Space group	*Pbcm*	*Pnma*	*Pnma*	$Pmn2_1$
a (Å)	7.13(2)	7.263(1)	7.298(1)	6.801(1)
b (Å)	18.104(5)	8.591(2)	8.504(3)	12.199(1)
c (Å)	8.612(1)	19.488(4)	19.472(2)	7.327(1)
α	90	90	90	90
β	90	90	90	90
γ	90	90	90	90
Volume[Å^3]	1111(1)	1216(1)	1208(1)	607.9(1)
Z	4	4	4	2
D_{calc} *(g/cm^3)*	1.20	1.17	1.29	1.293
F(000)	424	456	488	248
T, *K*	296.2	296.2	296.2	296.2
$2\theta_{max}$	60	68	70	65.92
Range *h*	0 to 10	-10 to 10	-11 to11	-0 to 13
Range *k*	-25 to 0	-12 to 12	0 to 13	11 to 12
Range *l*	0 to 12	0 to 27	0 to 31	-24 to 23
N-Total	1725	2927	5681	2150
N-independent	1725	2927	3014	1654
N-observed	674	609	959	1105
R_1	0.058	0.044	0.043	0.039
wR2	0.046	0.047	0.035	0.052
GOF	2.779	5.181	3.067	2.008
Parameters	85	91	109	90

Table 1. *Continued...*

Chapter 3				
6	**7**	**8**	**9**	**10**
$C_{13}H_{15}N_2OCl$	$C_{12}H_{12}N_2OCl_2$	$C_{12}H_{12}N_3O_4Cl$	$C_{13}H_{15}N_3O_4$	$C_{18}H_{16}N_2O$
Monoclinic	Monoclinic	Orthorhombic	Orthorhombic	Monoclinic
$P2_1/m$	$P2_1/m$	*Pnma*	*Pnma*	$P2_1/a$
7.304(1)	7.313(1)	26.880(3)	26.559(3)	12.602(2)
6.767(1)	6.668(2)	6.348(1)	6.373(1)	10.201(3)
13.444(2)	13.644(2)	8.102(1)	8.079(1)	23.118(6)
90	90	90	90	90
105.59(1)	105.23(1)	90	90	94.37(2)
90	90	90	90	90
640.1(1)	641.9(2)	1382.5(3)	1367.4(1)	2963(1)
2	2	4	4	8
1.301	1.403	1.430	1.347	1.239
264	280	616	584	168
296.2	296.2	296.2	296.2	296.2
60	79.5	60	59.92	35.16
-11 to 10	0 to 13	0 to 37	0 to 37	-12 to 13
-10 to 10	-11 to 12	-8 to 8	-8 to 8	-10 to 0
-11 to 11	-24 to 23	0 to 11	-11 to 11	-24 to 24
4953	8137	4354	4314	6240
2569	4195	2694	2333	3673
1448	1726	759	758	850
0.037	0.038	0.066	0.061	0.074
0.043	0.041	0.059	0.066	0.078
3.015	2.213	2.895	3.835	1.758
90	125	115	115	199

Table 1 *Continued...*

Chapter 4					
14	**15**	**16**	**17**	**18**	**19**
$C_{12}H_{11}BrN_2O$	$C_{12}H_{11}IN_2O$	$C_{12}H_{11}N_3O_3$	$C_{13}H_{14}N_2O$	$C_{13}H_{14}N_2O_2$	$C_{12}H_{10}FN_2O$
Triclinic	Triclinic	Triclinic	Monoclinic	Monoclinic	Orthorhombic
$P\bar{1}$	$P\bar{1}$	$P\bar{1}$	$P2_1/n$	$C2/c$	*Pnma*
7.1084(6)	7.531(1)	7.126(6)	7.1729(5)	21.324(4)	7.0475(10)
7.4863(6)	12.236(2)	7.635(1)	14.506(2)	7.2771(9)	7.438(3)
11.923(1)	7.154(1)	11.337(2)	11.384(1)	16.929(7)	20.763(4)
99.788(4)	106.27(1)	102.33(1)	90	90	90
107.055(3)	100.1(9)	103.28(5)	106.972(6)	111.81(3)	90
98.477(4)	74.90(1)	96.74(5)	90	90	90
584.50(9)	607.2(7)	577.4(5)	1132.9(2)	2439.0(11)	1088.4(4)
2	2	2	4	8	4
1.586	1.784	1.410	1.256	1.254	1.326
280	316	256	456	976	452
296.2	296.2	296.2	296.2	296.2	296.2
59.2	42.7	70	42.8	55.94	49.94
-9 to 8	-8 to 9	-11 to 11	0 to 9	-28 to 28	0 to 8
-9 to 9	-9 to 9	-12 to 12	0 to 18	0 to 9	-8 to 8
-15 to 15	-15 to 15	0 to 18	-14 to 14	0 to 22	-24 to 0
6418	5982	5276	2693	3249	2148
2647	2756	5071	2693	3148	1164
1717	1966	984	1355	1437	707
0.05	0.04	0.057	0.07	0.049	0.087
0.058	0.054	0.056	0.066	0.061	0.071
1.465	1.477	2.727	2.008	2.003	2.097
136	177	163	145	155	94

Table 1. *Continued...*

Chapter 4		*Chapter 5*		
21	**22**	**23**	**24**	**25**
$C_{12}H_{12}N_2O$	$C_{12}H_{12}N_2O$	$C_{15}H_{16}N_2O_3$	$C_{12}H_{13}BrN_2O_2$	$C_{13}H_{21}N_2NaO_8$
Orthorhombic	Monoclinic	Monoclinic	Monoclinic	Orthorhombic
Pbca	*C2/c*	*P2$_1$/a*	P2$_1$/a	*Pbcn*
10.1248(7)	18.468(3)	7.183(1)	11.184	17.1943(2)
17.625(2)	7.214(2)	13.586(1)	9.811	6.88470(10)
11.924(1)	15.603(3)	14.142(1)	11.4109	29.5336(3)
90	90	90	90	90
90	91.87(2)	92.99(1)	91.4820	90
90	90	90	90	90
2127.9(3)	2077.7(7)	1378.2(2)	1273.43(5)	3496.12(6)
8	8	4		8
1.280	1.248	1.312	1.550	1,354
848	848	576	600	1504
273.2	296.2	296.2	296.2	296.2
42.9	59.2	56	45.84	42.7
-13 to 0	-25 to 25	-9 to 9	0 to 15	0 to 22
0 to 22	0 to 10	0 to 17	0 to 13	0 to 8
0 to 15	0 to 21	0 to 18	-15 to 15	-38 to 0
4510	6672	3593	3751	4536
2756	6454	3463	3751	4536
1504	1057	1787	2705	2786
0.064	0.049	3.6	5.4	4.2
0.053	0.061	3.6	4.0	4.2
1.682	2.809	2.568	1.528	1.969
173	136	245	206	301

Table 1. *Continued...*

Chapter 6				
26	**27**	**28**	**29**	**30**
$C_{13}H_{10}IN_3O_3$	$C_{15}H_{11}N_3O_3$	$C_{15}H_{16}N_4O_3$	$C_{13}H_{10}BrN_3O_3$	$C_{13}H_{10}ClN_3O_3$
Monoclinic	Monoclinic	Triclinic	Monoclinic	Monoclinic
Cc	*Cc*	$P\bar{1}$	$P2_1/n$	$P2_1/n$
13.552(3)	13.422(3)	6.0710(12)	7.9974(8)	8.0360(5)
4.6722(9)	4.6511(9)	7.5613(15)	13.4826(13)	13.3397(8)
21.377(6)	21.261(4)	31.715(6)	12.0227(12)	11.8513(7)
90	90	89.95(3)	90	90
90.40(3)	94.97(3)	87.01(3)	94.671(2)	94.8820(10)
90	90	85.23(3)	90	90
1353.5(5)	1322.3(5)	1448.9(5)	1292.1(2)	1265.82(13)
4	4	4	4	4
1.880	1.413	1.377	1.728	1.531
744	584	632	672	600
293(2)	300	300	293(2)	293(2)
56.02	54.96	55.14	56.04	56.04
-17 to 17	-17 to 17	0 to 7	-10 to 10	-10 to 9
-5 to 6	-6 to 0	-8 to 8	-17 to 15	-9 to 17
-28 to 27	-27 to 27	-37 to 37	-15 to 15	-14 to 15
4355	3017	5543	8669	8434
2212	3017	5055	3120	3067
2036	1912	2329	1919	2201
2.88	4.75	8.01	4.91	4.68
7.39	12.32	20.95	13.81	13.57
1.005	1.067	1.023	958	1.058
182	190	397	181	181

Table 1. *Continued...*

Chapter 6				
31	**32**	**33**	**34**	**35**
$C_{13}H_{10}FN_3O_3$	$C_{14}H_{10}N_4O_3$	$C_{13}H_{10}IN_3O_3$	$C_{15}H_{16}IN_3O_4S$	$C_{15}H_{18}N_4O_4$
Monoclinic	Monoclinic	Monoclinic	Triclinic	Monoclinic
$P2_1/n$	$P2_1/n$	$P2_1/n$	$P\bar{1}$	$P2_1/c$
8.1241(8)	7.919(4)	8.4419(17)	10.184(2)	9.4442(19)
12.9932(12)	13.692(6)	12.987(3)	13.346(3)	7.3883(15)
11.6524(11)	11.777(6)	12.399(3)	15.502(3)	23.863(5)
90	90	90	66.82(3)	90
94.967(2)	94.517(10)	96.59(3)	88.22(3)	97.73(3)
90	90	90	68.75(3)	90
1225.4(2)	1272.9(10)	1350.4(5)	1790.0(6)	1650.0(6)
4	4	4	5	5
1.492	1.473	1.885	2.075	1.294
568	584	744	1090	670
293(2)	293(2)	293(2)	293(2)	293(2)
56	56.16	56.16	54.96	54.96
-10 to 10	-10 to 10	-10 to 10	0 to 13	0 to12
-14 to 17	-17 to 15	-16 to 17	-16 to 17	0 to 9
-14 to 15	-15 to 15	-16 to 12	-20 to 20	-30 to 30
8210	5981	5931	8625	4014
2958	3037	3075	8168	3789
1741	1606	1825	3868	1467
5.21	5.14	6.46	7.75	7.83
14.72	13.04	15.93	18.71	18.39
1.083	973	981	1.119	1.093
181	190	191	433	237

Table 1. *Continued...*

Chapter 6	
36	**37**
$C_{16}H_{19}N_3O_4S$	$C_{17}H_{19}N_3O_5S$
Monoclinic	Triclinic
$P2_1/n$	$P\bar{1}$
16.0665(10)	6.0509(6)
5.7448(4)	12.4575(12)
39.100(3)	12.5937(11)
90	78.120(2)
100.115(2)	82.891(2)
90	80.105(2)
3552.8(4)	911.30(15)
8	2
1.306	1.375
1472	396
293(2)	293(2)
56.08	56.06
-21 to 20	-8 to 7
-7 to 7	-13 to 16
-15 to 45	-9 to 16
23182	6233
8599	4313
3157	2218
6.64	5.34
19.50	13.79
861	889
442	235

ABOUT THE AUTHOR

Sumod George was born in Manimooly, a village in the Malappuram district of Kerala, India in 1971. He had his primary and high school education in Nilambur and Trichur. After completing M.Sc. from Barkatullah University, Bhopal in 1994 he joined for M.Phil in 1995 in Pondicherry University. In 1998 he joined School of Chemistry, University of Hyderabad for the Ph.D degree.

LIST OF PUBLICATIONS

1 C–H···O and C–H···N Hydrogen Bond Networks in the Crystal Structures of Some 1,2-Dihydro-*N*-aryl-4,6-dimethylpyrimidin-2-one.
M. Muthuraman, Yvette Le Fur, Muriel Bagieu-Beucher, René Masse, Jean-François Nicoud, **Sumod George**, Ashwini Nangia and Gautam R. Desiraju
J. Solid State Chem., **2000**, *152*, 221-228.

2. *N*-(4-Biphenylyl)urea.
Sumod George, Ashwini Nangia, and Vincent M. Lynch
Acta Cryst., **2001**, *C57*, 777-778

3. *N*-(3-Pyridyl)urea.
Sumod George and Ashwini Nangia
Acta Cryst., **2001**, *E57*, o719-o720.

4. Crystal Engineering of Neutral *N*-Arylpyrimidinones and their HCl and HNO_3 Adducts with a C–H···O Supramolecular Synthon. Implications for Non-Linear Optics.
Sumod George, Ashwini Nangia, Meiyappan Muthuraman, Muriel Bagieu-Beucher, René Masse and Jean-François Nicoud
New J. Chem., **2001**, *25*, 1520-1527.

5. Crystal Engineering of Two-Dimensional Polar Layer Strucutures: Hydrogen Bond Networks in Some *N-meta*-Phenylpyrimidinones.
Sumod George, Ashwini Nangia, Muriel Bagieu-Beucher, René Masse and Jean-François Nicoud
New J. Chem., **2003**, *27*, 568-576.

6. *N,N'*-Bis(4-biphenylyl)urea.
Sumod George and Ashwini Nangia
Acta Cryst., **2003**, *E59*, o901-o902.

7. Crystal Engineering of Urea α–Network via I···O_2N Synthon and Design of SHG Active Crystal *N*-4-Iodophenyl-*N'*-4'-nitrophenylurea.
Sumod George, Ashwini Nangia, Chi-Keung Lam, Thomas C. W. Mak and Jean-François Nicoud
Chem. Commun., (Accepted for publication).